Technical Transactions

Czasopismo Techniczne

Issue 2
Volume 2018 (115)

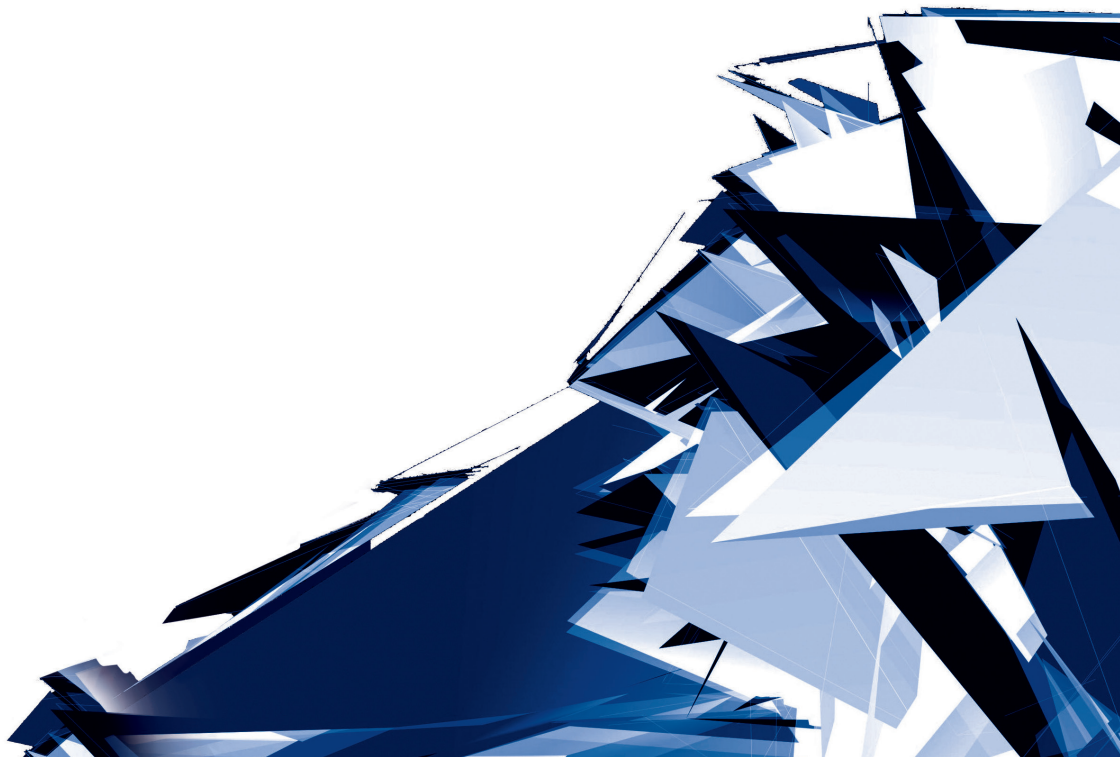

Chairman of the Cracow University of Technology Press Editorial Board
Przewodniczący Kolegium Redakcyjnego Wydawnictwa Politechniki Krakowskiej

Tadeusz Tatara

Editor-in-chief
Redaktor naczelny

Józef Gawlik
(jgawlik@mech.pk.edu.pl)

Scientific Council
Rada Naukowa

Jan Błachut – University of Liverpool (UK)
Wojciech Bonenberg – Poznan University of Technology (Poland)
Tadeusz Burczyński – Silesian University of Technology (Poland)
Massimo Corcione – Sapienza University of Rome (Italy)
Leszek Demkowicz – The University of Texas at Austin (USA)
Joseph El Hayek – University of Applied Sciences (Switzerland)
Ameen Farooq – Technical University of Atlanta (USA)
Zbigniew Florjańczyk – Warsaw University of Technology (Poland)
Marian Giżejowski – Warsaw University of Technology (Poland)
Sławomir Gzell – Warsaw University of Technology (Poland)
Allan N. Hayhurst – University of Cambridge (UK)
Maria Kušnierova – Slovak Academy of Sciences (Slovakia)
Krzysztof Magnucki – Poznan University of Technology (Poland)
Herbert Mang – Vienna University of Technology (Austria)
Arthur E. McGarity – Swarthmore College (USA)
Antonio Monestiroli – Polytechnic of Milan (Italy)
Ivor Samuels – University of Birmingham (UK)
Mirosław J. Skibniewski – University of Maryland (USA)
Günter Wozny – Technical University in Berlin (Germany)
Roman Zarzycki – Lodz University of Technology (Poland)

Native Speakers
Weryfikacja językowa

Tim Churcher
Robin Gill
Justin Nnorom

Series Editors
Redaktorzy Serii

ARCHITECTURE AND URBAN PLANNING
Mateusz Gyurkovich
(mgyurkovich@pk.edu.pl)

CHEMISTRY
Radomir Jasiński
(radomir@chemia.pk.edu.pl)

CIVIL ENGINEERING
Marek Piekarczyk
(mpiekar@pk.edu.pl)

ELECTRICAL ENGINEERING
Piotr Drozdowski
(pdrozdow@usk.pk.edu.pl)

ENVIRONMENTAL ENGINERING
Michał Zielina
(mziel@vistula.wis.pk.edu.pl)

PHYSICS, MATHEMATICS AND COMPUTER SCIENCES
Włodzimierz Wójcik
(puwojcik@cyf-kr.edu.pl)

MECHANICS
Andrzej Sobczyk
(andrzej.sobczyk@mech.pk.edu.pl)

Section Editor
Sekretarz Sekcji

Dorota Sapek
(dsapek@wydawnictwo.pk.edu.pl)

Editorial Compilation
Opracowanie redakcyjne

Aleksandra Urzędowska
(aurzedowska@pk.edu.pl)

Typesetting
Skład i łamanie

Anna Basista

Design
Projekt graficzny

Michał Graffstein

www.ejournals.eu/Czasopismo-Techniczne
www.technicaltransactions.com
www.czasopismotechniczne.pl

© 2018 Cracow University of Technology
ISSN 0011-4561

Basic version of each Technical Transactions magazine is its online version
Pierwotną wersją każdego zeszytu Czasopisma Technicznego jest jego wersja online

Creative Commons (CC BY-NC-SA 4.0)
https://creativecommons.org/licences/by-nc-sa/4.0/legalcode.pl

Contents

MECHANICS

TECHNICAL TRANSACTIONS 2/2018
ARCHITECTURE AND URBAN PLANNING
DOI: 10.4467/2353737XCT.18.017.7990
SUBMISSION OF THE FINAL VERSION: 5/1/2018

Mateusz Gyurkovich (mateusz.gyurkovich@pk.edu.pl)
Institute of Urban Design, Faculty of Architecture, Cracow University of Technology

Adolfo Sotoca (adolfo.sotoca@ltu.se)
Department of Civil, Environmental and Nature Resources Engineering,
Luleå University of Technology

Towards the Cracow Metropolis – a dream or a reality? A selected issues

W kierunku Krakowskiej Metropolii – marzenie czy rzeczywistość? Wybrane problemy

Abstract

Cracow, the former capital of Poland and currently the second-largest Polish city, dreams of becoming the most important metropolis – not only of the Lesser Poland region, but also of the entire southern and south-eastern part of Poland. This paper, based on long-term research and field studies, also refers, in part, to the "Model of the Spatial Structure of Cracow" research programme, which was conducted at the Institute of Urban Design of the CUT under the guidance of M. Gyurkovich with collaboration with A. Sotoca, between October 2016 and July 2017. This is the background against which the selected issues of spatial transformations that took place within the city limits and that influence the urban morphology of Cracow, will be presented against. The type of spatial structure that can currently be observed in Cracow, does not bring to mind an association with the urban form of a European Metropolis. Can the contemporary attempts to create a polycentric urban organism- that can compete with other, well-organised ones, internationally, ever be successful? Will the dream of the Cracow Metropolis ever come true?

Keywords: metropolis, polycentrism, density, exurbanisation, urban morphology, urban form

Streszczenie

Kraków, była stolica Polski i obecnie drugie polskie miasto, marzy o staniu się najważniejszą metropolią nie tylko regionu Małopolski, ale także całej południowej i południowo-wschodniej Polski. Niniejszy artykuł, oparty o długotrwałe badania i studia terenowe, również odnosi się częściowo do programu badawczego „Model Struktury Przestrzennej Krakowa", opracowanego w Instytucie Projektowania Urbanistycznego PK pod kierunkiem M. Gyurkovicha przy współpracy z A. Sotocą między październikiem 2016 a lipcem 2017 roku. Stanowi on tło, na którym będą prezentowane wybrane zagadnienia przekształceń przestrzennych, które miały miejsce w obrębie miasta, i które wywierają wpływ na morfologię urbanistyczną Krakowa. Rodzaj struktury przestrzennej, który można obecnie zaobserwować w Krakowie, nie wywołuje konotacji z formą urbanistyczną Europejskiej Metropolii. Czy współczesne próby stworzenia policentrycznego miejskiego organizmu, który mógłby konkurować z innymi, dobrze zorganizowanymi miastami na płaszczyźnie międzynarodowej mogą zakończyć się powodzeniem? Czy marzenie o Krakowskiej Metropolii kiedykolwiek się spełni?

Słowa kluczowe: metropolia, policentryzm, intensywność, eksurbanizacja, morfologia urbanistyczna, forma urbanistyczna

1. Focus of the paper

This article was written as one of the results of many years of studying the wealth of subject literature[1], cartographic and iconographic materials, as well as planning documents regarding Cracow, in addition to observations and on-site research. This research concentrated chiefly around the problems associated with the urban form and, even more broadly – the urban composition of a city that plays the *de facto* role of a very important metropolitan centre on the regional[2] and national[3] scale. It focused both on the city as a whole, but also on each of the distinct, characteristic elements that make up that whole. Cracow cannot be labelled as "compact city" and the roots of this issue are connected much more with the process of its urban growth over last 120 years, than with its more distant historical origins or geographic determinants of the location: between river plain and hilly areas. We can observe, within the city limits, the defragmentation of the urban form and the coexistence of dense urban fabric chaotically mixed with the sprawled areas of different kind and origin. That structures has been created mostly after the Second World War[4], on former rural areas, without changing the original partitions of the sites, and sometimes even- without changing the scale and typology of former villages to "more urban like". The main focus of the paper would be put on this strange coexistence of different typology and scales, which makes that the identifying of "local sub-centre" in numerous districts and areas within the Cracow city limits is almost impossible. That is one of the main reasons, why the problem of the polycentric nature of the spatial structure of Cracow, which has been declared in numerous planning documents and has been present in academic discourse on both the national and international level, is still not functioning at a satisfactory level – unlike throughout the city's history [38, 18].

---

1 Which focuses on numerous issues – from general urban planning theories (among others: [13, 34, 35, 54, 12, 15, 61, 55, 58, 10, 45, 36]); through the history of the spatial development of Cracow (including: [7, 47, 43, 44, 39, 60, 38, 9, 42, 57, 17, as well – 14] , in addition to problems that have been of particular importance in recent years, associated with the phenomenon of exurbanisation and of the loss of the urban form of cities – important sources include the documents of the European Commission, publications associated with international scientific conferences (those organised in Poland include, for instance, the Urban Landscape Renewal conference at the Silesian University of Technology or a series of conferences organised by the Institute of Urban Design of the CUT in the years 2001–2016), as well as the research work published both in the form of articles and scientific books (including: [2, 22, 37, 32, 33, 26, 31, 6]).

2 As the capital and the largest city of Lesser Poland, it is also an important university, cultural, economic and tourist centre (12,000,000 tourists in the year 2016 – according to data of the Tourist Information Service of the Office of the City of Cracow from 11.10.2017), and in the spiritual sense, a pilgrimage centre for Catholics, the seat of an archdiocese – metropolis, which is composed of four dioceses of the Catholic Church.

3 To which it is not limited, as it also exerts strong influence in this part of Europe (sometimes in tandem with the Upper Silesian Metropolis, or separately – depending on accepted conditions) – cf., among others, elements of the bibliography.

4 But also before, since the times of the Plan from 1910, which will be mentioned later on; they appear more and more often even nowadays.

2. Introduction

The rapid and largely uncontrollable development and growth of cities during the past century has taken place with varying intensity in different parts of the world. There is currently no single, widely accepted model of a metropolitan city – there exist many variations of it, depending on the different geographic, historical, economic and demographic conditions (as well as many others: [58, 45, 4, 17]. This process has often led to a situation in which, apart from fragments of composed urban tissue, relics of spatial layouts that are typical of rural areas can be observed in urban zones. The situation is no different in Cracow. The causes of this state of affairs can be sought both on the side of economic and legal conditions, political turmoil (which, apart from changes regarding the political system, also include military operations) that changed over time, as well as in the complex history of the spatial development of the city[5]. In Poland, the period of the last three decades, apart from a return to democracy, has also been a time of ongoing processes of the growth of urban areas. They are accompanied by a more and more observable loss of urban form and characteristic compositional elements that have so far shaped cities in our region of Europe (The situation is no different in Cracow, cf. for instance [1, 32, 33].

Cities and metropolitan areas inevitably become the natural environment of the life and habitation of modern humans. The 21st century has already been called the "century of cities", with over half of the global population living in cities (as of 2006). Against this background, Poland (38.45 million inhabitants in the year 2015 – according to information provided by GUS [71]) appears to fit in with the European average, although when compared to countries with a similar population from the circle of the European tradition of building cities (e.g. Canada – 36.5 million; Spain – 46.4 million or Ukraine – 45.1 million inhabitants in the year 2015 [71]) it can be observed that the share of medium-sized (up to 100,000 inhabitants) and small (up to 50,000 inhabitants) cities and towns is much greater in the overall number of urbanised areas. Cracow, the former capital of Poland, has a dream to become the most important metropolis, not only in the region of Lesser Poland, but also in the entire southern and south-eastern part of the country. Cracow is currently Poland's second largest city with a population of slightly over 765 thousand inhabitants in 2016 [72], while the populations of comparable (second-largest in their respective countries) cities in the aforementioned countries, as well as in the majority of EU member states are substantially larger and usually exceed 1.5 million inhabitants[6].

We can thus conclude (after A. Bitner [5]) that the indicator of the level of demographic urbanisation appears to be decidedly insufficient for the purpose of fully describing the complex phenomenon of urbanisation. The studying of the structure of a city from a morphological perspective can be exceptionally helpful. Urban morphology, understood as an interdisciplinary field bordering on urban planning and architecture, as well as geography,

[5] Confer numerous bibliographic positions that refer to the spatial development of Cracow or of its fragments, including those mentioned in previous notes.

[6] For comparison: in Canada – Montreal – 1,620 thousand; in Spain – Barcelona – 1,605 thousand; in Ukraine – Kharkiv – 1,450 thousand; in Germany – Hamburg – 1,686 thousand; cf. the websites of the aforementioned cities, as well as [73].

focuses on studying *urban form*. Depending on its current, it focuses its attention on such aspects of the space of a city like: streets (roads), plot division and the built environment or, even more generally: plots, the built environment and non-built-up spaces (solid/void). According to the basic principles of this discipline (Confer, for instance [46, 27–29]), a *city's morphological structure* (which is the structure of the visible, three-dimensional form of a city), which is sometimes described in literature as *morphogenetic* (which is the structure of the visible form with a reference to its genesis), is a part of its spatial structure. The latter term was used by the authors in the *Model of the Spatial Structure of Cracow* already during the 1st stage of this research study [20] and it appears to be more adequate in the context of a city with a historically shaped core that features unique assets, which Cracow, without a doubt, clearly possesses.

3. The *morphogenetic* structure of Cracow

The urban structure of Cracow, similarly to that of any city, is defined by the grid of the spatial layout outlined by urban units[7] that are connected with each other through the transport system[8] and are composed in a legible manner and are easy to identify, or, by using a different term – *morphogenetic units*. In theory, their mutual compositional relations should be legible both in terms of their plan, but chiefly in the third dimension – in the real-world spatial structure of a city. An urban composition built using these measures, under the guise of the urban form, should facilitate spatial orientation among its users, even those that are not familiar with a particular city or district [27]. Due to numerous problems that have been mentioned briefly in this paper, this is, however, not the case in Cracow.

The form of a city, in the case of Cracow, as it has already been mentioned earlier, is highly varied and not always legible. However, from the visual perspective of the city, we can identify individual fragments (districts, regions, architectural and urban complexes) which are easy to tell apart. The important thing here is legibility on both the layer of *urban grids*, understood as a system of public spaces (including roads and streets, as well as the still heavily fragmented system of green public spaces), as well as on the layer of *tissues*, which is formed from the architectural substance that constitutes the filling of these grids. The morphogenetic structure was recorded in the form of a scheme of the layout of the units of urban space that have become distinct due to their planning, form and genesis (called *morphogenetic units* [20, 21]).

---

7 According to urban composition theory – e.g.: K. Lynch, K. Wejchert – regions/areas, treated in this work as *tissue*.

8 Elements of which can be defined in accordance with numerous theories regarding urban composition (whose authors are, among others: G. Cullen, K. Lynch, or K. Wejchert), as: lines/and in reference to the methodological assumptions of the *Model of the Spatial Structure of the City of Cracow*, as *grids* [21].

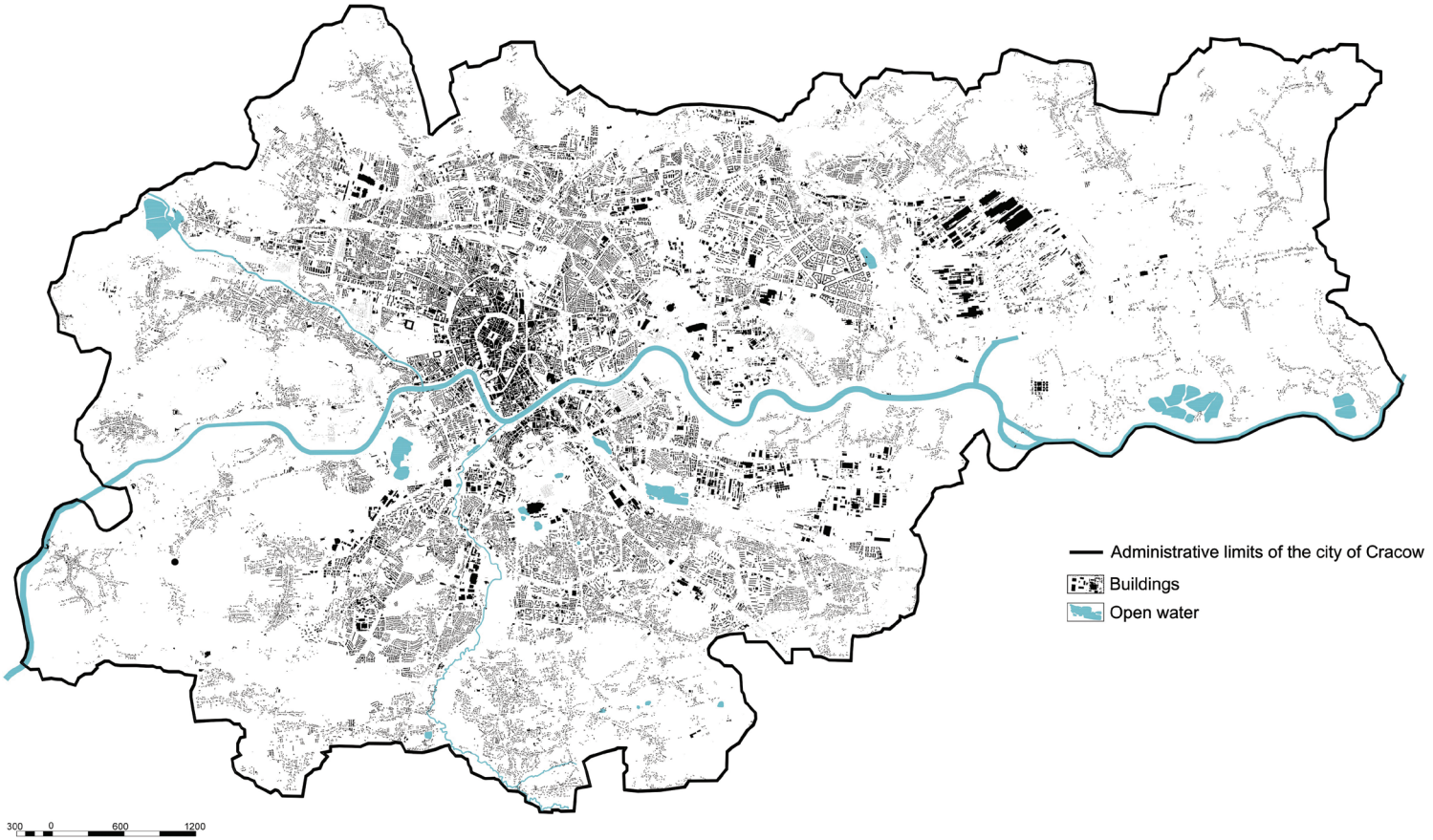

Fig. 1. Cracow 2016 – structure of the built environment – developed by P. Tota, K. Studencka (source: [21, pp. 41, 53–54])

Their delimitation was performed in reference to the *structural urban units*[9] established in the Spatial Development Conditions and Directions Study of Cracow[10], which aggregate areas with similar spatial features that are easy to delineate using linear elements of development (roads, railways, hydrological elements, etc.). Guidelines for the development of local plans for all 63 *structural urban units* were defined in the following, III volume of the Study in question. They already contained a detailed division of each SUU into areas of varying morphology. In order to properly evaluate the existing morphogenetic structure of Cracow, and, as a result, also its potential, it was thus necessary to introduce a finer division. This is why the final delimitation of *morphogenetic units*[11] was performed on the basis of the following three criteria: the features of the physiognomy of the urban form; the qualities of the layout of buildings; the genesis of the formation of the individual fragments of urban tissue. The scheme of the introduced morphogenetic units (Fig. 2) shows that many of them (80) are formed of unstructured or post-rural single-family housing of suburban character. So called "hybrid morphogenetic units" are treated as potential intervention sites and potential areas of the development of well-stucturized, urban fabric of Cracow linking the core of the city with the outskirts and Nowa Huta district. As for today, they are in fact no more than chaotic mixture of different kind of uses and typologies in which one can find the leftovers of former suburban villages, which has influenced very strongly[12] on the later development of those areas of the city.

The urban development of Cracow – from the earliest times of the pre-charter settlements grouped around the fortified princely castle on Wawel Hill from the IX century, through the tri-city polycentric layout that formed in the Middle Ages[13], to modern times – can, similarly to many other cities on the European continent, serve as a case study for the tracing of the role of urban composition, both in the crystallisation of urban and district cores, as well as of the residential building layouts that accompanied them. Cracow is currently not a compact city outside of its second bypass, which is a result of historical conditions[14]. It is characterised by a high loosening of the built environment as well as a high share of morphogenetic units associated with suburban

[9] This document specifies the division of Cracow into 63 structural urban units (SUU), which were assigned customary names, easily associated with a given area of the city. Even though their delimitation was mostly based on, among other things, conditions associated with the morphological structure of each area, in many cases other elements turned out to be more important and affected the final delimitation of SUU's. When performing the limitations, it was rightly acknowledged that "*there is no absolute necessity of reflecting the historical layout of the City, as current development has, in many cases already erased this layout and it is no longer possible to recreate*" [69, Vol. II, p. 37].

[10] This mention refers to the planning document from the year 2014 that is still in force – see *References*.

[11] 411 morphogenetic units were delimited in the work. This included as many as 80 units that featured the dominating role of single-family buildings of a suburban and rural character that occupy considerable areas of the city within its administrative limits – see Fig. 2, cf. [21, pp. 49–51].

[12] Most of all, thanks to the partition of the rural and building sites, which can be observed on numerous maps, plans and the aerial photos of the city from different times (including those presented in this paper).

[13] Which are: Cracow (Cracovia – 1257), Kazimierz (Casimiria – 1335) and Kleparz (Florentia, Claepardia – 1366), with the metropolitan layout having functioned, with small changes, for nearly 450 years. Over time, it was accompanied by a larger amount of suburbs, *jurisdictions* and satellite urban layouts (e.g. Podgórze from 1784).- cf. for instance [14, 44, 47].

[14] Which are touched upon in this article, but discussed much more in depth in the publications on the spatial development of Cracow, including a number of works by M. Gyurkovich, that have already been referenced here many times.

or even rural single-family buildings. These areas are mixed with dense, multi-family residential built-up areas from the second half of the XX century and even denser developer housing estates that have been built after the year 2003 on the basis of singular administrative decisions[15] and imperfect local plans that are not fully coordinated with each other[16]. It was observed that buildings are not the dominating form of development in many areas within the city. In such cases, morphogenetic units associated with forms of spatial development other than buildings were outlined, such as: the natural landscape, composed greenery (including parks and cemeteries)[17], larger watercourses and reservoirs, large railroad areas, the city's highway bypass, etc.[18]

Up to the time of the proclamation of the results of the competition for the *Greater Cracow Regulation Plan* in the year 1910 (and for a couple years longer), Cracow was a compact city, due to the slowing down of the growth after the relocation of the capital to Warsaw in the XVI century, as well as largely thanks to the status of a fortress-city, which was given to it by the Austrian partitioning authorities in the second half of the XIX century. The *Plan*[19] presented a spatial vision for a part of the areas that were newly incorporated into the city. The radial-concentric layout of the city – that was initiated inside the XIX-century urban tissue and which was also continued in the spatial structure of the Cracow Fortress – became crystallised in its provisions. Areas of the concentration of built-up areas featuring diverse forms of use and standards, with a clear underlining of the westward direction of the city's development (both on the northern and southern shores of the Vistula) were defined for the first time. Areas located to the west of the city were assigned to representative residential districts featuring diverse degrees of density[20]. Apartments of a lower standard, mixed in with industrial areas, were placed mainly in the eastern (Grzegórzki, Wesoła) and southern (Kazimierz, Dębniki) parts of the city[21].

The wedge of typologically diverse residential buildings that was featured in the Plan and that pierced the space between the city lawn of Błonia to the south and the railway line bound for Silesia in the north, constituted the largest development area of the city according to the document. This is roughly the area of the current fifth and sixth districts. Throughout the entire period of the two decades of the Interbellum, as well as during the Nazi occupation and in the years of the People's Republic of Poland, these areas were subjected to the processes of parcellation and urbanisation.

---

15 In areas where no local plans are in effect.

16 Or that are completely incompatible with each other, only very vaguely referring to the regulations of the Study in force at the time of their development, which, in light of Polish law, not even a legally binding document. This was written about by many authors of publications listed in the *References* (e.g. [32, 33, 6, 1, 61–63, 56, 57]).

17 Regarding their role in the shaping of the structure of Cracow – see, for instance [24].

18 The method used partially refers to, in spirit, to the works of professor Bogdanowski (*architectural and landscape units*), however, it appears to be much more objectivised: [8].

19 Whose authors were Józef Czajkowski, Władysław Ekielski, Tadeusz Stryjeński, Ludwik Wojtyczko and Kazimierz Wyczyński. It was the first significant planning document after several decades of blocking the city's development due to it being a fortified borderland stronghold – cf. for instance: [44, 14].

20 The urban multi-family residential buildings in these areas were placed adjacent to villa districts and city green areas, such as Błonia Krakowskie, Park Jordana and the future sports grounds of the Wisła and Cracovia sports clubs that were established in 1906.

21 The significance of the Plan of Greater Cracow to the later spatial development of the entire metropolitan layout is enormous and has been the subject of numerous scientific works many times. It was discussed in detial by, among others, Krystian Seibert in a previously cited book from 1983.

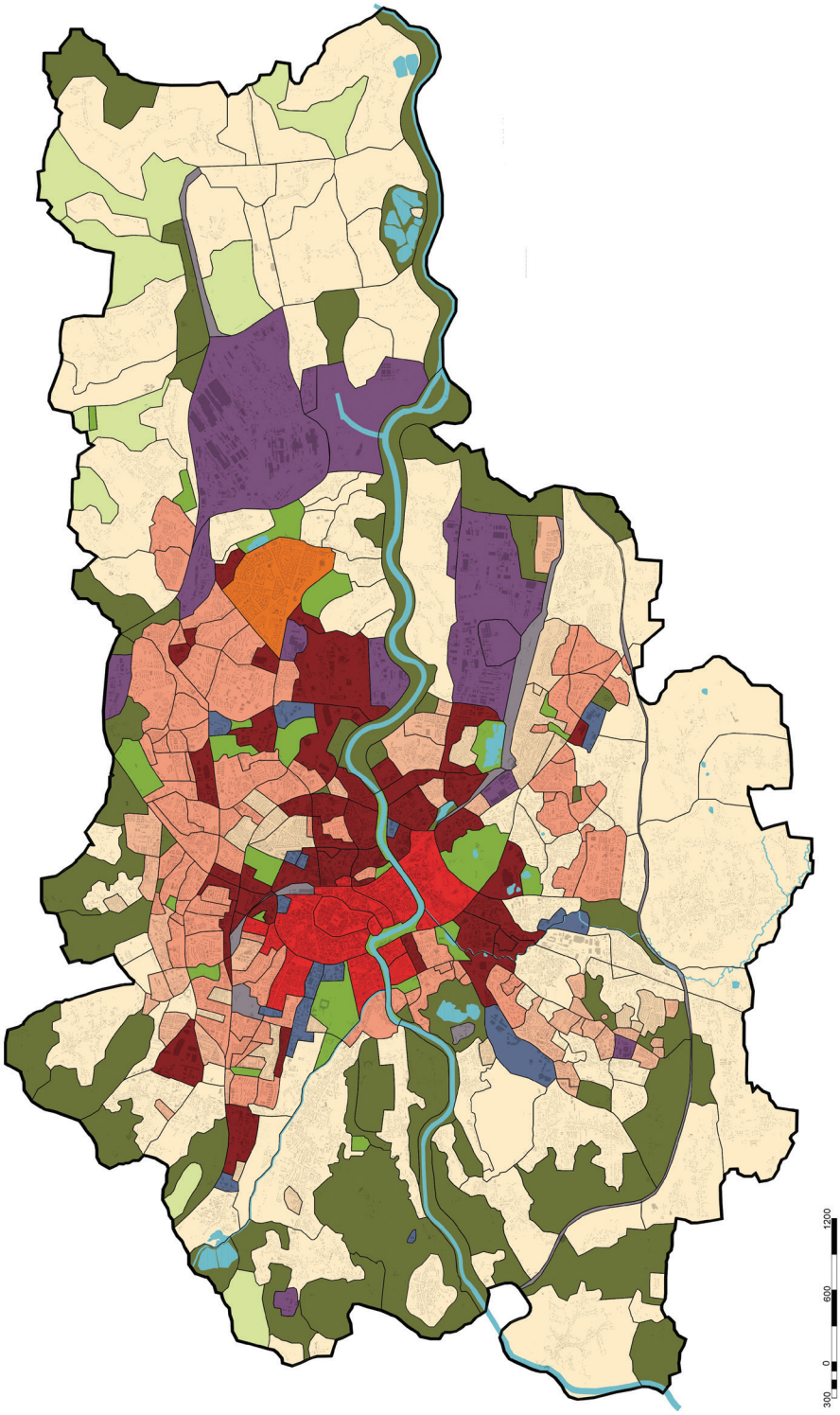
1200
600
0
300

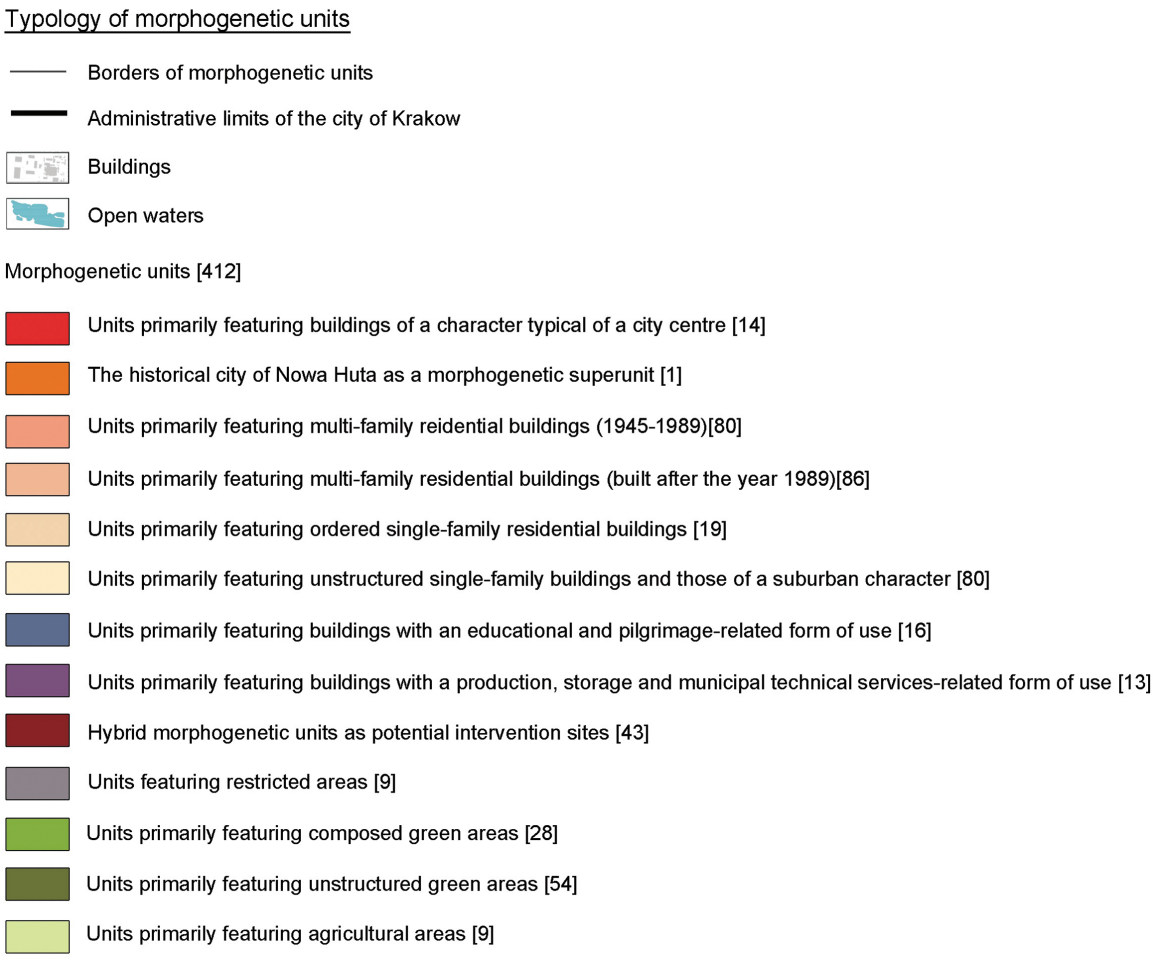

Fig. 2. Cracow 2016 – division into morphogenetic units along with their typology – developed by M. Gyurkovich, P. Tota (source: [21, pp. 41, 53–54])

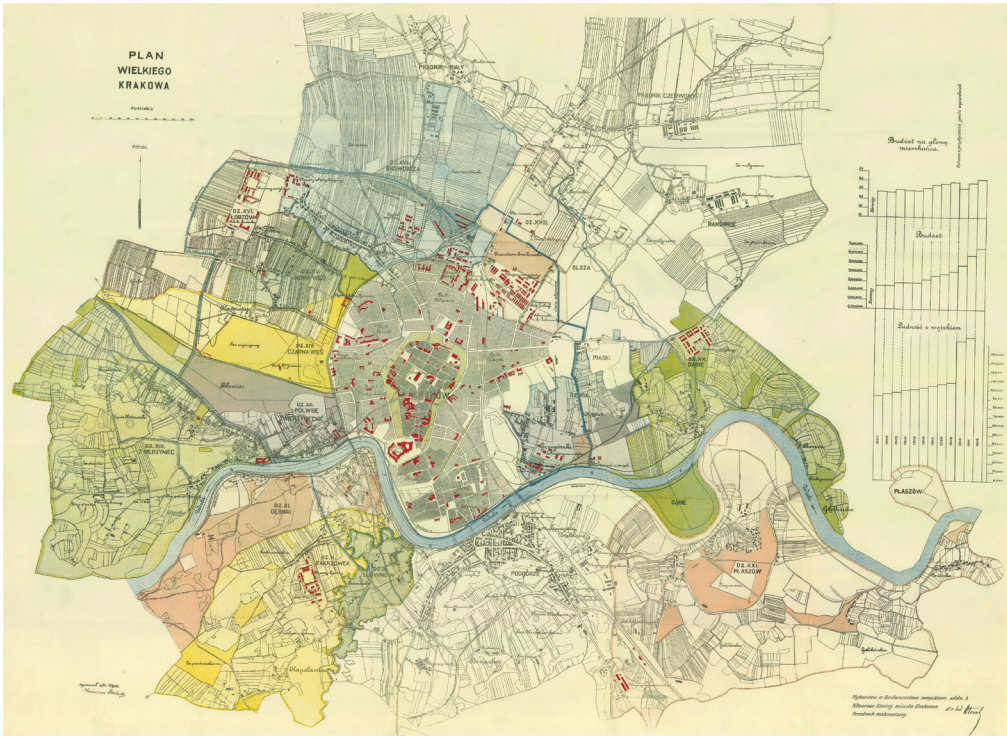

Fig. 3. Cracow – The Greater Cracow Plan, 1912 version
(source: archive of the Institute of Urban Design of the CUT)

Despite the demolishing of a part of the fortifications of the core of the fortress – the "noyau", we can still see significant areas exempted from civilian use (barracks and military storehouse complexes near Warszawska, Montelupich, Racławicka, Wrocławska streets and in the district of Grzegórzki) in the plans from the Interbellum period. To this day, despite a change of the form of use of most of these areas (despite one complex at Racławicka street and the area between Wrocławska and Głowackiego streets), they are easily recognisable in urban tissue, constituting, unambiguously, separate units, which can only serve to confirm the enormous influence of the XIX century Austrian fortress on the morphological structure of modern Cracow.

As a result of these transformations, it was possible to establish highly diverse urban tissue in this area, where Interbellum-period townhouses and urban villas, as well as representative residences are accompanied by relics of rural-type buildings, city block in-fills of a varied typology and form, as well as small complexes of prefabricated panel building apartment blocks of differing, yet easily predictable[22] heights. Today, these areas belong to the most centrally (despite the historical core of the city that has been shaped since the beginning of the XX century and has been placed on the UNESCO World Heritage Site List[23]) located districts of the city, irrefutably constituting the heart of a metropolis. This begs the question whether there is still a place for substandard urban substance

[22] Due to the solutions of industrialised construction employed in the 1960's and 1970's.

[23] Both as a protected area – the Old Town, Wawel and Kazimierz – since 1978; as well as the buffer zone within the core (noyau) of the Cracow Fortress – since the year 2010 [74].

in such a key area of the city – a substance that imitates the former layout of the villages from around Cracow[24] and that increases spatial chaos in the centre. Especially in light of the fact that this structure is constantly made denser, particularly in areas that have been reclaimed from former users (industry and the military). A striking example of such interventions is the residential development (built as a series of independent projects designed by different architects) that fills in the formerly industrial areas between Racławicka, Poznańska and Wrocławska streets and the railway tracks. Morphological dissimilarity, a disruptive scale and non-contextuality are the identifying traits of the – architecturally attractive, nonetheless – urban form of this heterogeneous complex.

Contrary to other Polish cities, whose urban structure has substantially suffered during the time of the Nazi German occupation of World War II, at the time of its ending Cracow[25] found itself enriched by 168 km^2 of land formerly belonging to suburban communities, a developed and modernised street network and a number of monumental urban layouts whose construction was just getting started. What is interesting, in their overall objectives, apart from plans of bombastic administrative districts at the foot of Wawel Hill, in Dębniki and in the area of Błonia, the German plans were a continuation of the pre-war plan by Dziewoński[26] in the western districts, which was also based on a continuation of the key features of the plan of 1910. The new residential district for the arriving civilian German population, located near the newly established Królewska street (then named Reichstrasse) [19] which was opened in 1941 and that led from the centre in the direction of the Palace in Łobzów (which was then used as a military barracks), deserves particular attention.

The form and urban composition of the areas that were planned and built during the period of the Interbellum and during World War II, based chiefly on city blocks and monumental public buildings connected to green areas and paved squares, resembles a traditional XIX century city, although the architectural forms themselves were different. Similar in both principle and construction is the urban structure of the oldest part of Nowa Huta[27],which was initially being built as a separate urban organism from 1949 onwards, but that was relatively rapidly incorporated into Cracow. Although the scale of the buildings is also somewhat different at times, a structure that mostly resembles the general idea of a European city was built nonetheless. The incorporation of the new urban organism that was Nowa Huta – which was located around 7 km to the east – caused the need to physically connect the city not only through the circulation system (roads and railways), but also through the layout of the

---

[24] In most cases the architectural substance was heavily modified or completely redeveloped, it thus has no historical or architectural value.

[25] The city remained under the authorities of the Nazi occupants from the 6th of September 1939 to the 18th of January 1945, when, along with the rest of the country, it was transferred under Soviet occupation. During this time it played the role of the capital of the so-called General Government, a rump state dependent on Nazi Germany, which was meant to lower the importance of Warsaw, as the capital of occupied Poland, and at the same time take over and germanise the historical role of Cracow [14].

[26] Developed in the years 1935–39; cf. [47, pp. 18–20].

[27] Nowa Huta, built based on a multi-axial, concentric layout, in which we can find inspiration with Baroque layouts, in combination with communist ideology and spatial principles that refer to neighbourhood units. The socialist realist city was built in accordance with a design developed by a team under the leadership of T. Ptaszycki. Nowa Huta has become the subject of numerous scientific works (e.g. [14, 47, 39, 38, 3].

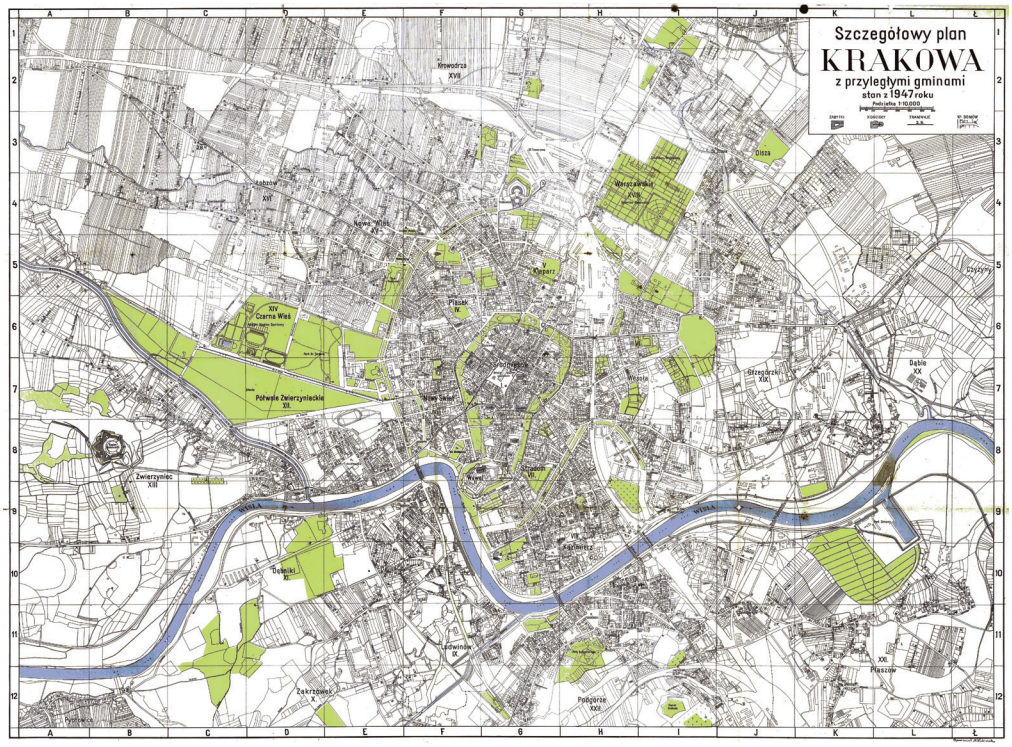

Fig. 4. Cracow – plan from the year 1947 (source: archive of the Institute of Urban Design of the CUT)

built environment. The current, historically conditioned development of the city became distorted and the new east-west development direction became dominant for several decades, something that has been confirmed by numerous planning and research works[28].

The newly established urban structure chiefly consisted of residential estates featuring prefabricated panel buildings as well as a number of small single-family residential complexes, featuring villas, terrace houses or other typologies[29], and which mostly (at least from the perspective of design objectives) constituted wholes composed in line with modernist and functionalist urban planning principles. Unfortunately, it was not possible to build all of the elements of these layouts. Especially those associated with circulation and service infrastructure were not implemented in a satisfactory manner. Similarly composed green areas or other types of public spaces do not constitute spatially legible and well-functioning systems on the scale of the city outside of Cracow's city centre[30].

[28] The administrative decision regarding its incorporation into Cracow on the day of 1.01.1951 as one of six districts (Cracow is currently divided into eighteen districts) brought with it additional changes and planning decisions, which have changed the spatial structure of the city forever. Instead of the historical axial layout that was developing along the N-S axis, subsequent city development plans (see References) feature belts of buildings oriented along the E-W axis, one in the north and another in the south of the city (cf. also, for instance [39, 47]).

[29] E.g. the immensely interesting Widok Zarzecze housing estate composed of atrial houses by M. Buratyńska-Seruga and her team.

[30] As shown in research by A. Ziobro in: [21, pp. 144–168].

4. Complicated contemporary *urban form* of Cracow

Multi-family structures that appeared around the entire city after the year 1945 (apart from the centre of Nowa Huta), are still mixed with agricultural areas and the aforementioned relics of the former villages that used to be located around Cracow and that were being incorporated into the city throughout almost the entirety of the XX century[31]. In general, regardless of location within the city's structure, the planning of residential buildings as a part of these groupings is the result of secondary divisions, as well as the combination and adaptation of the layout of parcels of former agricultural areas. At times, especially on the outskirts of the city, in the so-called *suburban zone*[32], but also in areas that are currently located closer to the city centre, they have legible centres of complexes that were once the centres of villages (Tyniec, Mydlniki, Skotniki, Bronowice Małe, Piaski Wielkie). Cracow's distinct quality is that single-family residential buildings are encountered practically all over the city, apart from the city centre inside the area encircled by the II bypass. They create typologically diverse groupings and groups – both large and small – either composed or chaotic in their layout.

A significant number of diverse projects, chiefly carried out by private developers on sites of varying size, spread nearly all over the administrative area of the city, could be seen in the space of Cracow during the last quarter-century. Residential projects, both multi and single-family ones, which were characterised more precisely in the oft-cited work [21], are the majority here. At times, they form composed wholes (units) or constitute a harmonious supplementation of earlier – currently historical – architectural and urban layouts. At other times they remain without any compositional connection with the extant context or even disrupt composed spatial layouts that have existed for decades (which is particularly visible in the case of residential and mixed-use residential and commercial projects that constitute the "densification" of multi-family residential estates from the second half of the XX century). They are sometimes built outside of built-up areas that have an urbanised character, amid green or agricultural areas, or in the area of the former villages that surrounded Cracow, which have currently found themselves inside the city's administrative limits[33]. The still-considerable amount of gated communities, built in such a manner that the continuity of the urban public domain is not being extended, also aids in the increasing of spatial chaos in many fragments of the city. Furthermore, we can also observe the tendency of the fencing off and fragmentation of the existing "modernist" spatial layouts of estates, and even the fencing off of individual buildings located in compact urban tissue and the reduction of common areas to, oftentimes, little more than road lanes.

[31] The last areas were incorporated into Cracow in 1986 – cf. [14].

[32] According to the terminology of the SUiKZP currently in force, however, as we know, this is a common occurrence in Polish cities (e.g. [22, 37, 32, 33, 6, 51]).

[33] Increases in the amount of residential buildings were discussed in detail by A. Ziobro in: [21 pp. 144–168].

Fig. 5. Cracow, north-western part – fragment of an orthophotomap from the year 2004 (source: [75])

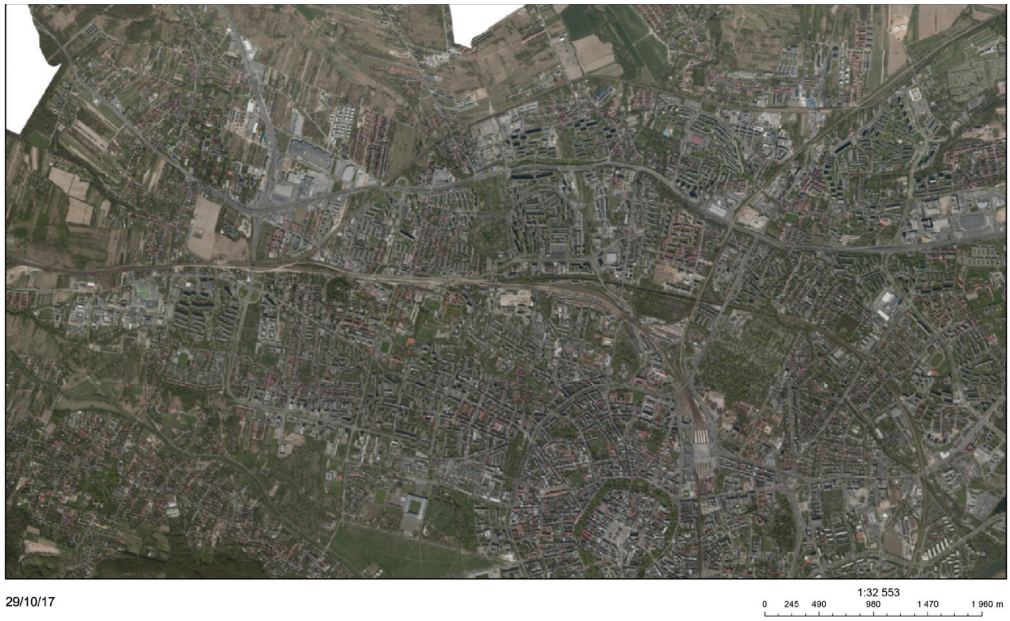

Fig. 6. Cracow, north-western part – fragment of an orthophotomap from the year 2015 (source: [75])

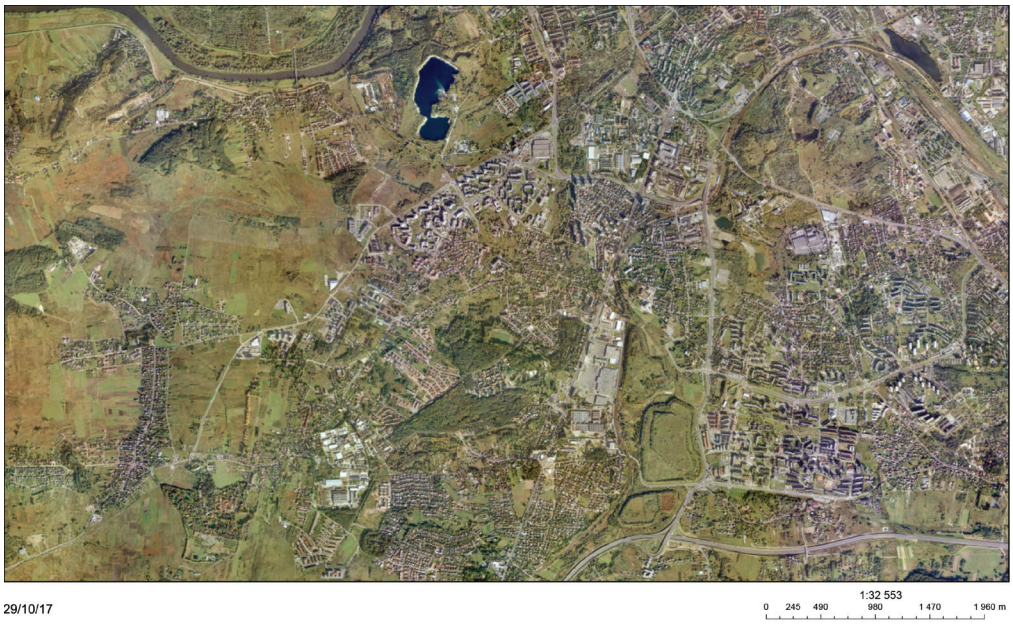

Fig. 7. Cracow, south-western part – fragment of an orthophotomap from the year 2004 (source: [75])

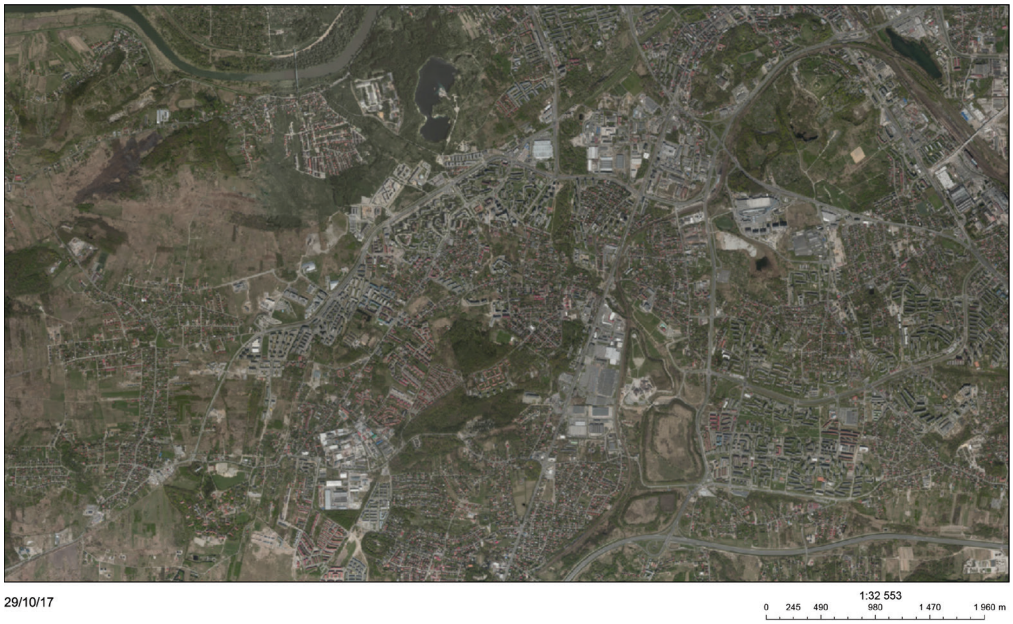

Fig. 8. Cracow, south-western part – fragment of an orthophotomap from the year 2015 (source: [75])




Fig. 9–12. Cracow, relics of rural and farm-type buildings in the context of Sienkiewicza, Wrocławska and Kijowska streets in the strict city centre (photo by M. Gyurkovich)

Fig. 13. Zarzecze street, currently also a central area of the city (the 6th district) – the preserved urban layout of a former village (photo by M. Gyurkovich)

Fig. 14. Cracow – Przegorzały. Prestigious villa district in the western part of the city at the foot of Las Wolski in the Sowiniec belt. The lack of common areas (sidewalk, composed greenery) and the Americanisation of the space of Cracow, making residents dependent on travelling by car (photo by M. Gyurkovich)

5. Summary

Quite interesting plans and projects that have the potential to change the city into one of the most important polycentric centres of the country seem to appear more and more often, proposed by the local administration of different levels[34]. Up until now, not many changes and projects of a metropolitan scale have been initiated. It is really hard to distinguish most of the declared local centres of the future metropolis from among the sprawled urban-rural fabric which surrounds the slightly more defined and composed central districts of Cracow. Even within the city's administrative borders one can still observe numerous areas featuring a sprawled, low-density structure[35]. Exurbanisation in Poland is founded on a completely different historical, social and economic basis than the one in North America or Western Europe [48]. The different spatial representation of sprawl is the result of the abovementioned situation. Administrative divisions and borders are imperceptible in space. Loosened, chaotic individual buildings mixed with new estates of detached and multifamily houses shape the landscape of the belt around the modern city, covering several dozen square kilometres[36].

The fall of the communist political system in Poland in 1989, combined with an increase in the possibility of building individual homes, has caused an increase in the number of houses within and around Cracow. At the same time, this process was not accompanied by any infrastructural projects on the municipal, metropolitan or regional scale, which can be observed on the examples of aerial photos from 2004 and 2015, that have been presented in the article, and which show parts of the modern urban fabric of Cracow. Situations like this are unusual in the abovementioned countries[37], where sprawl has appeared as one of the results of the growth of the traffic network. The Polish version of urban sprawl has more in common with the process of the creation of slums around the metropolises of Latin America, Africa or Asia, but the spatial effect and the developers of new buildings are entirely different [26]. This is mostly the result of the chaotic formation of new projects during the last three decades, in addition to contemporary attempts at creating a polycentric urban organism, that could compete with other, well organised ones, at the international level. Is such a spatial structure capable of evolving into the layout of a polycentric metropolis that has been declared for

---

34 See: *References*.

35 Unfortunately there seems to be, that there are no administrative policies against sprawl, on the contrary- more and more areas are changed from rural use or urban greenery to buit-up use. The above-mentioned Spatial Development Conditions and Directions Study of Cracow from 2014, which should be the basis for the local plans, secures vast areas for future housing use of different kind- many for single-family one. Altogether the surface devoted for housing areas in Cracow is already prepared to accommodate way much more of inhabitants, than the long-term demographic prognosis for entire region (see *Planning documents* [69, 70]). According to the demands of the land owners, those changes are constantly introduced in the uncoordinated local plans, which are still – by the way – not covering the 100% of the city limits [76].

36 Which has its justification in historical land ownership divisions that were typical of *Galicja* (the former Austrian partition) – see, for instance: [33].

37 Compare with US and situation in Portland [49].

years[38]? Is Cracow condemned to become an urban organism bereft of the principles known from the history of urban composition[39]? Will its metropolitan rank be preserved, despite its imperfect urban form? Can the dream of the Cracow Metropolis ever come true?

References

[1] Bajwoluk T., *Konflikty strukturalne w tkance miejskiej i podmiejskiej Krakowa*, [in:] Maciejewska A. (ed.), *Współczesne uwarunkowania gospodarowania przestrzenią – szanse i zagrożenia dla zrównoważonego rozwoju: proces inwestycyjny*, Oficyna Wydawnicza PW, Warszawa 2014.

[2] Bartkowicz B., *Przyczyny braku kompozycji i piękna w przeobrażeniach i rozwoju miast*, Teka KUiA PAN, Vol. XXXIII, Kraków 2001.

[3] Biedrzycka A. (ed.), *Nowa Huta. Architektura i twórcy miasta idealnego. Niezrealizowane projekty*, Muzeum Historyczne Miasta Krakowa, Kraków 2007.

[4] Biere Arenas R., Gyurkovich M. (eds.) *Back to the Sense of the City: 11th VCT International monograph book, Year 2016, July, Cracow*, CPSV, Barcelona 2016, www.upcommons.upc.edu/handle/2117/90350 (access: 09.03.20137).

[5] Bitner A., *Nowa metoda określania poziomu zurbanizowania obszaru na podstawie morfologii struktury podziału gruntu na działki*, [in:] *Infrastruktura i ekologia terenów wiejskich*, No. 3/2010, Polska Akademia Nauk, Oddział w Krakowie, Komisja Technicznej Infrastruktury Wsi.

[6] Blazy R., *Deformation of the City*, Technical Transactions 9/2017.

[7] Bogdanowski J., *Warownie i zieleń Twierdzy Kraków*, Wyd. Literackie, Kraków 1979.

[8] Bogdanowski J., *Metoda jednostek i wnętrz (JARK-WAK) architektoniczno-krajobrazowych w studiach i projektowaniu*, [in:] *Nowe idee i rozwój dziedziny architektury krajobrazu w Polsce*, III Forum Architektury Krajobrazu, materiały konferencyjne P. Wolski (ed.), Ośr. OZK, Warszawa 2000.

[9] Bojanowski K, *Strategia dla Krakowa – koncepcja rozwoju przestrzeni publicznych. Monolog o polskiej urbanistyce*, Wyd. PK, Kraków 2013.

[10] Böhm A., *O czynniku kompozycji w planowaniu przestrzeni*, Wyd. PK, Kraków 2016.

[11] Busquets J., *Urban compositions: City Design in the 21st Century*, [in:] Graafland A., Kavanaugh L.J. (eds.), *Crossover. Architecture, Urbanism, Technology*, 010 Publishers, Rotterdam 2006.

[12] Chmielewski J.M., *Teoria Urbanistyki*, Oficyna Wydawnicza Politechniki Warszawskiej, Warszawa 1996.

[13] Cullen G., *The Concise Townscape*, The Architectural Press, London 1986.

[14] *Encyklopedia Krakowa*, PWN, Warszawa–Kraków 2000.

[38] For instance in the concept of "Cracow of small towns" formulated in the plan of the city from the year 1988, developed by Z. Ziobrowski and his team. See [57, 58]

[39] See, for instance: [15, 27, 31, 40]

[15] Gyurkovich J., *Znaczenie form charakterystycznych dla kształtowania i percepcji przestrzeni. Wybrane zagadnienia kompozycji w architekturze i urbanistyce*, Monografia 258, Wyd. PK, Kraków 1999.
[16] Gyurkovich J., *The significance of contemporary transformations of urban areas for the global processes of urbanization*, Technical Transactions, 1-A/1/2012.
[17] Gyurkovich J., Matusik A., Suchoń F. (eds.), *Cracow: selected problems of the urban structure evolution*, Wyd. PK, Kraków 2016.
[18] Gyurkovich M., *In search of the urban composition of sub-centres in polycentric European metropolises*, [in:] ACE – Architecture, City and Environment / Arquitectura, Ciudad e Entorno No. 18, 2, February 2012.
[19] Gyurkovich M., *Transformations of public space in multifamily residential complexes in the western part of Cracow*, [in:] Gyurkovich M. (ed.), *Future of the city: mass housing estates or multifamily housing complexes?, Eco Rehab 3 Cracow 2012*, Cracow University of Technology, Cracow 2012.
[20] Gyurkovich M., Szarata A., Zuziak Z.K., *Model Przestrzennej Struktury Krakowa. Perspektywa planistyczna. Etap I – Założenia modelu strukturalnych zmian w zagospodarowaniu przestrzennym miasta Krakowa*, reaserch project prepared for the City Council of Cracow, Instytut Projektowania Urbanistycznego, Politechnika Krakowska, Kraków 2016.
[21] Gyurkovich M., Szarata A., Zuziak Z.K. et al., *Model Przestrzennej Struktury Krakowa. Perspektwa planistyczna. Etap II – Zdefiniowanie modelu przestrzennej struktury Krakowa*, reaserch project prepared for the City Council of Cracow, Instytut Projektowania Urbanistycznego, Politechnika Krakowska, Kraków 2017.
[22] Gzell S., Wośko-Czerankowska A., Majewska A., Świeżawska K., *Miasto zwarte. Problem terenów granicznych*, Międzyuczelniane Zeszyty Naukowe, Urbanistyka, Akapit-DTP, Warszawa 2011.
[23] Harvey D., *Bunt miast. Prawo do miasta i miejska rewolucja*, Fundacja Nowej Kultury Bęc Zmiana, Warszawa 2012.
[24] Hodor K., *Urban parks and their value: Cracow Examples*, Technical Transactions, 1-A/2016.
[25] Hrabiec A., Ziobro A., Baran S., *Reflection about the Future of Cracow Metropolis*, Space & Form No. 17/2012.
[26] Kajdanek K., *Suburbanizacja po polsku*, Nomos, Kraków 2012.
[27] Kantarek A.A., *O orientacji w przestrzeni miasta*, Monografia 368, Wyd. PK, Kraków 2008.
[28] Kantarek A.A., *Urban form and orientation in urban space*, [in:] Oliveira V. et al., *ISUF: Our Common Future in Urban Morphology*, Vol. 2, ISUF2014: 21st International Seminar on Urban Form, Porto, Portugal, www.isuf2014.fe.up.pt/ISUF2014%20ebook.pdf (access: 05.08.2017).
[29] Kantarek A.A., *Morfologia i typologia formy urbanistycznej*, [in:] Kantarek A.A., Gyurkovich J. (eds.), *Wyznaczniki kształtu współczesnej przestrzeni urbanistycznej*, Wyd. PK, Kraków 2015.
[30] Kochanowski M., Lorens P. (eds.), *Miasto – wspólne dobro i zbiorowy obowiązek*, Materiały I Kongresu Urbanistyki Polskiej, BU 2, Urbanista, Warszawa 2004.

[31] Kosiński W., *Paradigm of the City of the 21st Century. Between the Past of the Polis and the Future of the Metropolis*, Wyd. PK, Kraków 2016.
[32] Kowicki M., *Patologie/wyzwania architektoniczno-planistyczne we wsi małopolskiej studium na tle tendencji krajowych i europejskich*, Wyd. PK, Kraków 2010.
[33] Kowicki M., *Rozproszenie zabudowy na obszarach Małopolski a kryzys kreatywności opracowań planistyczno-przestrzennych*, Wyd. PK, Kraków 2014.
[34] Lynch K., *Good City Form*, The MIT Press., Cambridge Mass., London 1984.
[35] Lynch K., *The Image of the City*, The MIT Press., Cambridge Mass., 1960.
[36] Majda T, Mironowicz I. (eds.), *Manifesty urbanistyczne*, BU 15, TUP, Warszawa 2017.
[37] Mełges H. *Architectural transitory zone between city and village (based on chosen examples Kraków–Śląsk agglomeration)*, Technical Transactions, 1-A/2007.
[38] Motak M., *Historia rozwoju urbanistycznego Krakowa w zarysie*, Wyd. PK, Kraków 2012.
[39] Mydel R., *Rozwój urbanistyczny miasta Krakowa po drugiej wojnie światowej*, Secesja, Kraków 1994.
[40] Paszkowski Z., *Miasto idealne w perspektywie europejskiej i jego związki z urbanistyką*, Universitas, Kraków 2011.
[41] Podhalański B.M., *Building polycentricity of the Metropolitan Region of Kraków and Katowice*, Technical Transactions, 5-A/2008.
[42] Podhalański B.M., *Integrowanie przestrzeni metropolitalnych*, Monografia 443, Wyd. PK, Kraków 2013.
[43] Purchla J., *Jak powstał nowoczesny Kraków*, Wyd. Literackie, Kraków 1990.
[44] Purchla J., *Kraków w Europie Środka*, BOSZ, Olszanica, Kraków 2008.
[45] Salingaros N., *Eight City Types and their Interactions. The "Eight-Fold" Model*, Technical Transactions, 2/2017.
[46] Samuels I., Panerai P., Castex J., Depaule J.Ch., *Urban Forms. The Death and Life of the Urban Block*, Architectural Press, Oxford, Burlington 2005.
[47] Seibert K., *Plan Wielkiego Krakowa*, Wyd. Literackie, Kraków 1983.
[48] Sotoca Garcia A., Massuet Villamajó M., *The next city: low density territories in the metropolitan area of Barcelona*, Technical Transactions, 1-A2/2012.
[49] Sotoca A., *Lessons from the world: Urban growth in the USA: from tracing boundaries to complex management: the Metro Portland case study*, GRU Urbanism Reasearch Group 2014, http://urbact.eu/fileadmin/Projects/USE_ACT/documents_media/USEAct_III_report_ISTANBUL.pdf
[50] Sudjic D., *Język miast*, Karakter, Kraków 2017.
[51] *ULAR 5 – Urban Landscape Renewal- Between City and Non-City, proceedings of Scientific Conference*, Sulimowska-Ociepka A. et. al. (eds.), Silesian University of Technology, Faculty of Architecture, Gliwice 2010.
[52] *Urban Agenda for the EU 'Pact of Amsterdam'*, Agreed at the Informal Meeting of EU Ministers Responsible for Urban Matters on 30 May 2016 in Amsterdam, The Netherlands.
[53] *Urban Sprawl in Europe, The ignored challenge*, European Commission, Directorate-General, Joint Research Centre, European Environment Agency, EEA REPORT, No. 10/2006.

[54] Wejchert K., *Elementy kompozycji urbanistycznej*, Arkady, Warszawa 1974.
[55] Węcławowicz-Bilska E., *Directions of contemporary, spatial development of European cities*, Technical Transactions, 3-A/2011.
[56] Węcławowicz-Bilska E. et al. (eds.), *Skuteczność planów zagospodarowania przestrzennego. Potrzeby i możliwości*, materiały międzynarodowej konferencji naukowej, Instytut Projektowania Miast i Regionów, Wydział Architektury PK, Kraków 2004.
[57] Ziobro A.B, *Model interpretation of the metropolitan spatial structure in development plans of the Cracow and its region. Period 1960–2010*, doctoral thesis, Faculty of Architecture, CUT, Cracow 2014.
[58] Ziobrowski Z., *Urbanistyczne wymiary miast*, IRM, Kraków 2012.
[59] Zipser T., *Prediction of states, modelling of processes and building the decision*, Architectus, No. 3(47)/2016.
[60] Zuziak Z.K, *Sterowanie procesami suburbanizacji w obszarze wzajemnych oddziaływań Katowic i Krakowa – spojrzenie z Krakowa*, Czasopismo Techniczne, 15/2005.
[61] Zuziak Z.K., O tożsamości urbanistyki, Wyd. PK, Kraków 2008.
[62] [Zuziak, Z.K., *Metropolitan form and sustainable mobility*, Technical Transactions, 1-A/2010.
[63] Zuziak Z.K., *Urban structures and metropolitan planning*, [in:] Węcławowicz-Bilska E. (ed.), *New ideas in planning for territorial development*, Vol. 2, *The problems of metropolitan areas and big cities: collective work*, Monografia 546, Wyd. PK., Kraków 2017.
[64] Plan ogólny Krakowa (1967 r.), opracowany pod kier. Stanisława Hagera.
[65] Plan Ogólny Krakowskiego Zespołu Miejskiego (1977), opracowany pod kier. Krystiana Seiberta.
[66] Miejscowy Plan Ogólny Zagospodarowania Przestrzennego Miasta Krakowa (1988), opracowany pod kier. Zygmunta Ziobrowskiego.
[67] Miejscowy Plan Ogólny Zagospodarowania Przestrzennego Miasta Krakowa (1994), opracowany pod kier. Zygmunta Ziobrowskiego.
[68] Studium Uwarunkowań i Kierunków Zagospodarowania Przestrzennego (2003), opracowane pod kier. Roberta Kuzianika.
[69] *Zmiana Studium Uwarunkowań i Kierunków Zagospodarowania Przestrzennego Miasta Krakowa, t. I–III*, załącznik do Uchwały nr CXII/1700/14 Rady Miasta Krakowa z 9 lipca 2014 r., Biuro Planowania Przestrzennego UM Krakowa, Kraków 2014.
[70] *Strategia Rozwoju Województwa Małopolskiego Na Lata 2011–2020*, przyjęta Uchwałą Nr XII/183/11 Sejmiku Województwa Małopolskiego z dnia 26 września 2011 r., s. 37, 111, 127.
[71] www.stat.gov.pl/statystyka-miedzynarodowa/porownania-miedzynarodowe/tablice-o-krajach-wedlug-tematow/terytorium-i-ludnosc (access: 5.06.2017).
[72] www.Cracow.pl/biznes/1140,artykul,liczby_o_Cracowie.html (access: 5.06.2017).
[73] www.encyklopedia.pwn.pl (access: 5.06.2017).
[74] www.unesco.org (access: 02.05.2017).
[75] City Spatial Information System, http://msip.um.krakow.pl/obserwatorium (access: 29.10.2017).
[76] http://obserwatorium.um.krakow.pl (access: 06.11.2017).

TECHNICAL TRANSACTIONS 2/2018
ARCHITECTURE AND URBAN PLANNING
DOI: 10.4467/2353737XCT.18.018.7991
SUBMISSION OF THE FINAL VERSION: 11/1/2018

Anna Bijak (annabijak@yahoo.com)
Kinga Racoń-Leja (krleja@pk.edu.pl)
Institute of Urban Design, Faculty of Architecture, Cracow University of Technology

Political aspects of Tempelhof Field

Polityczne aspekty parku Tempelhof

Abstract

Tempelhof Field, one of the most interesting parks in the ever-changing city of Berlin, is not only an attractive, green, open space, but also an example of complex history entangled with the present political conflicts. Formerly, a symbol of Nazi megalomania, a forgotten site of terror, a witness of the heroic Berlin Airlift, an unprecedented example of a modern civil protest against rapid development and recently serving as the biggest refugee camp in Germany – Tempelhof continuously stirs controversy. In an attempt to understand the intricate situation and provide new solutions, the article presents the forgotten history of Tempelhof as well as analyses its significance for the city of Berlin.

Keywords: Tempelhof, Berlin, architecture and politics, urban history, city and film

Streszczenie

Jeden z najbardziej interesujących parków w Berlinie – Tempelhof jest nie tylko atrakcyjną zieloną przestrzenią, ale również przykładem złożonej historii odzwierciedlającej aktualne konflikty polityczne. Kiedyś symbol nazistowskiej megalomanii, zapomniane miejsce tragedii wielu ludzi, świadek bohaterskich działań alianckich pilotów podczas Blokady Berlina, niezwykły przykład współczesnego protestu obywatelskiego przeciwko nowej zabudowie deweloperskiej, a całkiem niedawno – największy obóz dla uchodźców w Niemczech. Tempelhof ciągle wzbudza kontrowersje. Aby zrozumieć skomplikowaną sytuację polityczną i znaleźć nowe rozwiązania dla tak trudnego miejsca, artykuł prezentuje zapomnianą historię Tempelhof oraz rolę, jaką odgrywa w Berlinie.

Słowa kluczowe: Tempelhof, Berlin, architektura i polityka, historia urbanistyki, miasto i film

1. Intricate history

Berlin is a significant city in Europe, home to almost 3.5 million people [10]. It is not the size, however, but the rich history, which makes Berlin a one-of a kind place in the world. No other city was divided for almost half a century with a wall. No other city was so profoundly the focus of the Nazi regime and the Second World War. Berlin was basically a representative of politics and cultural changes in the 20th century. "Paris is always Paris and Berlin is never Berlin", said Jack Lang, former French Culture Minister [31]. Paris is grounded in its history, but Berlin is constantly changing. Berlin is a city, which opens up an art gallery made out of graffiti next to a bustling street. Berlin is a city where a 2.5 by 2 km piece of land is fiercely protected and cannot be developed. This place is Tempelhof Field, a park in the centre of Berlin, a place with rich and difficult history.

Fig. 1. View of Tempelhof along the Germania axis, around 1948
(source: National Museum of the U.S. Air Force)

Tempelhof was first mentioned in a document from 1247 as it was established as a unit of the Knights Templar. Nowadays, it refers both to the previous airport and to the borough in Berlin. As the Order of Temple was abolished, the site was sold to the city of Berlin in 1435. In the early 19th century, Tempelhof was a village and a place for family excursions for Berliners. It also served as a military site for Prussian forces, dating from 1720 to 1914.

The first Tempelhof Airport was established on 8th October 1923. Its origins are associated with the Deutsche Luft Hansa company establishment in 1926. The first terminal at that place was constructed in 1927 and became one of the most important in Europe. At the beginning, while aviation was still in its infancy, the terminal was no more than a shed. Later on, it became a complex of a couple of buildings, which presently would be located in the northern-central part of the airfield. However, in 1934, due to Albert Speer's plan of Germania, the terminal was replaced with a new building, resembling in its form "an eagle". Since, in Hitler's plans, Berlin

was meant to be "Weltstadt" – a "world capital", then the shape of terminal had to evoke the intention of Berlin airport to become a gateway to Europe. Tempelhof was supposed to become a European *"Flugkreuz"*, a dominant flight crossing of the continent [13, pp. 112–114]. The size of the terminal reflected the scale of the whole Germania plan, a part of which was only realised. Had Speer's and Hitler's vision been realised, Berlin would have been transformed without recognition. That would include erasing around 50.000 buildings along with the Brandenburg Gate and the Reichstag [11]. The plan centred around two extensive north-south and east-west axes. The most important building, the Great Hall, set on the redirected river Spree, was inspired by Pantheon. It was to be covered by the biggest dome in the world. The plan also featured underground complexes of tunnels planned underneath Tiergarten and in other places around the city. The tunnels below the airport fields were supposed to house highways and railway tracks [45]. The terminal of Tempelhof was also designed with extensive underground structures. Sir Norman Foster called the terminal the "mother of all airports" [29]. Its advantageous location, with proper connectivity to the city centre, made it a busy airport during the first years. The striking structure is still considered as huge. Even though the building was not finished, it still appeared impressive, with an immense concrete skeleton covered with heavy natural stone [1]. Many innovative features were introduced in the design of the terminal, including separate levels for baggage and people. Around 80% of works on the airport have been finished [37].

What is usually left out in the history of Tempelhof is that the area served as one of the first experimental concentration camps. The Columbia Concentration Camp was established in 1933. Its name refers to one of the breaking-record longest flights landing in Tempelhof by Columbia airplane [1]. It was a scary training ground for what would become one of the biggest atrocities of all time. Many of the chiefs of Columbia would later become the chiefs of other big concentration camps. The majority of its 8000 prisoners were men, predominantly political prisoners, communists and intellectuals. Half of them were homosexuals [41]. In 1936, Columbia's inmates were moved to Sachsenhausen. The buildings of the camp are no longer standing, since they were demolished in 1938; however, the outlines of some of the structures are still visible [41]. Little public attention was given to the camp. The only commemorating sign of its historical presence is a steel sculpture. The monument is located on the other side of the street than the terminal, which, in terms of historical accuracy, should actually be opposite. There is a group of citizens concerned with the necessity of commemorating the place, who propose the creation of a memorial and information centre regarding the former Columbia Concentration Camp [41] (Fig. 2).

What seems interesting is that Tempelhof was not bombed during II WW, since the Allied Forces saw an opportunity to use the terminal after the war. Also, for the Luftwaffe, Tempelhof was not a military airfield. The airport was used mainly for assembling planes, with the use of forced labour. The planes were manufactured in underground tunnels and sent directly to the runways or transported by train. Many of the workers were of east European origin. They lived in miserable conditions, in barracks placed north of the terminal [39].

But this was not the end of the atrocities within the area of Tempelhof. Between 1942 and 1945, another labour camp was placed there, close to the Neukölln cemetery. It was run

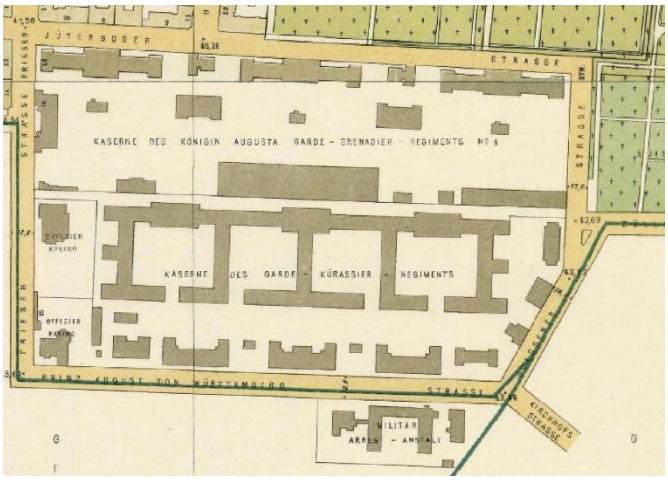

Fig. 2. Map showing the location of the Columbia Concentration Camp (source: *City Map of 1895*, Verlag Julius Straube)

by the Protestant church. Around 200 east European prisoners, marked with "Ost" patches, together with some German workers, were forced to work and live there in scary conditions. Their task was to dig graves in cemeteries around the city [3].

The Soviets took over Tempelhof in April 1945. The Yalta Agreement turned the terminal over to the U.S. Army. In August 1945, the Potsdam Agreement formally divided Berlin. The meaning of the airport grew immensely in 1948 with the beginning of the Berlin Blockade. The Soviets ceased all car and water access to the city. The only supply could be provided by air, using one of the three air corridors – coming from Hamburg, Frankfurt (Main) and Bückeburg. There were two options left for the Western forces – either to leave the city without the help, which would mean practically to abandon it, or to supply 2.5 million people with food from the air. Happily, they chose the latter. The "Berlin Airlift", as it was called, started in June 1948. Because of expanding requirements, new 1800-meter asphalt runways were built in September 1948.

People often stood by the fences of Tempelhof and watched arriving planes. Some of them were children. The airport also became the site of the famous "Candy Droppers", first of whom was Gail Halvorsen, an American pilot. He once took a walk to the children who gathered to ask about the aircraft. The pilot gave them candies and promised that he would come the next day. Soon, it became a custom for American pilots to drop small parachutes filled with candies to kids. The fact became widely renowned when children from West Germany sent their own candies and even major manufactures followed through. Finally, it became not only a touching custom, but also a big propaganda success, as it was even officially named "Operation Little Vittles". The last transport touched down on the ground on 30th September 1949. The Airlift was celebrated by changing the name of the U-Bahn to Platz der Luftbrücke. The monument, with the names of the pilots who died during the airlift engraved on the stone, is standing to this day on the plaza next to the terminal. Tempelhof became a legend and a hero of the city – a symbol of the resistance towards communism in Berlin [25].

Before 1951, Tempelhof was fully controlled by the American military. Later, it was taken over by civil transport and controlled only in part by military forces [37]. The American forces were deactivated in 1994. In 1996, it was announced that, in the upcoming years, all domestic and international air traffic would be slowly redirected to the Berlin-Schönefeld International Airport. The plan also ensured the closing of other two airports – first, Tempelhof, and then, Tegel. The final decision was confirmed in 2007; however, it faced some backlash. In 2008, a referendum opposing these decisions was carried out. The protest did not gain enough votes and the decision to close-off Tempelhof remained. Finally, the Tempelhof Airport was closed on the midnight of 30th October 2008.

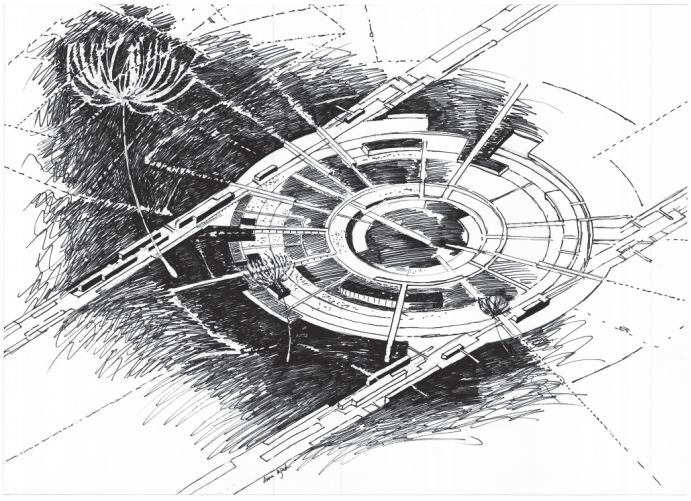

Fig. 3. Freehand drawing, part of "Urban Therapy – Tempelhof Hoffnung" – diploma project by Anna Bijak, promoter: M. Gyurkovich, co-promoter: K. Racoń-Leja [6]

Interestingly, up until today, Tempelhof has been the setting for some of the most interesting or absurd conspiracy theories, including "alien hotspot and sacred pagan ground", which means that this place exists in the common consciousness as a mysterious site. Some believe that the tower, built by the USA next to the northern edge of the terminal, is a transmitter of low-frequency waves used to test the possibility of brainwashing the population of Berlin and cause illnesses [46]. Tempelhof is also featured in a famous conspiracy theory that Hitler did not die in the bunker, but escaped to Argentina. Some also believe that he fled to Antarctica, where he set up a base with aliens. These theories are based on the assumption that a secret tunnel existed in between U6 metro line and Tempelhof airport.

The Tempelhof Terminal has, in fact, many secrets buried in the underground. There are three underground levels placed underneath the massive structure. The hidden parts contain around 300 air raid shelters, with paintings that still remain untouched after 70 years [40], as well as bunkers [16]. The lowest level was taken over by the storage of photographs, accidentally burnt by the Soviets. Also, some of the bunkers were burnt by Nazi troops, when their commander killed himself.

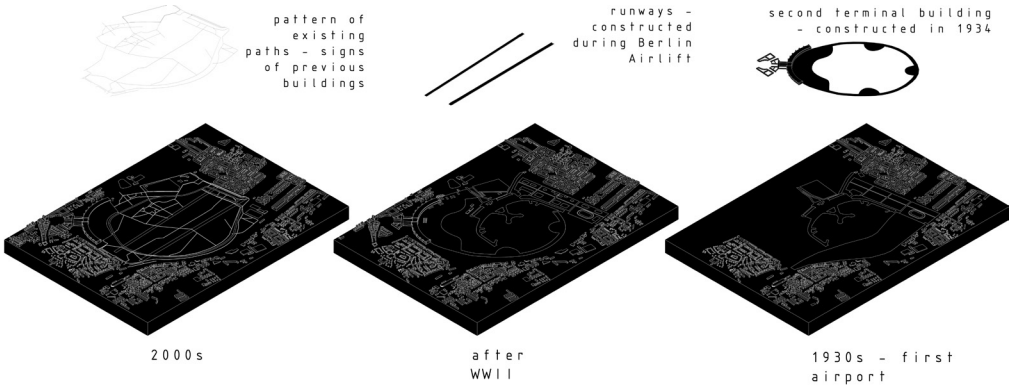

Fig. 4. Historical layers of Tempelhof; part of "Urban Therapy – Tempelhof Hoffnung" – diploma project by Anna Bijak, promoter: M. Gyurkovich, co-promoter: K. Racoń-Leja [6]

2. In the search for new ideas

It seems that the area of Tempelhof is an architect's *dream-come-true*. The huge area is filled with absolutely nothing, ready to be touched by the *hand of a master-architect*. It is just waiting for new ideas, a *carte blanche,* which can be filled with anything possible. At least that is what it seems at first glance. But what about its rich history and cultural connotations?

The competition shortlisted in 2009 has been a source for the new development strategy. Tempelhof has sparked major international interest in the architectural community; many designers have issued their proposals. The selected winning competition entry, a cooperation

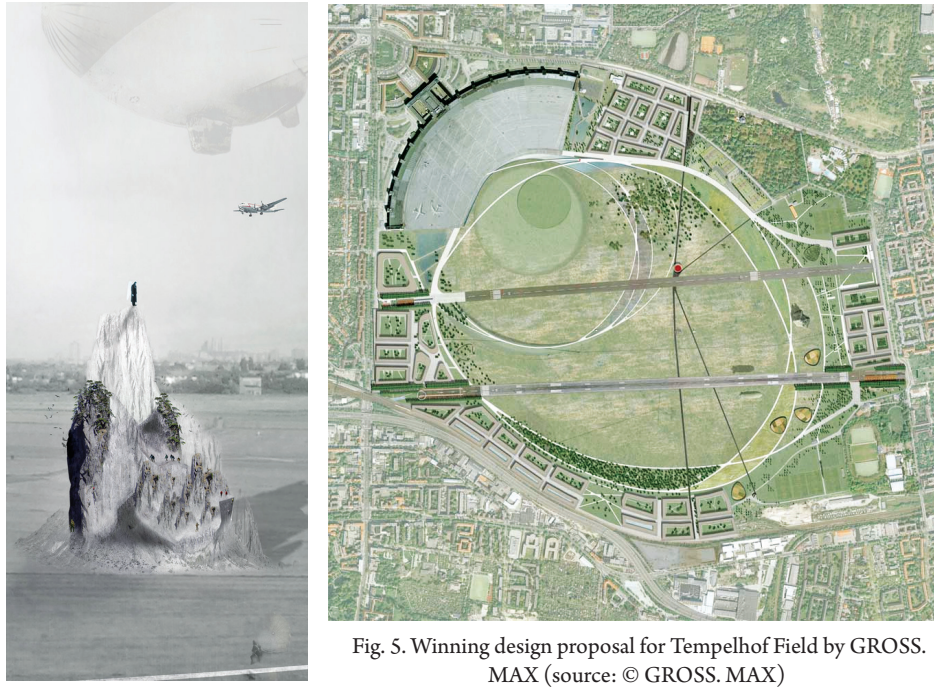

Fig. 5. Winning design proposal for Tempelhof Field by GROSS. MAX (source: © GROSS. MAX)

between three groups, has been awarded with partly commission to design the park as well as redesign the terminal [26], which ultimately did not happen. The landscape architecture was proposed by GROSS.MAX with Sutherland Hussey Architects. Chora was responsible for the architecture and urbanism. Happold office introduced sustainable technologies and infrastructure [26] (Fig. 5).

The proposal included a development in form of city blocks around the circle enclosing the green space. Various circular paths have been created. The circular building of the library stood in a strangely chosen point at the intersection of random paths. What seemed the most interesting part of the solution was the rock monument standing in the eastern part of the site. Illustrated with the inspiration from Wim Wenders' "Wings of Desire", it provided a symbolical meaning; however, with a rather pointlessly chosen location. This proposal did not seem to be providing very clear ideas; it was considered as an organic merger of different programs.

Fig. 6. "The Berg" by Jacob Tigges, one of the competition entries for Tempelhof Field (© THE BERG BY MILA/JAKOB TIGGES)

Another design, probably the most outlandish of all, was "The Berg", a "provocative, but not constructive" [27] idea of a phantom mountain designed by Jakob Tigges. The author stated: "I chose the idea of a mountain precisely because it can't be done. Instead it'll awaken people's imaginations" [8] Tigges' proposal was a manifest, which highlighted the dangers of the policy undertaken by the city years ago. In his project, Tigges warned that, by implementing a typical development logic, the city was risking destroying one of the most important landmarks of Berlin. He stated: "We can't lose this site that's got so much cultural and symbolic meaning just for more of the same old, mediocre housing development" [8], highlighting the cultural and historical importance of Tempelhof. It must have worked, along with the protests of the inhabitants of the city, since nothing has been built in Tempelhof and nothing would be. Tempelhof would remain one of the most intriguing parks in Berlin (Fig. 6).

After the competition, new proposals were still being created by students and architects alike. Probably the most interesting idea for developing Tempelhof is a conceptual design *Tempelhof Lu(f/s)twerks*, by Jack Holmes, graduate of Bartlett School of Architecture in London. The idea is presented by interventions transforming Tempelhof into a "landscape of a sublime" [21]. Taking advantage of the soil conditions in Berlin, the site is transformed into a wetland, with many bridges as well as hydro- and wind-powering machines. The strong composition of the site, flying elements as well as the symbolical aspect – connection between heaven and underground – elevate it into a site of sublimity. Of course, one can debate the shapes and axes as well as the strongly implied sci-fi inspirations. It seems that some of these elements may be a little out-of-place, but it is a strong concept, which explores new areas and, as one of the few, provides a strong and specific cultural narrative for this site, avoiding to sentimentally tackle the site as a monument (Fig. 7).

Fig. 7. *Tempelhof Lu(f/s)twerks* by Jack Holmes (© J. Holmes, Motionpicturesque)

A concept by Eleonora Viviani implies new public transport solutions adjacent to the Tempelhof area. She proposes adding a U-Bahn line to connect Berlin Mitte and Berlin-Schönefeld Airport with Tempelhof, and building a new S-Bahn station right in the southern edge of the area [42]. However, it is not only about changing the existing patterns, but also creating new ones. The reworked public transportation system is tied together by means of a new mobility ring created in Tempelhof. The ring has a common interchangeable node with the new U-Bahn Line. It connects with a new S-Bahn station as well. The ring is comprised of two elevated bridges, one for pedestrians and another one intended to be used by a light train. In this way, the Tempelhof area becomes more accessible.

Another proposal, which, even though it was part of the competition, seemed to be more forward-thinking than the 2009 entries. It was based on a flexible system of paths, which were cutting through the space on two levels, creating different functions. The project of by Studio SPTA reflected the future of cities, which, due to the lack of space, would have to be developed on several levels in order to sustain their needs [38]. The proposed park consisted of two levels. The upper level was devoted to a park; the lower one was devoted to various activities. The northern runway placed underground was designed as a space used for different functions, serving as a linkage between east and west. The southern runway was filled with water and served as a recreational space. The main goal was to create a lively space, which could be flexible [38]. The preliminary, very good idea of splitting Tempelhof into two levels was diminished by implementing too many elements (Fig. 8).

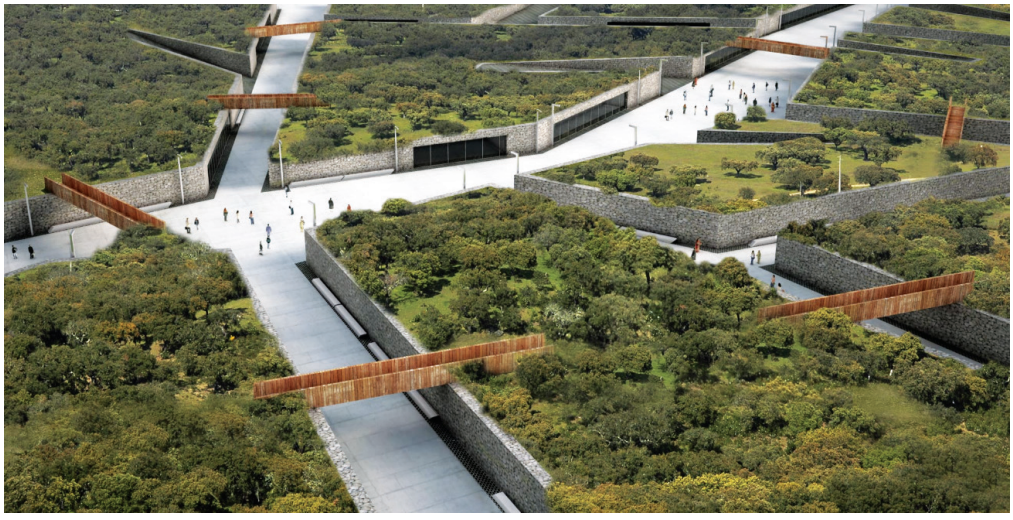

Fig. 8. Studio SPTA's competition entry for Tempelhof Field (©Studio SPTA)

As for the concepts regarding the existing terminal building of the former airport, most of the projects propose to use the space for various functions, such as start-ups, recording studios, film studios and offices. What links all of those designs together is that they never introduce any kind of change in the terminal in a formal sense. They allow for the introduction of new functions inside. These very minor interventions seem understandable, due to the

protected nature of the building. However, the reworking of a monument alike could, in this case, include some kind of an extension or superstructure, done both in a tasteful and also a symbolical way. New interventions should provide some sort of a dialogue with the building, taking into account its historical connotations.

3. Facing present conflicts

Tempelhof Field, the largest park in Berlin, has been established in May 2010. There are also other known names for this space, such as Tempelhof Freiheit – Tempelhof Freedom, referring to the Berlin Airlift as well as to the new function of the place, which is a refuge from the city's noise and traffic [15]. Some have expressed their discontent with the new name because, in the past, Tempelhof was not a place of freedom; quite the contrary. Berlin History Workshop [4], a non-profit organisation started in 1981, states that the usage of the word "Freedom" implies the neglect of Berliners to address and remember the history of the place. The organisation tries to commemorate the past of Tempelhof with the booklet *No place of freedom – Tempelhof Feld 1933–1945* as well as with different initiatives attempting to save the memory of the history of the place [22].

The park has been at risk of privatisation in 2014 due to the investors, who cooperated with the city of Berlin, and saw it as a space with huge potential for development. However, by referendum, Berliners supported the local citizens' initiative *100 percent Tempelhofer Feld*, and voted to keep Tempelhof solely as a green space [15]. The strategy of development has already been stated during the 2011 elections, with the project of Klaus Wowereit. The plan implied the usage of only 25% of the site for buildings, which, by the way, covers an area roughly of the size of New York's Central Park [36]. The planned housing was supposed to be an affordable option, highly desirable in a city like Berlin, which suffers from huge apartment shortages. But some critics had voiced their doubts about the purity of the intentions. "This government hasn't built a single social apartment for 10 years – are they going to start right when park-side real estate opens up?", said John Riceburg for Exberliner Magazine [15].

The situation was quite unique. Had it been in London, this huge area in a close proximity to the city centre, with an enormous market potential, would already be filled with apartments. But, in Berlin, Tempelhof Field was left as a completely green space due to the willingness of the inhabitants. If the city developed the space as it was planned, even with only 25% of the area filled with buildings, the character of the space would change forever. With new glitzy commercial buildings and developer housing, more boundaries would have to be marked. The space would no longer be public anymore, it would be a subject of private demands. The accessibility to greenery would be filtered. Like in New York, where the prices of apartments located by the Central Park are skyrocketing, similar situation would apply here. It would have to be a more polished, "classy" space. And sooner or later, it would be gentrified, which is not the case, as how revitalisation is done in Berlin. Even though there were a lot of spaces rebuilt as glamorous urban squares, like Potsdamer Platz, the city has built its legend on the raw charm of post-industrial buildings, now remade into hip bars, restaurants and hotels. Berlin

is the *hip capital* of Europe and this is due to filling gaps and reusing them in a creative and edgy way. It is not a *ready-made* city. Berlin is quickly growing and re-living itself after the reunification and it cherishes the process rather than the destination. Ulf Poschardt, editor of "Die Welt", claimed: "In the Prussian capital, hippie culture is state policy" [15].

Furthermore, Berlin is one of the greenest and environment-friendly cities in Europe. The number of bikers is constantly on the rise; closed zones for cars were first introduced here. And it is only suitable to look at the map of Tempelhof-Schönefeld to see how much the German people love allotment gardens, to understand their approach to green spaces. Also, many shortlisted birds and insects are occupying the area of Tempelhof.

After the incident with the failed plan, a careful policy route has been undertaken. The Tempelhof Conservation Act has been established, with the main presumption that no buildings are allowed to be built anywhere in Tempelhof. Only limited construction is permitted [15]. The growth of new trees is carefully controlled, with the restriction to not even replace the dead ones, and so is even putting new park benches. Participation has become very important for Tempelhof Field in the recent years. Raumlabor is a group of architects who pioneered this approach towards the park. They implemented small test facilities in different areas of the Field. They involved, e.g. Jupipark in Neukölln, which became a meeting point to organise discussions about affordable housing and different issues [2]. By using these facilities and social participation, the architects wanted to test what kind of functions were needed in this place and, most of all, how Berliners envision the regeneration of Tempelhof. The inhabitants of Berlin were also asked for their ideas in 2008, presented within "Tempelhof First Steps". Many of the ideas were very creative, including the "tallest building in the world, a zoo, a mosque, treehouses, a lake, casino, baseball, gardens, lake, mountain, funfair…" [34].

Since 2008, Tempelhof has been the site of various public events, involving music festivals or sporting events like marathons. The terminal served as a backdrop for fashion shows, product launches and fairs. Tempelhof Field is used on a daily basis for various activities, including biking, running and skateboarding. There are many smaller events (such as barbecues) organised in spontaneous open allotment gardens established in the Hippie Garden. It is hard to deny their charm: "(...) the allotments are often adorned with old couches for gardeners to entertain visitors; others have no gardens but bring their couches anyway. Beer is usually involved" [15]. It goes to show how much Berliners appreciate this sort of freedom, spontaneity and messiness that comes with reclaimed sites.

But the issue of the development of Tempelhof Field remains, and it is now even more plausible than in 2010–2011. There is a desperate need for affordable housing in Berlin in the wake of the refugee crisis. In 2015, Tempelhof Terminal has become the biggest open emergency refugee shelter in Germany. Around 6400 people lived there in one space at that time. There were problems with access to toilets and showers, since the terminal was not equipped with water plunges and canalisation to accommodate such a huge number of people. Most of the time, in order to take a shower, they had to be transported to the swimming pool. In this particular situation, it was difficult to avoid diseases. Also, due to the fact that, at the beginning, there was only one doctor per 2500 people [35]. The other issue was the lack of psychological care, necessary for deeply traumatised people. Refugees could not sleep, had no

privacy and sometimes were also visited by intruders. The very few social workers were not able to keep track of everything. Obviously, in such difficult conditions, conflicts occurred. Refugees' living conditions were miserable and could not promise them a change – simply because of a lack of any affordable housing in the city. According to humanitarian regulations, refugees can be put through these conditions for no longer than two weeks. The situation with the refugees in Germany got so complicated in the meantime that, since 2015, around 1000 of them still have not been relocated and are living in the terminal [12].

What also seemed difficult was that the totalitarian architecture of the terminal could not be altered, apart from having cubicles put inside. Some residents have tried to reshape their living spaces inside anyway, by introducing more colour and providing some sense of privacy and domesticity. At some point, refugees started to put graffiti on the walls of cubicles, which seemed an interesting and sometimes artful attempt of claiming their space. But after some controversial and offensive remarks, the authorities had to order to erase all the paintings. With the heavily scrutinised Tempelhof, where even a small fight in November 2015 has been hugely publicised and politicised, Berlin has been extremely careful not to make the already difficult situation any worse [30], which seemed a pity, because the only attempt at having a dialogue of cultures had to be silenced.

The organisation called "100% Tempelhofer Feld" came up with a proposal to tackle the issue head-on – providing refugees with buildings containing necessary functions and some housing. All of them would be located near the terminal, in a space previously used for events [5]. The main problem was that it was only a temporary proposal, which did not contribute to the plans of the city. The city could not say "we will see" what happens later, because a certain amount of money needed to be invested. And the city would already lose a lot of money due to the cancellation of many major events, for which Tempelhof was the perfect space. However, most of all, the city could not allow to form a ghetto at the space. The prolonged isolation of people would lead to far more serious problems later, which Paris learnt the hard way. It seems, however, that the city overlooked these problems, since it was announced that a similar plan will be undertaken. The construction of 976 temporary prefabricated homes in the area near terminal has already started. The resettlement of residents from Tempelhof altogether is planned in 2019, when the prefabricated houses will be removed [12].

A completely different proposal has been put forward by a former urban planner of Berlin, Bernhard Strecker. In his opinion, Tempelhof should be incorporated into the city tissue and provided with mixed functions of housing, work, recreation, schools etc. But most of all, in his project, Tempelhof becomes an international centre, which would mix people from different backgrounds, also including refugees [5]. From the political point of view, the proposal seems perfect. On the other side, it reinforces the urge to develop the whole site, leaving only the north part of the Fields as a green park, bordering with Volkspark Hasenheide. The proposal rose a very difficult question – is the location of a refugee camp at Tempelhof an excuse for developers to build apartments? [30] This lack of trust should not be surprising considering how easy it was for the city back in 2010 to assume that Berliners will allow for the development to happen.

Finally, Tempelhof is not a regular site in the city. It was already highly controversial before. As T. Parsloe writes: "The decision to use the airport as a camp merely intensified

the complexity of its associations. It now simultaneously acts as an international symbol of totalitarian megalomania and trauma, humanitarian intervention, and cold war propaganda, and is a cinematic icon" [30]. This comment seems very adequate. Maybe it is not good to demand one simple narrative for a piece of history; however, such a politicised site is probably not the best place to house refugees.

It is extremely difficult to build a proper narration for Tempelhof, which would respect all of the aspects of this space. On the other hand, it seems that there is not much willingness from the city to build such a dialog. The issue is approached mostly from the functional and the financial point of view. The authorities choose not to touch the subject of the troubled and ambiguous past, and problems arise.

4. Urban Therapy – "Tempelhof Hoffnung" [6]

The name of this chapter refers to the master thesis project of A. Bijak [6]. The most defining quality of Tempelhof is its ambiguity – as a place that possesses both strongly positive and strongly negative connotations. Now, it is a collage of different random functions scattered around the park. Almost no elements of this place are easy to define – the terminal was an important symbol of the Berlin Airlift, but it has been also a symbol of the horrible Nazi regime, along with its megalomaniac scale and the memories of Nazi gatherings. The runways are similar – place where ground connects with heaven, and from this heaven, food, coal and candies once came to Berlin. But these are also the same runways from which bombing planes were sent to many locations. There are no easy definitions here. And maybe there should be no easy definitions in this case. But, taking into account how much controversy Tempelhof continuously stirs, how many conspiracy theories and myths are built around this place and how much of its history remains forgotten, Tempelhof certainly needs some kind of a narrative.

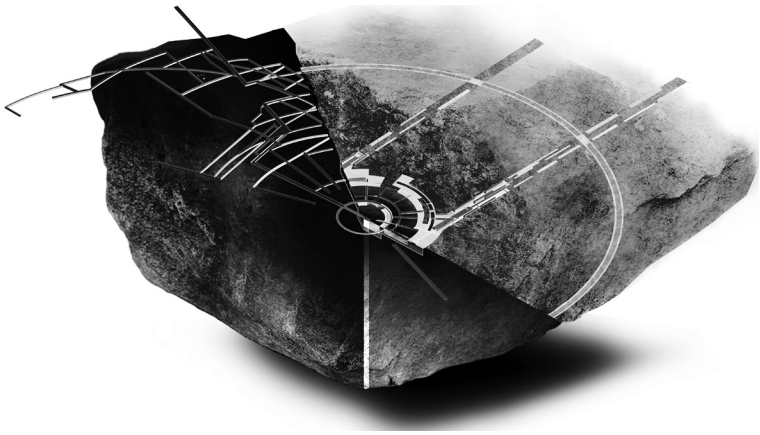

Fig. 9. Part of "Urban Therapy – Tempelhof Hoffnung" – diploma project by Anna Bijak, promoter: M. Gyurkovich, co-promoter: K. Racoń-Leja [6]

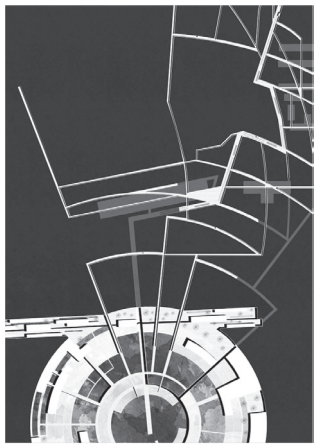

Fig. 10. underground tunnels and "Time Machine"– Tempelhof Hoffnung" – diploma project by Anna Bijak, promoter: M. Gyurkovich, co-promoter: K. Racoń-Leja [6]

In psychology, trauma is sometimes followed by holes in the memory. Some patients suffering from PTSD cannot recall certain memories and they repress them. What has to happen during therapy is digging up those memories, reliving them and healing the patient. If this is not done, it can then come up in unsuspected ways, slowly deteriorating the mental health of the patient. Maybe it can also be related to the whole society of Berlin, where "urban therapy" could be a solution for problems related to Tempelhof, a site which has not yet truly been claimed by the inhabitants as their own. Instead, it still belongs to the realm of mystery and darkness with unexplained questions and doubts. Some of the critics have touched on the subject of the history of Tempelhof and its cultural importance as well as the fact that the unresolved historical traumas can be the actual reason why this site is always so controversial. There never was any political and cultural narrative created for this site.

Interestingly, one of the very few supposed attempts to tackle the issue of taboo of Tempelhof seems to be one of the most intriguing movies set in Berlin, *Possession*, directed by Andrzej Żuławski [49]. One of the most important scenes of that film takes place at an underground station, Platz der Luftbrucke, which exists right next to the Tempelhof Airport terminal. The location must have been chosen deliberately, judging from the locations of the scene before and after this one. The main character is being possessed during this scene, or miscarries – it is not really clear. She runs around growling in the metro tunnel, then vomits and bleeds from different parts of her body. Needless to say, it is the most important, most gruesome and most memorable moment in the movie and, at the very same time, seems like the only artistic attempt to touch on the subject of the difficult topic of Tempelhof. In *Possession*, Tempelhof is a residue of evil forces –somehow, it triggers a break-down of the main character and becomes a defining moment in her story. Interestingly, Anna breaks down right when she passes by a supposed secret tunnel, which has been, according to conspiracy theories, dug to accommodate the escape of Hitler. Maybe it is a subtle attempt to involve Tempelhof into the whole narrative of Berlin. Tempelhof is, in this scenario, a dark underbelly of the city; a place where evil resides.

The whole topic of underground areas of the cities seems extremely interesting. The things that lie underneath the cities are probably one of the biggest components of what builds up their legends. The underground is usually mysterious; one can never be sure how many

structures lie underground. Even if one is discovered, something more may still remain. The underground is not seen by the naked eye easily. It usually demands great effort in unearthing its secrets or finding a hidden passage. In *Civilization and its discontents*, Sigmund Freud compared the working of the city to that of the human mind [17]. Later, art has developed metaphors to include the unseen underground – representing subconscious, ID, from which sometimes difficult memories or dark thoughts come out. In the analogy of the city, it could be represented by people on the margin of society.

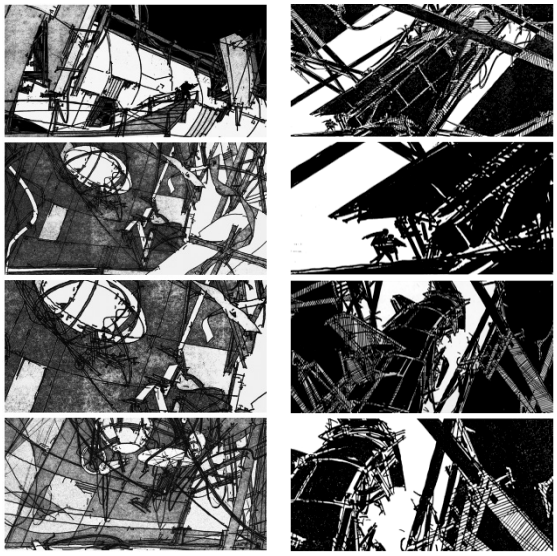

Fig. 11. Story synopsis "Underground Berlin" by Lebbeus Woods (© Lebbeus Woods)

Underground Berlin by Lebbeus Woods, highlighted the power and importance of the underground, relating it to a complicated cultural and political context of Berlin [43]. It showed the hidden and dark parts of cities, but most of all, the prevalent forces, which are always existing, no matter which ideology is currently in power. At the end of the story, the whole power of the underground, throughout the story used for different ideological purposes, is finally sunk in the depths. It is connected to the Nazi past – in L. Woods' story, the underground structure was built by Third Reich and it was a part of their plan for Berlin. The underground can be a powerful force of both good and evil, but it also has two different sides – as systematically utilised and as wild, unpredictable, primordial force of the city's subconscious. In the case of Tempelhof, the underground is a residue of darkness. *Possession* shows that fact by unveiling the darkness, which, for everybody, is a constantly existing ghost of the airport. And that makes Tempelhof a point in the city with immense political and cultural importance, not recognised by new architectural proposals.

Tempelhof is not just a park, but it does not only collect bad memories. Tempelhof needs to react to them, claim them and use them to teach society, relive the traumas and make itself a positive space, possibly also including a new, multicultural Berlin, where racism, antisemitism and homophobia are not acceptable. It cannot be just a grass, recreational plane. Not many places

in Berlin have a more symbolic meaning than Tempelhof, of which history is ambiguous, difficult and scary. And yet, it still can become the ground for something good. In this way, Tempelhof may become one of the most hopeful places in Berlin, a city of so many complex layers.

References

[1] *Abandoned Berlin blog,* March 2015, http://www.abandonedberlin.com/2015/03/tempelhof-mother-of-all-airports.html (access: 20.07.2017).

[2] Agile City, *Tempelhof Park Regeneration*, http://agile-city.com/community-project/tempelhof-park-berlin/ (access: 20.07.2017).

[3] Akopyan E., *Gravediggers Neukolln,* [in:] *Tempelhof Unfreiheit…*, http://www.tempelhofer-unfreiheit.de/en/walking-tour-tempelhof-field-7-gravediggers-neukolln/ (access: 20.07.2017).

[4] Berlin Gesichtswerkstat – Berlin History Workshop, http://www.berliner-geschichtswerkstatt.de (access: 20.11.2017).

[5] *Berliner Tempelhof geplant als erste Flüchtlings-<<Modell>>-Stadt für 7000 Migranten,* https://www.youtube.com/watch?v=bInTiIE9XYg (access: 20.07.2017)

[6] Bijak A., *Urban Therapy – Tempelhof Hoffnung,* master thesis project, promoter: M. Gyurkovich, co-promoter: K. Racoń-Leja, Faculty of Architecture, Cracow University of Technology 2017.

[7] Bodenschatz H., *Berlin Urban Design – A Brief History*, DOM Publishers, Berlin 2010.

[8] Brooke A., *Berlin's Tempelhof airport gets mountain rescue bid,* The San Diego Union Tribune, Jan. 2009, http://www.sandiegouniontribune.com/sdut-63912073339-tempelhof-airport-2009jan27-story.html (access: 5.07.2017).

[9] Burg, A., *Berlin Mitte – die Die Entsehung einer urbanen Architektur/Downtown Berlin – Building the Metropolitan Mix,* Bierhäuser Verlag, Berlin 1994.

[10] City of Berlin Population, https://www.citypopulation.de/Deutschland-Berlin.html (access: 03.07.2017).

[11] Connoly K., *How Hitler's plans for Germania would have torn Berlin apart*¸ The Guardian, https://www.theguardian.com/cities/2016/apr/14/story-of-cities-hitler-germania-berlin-nazis (access: 9.07.2017).

[12] Cruz L., *Turbulence ahead: hundreds of refugees set for Berlin's Tempelhof Airport,* Euronews, Sept. 2017, http://www.euronews.com/2017/09/22/turbulence-ahead-hundreds-of-refugees-set-for-berlins-templehof-airport (access: 21.11.2017).

[13] Düwel J., Gutschow N., *Städtebau in Deutschland im 20. Jahrhundert, Ideen-Projekte-Akteure,* Gebrüder Bornträger Verlagsbuchhandlung, Stuttgart 2005.

[14] Eliade M., *The Sacred and the Profane: The Nature of Religion,* Houghton Mifflin Harcourt, Boston 1987.

[15] Fahey C., The Guardian, *How Berliners refused to give Tempelhof Airport over to developers,* March 2015, https://www.theguardian.com/cities/2015/mar/05/how-berliners-refused-to-give-tempelhof-airport-over-to-developers (access: 10.07.2017).

[16] *Flughafen Tempelhof: Was befindet sich im Untergrund*, Rbb Abendschau, https://www.rbb-online.de/abendschau/serien/die-sonntagsfrage/Sonntagsfrage1.html (access: 20.07.2017).
[17] Freud S., *Civilization and its discontents,* W.W. Norton & Company, New York 1989.
[18] Frick M., Sippel J., Cacace M., Scheck-Wenderoth M.,*The geothermal field below the city of Berlin, Germany: Results from structurally and parametrically improved 3D Models, European Geosciences Union General Assembly 2016, EGU* Division Energy, Resources & Environment, ERE, 2016.
[19] Gyurkovich M., *Hybrydowe przestrzenie kultury we współczesnym mieście europejskim*, Wydaw. PK, Kraków 2013.
[20] Heathcote E., *Monument builders / Modern architecture and death,* Wiley, New York 1999.
[21] Holmes J., *Tempelhofer Lu(f/s)twerks,* Motionpicturesque, https://www.motionpicturesque.com/luftwerks (access: 20.07.2017).
[22] Klein B., *Contradictions between past and present,* [in:] *Tempelhof Unfreiheit…* , http://www.tempelhofer-unfreiheit.de/en/walking-tour-tempelhof-field-5-contradictions-past-present/ (access: 20.07.2017).
[23] Kosiński W., *Paradigm of the city of the 21st century: between the past of the polis and the future of the metropolis*, Wydaw. PK, Kraków 2016.
[24] Lee I.Y., *Form and Meaning: How Media's Representation Tells the Story of the Berlin Wall,* Richter Research Abroad Student Scholarship, http://scholar.oxy.edu/cgi/viewcontent.cgi?article=1006&context=rrap_student (access: 13.07.2017).
[25] *Legendarne Lotnisko Tempehof w Berlinie w nowej roli. Schronienie dla uchodźców z Syrii*, WP Wiadomości, November 2015, http://wiadomosci.wp.pl/legendarne-lotnisko-tempelhof-w-berlinie-w-nowej-roli-schronienie-dla-uchodzcow-z-syrii-6027729814950529a (access: 16.07.2017).
[26] Lomholt I., *Tempelhof Competition Berlin*, March 2016, https://www.e-architect.co.uk/berlin/tempelhof-competition (access: 15.07.2017).
[27] *Magic Mountain for Berlin?*, Spiegel Online, Jan. 2009, http://www.spiegel.de/international/germany/future-of-tempelhof-magic-mountain-for-berlin-a-602429.html (access: 29.07.2017).
[28] Menberg K., Blum P., Rivera J., Benz S., Bayer P., *Exploring the Geothermal Potential of Waste Heat Beneath Cities*, Proceedings World Geothermal Congress 2015, Melbourne, Australia, 19–25 April 2015 (access: 20.11.2017), https://pangea.stanford.edu/ERE/db/WGC/papers/WGC/2015/16063.pdf
[29] Mohr R., *Spiegel Online*, http://www.spiegel.de/international/germany/the-myth-of-berlin-s-tempelhof-the-mother-of-all-airports-a-549685.html (access: 29.07.2017).
[30] Parsloe T., *Berlin's Tempelhof*: *The camp too controversial to customize,* News Deeply, June 2017, https://www.newsdeeply.com/refugees/articles/2017/06/22/berlins-tempelhof-the-camp-too-controversial-to-customize (access: 24.07.2017).
[31] Pixart printing: *Berlin Lines,* https://www.pixartprinting.co.uk/content/berlin-lines/ (access: 18.07.2017).
[32] Racoń-Leja K., *Traces of the Second World War in European cities*, Technical Transactions, 1-A/2013, 101–118.

[33] Racoń-Leja K., *Urban heritage of Europe in the context of the Second World War,* [in:] *Tradition and heritage in the contemporary image of the city*, Vol. 1, *Fundamentals*, Wydaw. PK, Kraków 2015, 69–73.
[34] Raumforschung, Flickr, https://www.flickr.com/photos/raumforschung/5116761169 (access: 6.08.2017)
[35] Schwarzbeck M., *Fluchtlinge in Berlin: inside Tempelhof,* Nov. 2015, https://www.zitty.de/inside-tempelhof/ (access: 20.07.2017)
[36] Scott R., *Tempelhof Airport Plan Denied by Berlin Voters,* ArchDaily, May 2014, http://www.archdaily.com/510044/tempelhof-plans-denied-by-berlin-voters (access: 17.07.2017).
[37] Shead S., Business Insider, *The story of Berlin's WWII Tempelhof Airport which is now Germany's largest refugee shelter,* http://www.independent.co.uk/news/world/world-history/the-story-of-berlins-wwii-tempelhof-airport-which-is-now-germanys-largest-refugee-shelter-a7799296.html (access: 23.07.2017).
[38] Studio SPTA, *Parklandschaft Tempelhof,* Divisare, Jan. 2011, https://divisare.com/projects/155900-studio-spta-alessandro-pianetti-della-stufa-elisa-trapani-francesco-finelli-mauro-merlo-roberto-mazzer-roberto-simeone-alessandro-ciocci-elisa-trapani-rocco-smaldone-angela-arnone-parklandschaft-tempelhof (access: 20.07.2017).
[39] Todtmann J., *Forced Labor,* [in:] *Tempelhof Unfreiheit…*, http://www.tempelhofer-unfreiheit.de/en/walking-tour-tempelhof-field-3-forced-labor/ (access: 20.07.2017).
[40] Vail J., *Chasing the Ghosts of the past in Tempelhof,* Nov. 2016, https://www.reflectionsenroute.com/chasing-the-ghosts-of-the-past-in-tempelhof/ (access: 23.07.2017).
[41] Veerman T., *Columbia House – Forgotten Site of Terror,* [in:] *Tempelhof Unfreiheit…*, http://www.tempelhofer-unfreiheit.de/en/walking-tour-tempelhof-field-1-columbia-house-forgotten-site-terror/ (access: 15.07.2017).
[42] Viviani E., *THFZentrum/Evolution (A new Berlin connection/landmark)*, Feb. 2016, https://divisare.com/projects/309845-viviani-eleonora-thfzentrum-evolution-a-new-berlin-connection-landmark (access: 17.07.2017).
[43] Woods L., *Underground Berlin: the film treatment,* blog post, 2009, https://lebbeuswoods.wordpress.com/2009/09/15/underground-berlin-the-film-treatment/ (access: 20.07.2017).

Filmography:

[44] Berlin: Die Sinfonie der Großstadt, dir. Walther Ruttmann, 1927.
[45] Cities of the Underground – Hitler's Underground Lair, dir. Emre Sahin, 2007.
[46] Die Wahrheit über Berlin Tempelhof, Die WAHRHEIT, July 2015, https://www.youtube.com/watch?v=wUSRSVnPtns (access: 15.07.2017).
[47] Hedwig and the Angry Inch, dir. John Cameron Mitchell, 2001.
[48] Himmel über Berlin, dir. Wim Wenders, 1987.
[49] Possession, dir. Andrzej Żuławski, 1981.
[50] *Rabbit a la Berlin*, dir. Bartosz Konopka, 2009.

TECHNICAL TRANSACTIONS 2/2018
ARCHITECTURE AND URBAN PLANNING
DOI: 10.4467/2353737XCT.18.019.7992
SUBMISSION OF THE FINAL VERSION: 17/1/2018

Artur Jasiński (a.jasinski@ajbiuro.pl)
Department of Architecture and Fine Arts, The Andrzej Frycz Modrzewski Krakow University College

Protecting public spaces against vehicular terrorist attacks

Zabezpieczenie przestrzeni publicznych przed samochodowymi atakami terrorystycznymi

Abstract

The recent wave of terrorist attacks, where vehicles are driven into crowds of people, forces us to question the effectiveness of the current antiterrorism security measures in our cities, especially in open public spaces. Vehicular terrorism, a new form of Islamic terrorism, which involves the use of mechanical vehicles as a weapon against civilians, brings new challenges for the police, security agencies and mass event organisers, as well as for designers, architects and planners. This article considers the possibilities, costs and results of implementing actions and security measures that may reduce the risk of vehicular terrorism.

Keywords: vehicular terrorism, antiterrorist security, urban fortifications.

Streszczenie

Seria ataków terrorystycznych przeprowadzonych z użyciem samochodów taranujących ludzi każe na nowo postawić pytanie o skuteczność zabezpieczeń antyterrorystycznych naszych miast, a szczególnie ich otwartych przestrzeni publicznych. Nowa forma taktyki islamskiego terroryzmu, polegająca na wykorzystaniu pojazdów mechanicznych jako broni wymierzonej w ludność cywilną, stawia kolejne wyzwania służbom odpowiedzialnym za bezpieczeństwo publiczne i organizatorom masowych imprez, a w drugiej kolejności także projektantom, architektom i planistom. W artykule rozważane się możliwości, koszty i skutki wprowadzenia w życie działań i zabezpieczeń, które mogą służyć ograniczeniu ryzyka ataków terrorystycznych dokonywanych przy użyciu samochodów.

Słowa kluczowe: terroryzm samochodowy, zabezpieczenia antyterrorystyczne, fortyfikacje miejskie.

1. Introduction

Terrorists have used vehicles as weapons, or more specifically, for weapon transportation, for close on a century. The historic Morgan's building on Wall Street in downtown Manhattan still bears the scars of an August 1920 attack, when Italian-born anarchist Mario Buda blew up a horse-drawn wagon full of explosives, killing 40 and wounding more than 200. Mike Davis, who describes the rich history of vehicle terrorism, metaphorically calls the car bomb "the poor man's air force" [4, p. 4]. The growing popularity of recipes for the DIY production of explosives using generally available materials (organic fertilisers, oil) sparked a worldwide wave of bomb attacks in the late 20th century. The attacks carried out by the IRA in towns and cities across England, the series of attacks against US embassies, car bombs detonated indiscriminately in the streets of Middle Eastern cities and the Oklahoma Alfred P. Murrah Federal Building bomb attack of April 1995 have caused hundreds of casualties and inflicted significant material damage. The images of destruction reported in the media have sparked a fierce reaction from the public, followed by fear and dismay, and, in some cases, a destabilisation of the political situation.

Fig. 1. High security on London's Downing Street, where the seat of the British Prime Minister is located: police checkpoints, massive gates, and a clamshell road barrier in the background

Since the late 20th century, the Vehicle Borne Improvised Explosive Device (VBIED) has been seen as the most menacing type of weapon in the hands of terrorists. A variety of situational prevention tactics have been employed to counter potential car bomb attacks, such as setting up road barriers, reinforcing and fortifying essential buildings, and creating security zones around

whole city sections (London, New York, Washington). Comprehensive antiterrorism security tends to militarise the city space, "harden" the urban landscape, and restrict access to public facilities by residents, who are subject to continuous control and surveillance using state-of-the-art technologies. This poses the archetypical question of "safety versus freedom", which, in spatial terms, can manifest as a conflict concerning the essence of urban character: it involves risks to the functioning of the city's public space as a widely accessible zone of civic activity and freedom [7, p. 12].

2. The car as a weapon for attacking people

The Internet, along with the social media associated with it, is one of the most commonly used platforms for the dissemination of contemporary Islamic terrorism ideologies. In October 2010, the second issue of the English-language magazine "Inspire", published online by Al Qaeda cells, had an article titled "The Ultimate Mowing Machine". It described how a car could be used as a weapon for "mowing down the enemies of Allah", particularly in situations where attackers have no access to explosives or firearms. More detailed tactical guidelines on planning terrorist attacks using vehicles were featured in the third online edition of ISIL's (Daesh's) "Rumiyah Magazine", which included the expertise gained from recent attacks in the EU and Western Europe [10, p. 2].

On 22 December 2014, Sebastien Sarron ran down ten people at the Christmas market of the French city of Nantes in a van and then attempted suicide. One person died in the attack. The attack was inspired by a video, which urged ISIL supporters to attack infidels using cars. On 14 July 2016, another attack took place in Nice: Mohamed Lahouaiej Bouhlel, a Tunisian with a French residency permit, used a rented Renault Midlum truck to drive into people celebrating Independence Day along the city's seafront boulevard. The deadly rampage lasted 5 minutes and the attacker drove almost 2 kilometres, killing 87 and injuring more than 200 people, before he was shot by the police.

On 28 November 2016 in Columbus, Ohio, Somalian refugee Abdul Razak Ali Artan drove a Honda Civic into the courtyard of Ohio State University. After hitting a wall, he got out of the car and began stabbing random victims with a knife, wounding 13 people, before a police officer shot him dead. ISIL claimed to have inspired the attack. On 19 December 2016, a large Scania truck with a trailer carrying steel beams ploughed into the crowd at the Breitscheidplatz Christmas market in central Berlin. Moving at more than 60 kph, the truck was driven into market stalls for some 80 metres [2]. 12 people were killed and 56 were injured. The attacker was a Tunisian refugee, and his victims included Łukasz Urban, the Polish driver of the carjacked truck, found dead in the passenger's seat afterwards. The attacker fled the scene and was shot dead four days later by Italian police in Milan. The recording released after the attack suggests that Amiri was inspired by the ISIL.

The tactical guidelines on preparing and carrying out vehicular attacks in "Rumiyah Magazine" stressed the importance of meticulous preparation and the need to choose an appropriate spot for ramming with a speeding truck. It pointed out that, especially in the United States, attacks against civilians provoke more outrage than those against military targets. Some of the most sensitive potential targets specified in the article included outdoor assemblies and ceremonies, parades, fairs, festivals, political rallies and crowded inner-city streets. The article recommended

the use of sturdy trucks and all-terrain vehicles with a massive steel body and an all-wheel-drive system. "Inspire" also encouraged its readers to modify attack vehicles by welding thick sheets of metal to the vehicle front to act as blades to cut the victims' bodies. It was recommended to choose long and narrow spaces, such as boulevards or bridges, with limited escape routes and no other vehicles around that could stop the attacker's vehicle moving at speed. Walkways and inner-city main streets were indicated as perfect attack spots. Finally, drivers were encouraged to carry firearms or knives to complete their act of destruction after their vehicle comes to a halt, and to prepare for death by leaving a note with their motives in the vehicle or at home [10, p. 4].

The subsequent attacks in 2017 followed the same scenario. On 22 March 2017, British-born Islamic convert Khalid Masood rammed into pedestrians on Westminster Bridge, driving at over 120 kph, killing 4 people and injuring more than 50. When his SUV Hyundai Tucson crashed into a road barrier protecting the Parliament building, he exited the vehicle, stabbed a police officer with a knife and was shot down a few moments later while running away. The whole incident lasted 82 seconds [9]. In the recording that he left behind, he confessed that this was an act of vengeance against British society, responsible for wars with Islamic countries in the Middle East.

On 7 August 2017, 22-year old Younes Abouyaaqoub, a Moroccan-born Spanish citizen, killed 13 and injured 130 while driving a Fiat van on Las Ramblas Boulevard in central Barcelona. After driving more than 500 metres, the attacker was stopped by airbags and other safety systems; he escaped the car, stabbed another victim and fled the scene in a carjacked vehicle. A few hours later, five of his companions from the same terrorist cell rammed a passenger car into a group of pedestrians in the town of Cambrils, located to the south-west of Barcelona, killing one and injuring six people. The attackers were shot dead on the spot by the police; 4 days later Abouyaaqoub met the same fate.

These incidents prove that protecting public spaces against vehicular terrorist attacks is extremely challenging at the present time, perhaps even impossible, both because of the broad access to the terrorist's new weapon: the regular vehicle, and because of the virtually unlimited number of potential targets: pedestrians in cities. What can be done? Is it even possible to protect against vehicular terrorism attacks?

3. Measures that can reduce the risk of a vehicle-ramming attack

According to Brian M. Jenkins, an expert on contemporary terrorism and advisor to the influential think tank RAND, vehicular terrorist attacks cannot be prevented, only their results mitigated [8, p. 2]. He proposes 10 hostile vehicle mitigation measures:

3.1. Armed police patrols

Increased numbers of armed police improve security on the streets and at mass events. However, most vehicular attacks last for only a few dozen seconds or several minutes. Lightly-armed police officers will certainly not be able to prevent such an attack, but they can try to deter and neutralise the attacker, reducing the number of potential victims.

3.2. Increased traffic surveillance

In theory, digital technologies could be used for traffic surveillance (e.g. with algorithms to detect suspicious vehicles or unusual driver behaviour). Rental companies, especially those renting trucks and off-road vehicles, could be subject to meticulous scrutiny and their customers pre-emptively crosschecked with police databases, similar to passenger profiling in airports. It is also possible to put vans and trucks under GPS surveillance; a vehicle departing from its planned and electronically controlled route would then produce an alarm signal to call for police intervention.

3.3. Separate pedestrian and road traffic

To ensure pedestrian safety, it is always desirable to physically separate the roadway from the adjoining pavements; for example, with street furniture, bollards, reinforced street signs and various specialised barriers. Rows of trees and cars parked along the pavements also provide effective separation.

3.4. Restricted vehicle access to pedestrian zones

Fig. 2. A pedestrian crossing protected from car entry, Brussels (photo by A. Jasiński)

Walkways, squares, pavements and other pedestrian zones, particularly around pedestrian crossings and intersections, can be effectively protected from vehicle entry with reinforced bollards, elements of small architecture and hardened street furniture.

3.5. Traffic calming

Traffic speed can be reduced by installing speed bumps, obstacles that force drivers to zig-zag, etc. Long, straight road sections should be avoided, as these allow an attacker to accelerate, especially those near the entry-points to protected zones, where the vehicle's kinetic energy combined with its mass increases the risk of penetrating barriers and other security features if these are not sturdy enough.

3.6. Temporary security barriers for mass events

Fig. 3. Trucks, dumpsters and a police car blocking the city's main street during a sports parade, Rotterdam, 5 June 2017 (photo by A. Jasiński)

Trucks are often used to block areas holding mass events. One advantage of this solution is that the vehicles can be quickly deployed, and then moved if necessary to allow police and emergency services to cross the barrier. During the 2016 New Year's Eve celebration in Times Square, the access roads around the venue were blocked with 65 dumpsters and trucks filled with sand, and 100 police cars. At the same time, the public transport system was rearranged to ensure an efficient movement of people to and from the event. More than 7,000 police officers were responsible for maintaining order and safety [10, p. 2].

Other means of blocking access to mass event locations include temporary barriers made of water-filled tanks, Jersey Barriers road partitions from reinforced concrete and other innovative systems, such as X-Net from the British company Qinetiq. The latter is

Fig. 4. "Surface Guard" temporary barrier in a city centre street (source: [1])

a polyethylene net studded with sharp spikes that punctures the tyres and wraps around the wheels, effectively stopping vehicles with masses of up to several tonnes. X-Net can be quickly deployed by two people, and is used by the British police for securing mass events. The Surface Guard System, patented by ATG, uses another mechanism: its lightweight, three-dimensional plastic elements can be deployed on the road and linked together to set up a flexible barrier that provides full pedestrian and bicycle permeability but at the same time is capable of stopping a vehicle weighing up to 2.5 tonnes and travelling at 50 kph. It can be deployed and removed by four people in a short time, without damaging the surface.

3.7. Expanding the existing protection zones around buildings

The threat of car-bomb attacks has led to the construction of zone protection systems, such as rows of reinforced bollards, barriers and elements of small architecture, around a number of important buildings. These can be used or expanded to protect public spaces and the mass events they host. Some of the barriers are swivel-mounted or hydraulically collapsible to allow the crossing of emergency services. Deploying such systems is costly and time-consuming, but they provide the most effective form of protection against car-bomb

attacks. In many cities, it is not just the zones around single buildings that are secured this way, but whole streets with important public buildings, institutions and embassies, such as Wall Street in Manhattan and Wilhelmstrasse in Berlin.

Fig. 5. Double road barrier and police checkpoint at Wilhelmstrasse in Berlin, with the British embassy in the background (photo by A. Jasiński)

3.8. Terrorist-proof inner-city zones

In some cases, antiterrorist enclosures, road barriers and police checkpoints are used to protect whole inner-city areas. Examples include the Ring of Steel around the City of London, central Washington along Pennsylvania Avenue, and part of Lower Manhattan around the World Trade Center complex. In these cases, the "hard" terrain protection measures are supported by police patrols, CCTV surveillance systems, digital cameras for registration plate identification connected to police databases, and biometric devices (for identifying wanted individuals). Access to the zones is restricted by moving road barriers controlled by police checkpoints. These systems could be expanded, theoretically, but this would be extremely expensive and complicated due to the number of stakeholders and conflicting interests, and would interfere with the character of the public space.

Fig. 6. Road barriers and police checkpoints around the World Trade Center area in Lower Manhattan (photo by A. Jasiński)

3.9. Change car-accessible roads into pedestrian walkways

An easier solution, and one that is becoming increasingly popular and acceptable to the public, is to turn inner-city streets and squares, as well as main commercial streets, into pedestrian zones with completely or partly restricted motor traffic. This task is not a simple one, either, as they need to prevent a potential attacker's vehicle from penetrating the area without hindering access by delivery, emergency or repair services. This can be achieved with movable road barriers and hydraulic bollards installed at the entry points, controlled by police checkpoints or remotely by the drivers of authorised vehicles.

In many European cities, whole inner-city areas have already been transformed into pedestrian and bicycle zones, which improves pedestrian security while also promoting the development of local businesses and giving the city a friendly character. Some typical examples can be found in Venice, Copenhagen, Göttingen, Brussels and Kraków. This trend is now being popularised across the world, not least thanks to the design and journalistic efforts of Jan Gehl [5]. At the same time, busy inner-city streets and squares should be protected from unauthorised vehicle access, especially since those publications inspiring vehicular terrorism list crowded commercial streets as priority targets.

Fig. 7. Remotely-controlled hydraulic bollards blocking access to an inner-city pedestrian zone in Brussels (photo by A. Jasiński)

3.10. Use new technologies to prevent attacks against people

Most vehicle and software manufacturers are now carrying out intense research into developing vehicles that move automatically. The technology they use may, besides preventing road accidents, also counter vehicle-ramming attacks. The required blocking mechanisms could be installed in all vehicles.

4. Conclusions: on the need for measured and proportional reactions

In conclusion, the measures and protection systems mentioned above should be evaluated in terms of their cost and effectiveness. First of all, while terror attacks involving vehicles have been gaining much notoriety in the media worldwide, their actual significance is quite limited: they cause negligible damage to material property and have relatively few victims. Jenkins reports that a total of 167 people have been killed in all such attacks since 2000, which is less than two casualties per incident on average [8, p. 2]. Every death is a tragedy in itself, of course, but the number of fatal road accidents, which is more than 30,000 a year in the US alone, puts vehicular terrorism in a slightly different perspective.

Secondly, it is worth noting that terrorists continue to modify their tactics. Their targets and tools change. The worst terror attack in history was carried out using civilian aircraft as

flying bombs (New York, 2001), while real bombs have been used against trains (Madrid, 2004), buses and metro lines (London, 2005). In Israel, some desperate Palestinian attackers stab their victims with kitchen knives. Improving the security and protection against attacks in one place may force a change of target or method, and as a result increase the threat in another place, against softer and less protected targets. Particular attention should be given to the August 2017 article in "Inspire" urging Al Qaeda supporters in Europe and the US to target trains and railways [3].

The New York truck-ramming attack of 30 October 2017 committed by an Uzbek immigrant sympathising with the ISIL proves that such an act of terrorism can succeed even in a city better protected against terror attacks than any other, a city surrounded by multiple rings of electronic and physical fortifications. The attack took place in Lower Manhattan, on a bicycle path along the Hudson River, and finished with the attacker crashing into a school bus a few hundred metres away from the fortified zone around the WTC. It is extremely difficult to prevent this type of attack: to identify a potential perpetrator whose preparations involve nothing more than accepting online propaganda and self-indoctrination, and to restrict vehicle access. It is impossible to protect all the people in all the streets and squares of a city.

Attempts at restricting vehicular access or placing all drivers under surveillance would infringe upon the modern way of life, where the car plays an important role. Of course, an actual threat warrants appropriate countermeasures that are proportional to the threat, yet allowing an acceptable level of risk. Crowded inner-city streets, busy squares and outdoor mass events certainly require special attention, although it is important to realise that the threat of terrorist attacks can never be fully eliminated and must be accepted. We cannot give in to the fear syndrome fuelled by the mass media, which have effectively become the greatest allies of contemporary terrorism. The word "terrorism" can be more dangerous than the terrorist act itself, according to Tomasz Goban-Klas, who urges journalists to exercise restraint in reporting terror attacks, and calls for self-regulation of the media [6, p. 363–385].

The best response to the increased threat of terror in today's cities is to apply situational prevention measures in a skilful manner, to increase the threat prevention capabilities, and to improve emergency response in the wake of potential attacks, accidents and natural disasters. One way to reduce the threat of vehicular terrorism is to introduce comprehensive solutions that improve pedestrian safety and gradually restrict vehicular traffic. By redesigning streets, we can protect people from both careless and malicious drivers. Moreover, a well-conceived, holistic system of traffic security and regulation can contribute to inner-city revitalisation, thus improving the living and working conditions for the residents, and making the city more attractive to tourists.

References

[1] ATG Access Ltd. https://www.atgaccess.com/product/surface-guard-system (access: 20.11.2017).

[2] *Berlin lorry attack: what we know*, BBC News, http://www.bbc.com/news/world-europe-38377428 (access: 30.10.2017).

[3] Clarke C.P., *When a Car is a Terror, Can We Prepare for Attacks?,* The RANDBLOG, Rand Corporation, 18.08.2017, https://beta.theglobeandmail.com/opinion/when-the-car-is-a-terror-weapon-can-we-prepare-for-attacks/article36027840/?ref=http://www.theglobeandmail.com& (access: 20.11.2017).
[4] Davis M., *Buda's Wagon. A Brief History of the Car Bomb,* Verso, London-New York 2007.
[5] Gehl J., *Life Between Buildings. Using Public Space,* 1971, Polish edition: Życie między budynkami. Użytkowanie przestrzeni publicznych, Wydawnictwo RAM, Kraków 2009.
[6] Goban-Klas T., *Wartki nurt Mediów. Ku nowym formom społecznego życia informacji,* Universitas, Kraków 2011.
[7] Jasiński A., *Architektura w czasach terroryzmu. Miasto – przestrzeń publiczna – budynek,* Wolters Kluwer, Warszawa 2013.
[8] Jenkins B.M., *Vehicular Terrorism: Weighing the Benefits, and Worth, of Prevention,* The RAND BLOG, Rand Corporation, 5.09.2017, https://www.rand.org/blog/2017/09/vehicular-terrorism-weighing-the-benefits-and-worth.html (access: 30.10.2017).
[9] Warrell H., *Westminster attack lasted less than 90 seconds,* Financial Times, 25 March 2016.
[10] *Vehicular Terrorism. The Threat Behind the Wheel.* Corporate Risk Services. Intelligence Bulletin 2017 (access: 30.10.2017).

TECHNICAL TRANSACTIONS 2/2018
ARCHITECTURE AND URBAN PLANNING
DOI: 10.4467/2353737XCT.18.020.7993
SUBMISSION OF THE FINAL VERSION: 15/1/2018

Agnieszka Matusik (agnieszka.matusik@pk.edu.pl)
Institute of Urban Design, Faculty of Architecture, Cracow University of Technology

River Valley as a hydrological/urban dynamic system in the structure of the contemporary city

Dolina rzeczna jako hydrologiczno-urbanistyczny układ dynamiczny w strukturze współczesnego miasta

Abstract

Contemporary tendencies in shaping river valleys in cities constitute a clash and overlap of numerous aspects of contemporary urban planning. The range and diversity of interventions depict the whole array of new urban landscapes, the superior quality of which is constituted by the ecological aspect. Growing climatic changes, as well as limits of the natural environment within urban structures, pose special requirements for urban sections of river valleys. Urban strategies and projects proposed for these sections must face problems related to water resources management, and at the same time, they need to be activators of the new quality of the city in the context of its competitiveness. This paper focuses on two fundamental tendencies in designing river valleys in cities: anti-flood control, and increasing the share of the natural environment in the urban structure.

Keywords: river, watercourse, hydrological/urban system, city landscape

Streszczenie

Współczesne tendencje kształtowania dolin rzecznych w miastach to zderzenie i nałożenie się wielu aspektów współczesnej urbanistyki. Rozpiętość i różnorodność interwencji ukazuje pełen wachlarz nowych krajobrazów miejskich, których cechą nadrzędną staje się aspekt ekologiczny. Narastające zmiany klimatyczne, a także ograniczanie środowiska naturalnego w obrębie struktur miejskich, stawia przed miejskimi odcinkami dolin rzecznych szczególne wymagania. Proponowane dla tych odcinków strategie i projekty urbanistyczne muszą sprostać zarówno problemom dotyczącym gospodarowania zasobami wodnymi, jak i jednocześnie być stymulatorem nowej jakości miasta w kontekście jego konkurencyjności. Artykuł skupia się na dwóch podstawowych tendencjach w kształtowaniu dolin rzecznych w miastach: ochronie przeciwpowodziowej oraz zwiększaniu udziału środowiska naturalnego w strukturze miejskiej.

Słowa kluczowe: rzeka, cieki wodne, system hydrologiczno-urbanistyczny, krajobraz miasta

1. Introduction

Transformations of the course of river valleys in cities have been a permanent, continuous, and dynamic process for centuries. The very fact of locating an urban system at the edge of a watercourse sentences it to periodic transformations.

Questions concerning tendencies in shaping river valleys can be deemed to be simultaneously questions concerning the shape of the cities of the future. The river, the determinant of the establishment of cities, the stimulus for their development, takes place in a symbiotic relation: the built space – the natural landscape. The process of shaping its system within the territory of the city conditions the city life in the future, just like general urban actions determine the life of the river. Dynamic urbanisation processes make cities face the necessity to provide an answer to the structural form of this growth. Extreme densification of urban areas in their central parts is simultaneously connected with the excessive city sprawl, necessary in order to maintain its existence. At the same time, progressing climatic changes and flood risk connected with them, as well as the increasing temperature within urban structures, are linked with the need to take care of the natural system of the city.

What place and scenario in the process of forecasting and planning is occupied by corridors of river valleys? What will be the landscape of the river within the city and outside its limits in the reality of sprawling cities – regions? Sławomir Gzell poses a question: "Will (the city) have its suburban areas, will it have its urban areas, will we differentiate between urban and suburban (and rural) areas of the city at all, using landscape-related criteria?" [5, p. 31] What role in such a reality will be ascribed to corridors of watercourses, and what are the options for their protection? The more and more strongly marked need of coexistence of urban and open (rural) landscape and of their reciprocal overlapping, was emphasised already by Ildefons Cerdà. On the basis of experiences deriving from the extension of Barcelona, he observed that urbanisation is strictly connected with changing of the rural to the urban, and simultaneously with ruralisation [5, p. 29]. This assumption can serve as a base for formulating foundations for designing the shapes of watercourses to be keystones between the urban and the natural.

The search for something we call a 'good' city is still an open question. "It can be stated that cities combining an economic approach to the future with the protection of spatial values stand a bigger chance for desirable transformations". One of the desirable qualities of such a city is its spatial originality, uniqueness [5, p. 28]. Defining the relation between the built structure to the space of the urban section of a river valley slowly becomes an answer to the issues referred to above – how to make use of the originality and uniqueness of the system so as to succeed in economic terms? What is the role and meaning of urban strategies and projects connected with the river development in the city (and in the open landscape) for processes connected with issues of competitiveness of cities based on ecological aspects?

It can be recognised that two leading tendencies will be of key importance for the functioning of cities in the future [7, p. 97]. These are:

1. Urbanisation of waterfronts of urban sections of river valleys;
2. Naturalisation of waterfronts of urban sections of river valleys.

These two tendencies occur in their pure form extremely rarely – they usually complement each other, to the benefit of the urban structure. This interdependence can be dubbed a hydrological/urban dynamic system, where individual factors exhibit variable behaviour, and simultaneously maintain a reciprocal balance. The paper presents cities and projects in which the tendencies referred to above can be demonstrated in a clear way.

The first trend concerns predominantly the phenomenon of recovery and transformation of post-industrial sections of river valleys, located in the direct vicinity of city centres. The second trend comprises a whole spectrum of solutions aiming to maintain or recreate the natural ecosystem of the river valley in the city, whereas the term 'naturalisation' refers to the processes of recreation, revitalisation, and extension of the natural hydrological system of a river valley in the city. Both these tendencies entail the need to address problems connected with providing anti-flood protection with the simultaneous high-quality urban structure, the quality which is conditioned by the new hydrological/urban system of the city, operating and reacting to the variability of conditions in a dynamic way.

2. Urbanisation of waterfronts of urban sections of river valleys

Strategic projects implemented within the area of urban sections of river valleys have a determining effect on the shape of the urban model and are closely connected with the need to regulate the edge of waterfronts. The specificity of the location, resulting from low altitudes above sea level, and consequently entailing a high level of flood risk, also causes the need of far-fetched transformations within the urban structure, based on building a coherent water and greenery system. This fact, which is often an aspect that reduces the city attractiveness, may become a fundamental element of the process of creating its identity and potential. This need of structural transformations often entails a growing tendency of giving water bigger possibilities of penetrating the city structure. Contemporary metamorphoses of cities based on the dynamic relation between water and the city structure can be defined as new attractors building the position of cities in competitiveness rankings.

This is the case in Rotterdam. The structure of the city, located in the delta system of the river Meuse, has been conditioned by the water situation since its very beginnings. The historical layout of the city was already determined by water canals (Fig. 1). The contemporary Rotterdam has developed this typology, creating a water/greenery skeleton of the model of the city.

The strategy of Rotterdam was to address the problem of the excessive pressure of water coming from four potential sources: the sea, the river, precipitation, and waters drained from the surface of the land. The answer consisted in building a system of canals, which were to take over the excessive inflow of water. At the same time, this system, implemented in the form of blue-green corridors, becomes the fundamental skeleton of the urban structure, conditioning high-quality residential environment. The entire strategy has been described as 'Rotterdam – Watercity' (Fig. 2), and it is planned to the time horizon of 2035 [13]. The implementation of the anti-flood system at the same time provides grounds for the creation of an original urban structure.

Fig. 1. Rotterdam in 1650 and Rotterdam – Watercity 2035 (diagram: A. Matusik)

Looking at the city in a closer scale and considering the relations referred to above in the context of urban projects, it is possible to observe the continuation of the characteristics of the hybridity of the water/urban system. Simultaneously, the clash of climatic, ecological, and economic aspects becomes a foundation for urban marketing and promotion of the city. Addressing these needs, cities create spectacular engineering projects, allowing to introduce new types of space in the urban structure – attractive spaces, offering a high-quality living environment for their residents. This phenomenon is gradually becoming a determinant of the quality of life of a contemporary metropolis, operating with new tectonics and entering areas which so far have been impossible to inhabit.

2.1. HafenCity Hamburg: new tectonics

An example which has become the classics of including the floodplain in the public space of the city is the HafenCity Hamburg project. Elevating the level of the ground within the entire territory of the investment by 8 metres on average towards the set water surface allowed for the safe functioning of the new structure. At the same time, an incredibly important element of this strategy, or even the essence of the way in which the public space functions in this area, were designing assumptions pertaining to solutions in the scope of details of the waterfront edge, which define the quality of the contact point between the built structure and the water level. Building three additional levels of anti-flood protections entailed the application of specific typologies of public spaces, as well as typologies of development, which allowed to introduce full protection of the internal structure.

An element, which proved to be an essential assumption in this respect, was combining these two components – through gradually increasing water levels the fluidity of contact with water was made possible, simultaneously blurring the considerable difference in the altitude of the public space associated with entrances to buildings fulfilling residential and service functions.

Fig. 2. HafenCity Hamburg. The development plan of the former port area (source: [15])

Fig. 3. Fragment of the structure of the waterfront – Magellan Terassen (photo by A. Matusik)

2.2. Sluseholmen, Copenhagen: to live by water

Life 'on water' is the domain strongly bound with the way the Danish society functions, and how its customs and sense of identity are stimulated. The example of Copenhagen illustrates how the use of plans to regulate the shoreline – its incredibly deep modification – has allowed for the traditional functioning of the new residential structure. The post-industrial peninsula Sluseholmen, located in the southern part of the city, has been subjected

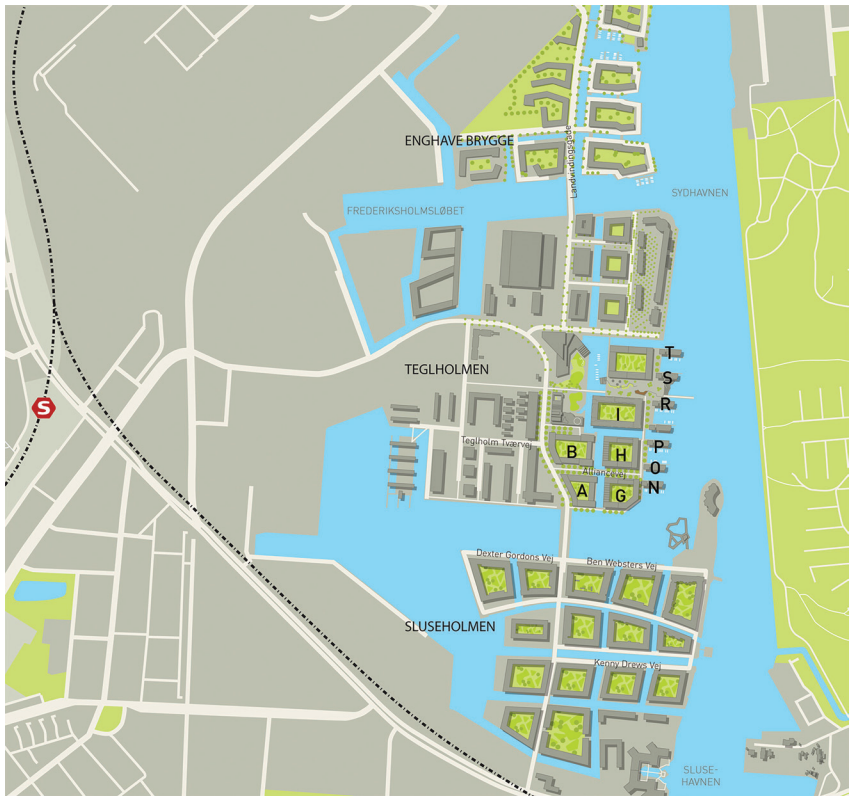

Fig. 4. Copenhagen, Sydhavn. Land development plan (source: [16])

Fig. 5. Copenhagen, Sluseholmen – view on the urban structure (source: [17])

to such modifications[1]. A strategic assumption was to adopt the principle of cutting the land and preparing the infrastructure in a way that would enable each of the urban blocks to have direct contact with the water space. The water canals, embedded deeply into the structure, become a natural extension of the public space connected with the publicly accessible squares and pedestrian routes, as well as of the semi-public/semi-private space, connected with the interiors of the development blocks.

3. Naturalisation of waterfronts of urban sections of river valleys

Protection of the natural landscape of the river within urban zones becomes a prerequisite in the situation of more and more dynamic urbanisation processes. This trend remains in close relation with the model of an ecological city, the importance of which in the contemporary urban planning has been constantly growing. Maintaining the natural landscape, often connected with the leading framegenic elements for the city, constitutes a fundamental part of this model. Simultaneously, the natural system of the city the essential part of which is a river and watercourses accompanying it, becomes a subject of attempts of aggressive city sprawl processes to take it over. Its protection is connected with not only local policies, but also – or even most of all – with supralocal ones.

The element that becomes a prerequisite in this respect is forming a clear natural (hydrological)/urban system, guaranteeing safe co-existence of these two layers of the city [14, pp. 80–87]. This forming takes place in the macro scale, covering the entire urban structure, as well as in the micro scale, which constitutes a solution of structures in the local context.

4. Macroscale – systems of river parks

One of the possibilities of moulding a coherent system is the creation of a system of river valleys linked with a system of green corridors. Such practices were adopted e.g. in Cracow and Warsaw, where the Vistula became the axis for a system of parks, combining urban areas of the city with the open landscape [14, pp. 82, 85]. The system of parks based on the restored natural river ecosystem is also proposed in the strategy of the transformation of Zaragoza. Protection of the natural system becomes not only a tool that moulds the internal structure of the city. A very distinct form of this tool being applied is shaping peripheral, nearly border areas.

A classic example of such transformations is the project of a park along the river Besos in Barcelona. Recultivation of the river itself, and next organising a natural park along its entire urban section was a huge success. Restoring the natural corridor of the river had its economic as well as ecological consequences. The park, with the clearly separated tidal frame, became an element of special and social/functional integration of the north-eastern suburbs of Barcelona and its neighbouring communes. High-quality public recreation spaces had their effect on increasing the economic values of adjacent areas. At the same time, in the

[1] Sluseholen, Copenhagen: urban planning design – Arkitema Architects + Sjoerd Soeters, 2008.

supralocal scale, this park is included in an ecological natural system linking mountainous areas which constitute natural limits of Barcelona from the north-east, with the seashore closing it from the south-west. Recultivation of the valley of the river Besos brought about an increased interest in the surrounding areas. Previously perceived as suburban, associated with a disadvantageous situation of being locked between a degraded watercourse and huge road infrastructure, today these areas are an extremely desired location in the city. The example in this respect is a project of a big residential complex La Catalana[2].

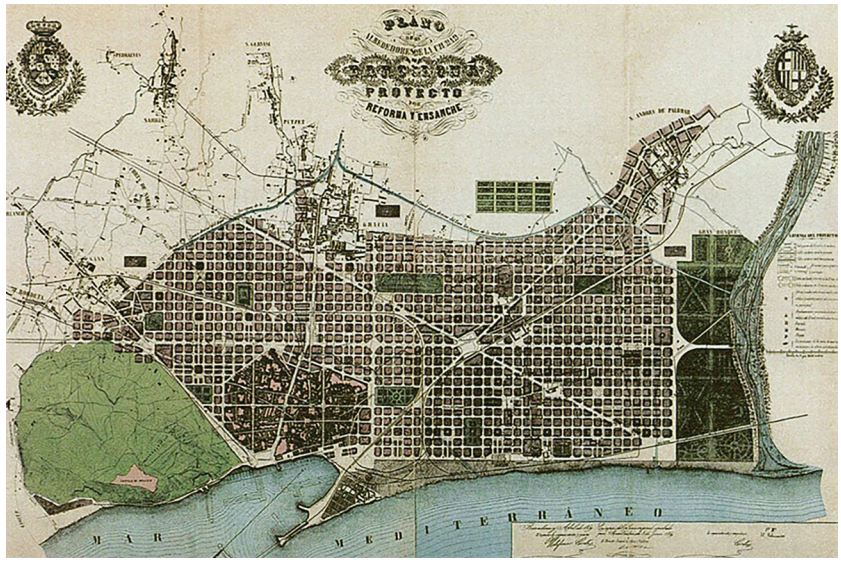

Fig. 6. Barcelona 1859, a map of Ildefons Cerdà – visible canal of the river Besos along with the park (source: [2, p. 127])

Fig. 7. Barcelona, 2001 – design of the transformation of the valley of the river Besos (source: [10, p. 96])

[2] This complex has contributed to a considerable change of the image of this part of Barcelona. On one hand open to natural spaces of the water park of the Besos, on the other it is closed with a linear park separating it from the city ring road [cf. 10, p. 96].

5. Microscale – green waterfronts (Hunters Point and Houtan Park)

The awareness of the need to protect the river landscape and building an urban model on its basis is not only the domain of the macro-scale policy. More and more cities conduct operations focusing on the renewal and recovery of natural water edges along selected sections. These tendencies can be particularly clearly visible against the background of such dense urban structures as New York, or Shanghai.

Both cities referred to above bear traces of their industrial past. Despite the fact that the cities have different geopolitical conditions, both New York and Shanghai can be proud of similar projects devoted to the ecological protection of waterfronts. The definition of a new edge in these two cities, so culturally different, is surprisingly similar. The waterfront of Hunters Point in New York, as well as the waterfront within the limits of Houtan Park in Shanghai, demonstrate a new ecological standpoint, and for this reason, they have become a specific urban manifesto.

The vision of the spatial development of New York 2020 defines the basic directions of the urban policy, aiming to demonstrate natural values of the urban structure deriving from its location. The flagship example of this direction is the project of Hunters Point. The structure of the waterfront, once dominated by railway infrastructure servicing the port and generating the export-related 'to be or not to be' of New York, was transformed into a wild municipal garden. The very area of Hunters Point is a place of predominantly dense residential development. The new waterfront, based mainly on natural forms of greenery, with the ecosystem playing the main role, was designed predominantly to serve this area as a kind of counterpoint. In line with the key assumptions, the post-industrial past represented by preserved relics and remains of the old infrastructure clashes here with the water edge, restored in its natural form. Along with it, a system of greenery was organised, embedded in the structure of the city and linking the waterfront itself with it.

A similar approach to shaping the waterfront line is proposed by Shanghai, making use of the potential offered by a great event of EXPO 2010 [1, pp. 104–133]. An integral element

Fig. 8a. Hunters Point New York. Waterfront development concept of the green waterfront, 2010 (source: [18])

Fig. 8b. Hunters Point, New York. Waterfront's view (photo by A. Matusik)

Fig. 9a. Huntan Park, Shanghai (source: [19])

Fig. 9b. Huntan Park, Shanghai. View on a fragment of the green – water structure of the waterfront (source: [19])

of the exhibition grounds is the project of a waterfront park – Houtan Park[3]. The strategy of the project is based on the recultivation of polluted banks and waters of the river Huangpu through the creation of a boggy ecosystem filtering rainwater, and at the same time acting as a buffer zone of the anti-flood protection. This very attractive solution of technical issues is also connected with the introduction of new forms of use of urban public spaces, such as e.g. urban agriculture.

6. Summary

Urban planning measures implemented in areas of river valleys in their urban sections become a stronger and stronger driving force in the process of creating visions for the future of urban structures. Their special meaning needs to be perceived in their position described by Anna Januchta-Szostak as "a keystone of anthropogenic and biocentric systems" [7, p. 92]. As spaces inseparably associated with the effect of climatic changes, they become a testing field for projects interpreting and predicting threats resulting from them. At the same time, the increasing ecological awareness imposes new forms of waterfronts, never encountered so far. All these factors, interconnected and dynamically harmonised, created contemporary hydrological / urban systems. The dominating meaning of such systems is their ability to transform – a desired aspect, allowing to mould the image of the contemporary city creatively and flexibly.

The constantly growing dynamics of transformations of urban structures are accompanied with the need to control the relation between the built and the natural: "balancing the needs of man and nature, defining relations between developed and open areas, including green areas, and finally, an appropriate attitude towards hydrological issues when designing cities" [11, p. 8] – these are ones of key issues for spatial and urban planning, as well as for architecture itself. Focusing on contemporary ways in which urban sections of river valleys are developed,

[3] Design: Turenscape, 2010.

one can clearly see a reflection of tendencies referring to the problem of the co-existence of the urban structure and the matter of the natural environment.

Referring to the aspects described above, one can conclude that their fulfilment becomes a prerequisite for the functioning of the city of the future, perceived as an eco-city. Regarded through the prism of competitiveness, the city faces a challenge of taking care of its 'skeleton' – the hydrological/urban system, which is a guarantee for stable water management, as well as for the high quality of life of the contemporary man.

References

[1] Burdett R., Sudjic D., *The endless city*., Phaidon Press Ltd, 2007.
[2] Busquets J., *Barcelona. The urban evolution of a compact city*, Harvard University, Nicolodi, Rovereto 2006.
[3] Charlesworth E., *City Edge. Case Studies in Contemporary Urbanism*, Architectural Press, 2005.
[4] Gonzalez Gonzalez M.J., Lopez Gonzalez A., *Strategic planning and change management. Examples of Barcelona, Seville and Saragossa (Spain)*, Bulletin of Geography. Socio-economics series, 2015, No. 29, 47–64.
[5] Gzell S., *Wykłady o współczesnej urbanistyce*, Politechnika Warszawska, Warszawa 2015.
[6] Hölzer Ch., Hundt T., Lüke C., Hamm O.G., *Riverscapes. Designing Urban Embankments*, Birkhäuser Verlag 2008.
[7] Januchta-Szostak A., *Usługi ekosystemów wodnych w miastach*, Politechnika Poznańska, Poznań.
[8] Januchta-Szostak A., Biedermann A., *The impact of great cultural projects on the transformation of urban water-side spaces*, Technical Transactions, 1-A/2014, 69–88.
[9] Marshall R. (red.), *Waterfronts in Post-Industrial Cities*, Spon Press, 2001.
[10] Marti C., Casas E., Vicente E., Marti J., Rubert M., Campillio J., Figuerola G., Gimeno V., Dalmau J.A., Gibert C., Freijo P., *Barcelona, Transformación. Planes y Proyectos*, Ajuntament de Barcelona, Barcelona 2008.
[11] Solarek K., Ryńska E.D., Mirecka M., *Urbanistyka i architektura w zintegrowanym gospodarowaniu wodami*, Politechnika Warszawska, Warszawa 2016.
[12] Stern R.A.M., Fishman D., Tilove J., *New York 2000. Architecture and Urbanism Between the Bicentennial and the Millenium*, The Monacelli Press, New York 2000.
[13] *Water Plan 2 Rotterdam. City of Rotterdam 2007*, https://www.rotterdam.nl/wonen-leven/waterplan-2/Waterplan-2-samenvatting-Engels.pdf (access: 10.07.2017).
[14] Ziobrowski Z., *Urbanistyczne wymiary miast*, Institute of Urban Development, Kraków 2012.
[15] http://www.hamburg.de/stadtplanung/projekte/hafencity (access: 15.08.2017).
[16] http://www.skyscrapercity.com/showthread.php?t=1495544&page=17 (access: 15.08.2017).

[17] https://www.google.pl/earch?q=copenhagen+sluseholmen&source=lnms&tbm=isch&sa=X&ved=0ahUKEwjAqOmfs9nWAhXQzRoKHeQwDjkQ_AUICygC&biw=1366&bih=588#imgrc=K9TSmnYesFU-BM (access: 16.08.2017).
[18] http://waterfrontalliance.org/2015/10/08/waterfront-alliance-celebrates-archtober (access: 16.08.2017).
[19] https://www.designboom.com/architecture/turenscape-shanghai-houtan-park-best-landscape-project-at-waf-2010 (access: 16.08.2017).

TECHNICAL TRANSACTIONS 2/2018
ARCHITECTURE AND URBAN PLANNING
DOI: 10.4467/2353737XCT.18.021.7994
SUBMISSION OF THE FINAL VERSION: 16/1/2018

Urszula Nowacka-Rejzner (nowacka.rejzner@gmail.com)
Institute of City and Regional Planning, Faculty of Architecture, Cracow University of Technology

Water in the creation of revitalised urban areas. The case of King's Cross Central

Woda w kreacji rewitalizowanych obszarów miejskich. Przykład King's Cross Central

Abstract

The case study selected to illustrate the author's considerations is the area in the northern part of London – the site of the next stage of the King's Cross Central revitalisation project. The site has been selected mostly because of its location in the close vicinity of the historic centre of the city and because of its valuable cultural and natural assets. The author discusses the spatial transformations of the area focusing primarily on various options of using the qualities and properties of water and its relations with elements of built environment and greenery in shaping urban spaces of a new quality, yet preserving their identity.

Keywords: revitalisation, public space, water components

Streszczenie:

Jako przykład rozważań wybrano tereny w północnej części Londynu, na których jest realizowany kolejny etap projektu rewitalizacyjnego King's Cross Central. Istotnym kryterium wyboru przykładu do badań było położenie rewitalizowanego terenu w bliskim sąsiedztwie historycznego centrum miasta, a także cenne walory kulturowe i przyrodnicze obszaru. Na tle zarysowanych przemian przestrzennych obszaru szczególną uwagę zwrócono na różnorodne możliwości wykorzystania cech i właściwości wody i jej relacji z elementami środowiska zbudowanego i zielenią w kształtowaniu nowej jakości przestrzeni miejskiej i zachowaniu jej tożsamości.

Słowa kluczowe: rewitalizacja, przestrzeń publiczna, elementy wodne

1. Introduction

The New Athens Charter of 2003, outlining the vision of the European cities of the 21st century, speaks of the need to create high-quality sustainable urban structures: "cities, which will connect the past with the future, through a vital and vibrant present" [7, p. 14]. The need to preserve, protect and make a full use of the cultural heritage and natural resources in urban areas has also been emphasised in the Charter of European Planning, Barcelona 2013, where we may find the proposition that: "The relationship between people and their environment is fundamental. It builds a shared identity and quality of life that is based on a shared cultural and natural heritage" [8, p. 8].

Elements of nature occupy a prominent place among the components shaping a space for living, work or leisure, i.e. components determining the quality of the urban environment. One of such elements is water. Nowadays, water is present as an important ingredient making up spaces of urban squares, parks, new housing developments and revitalised former industrial sites alike, not only in their compositional aspect. It is precisely the diverse use of water components in designing developments and public spaces in European cities that has primarily defined their beauty and high quality.

The specific role and various applications of water components in urban spaces, the way they affect humans and the environment we live in, all result from the special character of water – its unique physical features, which are so distinctly different from other components making up the world around us.

2. London – the city with "water history"

Water has always been a part of London history. The "water history" of London has been mostly created by the Thames, its tributaries and the London docks and canals. The London Docklands used to be the symbol of British economic power until the early 20th century. Closing the first dock in 1960 started the slow decline of this once the largest port in the world and the multi-aspect degradation of its area. The early 80s marked a new beginning in the history of London Docklands – the docks and canals were subjected to a complete make-over and they re-emerged as an important component of the city life and image[1]. Considerable transformations also took place in other waterfront areas, e.g. on the Thames or in the valley of the Lee River.

For several years now, the Thames, together with its tributaries of different sizes as well as the channelised sections of the rivers and streams, channels, docks and quiescent water reservoirs of various origin, have been covered by the programme *The Blue Ribbon Network*. The programme is a part of the authorities' policy related to putting London waterways to a new use and the principles governing the shaping and protection of their environment,

[1] The issue was discussed, among others, by S. Kaczmarek in [2].

comprised in *The London Plan*[2]. The document points out not only to the need to put the waterways to transportation, recreation or tourist use, but also to the need of protection and reconstruction of waterfront habitats, floodplains and landscapes. Strong emphasis has also been put on the need to protect and utilise properly the preserved buildings and technical infrastructure components contributing to the identity of these areas.

An important part of this blue network is Regent's Canal – a listed industrial monument and a unique area of greenery and water situated on the edge of the strict centre of one of the largest European metropolises. The plan to build the canal was part of a larger project of 1811, authored by John Nash, featuring development of the areas in north London. The decision to build the canal to the design by Nash was made in 1812. It was executed in two stages. The first section – between Paddington and Camden – was opened for navigation in 1816, and the remaining part was put into operation in 1820. The canal was performing the role of a transportation route until 1969, and the goods transported on its waters included *inter alia* coal, grain and building materials brought to London by rail from northern England.

The barges navigating the canal at present are playing a different role – they transport tourists or provide an alternative, increasingly more popular form of habitation. The almost 14 km long water course, cutting through nearly the centre of the city[3] is now beginning to be seen as a special asset. The areas neighbouring on the canal are becoming an attractive place for living, e.g. the area of Primrose Hill or the district of Marylebone, lying on the southern bank of Regent's Canal, between Paddington and Camden. Restaurants, cafés, music clubs and pubs located in revitalised former industrial facilities all open up to the riverfront areas. The former towpath along the bank of the canal is now a route for pedestrians and cyclists. Waterfront areas are a place for recreation, socialising and events of various kinds, such as e.g. festivals organised in Little Venice promoting living on barges.

Areas in the vicinity of Regent's Canal have undergone a special transformation in the recent few years; the area to the north of King's Cross and St. Pancras Railway Stations is the site of the project *King's Cross Central* implemented here for several years now[4]. Accepted towards the end of 2006, the plan to redevelop these areas, amounting to 27 ha in size, featured two components: one referring to *King's Cross Central. Main Site* and the other to *King's Cross Central. Triangle Site.* According to the design guiding principles[5], the new urban space, which has been under construction since 2007, is going to offer a rich and varied range of functions as well as a number of interesting solutions regarding public spaces design, architecture and environmental protection, it is also to be easily accessible for all and attractive for tourists [3, p. 28]. As regards public spaces, the revitalisation project stipulates the creation of a network of commons. The combined area of the squares, pedestrian routes, parks, gardens and avenues

---

2 See: *London's Living Spaces and Places. Blue Ribbon Network*, Policy 7.24 – Policy 7.30 [9, p. 325–335], Map 7.5 Blue Ribbon Network [9, p. 325].

3 Regent's Canal connects Grand Union Canal in the area of Paddington Railway Station with the Thames in the area of Limehouse Basin in the eastern part of London.

4 Since 2008, the owner of the area under revitalisation has been King's Cross Central Limited Partnership.

5 The landscaping concept was developed by Townshend Landscape Architects, the master plan was authored by Allies and Morrison & Porphyrios Associates.

making up this network is to constitute 40% of the revitalised site total area. One undoubtedly striking feature of the designs of individual public spaces is the large and diverse contribution of water and greenery to their overall composition.

A water element that makes a particularly strong presence in the area now being revitalised is Regent's Canal. The Canal runs across the centre of the area and cuts it into two parts – the northern part and the much smaller southern one. At the same time, along the direction of the flowing water, it connects the areas of two boroughs in its vicinity: Camden to the west and Islington to the east. The connecting element is the towpath, once used for towing barges along the canal, now – a popular pedestrian and cycling route. This characteristic location of the canal both in the space of the whole city and within the revitalised area has made it an important component of the whole new project and, simultaneously, a special reference point for the currently created public spaces of this new urban development.

3. Regent's Canal – a corridor filled with greenery and water – an urban public space

The revitalised area contains the section of Regent's Canal between St. Pancras Dry Dock and the bridge in York Way[6]. Just outside the area covered by the revitalisation project, the canal opens up to form Battlebridge Basin, on the waters of which is situated the building of the former ice warehouse built in the 1860s – since 1992 the house of the London Canal Museum presenting the history of London waterways.

The waters of the canal and the areas in its direct vicinity together create a new urban space, which is, at the same time, a water space and a space open to water. Water is not only a route for cruise barges, but, first, it plays an important role in shaping spatial, compositional and functional relations of this new urban development; it significantly influences the microclimate of the area. Both the water corridor itself and the areas directly adjacent to it are also the scene of numerous artistic and environmental activities. The new public spaces, which have already been opened for use in the direct neighbourhood of the canal, are: on its left bank – Gasholder Park, Canalside Steps and Wharf Road Gardens, on its right bank – Camley Street Natural Park.

The facilities and areas on the right bank of the canal play a special role in the promotion of eco-friendly attitudes and actions. It was exactly at this site that the local nature reserve Camley Street Natural Park was established in 1985[7]. The area now occupied by the reserve used to be a coal drop until the late 70s of the 20th century. At present, the narrow strip of land of merely 0.8 ha, characterised by large biodiversity, plays an important role in the provision of environmental education. This special place offers contact with nature only a 5-minute walk away from the busiest place in London, which is the area of King's Cross railway station. Just

[6] The canal in this area initially runs parallel to Camley Street, then it turns at the almost right angle to the east and runs parallel to Goods Way up to the bridge in York Way.

[7] The park is one of 142 local nature reserves in the area of London (data as of the 11th June 2014, according to the list published by Natural England).

at the bank of the canal, the reserve features two small water reservoirs – hidden in greenery and surrounded by wetland vegetation. The wooden bridge that separates them is fitted with seating areas, which encourage visitors to pause and relax, especially so that the bridge offers the opportunity to look down the canal from a unique perspective.

A narrow path leads from the reserve area down to the waters of the canal, where, since February 2002, an unusual object has been located – a floating platform called *Viewpoint*. In spite of its small size, the geometric form, with walls in the colour of rusty orange, is clearly visible against the background of Camley Street Natural Park greenery and the waters of the canal. The platform, featuring triangular walls sheltering seating places within, has been fixed to the canal bank with the use of a steel structure. The outer side of the walls has been clad in corten steel, whereas the inner side, for the sake of acoustics, with wood, similarly to the seating areas placed between the walls. Small triangular openings have been cut in the walls at various heights offering unique views of the canal and its surrounding wildlife. The platform floor is made of grey concrete slabs decorated with a pattern resembling bird and animal footprints. The *Viewpoint* floating platform is a place for organising workshops and meetings, a chance to experience close contact with the natural environment without interfering into its functioning. The authors of this object, which is an artistic contribution to the ongoing discussion on the relations between the built environment and nature are a team of young Finnish architects: Erkko Aarti, Arto Ollila and Mikki Ristola. The design was developed under the auspices of the Finnish Institute in London and the Architecture Foundation, in cooperation with the London Wildlife Trust, within the framework of Finland UK_Exchange Project dedicated to young architects in Finland and the UK who are especially interested in the problems of shaping the relations between water and the city.

Since August 2014, there have been four more floating objects to be seen on the waters of the canal in the vicinity of the viewing platform. Artificially created floating islands are covered by carefully selected species of water plants. The roots of the plants cleanse the water, at the same time providing habitat for water wildlife. The above-ground parts of the plants, apart from being aesthetically pleasing, play a function in the canal's ecosystem as they provide shelter and nesting site for birds. The islands are situated in a part of the canal separated from the main stream with buoys.

A little further to the north, there is yet another floating object – Floating Forest Garden – which is moored at the bank of the canal. The garden on a barge, composed of over 100 plant species placed in containers, is part of the project called Wildlife on your Waterways. The project covers the areas adjacent to Regent's Canal in the section between Camden and the Islington Tunnel. The aim of the project is to explore and monitor the habitats existing within this unique waterway. The garden, accessible from the area of the reserve, plays an educational and scientific role, promotes organic farming and eco-friendly lifestyles. A footbridge is due to be built by 2017 in the area where the barge is currently moored, which is to connect the reserve and the new information centre facility planned here with the green area of Gasholder Park situated on the other side of the canal. This exceptional park was opened for use in early 2016. The design of the park by Bell Phillips Architects was selected in the contest resolved in 2009. The park is an interesting combination of King's Cross industrial heritage and

contemporary tendencies in designing green areas. The spatial frame of the park is created by the beautiful cast iron structure of the largest gas container Gasholder No. 8, until the year 2000 functioning as part of the Pancras Gasworks. In 2011, the container structure was disassembled, renovated and, in 2013, reassembled at its present location on the left bank of Regent's Canal, opposite St. Pancras Basin. The area of the park, elevated above the waters of Regent's Canal, is a place offering unique views over the canal, the barges mooring at the basin and the greenery of Camley Street Natural Park (Fig. 1.)

Fig. 1. View over the waters of the canal from the *Viewpoint* platform. Floating islands, barge with the floating garden and the cast iron structure of Gasholder No. 8 are to be seen in the background (photo by U. Nowacka-Rejzner, 2014)

A different aesthetic and visual experience is brought by another space occupying the central place on the left bank of the canal – the Canalside Steps. The function of this space and its relations with the waters of Regent's Canal are also different. Wide concrete terraces stepping down to the waters of the canal have been located at the place where canal barges used to moor if they had some business with the granary building nearby. Now the terraces provide a venue for various small-scale events or happenings. The Canalside Steps are sometimes turned into the audience of a summer cinema, but every day they serve as a resting area for tourists and students of Central Saint Martins University of the Arts (Fig. 2).

The towpath, which as a pedestrian and cycling route running along the left bank of the canal, provides direct visual contact with the waters of the canal and it connects the Canalside Steps with yet another public space created on its waters – Wharf Road Gardens. A slightly inclining ramp running towards Granary Square from the side of the towpath, provides

Fig. 2. View over the Canalside Steps located on the left bank of the canal; in the background the building of Central Saint Martins University of the Arts situated at Granary Square (photo by U. Nowacka-Rejzner, 2014)

convenient access both to the square and to the Wharf Road Gardens space. The green areas may be reached, also from the side of Granary Square, by smoothly outlined pedestrian routes along Regent's Canal. The green expanses of lawns placed at different heights have been enclosed in *frames* made of corten steel. Numerous eateries occupy the area in the close vicinity, some of them spilling out directly into the space of the garden. This is another place to take a break, eat a meal and watch the barges move along the canal. The opportunity is eagerly seized by tourists, Central Saint Martins students and, at lunchtime, by people working in the offices nearby. The garden, opened for users in 2015, was designed by Townshend Landscape Architects in cooperation with Don Person Studio. Wharf Road Gardens are a continuation and a peculiar functional and compositional link to the part of Handyside Gardens, established earlier, which is situated on the canal. Handyside Gardens were the first public garden opened in the revitalised area of King's Cross. It occupies a narrow space between the Art House and the Midlands Goods Shed. A narrow water canal runs through the middle of the garden towards Regent's Canal. The shining stream of water flowing in a bed slightly sunk below the level of the ground takes its origins in the northern part of the gardens, at the playground area, where the water is a great attraction for children and adults alike. The linear shape of the garden has been additionally emphasised by the arrangement of pedestrian routes and the terrain configuration of the site. Similarly to the above-mentioned design, the spatial organisation of this garden makes clear references to the railway heritage of the area in the characteristic outline of the pedestrian routes, which – like railway tracks – run towards the buildings of King's Cross railway station, visible at a distance. The railway function has

also affected the technical solutions applied in the garden design. The railway tunnels running under the garden grounds to King's Cross railway station determined the way in which all vegetation was planted, the selection of species as well as their amount and distribution in the space of the garden. The landscaping design of this garden, similarly to the Wharf Road Gardens design, has been authored by the team of Don Person Studio. The vegetation used by the designer, typical of rail embankments – various grass species, perennials, shrubs and flowers, has been planted on soil piles elevated above the ground. The edges of the piles have been reinforced with corten steel, whose characteristic rusty colour makes a splendid combination with the greenery, at the same time emphasising the industrial character of the site. The garden area also features various forms of seating places: from wooden seats placed at the edges of piles to wave-shaped bent wooden forms resembling reclining chairs placed on the canal banks. The Handyside Gardens project, combined with its functional and spatial complement of Wharf Road Gardens, has created in the vicinity of Regent's Canal a place of special atmosphere – preserving and promoting cultural values of the area – and at the same time a place with modern spatial expression.

Looking at subsequent projects realised in the area of the canal, we get the impression that, designed by an exquisite designer who John Nash certainly was, Regent's Canal is now regaining its exceptional, though functionally different, significance in the structure of the city.

4. Water in the space of the squares and the park

Public spaces in the direct vicinity of Regent's Canal enter into functional and compositional relations with the squares and green areas located a little further away from the canal, together creating a system of public commons. A special place among these areas is occupied by Granary Square, executed to the design by Townshend Landscape Architects.

Due to its location and area, the square is often referred to as the heart of King's Cross. In its southern part, the square opens to the waters of the canal through the Canalside Steps, from the north – through Stable Street – it is connected with Lewis Cubitt Square and Lewis Cubitt Park, and from the east – through Wharf Road Gardens – with Handyside Gardens. The central feature of the Granary Square space is the four rectangular water plazas, whose shapes have been outlined by 1080 water jets placed at equal distances. The plazas have their narrow sides run parallel to the façade of the former granary building, currently used by Central Saint Martins University students, situated at the northern side of the square. Water appears in the space of the square in 100 different computer-controlled choreographic patterns, the majority of which are dynamic routines using intensive colours of the spouts of water. Water fills the space of the square, it is visible and audible, it squirts up to the height of several metres or just a few centimetres, it ripples and sways, rises in the form of mist or with a thin film covers the stone surface of the square creating four water tables. Diverse water arrangements are adjusted to the frequently changing function of the square, which may be a venue for a large open-air event (accommodating up to 2,000 people), a city beach, or a place for concerts, happenings, art installations and light and sound events. The area of the water tables or among

the squirting jets serves as a platform for dancers to practice their routines, for dance shows or simply as a playground for children and adults alike. The designers have created a vibrant, changing and colourful space, which attracts various users: those who like to just watch and those who actively participate in water spectacles or events organised here, always in a unique atmosphere. Water tables in the space of the square are not only a compositional element but they also bring to mind its water-related past – the reloading basin that existed here in the 19th century. Another reference made to the past of this place is the line of the former canal bank worked into its surface and a preserved mooring stanchion. On the other hand, a renovated rail turntable, covered with a glass panel, located in the north-western part of the square, and a preserved part of the former railway track are reminders of the industrial and rail history of Granary Square. Opening the square to the waters of the canal by the terraces of the Canalside Steps makes the space seem even larger (Fig. 3).

Fig. 3. Granary Square (photo by U. Nowacka-Rejzner, 2014)

Two new public spaces featuring water elements have been created in the vicinity of Granary Square, to the north-west of the square. The first of these spaces is Lewis Cubitt Square[8]. The place is connected with Granary Square by Stable Street, which is in turn separated from Lewis Cubitt Square by a green strip of trees, shrubs and various species of perennials with semi-circular enclaves hiding seating areas opened towards the square and the main pedestrian route cutting across the square. A row of wide wooden benches separates

[8] The square has been designed by Laurie Olin, who is also the author of *inter alia* Bryant Park in Manhattan, New York.

the route from the main area of the square. The linear arrangement of the wooden seats and their distribution is repeated in the arrangement and distribution of five water tables, which have been located in the eastern part of the square. Smooth water tables, like mirrors, reflect the sky and the street furniture featured on the square. Yet, they are not the only water attraction in this space. The designer has also proposed using other qualities of water – its movement and changeability. The water tables outlined in the grey stone paving of the square are accompanied by water jets, placed in two rows along their longer sides, which squirt water to make a water tunnel. The arched water spouts squirting from 55 jets are illuminated at night with white light focused on the water streams highlighting water drops flying through the air. The water jets applied in the space of the square, typical of this designer, are an attraction not only for children, who, as long as the weather conditions are favourable, never want to leave this place. The square, which may accommodate 2,000 people, is a place of recreation and play, but also a venue for various events and happenings. Concerts are organised here, there is an open-air cinema. In June 2015, the square housed a festival of architecture and art, which brought two characteristic pavilions – a yellow and a red one – into its space (Fig. 4).

A green extension of Lewis Cubitt Square to the north is Lewis Cubitt Part[9] open to users since 2015, the main green common of the revitalised area in King's Cross. The park has the shape of a rectangle of the area equal to 0.65 ha. On both sides of the park, the ground has been raised along longer ends. The gentle variation of the ground levels, defined by soft elevation lines, outlines subtly semi-private places in the space of the park encouraging individual relaxation and leisure.

Fig. 4. Water in the space of Lewis Cubitt Square (photo by U. Nowacka-Rejzner, 2014)

[9] The park was created to the design of Townshend Landscape Architects.

At present, the greatest attraction in this part of the King's Cross revitalised area is the pond[10] situated at the end of the green space of Lewis Cubitt Park and with a building site in the adjacent area. The water reservoir, open for use on the 15th May 2015, is a temporary art installation[11] promoting water recycling realised within the framework of Relay Arts Programme. Water in the pond is cleansed in a closed cycle with the use of various species of water plants. Vegetation typical of wetland has been planted to the north of the pond, in its direct vicinity. Similarly to the floating islands placed on the waters of Regent's Canal, the Floating Forest Garden or the *Viewpoint* floating platform, the pond is to draw attention to the dependencies and mutual relations between humans and the natural environment as well as to the results human activity brings to the environment. It is yet another place to stop and look for the answer to the question what significance has sustainable development, where is the place for humans, water and greenery in the space of the city. Simply by staying in this space of water and greenery and by looking at it and at the neighbouring building site from the viewing platform located on the northern side of the pond, visitors have the possibility of watching the ongoing transformations and, in a certain way, participating in them (Fig. 5).

Fig. 5. Art installation *Of Soil and Water: King's Cross Pond Club* in the area of Lewis Cubitt Park (photo by U. Nowacka-Rejzner, 2015)

[10] The "natural" bathing pond is 40 m long, 10 m wide and it is elevated approx. 2 m above the level of the ground.

[11] The authors of the project called *Of Soil and Water: King's Cross Pond Club* are: Eva Pfannes and Sylvain Hartenberg of Ooze Architects from Rotterdam and Marjetica Potrč.

An example of how the phenomenon of water may be used differently in arranging an urban space is Pancras Square, opened to the public in 2015[12]. The difference in ground levels between the two ends of this little triangular square of the area amounting to mere 0.4 ha (from the side of Regent's Canal to King's Cross railway station) is several metres. This terrain configuration has been used for creating an extremely interesting water feature. The designers proposed placing three water elements in the space of the square at different levels and shifted sideways in relation to each other. Each of these elements is composed of water cascades separated by flat shallow pools. Such spatial arrangement of the water elements and their form results in that the water feature seems different depending on the place from which it is viewed. When we enter the square from the Gateway of Battle Bridge, we see a very dynamic water system created by water cascades flowing towards us from the side of Regent's Canal. We get the impression that the water flows down from the canal and from the main public space in King's Cross – Granary Square. The same space seen from the north is completely different, water cascades are invisible, and the stepped terraces of water pools create a mirror floor reflecting the greenery of the square and the architecture flanking this urban enclosure. An important component, making this space a top-quality realisation, is the vegetation filling the terraces of the square – carefully selected and sculptured, along with the elements of street furniture. The square lighting design also deserves to be mentioned as it showcases the characteristic components of the water feature and emphasises the arrangement of greenery.

Fig. 6. Pancras Square (photo by U. Nowacka-Rejzner, 2015)

[12] This is yet another project realised in the revitalised area under consideration that has been designed by landscape architects of Townshend Landscape Architects.

The square is both a route leading from King's Cross station to Regent's Canal, flanked by water and greenery, and a place to relax and enjoy services offered by the facilities located at ground floors of the buildings surrounding the square (Fig. 6).

In the future, a footbridge is to connect the square with Granary Square, situated on the left bank of the canal, which will result in creating a chain of public commons – from Granary Square, through Pancras Square and Battle Bridge Place up to King's Cross Square outside King's Cross railway station. At present, the major pedestrian traffic from the area of Granary Square towards King's Cross station takes place over King's Bridge and further on along green King's Boulevard.

5. Summary and conclusions

The water world of King's Cross is created by the waters of the canal and the water features located in the squares, parks and gardens emerging in the area now being revitalised. Water takes different forms in these spaces: brooks, mirrors, cascades or jets, it lures visitors with its murmur and light reflexes, brings cool refreshment, relaxation and vibrancy into the spaces of the squares and green commons, reminds us of the incessant change going on in nature.

The organisation of the canal waterfront areas, as well as the form of the water features installed in the analysed public spaces, promote the creation of diverse relations between water and its users. The options include both direct contact with water – touching it, playing with it or participating in the happenings taking place on water plazas – and more passive visual contact by watching artistic actions performed in the squares or in the space of the canal from various perspectives – from King's Bridge, from the Canalside Steps or from the boulevards of Wharf Road Gardens. A special cognitive experience is a participation in the project *Of Soil and Water: King's Cross Pond Club*. A more intimate form of contact with water spaces: observation and learning the rules and conditions of water eco-systems' functioning, is offered by footbridges over water reservoirs in the area of Camley Street Natural Park and, on the waters of the canal, by the *Viewpoint* floating platform and the barge with Floating Forest Garden on it.

Offering various forms of contact with water – from visual to direct – makes water something more than just a component of the composition; it also acquires a cognitive and educational role, encourages and inspires various types of activity.

Special attention should also be paid to the various ways water elements highlight the identity of the now revitalised area, both the one related to water and rail transportation and the industrial one related to the Imperial Gas Light and Coke Company operating in this area in the past. Water also plays an important role in promoting sustainable development of urban structures and creating adequate relations between man and nature. This is precisely the function of the objects located on the waters of the canal, which have been discussed above: the floating islands, the *Viewpoint* platform, Floating Forest Garden and the art installation in the green space of Lewis Cubitt Park.

The projects listed above, which combine in an interesting way the 19th-century industrial heritage of the area and its natural assets, may certainly provide inspiration for seeking innovative design solutions in areas to be revitalised.

The way in which the whole process of the project execution and promotion among the general public is approached may also be an inspiration to implement similar solutions. Since the moment when this long-term project realisation was first initiated, the building site has been treated as an attractive public space and the area where both the industrial past of the site and the contemporary design solutions implemented now could be effectively promoted. There is a system of signposted routes leading to individual public spaces or facilities that have already been completed, which ensures a safe and attractive way of moving around the building site. The system of informing the public of the whole project and the individual stages of its execution also works extraordinarily well, all the desired information is to be found at King's Cross Visitor Centre. There is also an option of viewing the areas under revitalisation from specially built viewing platforms, e.g. the one located on King's Boulevard. Londoners and tourists alike have thus a unique opportunity to participate in the ongoing process of revitalisation of this space, to watch the transformation as it is happening and to use the individual parts of the redevelopment as they are opened to the public one after another.

Besides improving the image of the area, the revitalisation project has also brought environmental, social and economic benefits, to which the various water arrangements installed in the discussed public spaces contributed considerably.

It must be emphasised that water has enormous potential when it comes to the creation of urban spaces, which potential is still not quite fully exploited. New projects, emerging incessantly, proposing ever more ingenious admirable artistic and technological solutions are examples illustrating the above statement.

References

[1] Drapella-Hermansdorfer A., *Zieleń – woda – recykling przestrzeni: Wybrane aspekty przyrodniczej rewitalizacji miast,* Teka Komisji Architektury, Urbanistyki i Studiów Krajobrazowych – OL PAN, I/2005, 35–43.

[2] Kaczmarek S., *Rewitalizacja terenów poprzemysłowych: nowy wymiar w rozwoju miast.* Wydawnictwo Uniwersytetu Łódzkiego, Łódź 2001.

[3] *King's Cross Opportuity Area Planning & Development Brief.* Islington and Camden, London January 2004, https://www.camden.gov.uk/ccm/cms-service/download/assey?asset_id=2849324, (access: 15.09.2016).

[4] Nyka L., *Architektura i woda – przekraczanie granic,* Wydawnictwo Politechniki Gdańskiej, Gdańsk 2013.

[5] *Rewitalizacja miast w Wielkiej Brytanii,* [in:] *Rewitalizacja miast polskich,* vol. 1, R. Guzik (ed.), Instytut Rozwoju Miast, Kraków 2009.

[6] Społeczne i krajobrazowe *walory wody w środowisku miejskim*, [in:] *Woda w krajobrazie miasta-Water in the Townscape*, Vol. 3, A. Januchta-Szostak (ed.), Wydawnictwo Politechniki Poznańskiej, Poznań 2011.
[7] *The New Charter of Athens 2003. Vision for Cities in the 21st Century*, the European Council of Town Planners, Lisbon, 20th November, 2003; http://www.ectp-ceu.eu/index.php/en/?id=85 (access: 15.09.2016).
[8] The Charter of European Planning, Barcelona 2013. The Vision for Cities and Regions – Territories of Europe in the 21st Century, the European Council of Urban Planners; http://www.ectp-ceu.eu/images/stories/PDF-docs/The%20Charter%20of%20European%20Planning-LowResV2.pdf (access: 15.09. 2016).
[9] *The London Plan. The Spatial Development Strategy for London. Consolidated with Alterations Since 2011*. Greater London Authority, March 2016; htpps://www.london.gov.uk/sites/default/files/the_london_plan_malp_final_for_web-0606_0.pdf, (access: 15.09.2016).
[10] Węcławowicz-Gyurkovich E., *Woda w mieście jako przestrzeń publiczna*, Czasopismo Techniczne, 3-A/2010, 281–287.
[11] *Woda w mieście*, [in:] *Zrównoważony Rozwój – Zastosowania,* No. 5, T. Bergier, J. Kronenberg, I. Wagner (eds.), Fundacja Sendzimira, Kraków 2014.
[12] https://www.london.gov.uk (access: 15.09.2016).
[13] https://www.opsi.gov.uk (access: 15.09.2016).
[14] https://www.kingscross.co.uk (access: 15.09.2016).

TECHNICAL TRANSACTIONS 2/2018
ARCHITECTURE AND URBAN PLANNING
DOI: 10.4467/2353737XCT.18.022.7995
SUBMISSION OF THE FINAL VERSION: 18/1/2018

Rafał Zieliński (rzielinski@pk.edu.pl)
Division of Descriptive Geometry, Technical Drawing & Engineering Graphic, Faculty of Architecture, Cracow University of Technology

The issue of the linearity of the waterfront based on the redevelopment of Lyon's river banks

Zagadnienie liniowości nabrzeża na podstawie przemian brzegowych Lyonu

Abstract

The article discusses the issue of the redevelopment of Lyon's waterfront areas and long-term development strategy following the process of redevelopment. Owing to the large scope of the operations in question and a radically different approach to the problem of the revitalisation of the areas where the city and water meet, it is possible to conduct comparative analyses by pointing out specific factors, which determine the success of the enterprise. That is why it is reasonable to consider the latest example of redevelopment, which is that of Confluence, a post-industrial district of Lyon. The degree of activation of this peninsula can be related to various factors, which create the linearity of the waterfront.

Keywords: linearity, redevelopment, waterfront, Lyon

Streszczenie

Artykuł dotyczy problematyki rewitalizacji frontów wodnych Lyonu oraz związanemu z nią zagadnieniu liniowości nabrzeża. Dzięki dużemu zakresowi rozwiązań oraz diametralnie różnym podejściom do rewitalizacji styku miasta z wodą można przeprowadzić analizy porównawcze, wskazując konkretne czynniki decydujące o skuteczności inwestycji. W tym celu zasadne staje się odniesienie do najnowszego przykładu transformacji obszarów poprzemysłowych dzielnicy Lyonu, Confluence. Stopień aktywizacji tego półwyspu można stopniować względem czynników tworzących liniowości nabrzeża.

Słowa kluczowe: liniowość, rewitalizacja, front wodny, Lyon

1. Introduction

The second half of the 20th century brought a growing awareness of urban ecology and the need to transform it and bring it closer to the environment. Cities located above water reservoirs began to turn back to forgotten waterfronts that had remained deserted for several decades. The changes also affected the largest French cities, among which Lyon has become a leader. Located between the Saone and the Rhone rivers, this city is characterised by a long coastline. Therefore, the possibility of its re-adaptation and transformation became a huge challenge for the city authorities. With a wide range of solutions and diametrically different approaches to waterfront redevelopment, analyses can be carried out to identify the specific determinants of investment effectiveness. For this purpose, it is reasonable to refer to the linearity of the waterfront and the factors influencing it. By examining the degree of activation of individual districts of Lyon, we can distinguish features contributing to the successful transformation of the waterfront.

2. Degradation of the Lyon waterfront – the need for change

The slow degradation of the Lyon waterfront has been in progress since the 18th century. The Saone waterfront was largely inaccessible since it was built up by houses located directly by the river bank. Due to the slow current, it was only possible to sail and transport goods on this side of Lyon. The waters of the Rhone were much more rapid, making it possible to locate mills near the river. However, the fast current weakened and destroyed the waterfront to a great extent. The second half of the 19th century brought only minor changes involving the reconstruction of several docks and, due to river transport, digging several channels on the Rhone. In the second half of the 20th century, Lyon lost all contact with its rivers. Water transport moved to peripheral ports, while vessels, already reduced in number, disappeared completely from the waterscape of the rivers. A part of the waterfront was degraded due to being cut off by road sections and car parks. The A7 motorway was constructed along the banks of the Rhone, which not only makes contact of the residents with the river impossible now, but also visually spoils a very large section of the waterfront. At the end of the 1980s, the need for change began to be noticed, and major issues and recommendations were identified to restore the city's rivers [1, 2].

3. The Blue Plan – Lyon's new strategy

In 1991, the Lyon City Council adopted the "Blue Plan", a new strategy to bring the rivers Rhone and Saone closer to urban areas. The plan was focused on 27 municipalities and based on integrating their activities. Within a few years, communication was improved along the river bank, creating new cycling and pedestrian trails. In addition, river stops were upgraded or introduced. The implementation of the plan also had an impact on the environmental and

water quality issues as well as the improvement of the quality of life in the river areas. The economic factor was also taken into account, determining the following steps:

- Introduction of water sports on rivers;
- Adaptation of river banks and making them available to residents;
- Restoration of the natural and historical character of the banks [3].

Together with the development of ecological and economic awareness of the residents and city authorities, the scope of the Blue Plan was widened, predicting that the process of restoration of Lyon's rivers would take place in three main spheres:

- Ecology:
  - Protection of the landscape and improvement of the natural heritage quality. The impact of the environment is directly related to the quality of life;
  - Reinforcement or protection of the river banks against floods;
  - Limitation of river pollution.
- Restoration of the river to residents:
  - Preservation of the continuity of communication solutions for pedestrians and cyclists;
  - The inclusion of urban organisations in tourism projects and recreation;
  - Utilisation of the river as a binder connecting municipalities and districts.
- Economy:
  - Support for economic activities in river areas;
  - Development of river transport, water sports and tourism [3].

The Blue Plan became a catalyst for change both for Lyon and for other municipalities, revising the perception of the river's role and becoming the basis for further projects and implementations aimed at restoring the Rhone and Saone to the residents. As a result of growing public awareness among the population and authorities of Lyon, further projects and initiatives were developed:

- Banks of the Rhone project [4, 5];
- Confluence district project – stage I and stage II, at the confluence of the Saone and the Rhone;
- Saone River Project, including the development of the following projects: Rochetaillée and Fontaines promenades, a path at Caluire-et-Cuire, Port Gillet, a promenade at Rambaud docks, the opening of the bridge at Palais de Justice, and others;
- The "Peninsula Terraces" project (les terrasses dela presqu'île) [6].

4. Linearity as the main factor in the revitalisation of the Lyon waterfront – comparison with the transformation of the Lisbon coastline

When comparing large urban planning projects associated with the waterfront, it is helpful to refer to similar implementations that have continued to confirm their success over the past decades since the transformation. A model illustration of an efficient transformation of the waterfront is a section of the Lisbon waterfront, the Oriente district. By analysing this

example, we can distinguish factors that characterise the linearity of this investment, the level of which determines the degree of the waterfront activation, including:

- Earlier analyses and studies of planned revitalisation on a large area – a larger area and development of a wider strategy allows for continuity of investment and avoidance of less effective point-based activities;
- The linearity of investment – connecting the river bank into a coherent whole with a continuous line of pedestrian trails related to recreation;
- Integration of the coastline with the city – boosting the coastline by connecting the river bank to the city with arteries, streets, pedestrian trails, bridges or crossings (e.g. water tram), connected with investment linearity.
- Providing the diversity of functions – thanks to the diversity due to the type and design of buildings, a well-functioning and constantly developing labour and property market has been created. Enriching the space with squares, parks and recreation areas integrates the new part of the city with its adjacent districts;
- A solution of environmental issues and enlargement of green areas – while diversifying the coastline, the recreational areas and parks were not forgotten. Today, they are one of the most popular places visited both by residents and by tourists. This demonstrates the important role of urban greenery and its significance in shaping revitalisation transformations [7].

The definition of linearity refers to the term "linear settlement", a group of buildings located along roads or rivers due to physical limitations such as the coastline. In the context of urban development, thoughts about conscious linear systems were initiated at the end of the 19th century by Soria y Mata. In his plans for Madrid, he proposed an axial system developing in parallel along the main communication line [8]. Linearity is also connected with the concepts of the edge in urban space of the city. In his work "The Image of the City", Kevin Lynch defines the edge as a linear element, the border [9, 10]. Taking into account the example of Lisbon and attempting to characterise the model example of linearity of the waterfront fully integrated with a city, the following factors need to be considered (Fig. 1).

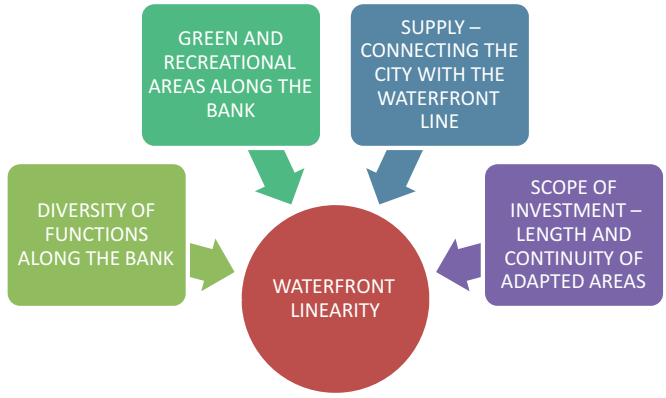

Fig. 1. Waterfront linearity – fundamental factors included in the linearity range and affecting the degree of waterfront activation

The above guidelines can be compared with Lyon's revitalisation plan, and consequently, the evaluation and classification of individual parts thereof. When analysing the waterfront transformation, reference should be made to the specific linearity factors and how they are met. The Confluence peninsula is an excellent example described in the following chapter.

5. Confluence peninsula as an example of the application of the waterfront linearity principle

The adaptation project at the confluence of the Rhone and the Saone, one of the largest urban projects in Europe in recent years, was launched in 1998. It was divided into two stages covering a total of 150 hectares. The first stage began in 2003, covering an area of 41 hectares. The investment was supposed to refer to the industrial character of the place while adapting it to the new infrastructure of the emerging district.

The anticipated end of stage I is supposed to take place in 2018, yet the first effects of the undertaken activities are already visible. Referring to the previously mentioned waterfront linearity pattern and principle, we can characterise the above transformation of the peninsula [11].

5.1. Scope of investment – length and continuity of adapted areas

1.5 km of the waterfront from the Saone's side was changed. The area extends from Confluence Museum to Perrache Station. There are paths and cycling trails along the waterfront, the courses of which are interrupted from both directions due to the A7 and A6 motorways. This issue was partly resolved by the completion of the Raymond-Barre Bridge completed in September 2013, which is a pedestrian walkway with a cycling trail and a tramline, leading to the other banks near the North Sea Park (Parc des Berges Nord). It should be noted that areas where the promenade line has been disturbed and its continuity interrupted are much less activated or not activated at all. As a result, there is a continuation of the promenade provided near the Nautique Square by establishing the Pont des Arts footbridge over the channel. Only this solution allows for continuity and connection with other already revitalised areas at the Rhone (Fig. 2 & 3).

5.2. Boost – connecting the city with the waterfront line

At the completion of stage I of the peninsula revitalisation, some of the areas will remain undeveloped. There is still only one row of office buildings by the promenade, stretching from Confluence Museum to Jean Couty aquatic garden. In this section, we cannot talk about a full boost of the waterfront with of with pedestrian trail axes or streets. The completion of stage II and the construction of residential building and green areas behind the offices will create new connections to the coastline and contribute to greater activation of these areas in the long run.

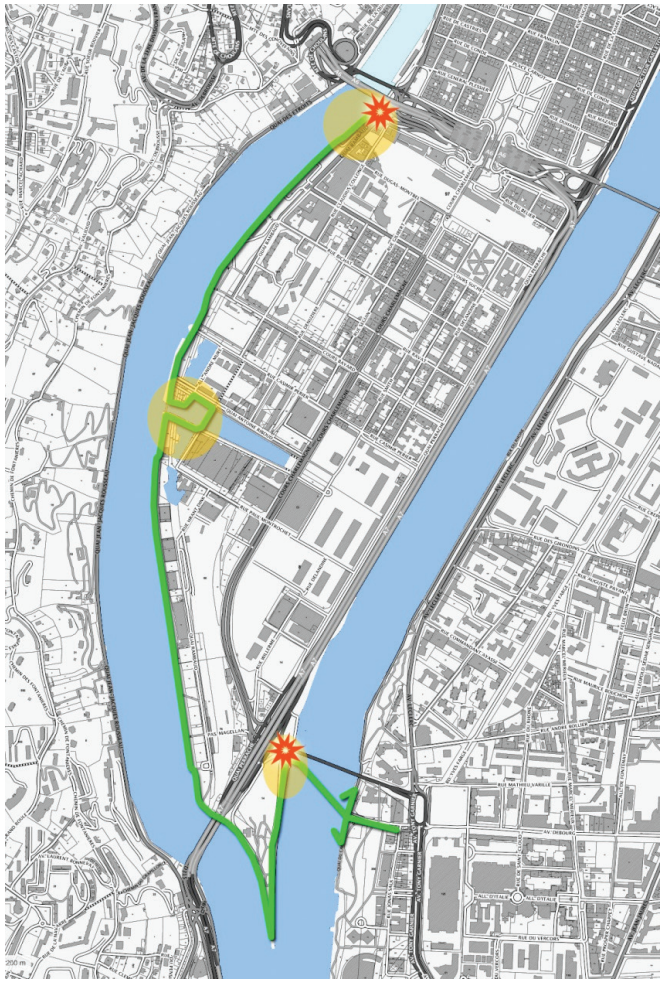

Fig. 2. The scope of investment – length and continuity of adapted areas: a) Green – the line of pedestrian and cycling trails, b) Red – interrupted linearity, c) Orange – disturbed linearity caused by lack of continuity or unusual promenade course (by Rafał Zieliński based on https://www.geoportail.gouv.fr)

Fig. 3. Left: The line of pedestrian and cycling trails near Confluence Museum; Right: Interrupted linearity near Raymond-Barre Bridge (photo by R. Zieliński)

The area that boosts the waterfront more effectively through the pedestrian trails and road sections stretching to the shore begins at the shopping centre above La Place Nautique. Such a combination results in much greater integration with the waterfront. The river bank on the east side of the peninsula is significantly degraded due to it being cut off with the A7 motorway. This area remains dead and one rational solution to this situation would be to change the course of this communication artery, e.g. by setting out a new bypass (Fig. 4 & 5).

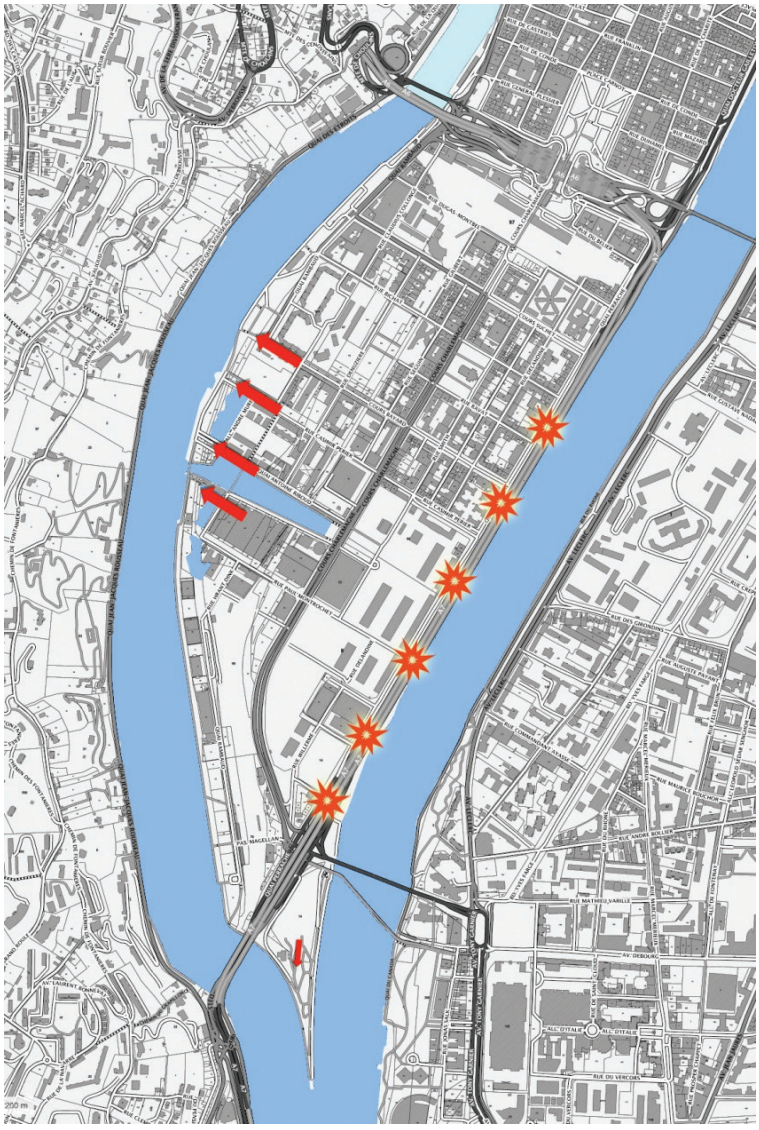

Fig. 4. Boost – connecting the city with the waterfront line. The arrows indicate areas connected by axes to the bank of the river. The red stars indicate a break in connection due to the A7 motorway, which makes the waterfront boost impossible, contributing to the waterfront degradation
(by Rafał Zieliński based on https://www.geoportail.gouv.fr)

Fig. 5. Left; Right: The break in connection due to the A7 motorway (photo by R. Zieliński)

5.3. Diversity of functions of buildings and services along the river bank

Another factor discussed is connected to the proper spatial organisation and functional diversity near the waterfront. The examples of Seville and the Expo'92 area show how the absence of the above can cause numerous problems. In the case of waterfront linearity, this is not a necessary element, but it certainly supports the connection between the city and the new districts with the river in a crucial way. Moreover, it is a factor influencing the economy of revitalised areas and increasing their investment value [12]. In the case of Lyon and Confluence peninsula, we can distinguish areas where the diversity of functions stimulates the waterfront to a greater extent and areas where the lack thereof proves to be negative:

- Lack of diversity – the section by the Quai Ramboud promenade is largely built up by offices, and only during stage II, it will be complemented with residential quarters. In addition, recently completed Confluence Museum is located in on the peninsula's spike. In this case, the lack of urban diversity is caused not only by natural constraints, but also by the course of the A7 motorway and the unfinished stage II of the new district. The situation will change after the second stage of revitalising post-industrial areas. Additional green areas, as well as new residential and service buildings, will also be created;
- Functional diversity – from Place Nautique channel to Cours Bayard Street. This section includes the design of hotels, office and service buildings, a shopping centre, over 1,600 flats, a playing field, squares, gardens and recreation areas. In addition, according to the Great Lyon plan, it was predicted that social flats will constitute approximately 25% of residential housing [13, 14] (Figs. 6 & 7).

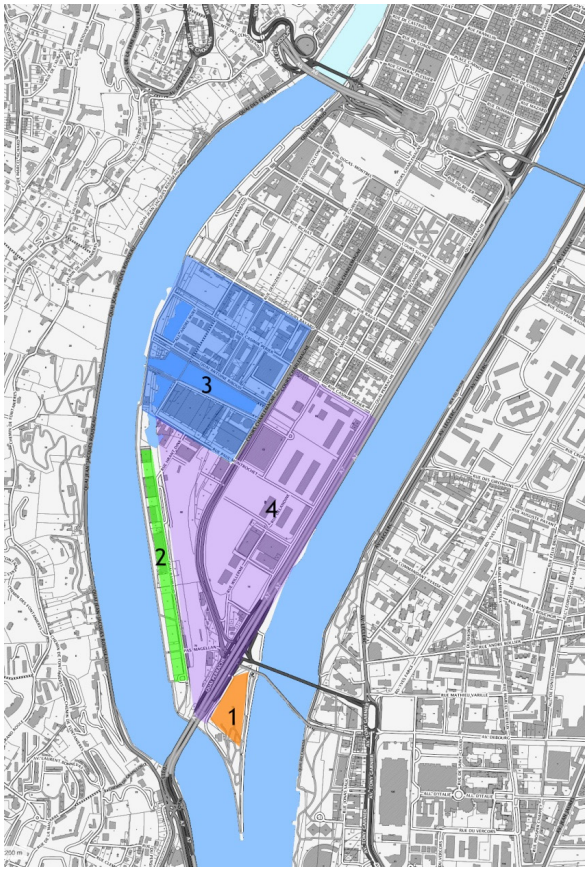

Fig. 6. The diversity of functions of buildings and services along the river bank: 1. Confluence Museum; 2. Office buildings; 3. Correct functional diversity – office buildings, sports facilities, recreation areas, service centres, shopping centres, squares, playgrounds, etc., 4. Areas not yet revitalised. This will only happen after the end of stage II (by R. Zieliński based on https://www.geoportail.gouv.fr)

Fig. 7. Diversity of functions of buildings and services along the river bank – the panoramic view is showing a part of correct functional diversity (on the left) and areas not yet revitalised (on the right)

5.4. Green and recreational areas along the river bank

Waterfront linearity is connected not only with the continuity of pedestrian and cycling trails, but also with their connection to recreational areas and urban greenery. This is a feature shared with the Blue Plan, which concentrated on making the banks accessible to residents and restoring natural features to the waterfront. Along the Saone, on the left side of Confluence peninsula, 5 km of promenades were built, and after the completion of stage I, the public space will occupy approximately 22.5 ha. The concept was also supposed to refer to the industrial nature that characterised these areas before transformation. Due to the above requirements, the old infrastructure (e.g. railways and port structures, a part of docks) was preserved and incorporated into emerging squares and pedestrian areas. The old port channel with an area of 2 hectares was adopted as a new centre of the district around which concerts and festivals are to take place. By building a bridge over the channel, the continuity of the cycling trail along the bank was maintained. There are also new sports facilities and parks established. It is estimated that after completion of the first stage, about 35ha of green areas will be created (Figs. 8 & 9).

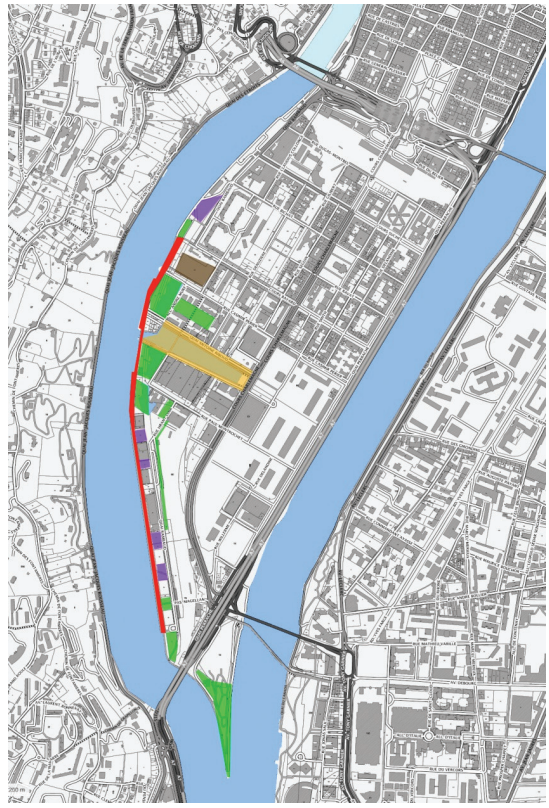

Fig. 8. 4th linearity feature – Green and recreational areas along the river bank. Red – promenades; Green – parks and larger green areas; Purple – small squares; Yellow – the main square; Brown – sports grounds, a playing field (by R. Zieliński based on https://www.geoportail.gouv.fr)

Ill. 9. Left; Right: Green recreation areas along the river bank near Confluence Museum (photo by R. Zieliński)

6. Conclusions – using the principle of waterfront linearity to assess revitalised areas and to grade their activation

Using waterfront linearity as a determinant, the transformation quality of the remaining sections of the Lyon waterfront can be assessed. In this way, it is easier to define possible problems and disturbances resulting from specific cases of negligence. The degree of linearity can be determined by the number of factors involved. Obviously, the key question is whether all of them prove a successful revitalisation. An example of Confluence district helps to address this issue.

The lack of some waterfront linearity elements does not exclude the success of the investment, yet it affects the degree of waterfront activation. By removing some elements, such as the waterfront boost factor, less movement is introduced, making the areas more intimate and peaceful. The change of the location of recreational areas or the lack of diversified functions of the buildings can be influential in a similar way. Another issue is the continuity and length of revitalised areas, the disturbances of which have a greater impact on the possible degradation of the waterfront. Conscious planning and using the principle of linearity can serve to highlight the areas where appropriate, thus increasing the value of the waterfront.

References

[1] Gerardot C. *Les élus lyonnais et leurs fleuves: une reconquête en question*, Le Yangzi et le Rhône, regards croisés, Géocarrefour, Vol. 79/1, 2004.

[2] Biaggioni S., *La requalification des berges en milieu urbain: comment répondre aux nouvelles attentes un espace contraint ?*, HAL – archiwum otwarte, https://dumas.ccsd.cnrs.fr/dumas-01373025, September 2016.

[3] Grand Lyon, Communaute Urbaine de Lyon, *Orientation d'aménagement des berges du Rhône et de la Saône: Plan bleu*, 2001.

[4] Angers.fr, Angres Rives Nouvelles, *Déplacement sur les berges du Rhône à Lyon*, June 2010, http://docplayer.fr/25331983-Deplacement-sur-les-berges-du-rhone-a-lyon.html (access: 02/2017).

[5] Calibre E., Simon E., Turpin M., *Berges du Rhône*, POPSU, June 2007, http://www.popsu.archi.fr/popsu1/lyon/projets/berges-du-rhone (access: 02/2017).
[6] Rives de Saone, http://www.lesrivesdesaone.com/au-fil-de-leau/debouche-de-la-passerelle-du-palais-de-justice (access: 02/2017).
[7] Zieliński R., *Integracja rzeki z miastem na przykładzie przemian frontu wodnego Lizbony*, [in:] *Współczesne problemy w architekturze i urbanistyce*, Politechnika Krakowska, Kraków 2016.
[8] Tufek-Memisevic T., Stachura E., *A linear city development under contemporary determinants*, Środowisko Mieszkaniowe, Politechnika Krakowska, Kraków 2015.
[9] Lynch K., *The Image of the City*, The MITPress, Cambridge 1990.
[10] Paszkowski Z., *Mieszkać na krawędzi*, Czasopismo Techniczne, 3-A/2007, 203–214.
[11] Lyon-Confluence, *Key figures*, http://www.lyon-confluence.fr/en/urban-project/key-figures.html (access: 02/2017).
[12] Gigler U., Tötzer T., Knoflacher M., *Examples of Revitalised Urban Industrial Sites Across Europe*, December 2004.
[13] Genevois S., *Lyon-Confluence, un exemple de rénovation urbaine*, Geo confluences, July 2005, http://geoconfluences.ens-lyon.fr/doc/territ/FranceMut/FranceMutDoc2.htm (access: 02/2017).
[14] Lyon-Confluence, *Chiffres clés. Projet d'ensemble, L'extension. d'un centre-ville, durable*, www.normandie-metropole.fr/Files/35_lyon_confluence.pdf (access: 02/2017).

TECHNICAL TRANSACTIONS 2/2018
ARCHITECTURE AND URBAN PLANNING
DOI: 10.4467/2353737XCT.18.023.7996
SUBMISSION OF THE FINAL VERSION: 10/1/2018

Anna Ziobro (aziobro@pk.edu.pl)
Chair of Spatial Planning and Environment Protection, Institute of Cities and Regions Design, Faculty of Architecture, Cracow University of Technology

Planning-related factors of the quality of the residential environment in the modelling of the functional spatial structure of Cracow

Planistyczne czynniki jakości środowiska zamieszkania w modelowaniu struktury funkcjonalno-przestrzennej Krakowa

Abstract

Models of functional spatial structures, thanks to information aggregation, facilitated the decision-making process in terms of the development of cities. Considering the quality of the residential environment in the planning-related approach, in the scale of the entire city, the Author investigates which elements should be presented in the analysed model. To this end, the Author undertakes an attempt at defining planning-related factors of the quality of the residential environment and at assigning relevant indicators to them. These reflections focus on the example of Cracow.

Keywords: quality of the residential environment, model of the functional spatial structure, spatial planning, development of Cracow

Streszczenie

Modele struktur funkcjonalno-przestrzennych, dzięki zagregowaniu informacji, ułatwiają proces decyzyjny w zakresie rozwoju miast. Rozpatrując jakość środowiska zamieszkania w ujęciu planistycznym, w skali całego miast, a autorka rozważa, jakie elementy winny być przedstawiane w analizowanym modelu. W tym celu podejmuje próbę zdefiniowania planistycznych czynników jakości środowiska zamieszkania wraz z przypisaniem ich wskaźników. Rozważania prezentowane są na przykładzie Krakowa.

Słowa kluczowe: jakość środowiska zamieszkania, model struktury funkcjonalno-przestrzennej, planowanie przestrzenne, rozwój Krakowa

1. Modelling

Special place in the history of urban planning is occupied by models of an ideal city of the industrial era. Equal importance is attached to planning models of the transformations of functional spatial structures developed later, among which the model of functional Warsaw from 1934 was a truly remarkable achievement. Model interpretations of existing urban tissues, as well as simulations of their development, were still a real strength of Polish spatial planning in the 1980s; today, they are a rarity. Meanwhile, many European metropolises are still being developed consequently on the basis of urban models, frequently supported with computer tools. Leaving aside, however, complex mathematical models, requiring extended databases, in this paper, the Investigator's attention is focused around quality factors of the residential environment, as components of the planning model.

2. Environment quality factors

Research work on gauges of the quality of the residential environment of a macro- and micro-range of influence was carried out by G. Schneider-Skalska [13] and J. Kobylarczyk [10] at the Faculty of Architecture, Cracow University of Technology. This study develops this topic for the needs of spatial planning in the scale of a city or an urban functional area. Therefore, it is proposed to introduce a new group of indirect factors of a mezzo-range of influence and to relate them to the details of the study of spatial development conditions and directions or the plan of an urban functional area.

The quality of the residential environment is influenced by factors with the macro-range of influence, characteristic for a specific region, mezzo-factors, moulding the environment of a city or an agglomeration/urban functional area, and micro-factors, referring to conditions in the scale of local planning, urban projects, and revitalisation projects.

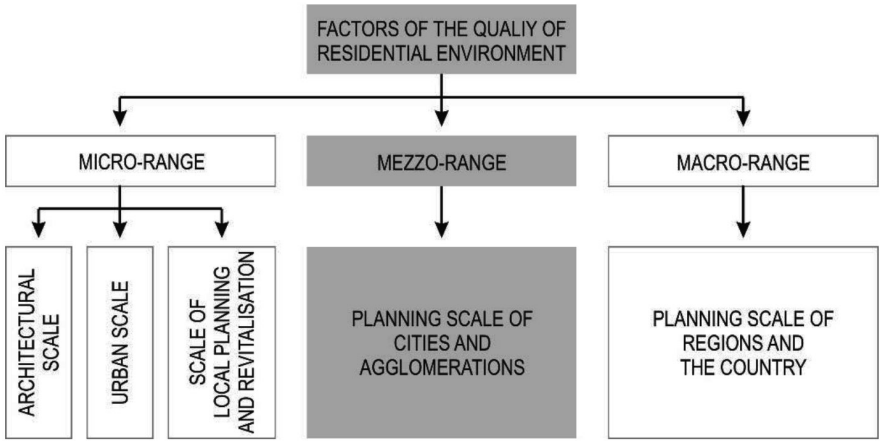

Fig. 1. Factors of the quality of the residential environment in the process of modelling the spatial structure of a city (by A. Ziobro)

The category of factors of the quality of the residential environment with the mezzo-range of influence covers: 1. Population density; 2. Accessibility to the public transport; 3. Accessibility to concentrations of primary services; 4. Accessibility to public spaces, greenery; 5. Morphogenetics of the layout.

1. Population density

The number of residents per one hectare is a leading factor in studies devoted to the quality of the residential environment. The other four quality-related factors of the residential environment are provided with reference to population density. The foundation for such analyses is an assumption that as population density increases, the demand for access to effective public transport, easily accessible primary services, easily accessible public spaces, which, along with the morphogenetic quality of the tissues, strengthen the cultural identity of residents, increases, as well. Owing to the conditions of the natural and cultural environment, cities around the world have different development density, different concentration of city inhabitants. Therefore, density classes should be selected on the individual basis, addressing the specificity of a given city. In order to maintain the legibility of the presentation of the research effects, the Author limited the number of classes of population per hectare to four.

2. Accessibility to public transport

One of the important aspects of the quality of the residential environment are comfortable transport options, which, in the case of big cities, are closely connected with the concept of TOD (Transit Oriented Development). As J. Gehl emphasised, "The concept of a sustainable city strengthens when most transport in the city is constituted by 'green mobility', that is pedestrian traffic, cycling, and public transport. (…) A good public space and a good public transport system are actually inseparably linked" [5, p. 7]. This means that the most densely populated areas are located within the distance of ca. 400–800 m from a highly efficient public transport stop, such as underground or rapid transit rail.

3. Accessibility to concentrations of primary services

The proximity of the concentrations of primary services has a direct effect on the sense of comfort of residence, and at the same time, it is connected with sustainable mobility. Regular distribution of service centres and corridors adjusted to the distribution of inhabitants within the city limits the need to move around to satisfy primary needs.

4. Accessibility to public spaces, greenery

The issue of public spaces and greenery calls for clarification. The typology of public spaces has been presented by, e.g. J.M. Chmielewski, who differentiated between the cultural and technical public space (Fig. 2). "Public spaces in the city are understood as generally accessible systems of passages and places, creating a rich mosaic of urban interiors, where cultural values or technical solutions prevail" [4, p. 429]. It should be pointed out that the division of streets into technical public spaces, dominated by car traffic, and cultural public spaces, where pedestrian traffic prevails, does not exhaust this topic, as the co-existence of space users: drivers

and pedestrians within the area of a street, is possible in the form of a shared zone, as well as a separate form (road and pavements), in a way allowing the pedestrian part to be also a cultural public space. It is possible by means of an appropriate design, by introducing elements enabling to use the pavement in a different way than only for moving from one point to the other.

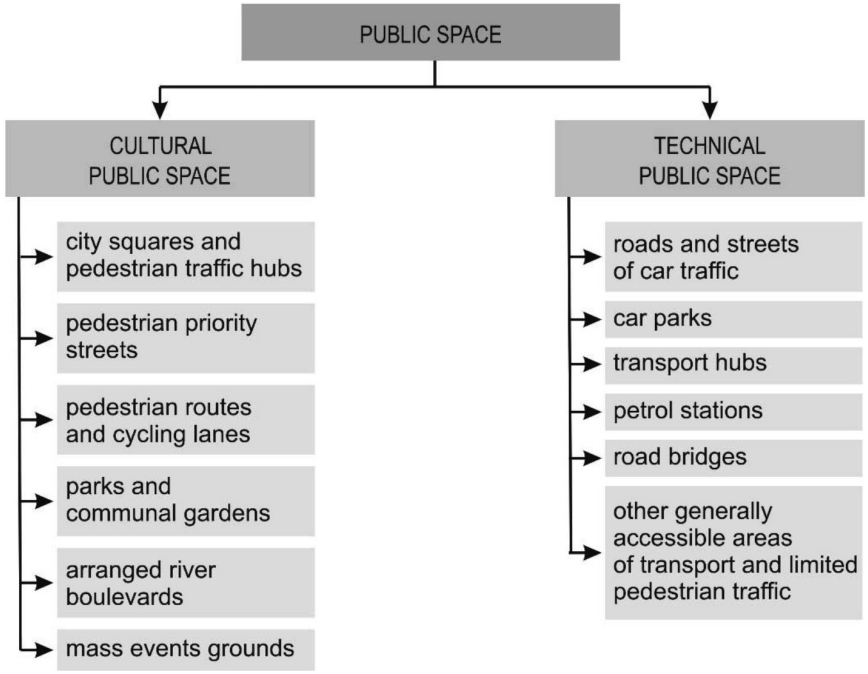

Fig. 2. Types of public spaces (source: [4, p. 429])

Linear public spaces should integrate point and area public spaces, creating a 'white-green'[1] rhizome of public spaces. "The layouts constantly encourage to take a stroll, eliminate unnecessary driveways, integrate the community, consolidate the city, and in the social reception they demarcate a clear skeleton, which crystallises the structure of the city" [4, p. 436].

The density of the rhizome should take into account the population density of specific areas, so as to make sure that the priority of several-minute accessibility (below 1 km) for the biggest concentrations of residents is satisfied. The 'white-green' rhizome of public spaces covers:

[1] The term 'white-green' public spaces corresponds to the method of recording public spaces in the planning practice: green public spaces are marked as parks and arranged greenery, and white public spaces stand for piazzas, market squares, pedestrian routes, etc. Meanwhile, most publications are devoted to either greenery, or public spaces, whereas these two elements intermingle. According to the Author, the quality of residential environment is influenced by greenery accessible to residents, and therefore greenery in the form of a public space. Unarranged greenery inaccessible to the public has only minor importance for the residential environment model – comparable to a private garden, which has a positive effect on the microclimate, allows to be contemplated from a distance, but is not utilised by the community.

- 'green' public space: points (parks, communal gardens), lines (avenues, boulevards), areas (vast recreational grounds, lakes, forest parks);
- semi-private 'green' space (housing estates);
- 'white' public space: points (piazzas, market squares), lines (pedestrian routes or zones shared with transport), areas (historical city centres excluded from car traffic).

5. Morphogenetics of the layout

A housing environment, where architecture is well composed and harmonious, is perceived as valuable. The period in which buildings were erected is important, too. The priority of the evaluation was the planning-related usefulness for the general scale of the city, i.e. defining whether a specific unit exhibits coherence of the general layout and is fully moulded, or whether it requires structural strengthening in the provisions of the study of spatial development conditions and directions.

3. Structural urban units

Four-degree scales were developed for all the factors, allowing for legible graphical representation, making use of structural urban units (SUU) defined in the study of spatial development conditions and directions. The decision to adopt such SUUs as research units was supported by:

- The accuracy of the image granulation – 63 units form an image general enough to be able to emphasise the development designing principles, and at the same time, they take into account the principal structural and spatial diversification of the city,
- The alignment of the research study with the study of development conditions in force, enabling to transfer the research conclusions onto further planning documents,
- The availability of statistical data for individual units.

4. Summary of the model of the residential environment in Cracow in 2016

The biggest concentrations of residents are located in the north parallel belt and in the historical centre of the city. In the southern belt, on the other hand, the highest densities of residents are observed only in two structural urban units: No. 32 Wola Duchacka and No. 52 Prokocim, located in the S/E part of Cracow. The distribution of residents within the city is not uniform. Despite the concentric layout of compact development areas towards the Old Town (except for the western greenery wedge and Rybitwy, which has an industrial character), the analysis of individual population density values in the SUUs demonstrated strong dominance of the belt located north of the Vistula (Fig. 3).

The geometry of effective public transport does not correspond to the geometry of population density. This means that the most densely populated northern belt only has very good accessibility via rail transport in selected locations, and in some cases, it does not have this type of accessibility at all. In the S/E part of the city, the accessibility of the rapid transit rail combined with tramway

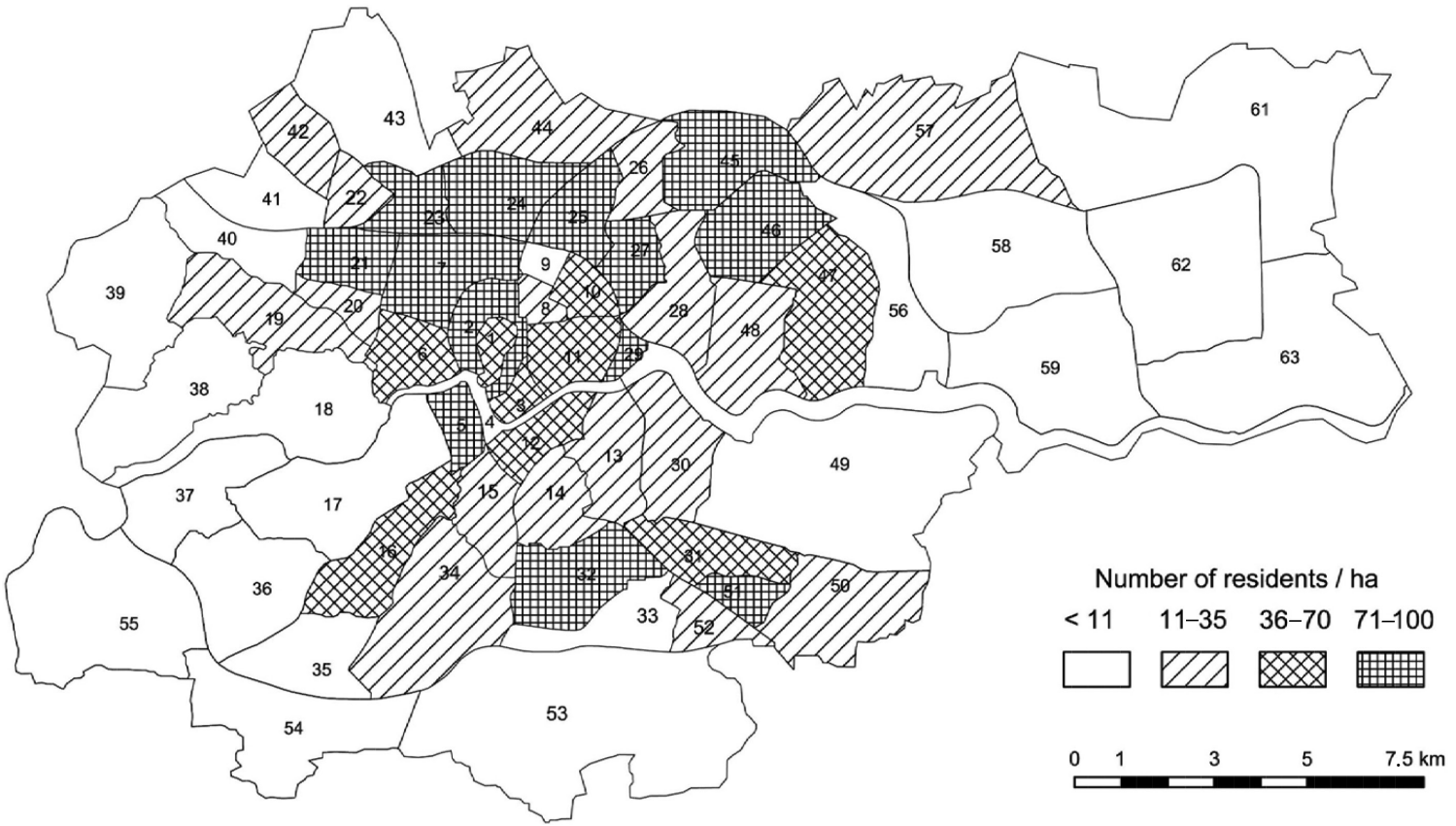

Fig. 3. Population per hectare in SUUs, 2016

is the most beneficial, but it misses units with the highest number of residents per hectare that are located in this part of the city. The logic of the transport form is also contradicted by the good accessibility of peripheral units (N/S, E, and S/E), which do not provide the passenger potential necessary for the feasibility of frequent connections, encouraging to use public transport (Fig. 4).

Primary service clusters (service centres and corridors) in SUUs demonstrate a concentric layout towards the Old Town (except for the western greenery wedge). A big concentration of the services in question is located in the central zone of the city, in the northern belt, and in the south. Peripheral areas, including the territory of Nowa Huta-East, are deprived of any local centres and corridors, which generates travelling to better equipped units, located in the city centre. This situation is even strengthened by analogous patterns in the dysfunctional suburbs of Cracow.

The juxtaposition of primary services clusters to population density in SUU emphasises the problems in the area of Górka Narodowa (SUU 44a), where the average population density exhibits a growing tendency, and there is no local service centre or corridor there (Fig. 5).

White public spaces, especially the high-quality ones, concentrate in the area of the historical part of the city, forming a relatively continuous system, which could be even classified as an attractive public space area, whereas in other areas of Cracow, especially where the population density is high, deficits are observed in this respect. As far as the green public spaces are concerned, a relatively good situation is in Stara Nowa Huta, Bieńczyce, and Mistrzejowice, thanks to vast areas of semi-public greenery of housing estates and Bieńczycki Park. In other parts of the city, the arranged greenery is in the form of islands, and it is too scarce considering the number of residents. In general, 'white-green' spaces do not form a coherent system (Fig. 6).

The island-like character of greenery, and at the same time, the small area of most parks and squares in areas with the highest population density, hinders diversified forms of everyday recreation on short distances, which is particularly important for individuals with worse mobility (the elderly and young children). Reaching few green enclaves along uneven pavements, which are even made narrower by cars often parked on them, along streets deprived of any trees, which would offer some shade on hot days, is a big challenge for people with limited mobility, sometimes even too big. Securing equal opportunities in the everyday access to attractive green areas, creation of walking lanes encouraging to spend free time actively and do sports all year round, constitutes a foundation for a healthy society. Meanwhile, for the majority of SUUs from the N/W and S belt, reaching bigger recreation grounds where one can jog, roller blade, etc. is connected with using an expensive means of transport. The problem is additionally intensified by the lack of attractive recreational areas in the suburbs of Cracow and the resultant migrations of residents of the neighbouring communes, especially at weekends.

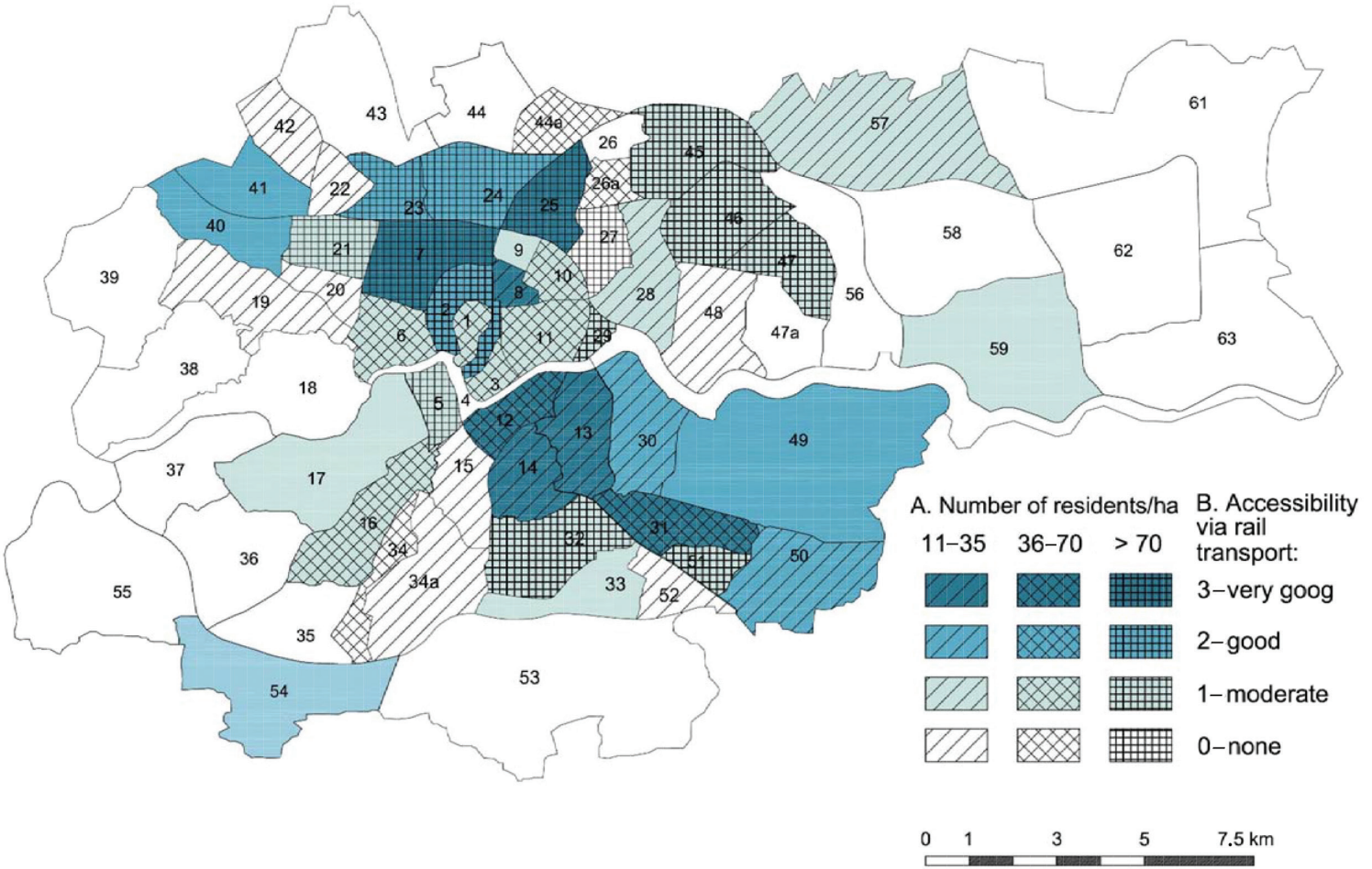

Fig. 4. Rail transport vs. population density in SUUs, 2016. Prepared by: A. Ziobro, in cooperation with: A. Derlatka, A. Matusik, D. Pokielski-Kozieł, A. Sarga, F. Suchoń, P. Tota

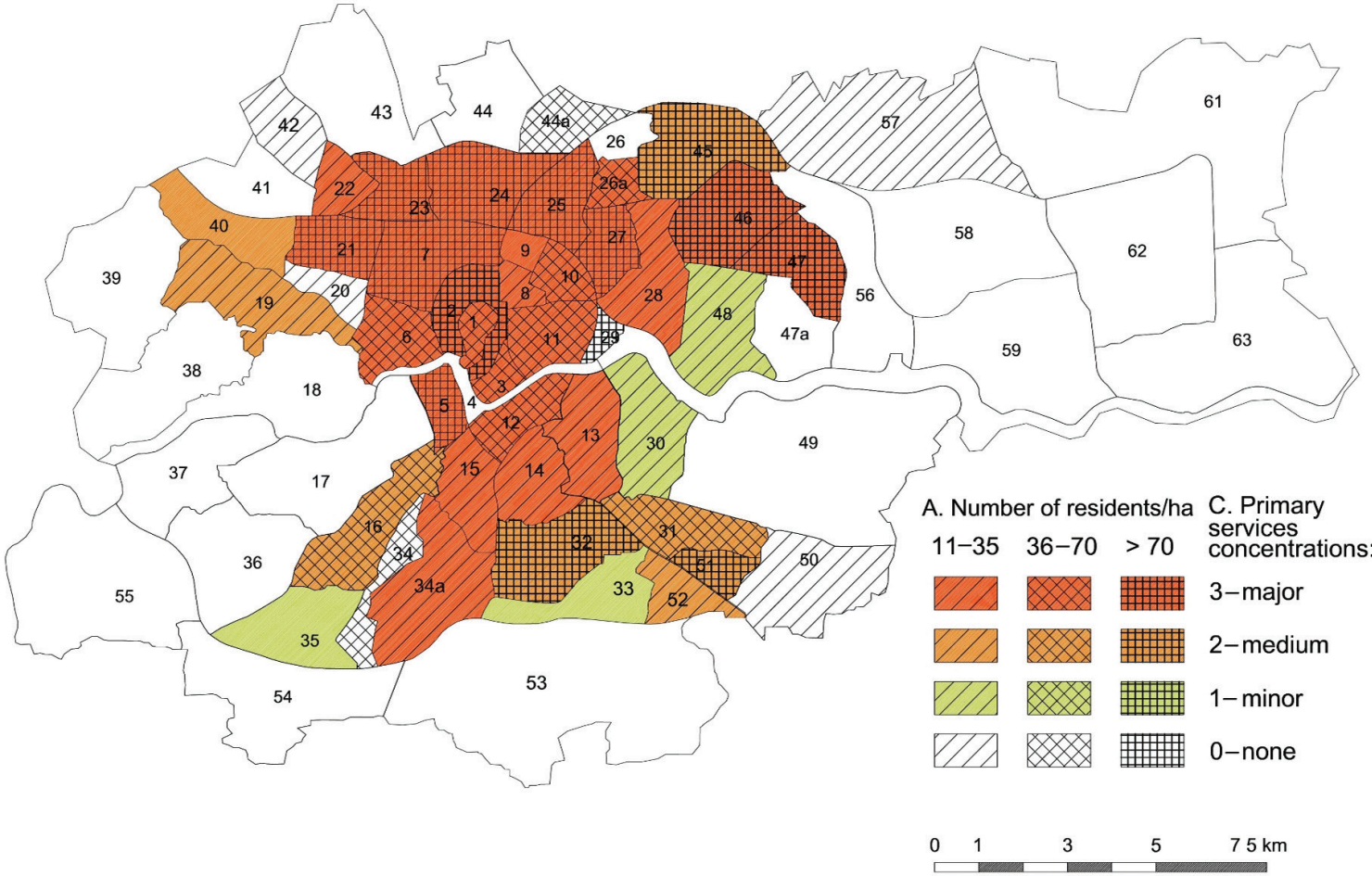

Fig. 5. Primary service concentrations vs. population density in SUUs, 2016. Prepared by: A. Ziobro on the basis of research by D. Ogrodnik; in cooperation with: A. Derlatka, A. Matusik, D. Pokielski-Kozieł, A. Sarga, F. Suchoń, P. Tota

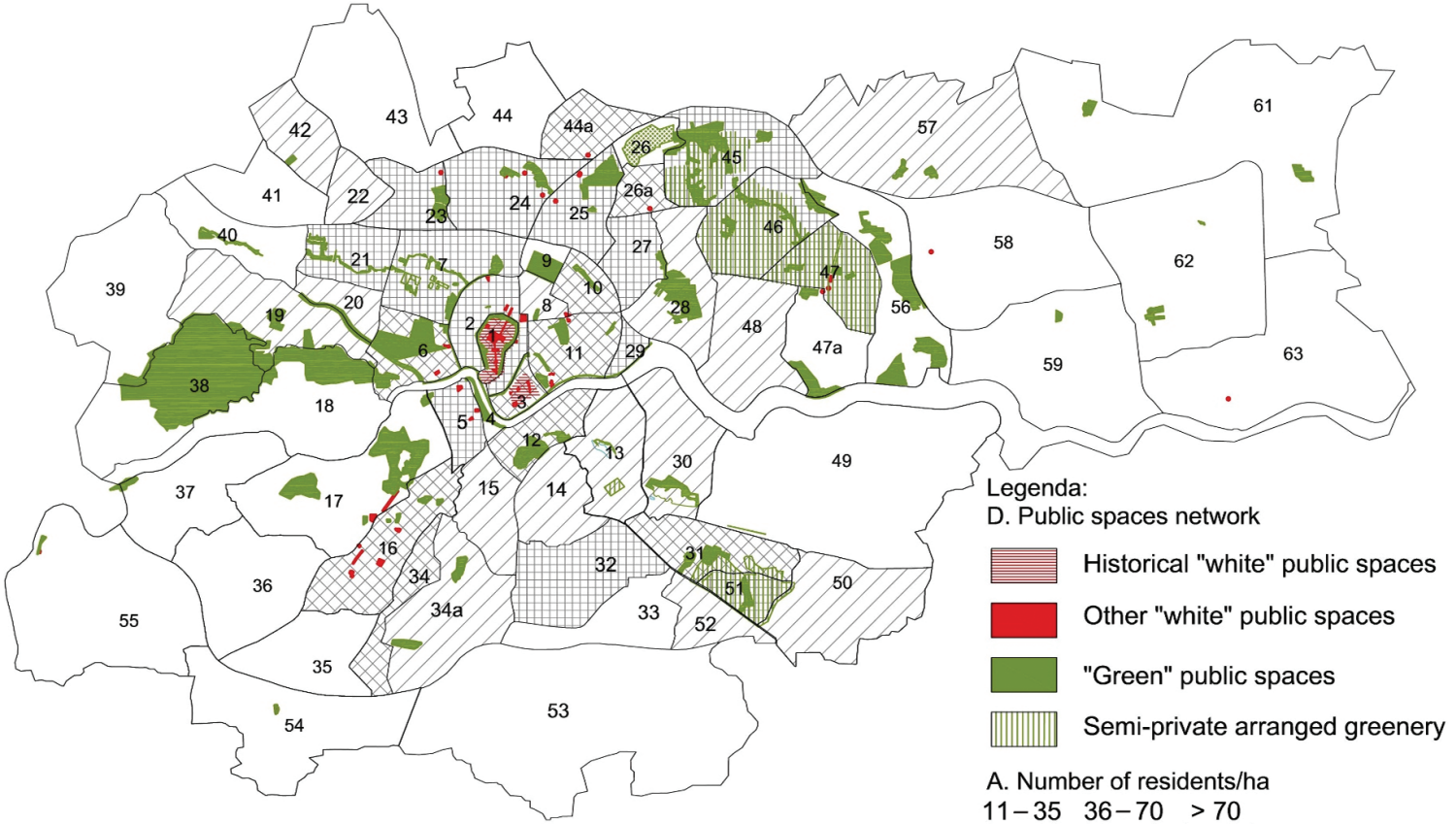

Fig. 6. 'White-green' public spaces vs. population density in SUUs, 2016. Prepared by: A. Ziobro, in cooperation with A. Derlatka, A. Matusik, D. Pokielski-Koziel, A. Sarga, F. Suchoń, P. Tota

5. Conclusions

The factors and indicators developed as components of the model of the quality of the residential environment allowed to illustrate the spatial dysfunctions of Cracow. A solution for many of the demonstrated problems is the implementation of investments already included in the study of spatial development conditions and directions. For other areas, recommendations for amending the aforementioned planning document were formulated. These experiences, as well as planning practices in such cities as Copenhagen or Stockholm, testify to the great usefulness of model interpretations.

References

[1] Böhm A., *O budowie i synergii wnętrz urbanistycznych*, Monografia, Politechnika Krakowska, Kraków 1981.

[2] Bojanowski K, *Strategia dla Krakowa – koncepcja rozwoju przestrzeni publicznych. Monolog o polskiej urbanistyce*, Wyd. PK, Kraków 2013.

[3] Cęckiewicz W., *Problemy rozwoju przestrzennego Krakowa w świetle współczesnych teorii urbanistycznych*, Zeszyty Naukowe Instytutu Projektowania Urbanistycznego Politechniki Krakowskiej, No. 1/92, 1993, 73–80.

[4] Chmielewski J.M., *Teoria i praktyka planowania przestrzennego. Urbanistyka Europy*, Oficyna Wydawnicza Politechniki Warszawskiej, Warszawa 2016.

[5] Gehl J., *Miasta dla ludzi*, RAM, Kraków 2017.

[6] Gyurkovich M., *Hybrydowe przestrzenie kultury we współczesnym mieście europejskim*, Monografia 438, Wyd. PK, Kraków 2013.

[7] Jacobs J., Śmierć i życie wielkich miast Ameryki, Fundacja Centrum Architektury, Warszawa 2014.

[8] Jaskulska M. (ed.), *Poradnik o przestrzeniach publicznych*, Biuro Rozwoju Gdańska, Gdańsk, 2014, http://www.brg.gda.pl/attachments/article/62/poradnik_o_przestrzeniach_publicznych.pdf (access: 24.01.2018).

[9] *Kierunki rozwoju i zarządzania terenami zieleni w Krakowie na lata 2017–2030*, Wydział Kształtowania Środowiska Urzędu Miasta Krakowa, 20/12/2016.

[10] Kobylarczyk J., *Ocena jakości środowiska zamieszkania w wybranych miastach województwa podkarpackiego po okresie „transformacji" w pierwszej dekadzie XXI wieku*, Politechnika Krakowska, Kraków 2013.

[11] Mydel R., *Rozwój urbanistyczny Miasta Krakowa po Drugiej Wojnie Światowej*, Wydawnictwo i Drukarnia „Secesja", Kraków 1994.

[12] Rudnicki, A., *Zrównoważona mobilność* a rozwój przestrzenny miasta, Czasopismo Techniczne 1-A/2010, 57–74.

[13] Schneider-Skalska G., *Kształtowanie zdrowego środowiska mieszkaniowego*, Politechnika Krakowska, Kraków 2004.

[14] Szarata, A., *Zrównoważona mobilność a rozwój przestrzenny miasta*, Czasopismo Techniczne 1-A/2010, 249–261.
[15] Ustawa o planowaniu i zagospodarowaniu przestrzennym z dnia 27 marca 2003 r., Dz. U. 2003 Nr 80 poz. 717 z późn. zm.
[16] Zachariasz A., *Zieleń jako współczesny czynnik miastotwórczy ze szczególnym uwzględnieniem roli parków publicznych*, Politechnika Krakowska, Kraków 2006.
[17] *Zmiana Studium Uwarunkowań i Kierunków Zagospodarowania Przestrzennego Miasta Krakowa*, U. Nr XII/87/03 Rady Miasta Krakowa z dnia 16 kwietnia 2003 r.
[18] Ziobro A., *Modelowe interpretacje przestrzennej struktury metropolitalnej w planach rozwoju Krakowa i jego regionu. Okres 1960–2010*, PhD Thesis, Politechnika Krakowska, Kraków 2015.
[19] Ziobrowski Z., *Urbanistyczne wymiary miast*, IRM, Kraków 2012.
[20] Zipser T., *Powiązania transportowe jako generatory struktury przestrzennej systemu osadniczego*, Czasopismo Techniczne, 3-A/2010, 21–30.
[21] Zuziak Z.K., *Nowe przestrzenie podróży. Przestrzenie publiczne węzłów transportu*, [in:] *Przestrzeń publiczna miasta postindustrialnego*, M. Kochanowski (ed.), Wydawnictwo Politechniki Gdańskiej, Gdańsk 2002.
[22] Zuziak, Z.K., *Forma metropolitalna i zrównoważona mobilność*, Czasopismo Techniczne 3-A/2010, 75–91.
[23] Zuziak Z.K., *Strategiczne węzły w przestrzeni przepływów*, Czasopismo Techniczne 10-A/2011, 41–47.
[24] Zuziak Z.K., *O tożsamości urbanistyki*, Politechnika Krakowska, Kraków 2008.

TECHNICAL TRANSACTIONS 2/2018
CHEMISTRY
DOI: 10.4467/2353737XCT.18.024.7997
SUBMISSION OF THE FINAL VERSION: 9/1/2018

Przemysław Woliński
Radomir Jasiński (radomir@chemia.pk.edu.pl)
Faculty of Chemical Engineering and Technology, Cracow University of Technology

Chemistry of 2-aryl-1-cyano-1-nitroethenes. Part I. Synthesis and physical properties

Chemia 2-arylo-1-cyjano-1-nitroetenów. Część I. Otrzymywanie i właściwości fizyczne

Abstract

In this paper, we present the methodology of preparation of 2-aryl-1-cyano-1-nitroethenes and the synthesis of their main precursor – nitroacetonitrile. We have also gathered the physical properties of all compounds of this group known in the literature.

Keywords: 2-aryl-1-cyano-1-nitroethene, 3-aryl-2-nitro-2-propenenitrile, nitroacetonitrile, ACN, NAN, synthesis

Streszczenie

W niniejszej pracy przedstawiliśmy metodologię otrzymywania 2-arylo-1-cyjano-1-nitroetenów oraz ich głównego prekursora, jakim jest nitroacetonitryl. Przedstawiliśmy również właściwości fizyczne wszystkich znanych w literaturze związków ze wspomnianej grupy.

Słowa kluczowe: 2-arylo-1-cyjano-1-nitroeten, 3-arylo-2-nitro-2-propenonitryl, nitroacetonitryl, synteza

1. Introduction

Conjugated nitroalkenes (CNA) are highly effective synthons in organic synthesis. The presence of the nitro group in CNA molecule provides almost unlimited possibilities for its further functionalization towards, for example, carbonyl compounds (Nef reaction) [1–3], nitrile N-oxides (Mukuiyama reaction) [4], amino alcohols (via a Henry reaction/reduction sequence) [2, 5–7], salts and esters of nitronic acids [2, 4, 8] and many others [1, 2, 6, 9]. Additionally, due to their evidently electrophilic character, CNA are valuable reagents in cycloaddition processes leading to five- and six-membered cyclic systems [1, 10, 11].

In this group of nitro compounds, 2-aryl-1-cyano-1-nitroethenes (ACN) are especially interesting. This type of CNA was first prepared in 1956 by Ried and Köhler [12]. Currently, more than 30 ACNs have been prepared and characterized. It is interesting that most experiments in this area have been performed recently. This confirms a growing interest in ACNs, and so we decide to review all physical and chemical aspects of the ACNs known. In the first part of our study, we characterized the synthetic protocols as well as the physical description of the compounds studied.

Preparation of nitroacetonitrile as a precursor for synthesis of ACNs

The methodology described in 1956 [12] for the preparation of nitroacetonitrile (NAN) is based on commercially available nitromethane [13, 14]. In the first step, nitromethane is converted into methazonic acid (MAC) via a condensation reaction catalyzed by NaOH, and in the next step acidification using concentrated HCl takes place. In this way methazonic acid can be prepared with a yield of 50% [14].

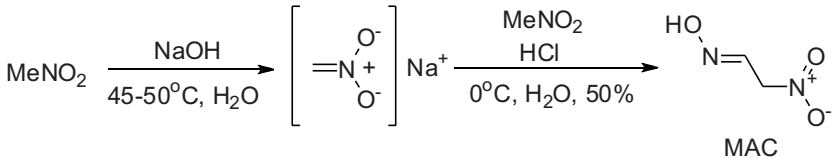

Dehydration of MAC leads to the formation of NAN. This process proceeds via a reaction involving thionyl chloride in a dry diethyl ether solution. Under these conditions, the final product may be synthesized with yields up to 47% [12, 14–18]. After purification using column chromatography (SiO_2/benzene) NAN of a purity suitable for use in Knoevenagel condensation is obtained. NAN is a pale yellow, unstable liquid, which at temperatures higher than 50–60°C is capable of exploding. Therefore, attempts to purify it via vapour distillation are potentially very dangerous [13].

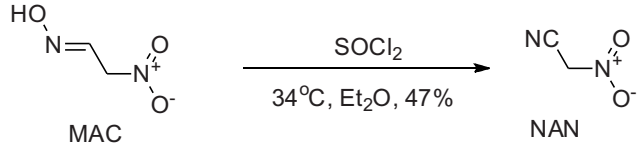

Kislyi and coworkers [19] have described an alternative, more effective synthetic way for preparing NAN. In this approach, NAN is synthesized according to a two-stage procedure: (i) nitration of cyanoacetone (CA) in a two-phase system, and next, (ii) deacylation of the nitrocarbonyl intermediate product (NCA).

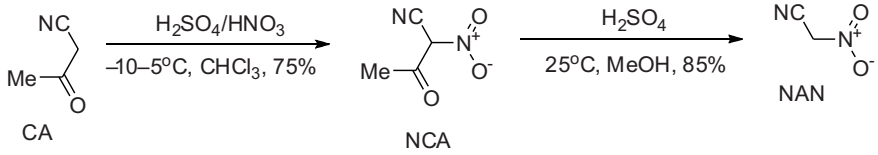

Unfortunately, no literature examples of a successful repeat of this procedure exist.

Very recently, a new procedure for NAN preparation was reported [20]. Based on ethyl ester of isonitrosocyanacetic acid (INCE), pure NAN was obtained with a moderate yield.

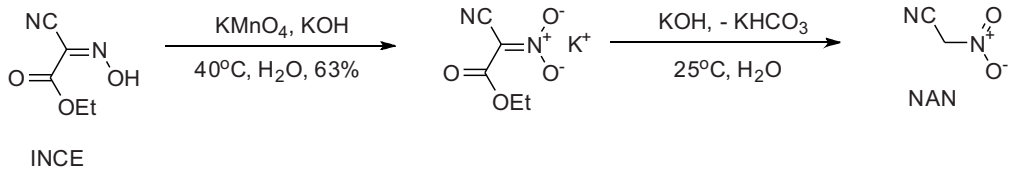

2. Preparation of ACNs

The first compounds in the ACN group were prepared by Ried and Köhler [12]. These authors described synthesis based on NAN and a series of aromatic aldehydes in the presence of a catalytic amount of methylamine generated *in situ*. This way, 11 new compounds (**1**, **3**, **13**, **17–21**, **24**, **28, 29**) were prepared with very different yields. An analogous methodology was also applied later in the case of ACNs **2**, **7**, **10**, **14**, **15**, **23** and **25** [21–24].

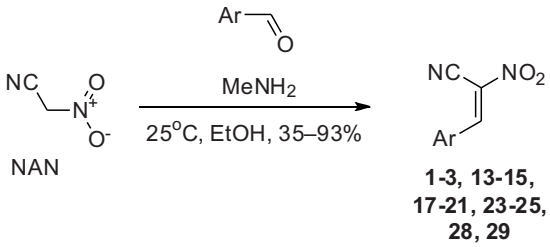

Later [18, 25–27, 28], other aliphatic and alicyclic amines (n-propylamine, n-pentylamine, morpholine, ethylenediamine, β-alanine) were also tested as catalysts in similar syntheses. In these syntheses several new compounds were prepared. It is interesting that these series contain many compounds (**2–4**, **9**, **11**, **12**, **16**) with electron-withdrawing groups (F, Br, COOMe) in aryl rings, which was not been prepared earlier.

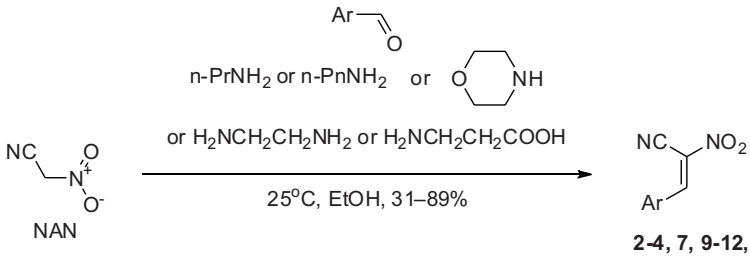

2-4, 7, 9-12, 14, 16, 24-27

In an alternative protocol, 1-butyl-3-methylimidazolium chloride has been used as a catalyst and as a reaction medium [17]. According to this procedure, six known earlier compounds (**1**–**5**, **7**) have been prepared with very high yields (>92%).

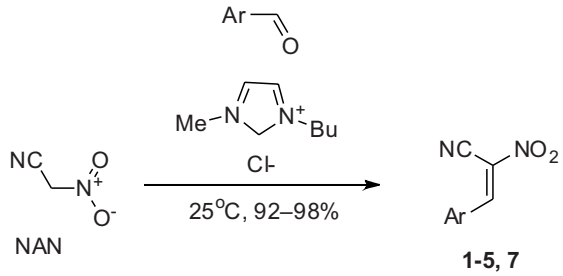

1-5, 7

For preparation of CNA **10** containing the EDG dimethylamino group in a phenyl ring, an alternative procedure using various acidic catalysts (A = $SOCl_2$, $AlCl_3$, 4-toluenesulphonic acid, HCl) was developed [29]. In particular, by this method compound **10** may be obtained with a yield up to 72%.

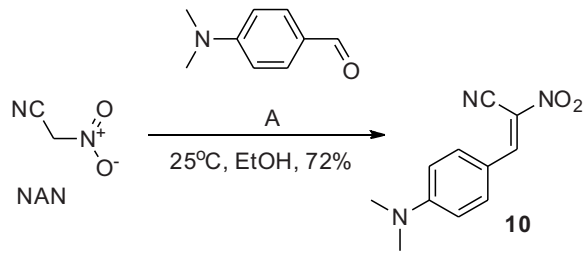

10

Heterogeneous catalysts have also been applied for the synthesis of ACNs. It was found that in the presence of dolomite $CaMg(CO_3)_2$ some aromatic aldehydes undergo condensation with the NAN yielding an expected CNA with a high yield [30]. In analogous processes, an SiO_2 catalyst was also applied [31].

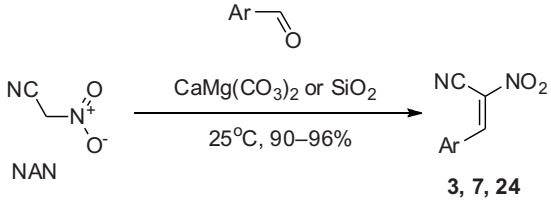

3, 7, 24

Recently, a "green" protocol for synthesis of series of ACNs has been described by Pizzo et al [32]. According to this procedure, 11 different compounds (**1**, **3**, **5–8**, **14**, **15**, **22**, **24**, **25**) were prepared in a water environment after 7h with high yields up to 95%.

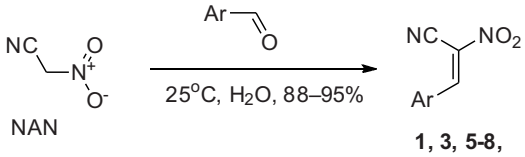

1, 3, 5-8, 14, 15, 22, 24, 25

Relatively faster than earlier methods are similar syntheses preformed in the presence of a catalytic amount of ammonium chloride [33]. Microwave irradiation of mixtures of NAN and appropriate aldehydes under these conditions give the expected products after 2–3 min(!).

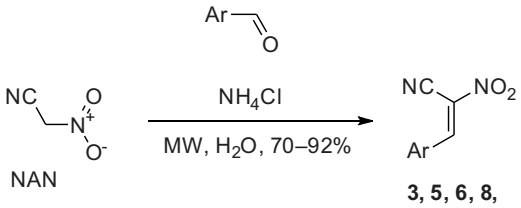

3, 5, 6, 8, 14, 15

Independently of condensation between NAN and aromatic aldehydes, other strategies have been also tested for synthesis of ACNs. In particular, Blaha et al [34], analogously to earlier studies [35], analysed the possibility of preparing CNA **1** via chloronitration using nitryl chloride. Unfortunately, no attempts to obtain 1 were successful. On the other hand, Ariga et al [36] described an alternative synthetic pathway based on the pyridinium salt of 4-nitroisoxazolin-5(2H)-one. This way, the authors synthesized two ACNs (**1**, **7**) with almost quantitative yield. Unfortunately, at this time it is not known whether this is a universal method.

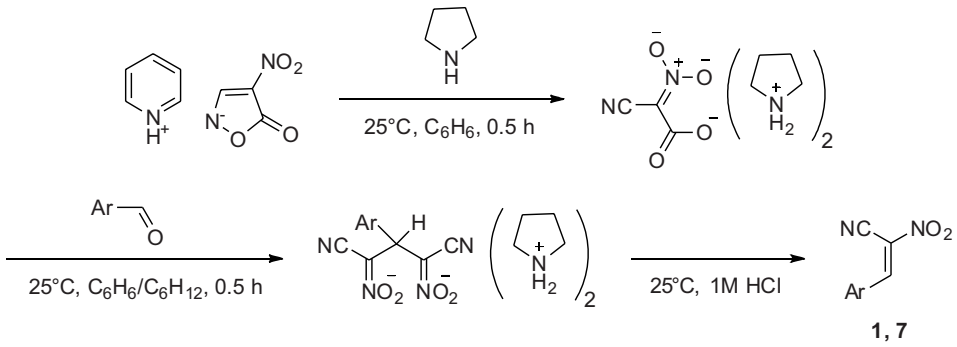

1, 7

Fundamental physical properties of all known ACNs are collected in Table 1.

3. Conclusion

The literature describes many methods for the preparation of conjugated nitroalkenes (CNA). Most universal strategies are based on the thermal or catalytic decomposition of nitroalkyl esters [37–41] and dehydrohalogenation of 1,2-dihalo-1-nitroethane derivatives [35, 42]. Unfortunately, all these protocols are inadequate for preparation of 2-aryl-1-cyano-1-nitroethenes. For this purpose only Knoevenagel condensation involving nitroacetonitrile is dedicated.

It should be mentioned at this point that most known ACNs were applied for synthesis of different type carbo- and heterocyclic compounds. These issues are the subject of the next part of our study.

References

[1] Barrett A.G.M., Graboski G.G., *Conjugated nitroalkenes: versatile intermediates in organic synthesis*, Chemical Reviews, 1986, 86, 751–762.
[2] Ono N., *The nitro group in organic synthesis*, Wiley-VCH, Weinheim 2001.
[3] Ballini R., Petrini M., *Recent synthetic developments in the nitro to carbonyl conversion (Nef reaction)*, Tetrahedron, 2004, 60, 1017–1047.
[4] Belenkii L.I., [in:] *Nitrile oxides, nitrone and nitronates in organic synthesis*, Ed. H. Feuer, Wiley, 2007.
[5] Boruwa J., Gogoi N., Saikia P.P., Barua N.C., *Catalytic asymmetric Henry reaction*, Tetrahedron: Asymmetry, 2006, 17, 3315–3326.
[6] Agrawal J.P., Hodgson R.D., *Chemistry of explosives*, Wiley, 2007.
[7] Bergmeier S.C., *The Synthesis of Vicinal Amino Alcohols*, Tetrahedron, 2000, 56, 2561–2576.
[8] Denmark S.E., Cottell J.J., [in:] *The chemistry of heterocyclic compounds*, Eds. A. Padwa, W.H. Pearson, New York 2002.
[9] Novikov C.C., Shvekhgeimer G.A., Sevastyanova V.V., Shlaposhnikov V.A., *Khimiya alifaticheskikh i alitsiklicheskikh nitrosoedinenii*, Khimya, Moscov 1974.
[10] Nguyen T.B., Martel A., Gaulon-Nourry C., Dhal R., Dujardin G., *1,3-Dipolar Cycloadditions of Nitrones to Hetero-substituted Alkenes Part 2: Sila-, Thia-, Phospha- and Halo-substituted Alkenes*, Organic Preparations and Procedures International, 2012, 44, 1–81.
[11] Terrier F., Dust J.M., Buncel E., *Dual super-electrophilic and Diels–Alder reactivity of neutral 10π heteroaromatic substrates*, Tetrahedron, 2012, 68, 1829–1843.
[12] Ried W., Köhler E., Königstein F.J., *Reacktionen mit Nitro-acetonitril*, Liebigs Annalen, 1956, 598, 145–158.
[13] R. Jasiński, *Preparatyka alifatycznych nitrozwiązków*, RTN, 2013.
[14] Matthews V.E., Kubler D.G., *Improved Synthesis of Salts and Esters of Nitroacetic Acid*, Journal of Organic Chemistry, 1960, 25, 266–268.
[15] Steinkopf W., Bohrmann L., *Das Nitro-acetonitril*, Liebigs Annalen, 1908, 41, 1044–1052.

[16] Kanishchev M.I., Korneeva N.V., Shevelev S.A., *Synthesis of 3-amino-5-benzylamino-4-nitropyrazole*, Bulletin of the Academy of Sciences of the USSR, Division of chemical science, 1986, 35, 2145–2147.
[17] Boguszewska-Czubara A., Lapczuk-Krygier A., Rykala K., Biernasiuk A., Wnorowski A., Popiolek L., Maziarka A., Hordyjewska A., Jasiński R., *Novel synthesis scheme and in vitro antimicrobial evaluation of a panel of (E)-2-aryl-1-cyano-nitroethenes*, Journal of Enzyme Inhibition and Medical Chemistry, 2016, 31, 900–907.
[18] Jasiński R., Miroslaw B., Demchuk O.M., Babyuk D., Łapczuk-Krygier A., *In the search for experimental and quantumchemical evidence for zwitterionic nature of (2E)-3-[4-(dimethylamino)phenyl]-2-nitroproprop-2-enenitrile – an extreme example of donor-π-acceptor push-pull molecule*, Journal of Molecular Structure, 2016, 1108, 689–697.
[19] Kislyi V.P., Laikhter A.L., Ugrak B.L., Semenov V.V., *Synthesis of a-functional nitro compounds by the nitration of activated carbonyl compounds in a two-phase system*, Russian Chemical Bulletin, 1994, 43, 70–74.
[20] Voinkov E.K., Ulomskiy E.N., Rusinov V.L., Savateev K.V., Fedotov V.V., Gorbunov E.B., Isenov M.L., Eltsov O.S., *New stable form of nitroacetonitrile*, Mendeleev Communications, 2016, 26, 172–173.
[21] Acheson R.M., Dearnaley D.P., Plunkett A.O., Porter V.C., *The amino-acid Analogue of Mescaline*, Journal of Chemical Sciences, 1963, 0, 2085–2087.
[22] Мечков Ц.Д., Демирева З.И., Синтез некоторых бисаммониевых солей *2,4-динитро-3-(4-фторфенил)*глутаронитрила, Журнал органической химии, 1985, 21, 1884–1887.
[23] Baichurin R.I., Aboskalova N.I., Trukhin E.V., Berestovitskaya V.M., *Aryl(hetaryl)-Containing gem-Cyanonitroethenes: Synthesis, Structure, and Reactions with 2,3-Dimethyl-1,3-butadiene*, Russian Journal of General Chemistry, 2015, 85, 1845–1854.
[24] Metchkov T., Demireva Z., *Die Synthese einiger Bis-Ammoniumsalze von 3,4-Dinitro-8-(methoxyphenyl)glutarnitrilen*, Zeitschrift für Chemie, 1985, 25, 169–170.
[25] M. Kwiatkowska, Praca doktorska, Politechnika Krakowska 2008.
[26] Nesterov V.N., Kislyi V.P., Timofeeva T.V., Antipina M.Yu., Semenov V.V., *trans-1-Cyano-2-(2-methoxyphenyl)-1-nitroethylene*, Acta Crystallographica Section C, 2000, C56, e107–e108.
[27] Полянская А.С., Перекалин В.В., Абоскалова Н.И., Демирова З.И., Соколова Л.Н., Абдулкина З.А., Химия замещенных цианонитроалкенов *II.* Синтез и строение гетерилцианонитроалкенов, Журнал органической химии, 1979, 15, 2057–2061.
[28] Troschütz R., Grün L., *Synthese von basisch substituierten 5H-Pyrimido[4,5-c]-2-benzazepinen*, Archiv der Pharmazie, 1993, *326*, 857–864.
[29] Абоскалова Н.И., Полянская А.С., Перекалин В.В., Демирова З.И., Соколова Л.Н., Реакция алкенилирования в присутствии кислотных катализаторов, Журнал органической химии, 1972, 8, 1332–1333.
[30] Tamaddon F., Tayefi M., Hosseini E., Zare E., *Dolomite ($CaMg(CO_3)_2$) as a recyclable natural catalyst in Henry, Knoevenagel, and Michael reactions*, Journal of Molecular Catalysis A: Chemical, 2013, 366, 36–42.

[31] Brillon D., Sauvé G., *Silica Gel-Catalyzed Knoevenagel Condensation of Peptidyl Cyanomethyl Ketones with Aromatic Aldehydes and Ketones. A Novel Michael Acceptor Functionality for C-Modified Peptides: The Benzylidene and Alkylidene Cyanomethyl Ketone Function*, Journal of Organic Chemistry, 1992, 57, 1838–1842.
[32] Amantini D., Fringuelli F., Piermatti O., Pizzo F., Vaccaro L., *Water, a clean, inexpensive, and re-usable reaction medium. One-pot synthesis of (E)-2-aryl-1-cyano-1-nitroethenes*, Green Chemistry, 2001, 3, 229–232.
[33] Valizadeh H., Mamaghani M., Badrian A., *Effect of Microwave Irradiation on Reaction of Arylaldehyde Derivatives with Some Active Methylene Compounds in Aqueous Media*, Synthetic Communications, 2005, 35, 785–790.
[34] Bláha I., Lešetický L., *Preparation and Z-E isomerization of substituted nitrostyrenes*, Collection Czechoslovak Chemical Communication, 1986, 51, 1094–1099.
[35] Shechter H., Conrad F., Daulton A. L., Kaplan R. B., *Orientation in Reactions of Nitryl Chloride and Acrylic Systems*, Journal of American Chemical Society, 1952, 74, 3052–3056.
[36] Nishiwaki N., Nogami T., Tanaka C., Nakashima F., Inoue Y., Asaka N., Tohda Y., Ariga M., *Aplication of Cyano-aci-Nitroacetate to Organic Synthesis. 1. Facile Synthesis of Pentanedinitrile-2,4-dinitronates*, Journal of Organic Chemistry, 1999, 64, 2160–2162.
[37] Kącka-Zych A., Domingo L.R., Ríos-Gutiérrez M., Jasiński R., *Understanding the mechanism of the decomposition reaction of nitroethyl benzoate through the Molecular Electron Density Theory*, Theoretical Chemistry Accounts, 2017, 136, 129.
[38] Kącka A., Jasiński R., *A dramatic change of kinetic conditions and molecular mechanism of decomposition processes of nitroalkyl carboxylates catalyzed by ethylammonium cations*, Computational and Theoretical Chemistry, 2017, 1104, 37–42.
[39] Kącka A., Jasiński R., *Triethylsulfonium and triethylphosphonium cations as novel catalysts for the decomposition process of nitroethyl benzoates*, Phosphorus Sulfur and Silicon and the Related Elements, 2017, 192, 1252–1258.
[40] Kącka A., Jasiński R., *DFT study of the decomposition reactions of nitroethyl benzoates catalyzed by the 1,3-dimethylimidazolium cation*, Current Chemistry Letters, 2017, 6, 15–22.
[41] Kącka A., Jasiński R., *A DFT mechanistic study of thermal decomposition reactions of nitroethyl carboxylates: undermine of pericyclic insight*, Heteroatom Chemistry, 2016, 27, 279–289.
[42] Łapczuk-Krygier A., Ponikiewski Ł., *Single crystal X-ray structure of (Z)-1-bromo-1-nitro-2-phenylethene*, Current Chemistry Letters, 2015, 4, 21–26.

No.		t_t [°C] (solvent)	1H-NMR δ [ppm]	IR [cm^{-1}]	UV λ (log ε) [nm]	Ref.
1	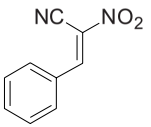	102(EtOH) 101(CCl_4) 103-104($CHCl_3$)	9.01 (1H, s, CH) 8.11 (2H, m, 2CH) 7.60-7.74 (3H, m, 3CH) d_6-DMSO 8.66 (1H, s, CH) 8.01 (1H, dd, J_{23}=8.24, 2CH) 7.59 (1H, dd, J_{23}=8.24, 3CH) 7.69 (1H, tt, J_{24}=1.20 J_{34}=7.45, 4CH) $CDCl_3$	2229 (CN) 1615 (C=C) 1537 (NO_2) 1320 (NO_2)	328(4.23)	[12], [17], [18], [20], [23], [32], [34], [36]
2	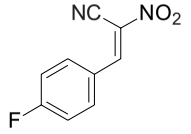	116-117(EtOH)	8.65 (1H, s, CH) 7.19-8.18 (4H, m, Ar) $CDCl_3$	2231(CN) 1616(C=C) 1537(NO_2) 1327(NO_2)		[17], [18], [22], [25]
3	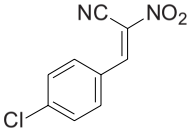	116-117(EtOH) 115-117(hex/AcOEt)	8.65 (1H, s, CH) 7.54-8.11 (4H, m, Ar) $CDCl_3$	2230(CN) 1615(C=C) 1548(NO_2) 1330(NO_2)		[12], [17], [18], [25], [30], [32], [33]
4	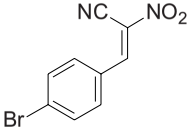	112-113(EtOH)	8.61 (1H, s, CH) 7.67-7.95 (4H, m, Ar) $CDCl_3$	2229(CN) 1620(C=C) 1538(NO_2) 1328(NO_2)		[17], [25]
5	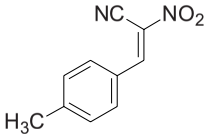	93-94(EtOH) 94-96(hex/AcOEt)	8.63 (1H, s, CH) 7.92 (2H, d, J=8.80, 2CH) 7.40 (2H, d, J=8.80, 3CH) 2.51 (3H, s, CH_3) $CDCl_3$			[17], [32], [33]

No.		t_t [°C] (solvent)	1H-NMR δ [ppm]	IR [cm^{-1}]	UV λ (log ε) [nm]	Ref.
6	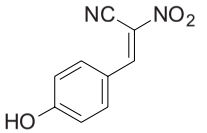	215-218(hex/AcOEt) 216-217(EtOH)	9.97 (1H, s, OH) 8.78 (1H, s, CH) 8.12 (2H, d, *J*=8.80, Ar) 7.11 (2H, d, *J*=8.80, Ar) d_6-acetone			[32], [33]
7	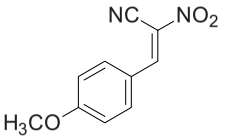	97-98(EtOH) 101(CCl_4) 104-105($CHCl_3$)	8.58 (1H, s, CH) 8.01 (2H, d, *J*=9.00, 2CH) 7.06 (2H, d, *J*=9.00, 2CH) 3.94 (3H, s, CH_3) $CDCl_3$	2229(CN) 1589(C=C) 1505(NO_2) 1317(NO_2)	382(4.48) CH_3CN 247(3.99) CH_3CN 367 MeOH 244 MeOH 390 EtOH	[12], [17], [18], [20], [23], [31], [32], [36]
8	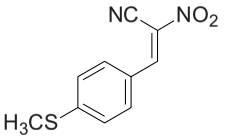	115-117(hex/AcOEt) 117-118(EtOH)	8.55 (1H, s, CH) 7.90 (2H, d, *J*=8.80, Ar) 7.34 (1H, d, *J*=8.80, Ar) 2.55 (3H, s, CH_3) $CDCl_3$			[32], [33]
9	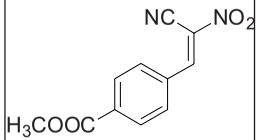	166-167(EtOH)	8.70 (1H, s, CH) 8.01-8.30 (4H, m, Ar) 3.99 (3H, s, CH_3) $CDCl_3$	2233(CN) 1624(C=C) 1542(NO_2) 1332(NO_2)		[18], [25]
10	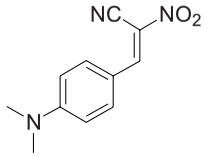	189(EtOH) 182-183(C_6H_6)	8.49 (1H, s, CH) 7.93 (2H, d, *J*=8.50, 2CH) 6.76 (2H, d, *J*=9.50, 3CH) 3.20 (6H, s, $2CH_3$) $CDCl_3$	2213(CN) 1618(C=C) 1542(NO_2) 1389(NO_2)	485(4.67) 481(4.70)MeOH 275(3.90)MeOH	[18], [20], [23], [29]
11	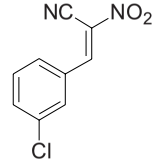	67-68(EtOH)	8.60 (1H, s, CH) 7.42-8.02 (4H, m, Ar) $CDCl_3$	2235(CN) 1622(C=C) 1532(NO_2) 1334(NO_2)		[25]

12	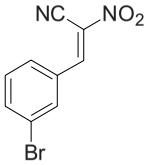	85-86(EtOH)	8.59 (1H, s, CH) 7.37-8.09 (4H, m, Ar) $CDCl_3$	2233(CN) 1618(C=C) 1532(NO_2) 1331(NO_2)		[25]
13	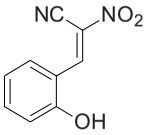	136(CCl_4)				[12]
14	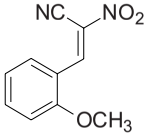	129-131(hex/AcOEt) 126(CCl_4) 130-132(EtOH)	9.21 (1H, s, CH) 6.97-8.31 (4H, m, Ar) 4.01 (3H, s, CH_3) $CDCl_3$	2235(CN) 1590(NO_2) 1330(NO_2)		[24], [32], [33]
15	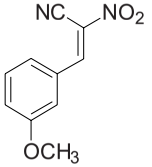	118-120(hex/AcOEt) 118-119(CCl_4) 119-122(EtOH)	8.62 (1H, s, CH) 7.22-7.60 (4H, m, Ar) 3.88 (3H, s, CH_3) $CDCl_3$	2235(CN) 1590(NO_2) 1335(NO_2)	241 208	[24], [32], [33]
16	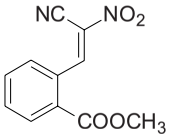	117-118(EtOH)	9.49 (1H, s, CH) 8.25-8.15 (1H, m, 3-H) 7.90-7.67 (3H, m, 4-H 5-H 6-H) 3.98 (3H, s, OMe) $CDCl_3$	2238 (CN) 1697 (COOMe) 1543 (NO_2)	303 (4.05) MeOH 223 (4.07) MeOH	[28]
17	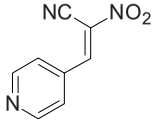	100(CCl_4)				[12]

No.		t_t [°C] (solvent)	1H-NMR δ [ppm]	IR [cm^{-1}]	UV λ (log ε) [nm]	Ref.
18	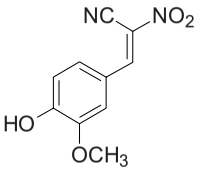	168(CCl_4)	8.57 (1H, s, CH) 7.78 (1H, d, 2CH) 7.49 (1H, dd, 3CH) 7.08 (1H, d, 3CH) 6.50 (1H, s, OH) 4.01 (3H, s, CH_3) $CDCl_3$	2225(CN) 1620(C=C)	390(4.45)	[12], [23]
19	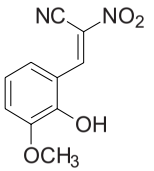	155-156(CCl_4)				[12]
20	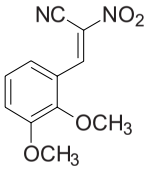	101(CCl_4)				[12]
21	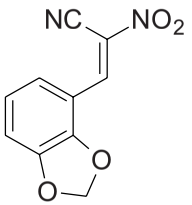	149(CH_3COOH)				[12]
22	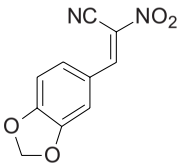	142-143(EtOH)	8.56 (1H, s, CH) 6.94-7.70 (3H, m, Ar) 6.17 (2H, s, CH_2) $CDCl_3$			[32]

23	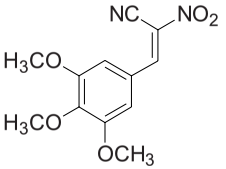	180(CCl_4)		2240(CN) 1570(NO_2) 1310(NO_2)		[21]
24	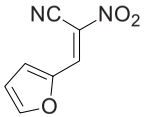	130(CCl_4) 126-127(EtOH)	8.43 (1H, s, CH) 7.93 (1H, d, J^3=1.55, CH) 7.54 (1H, d, J^3=3.43, CH) 6.81 (1H, dd, J^3=3.43, J^3=1.55, CH) $CDCl_3$	2234(CN) 1607(C=C) 1514(NO_2) 1307(NO_2)	371(4.33)EtOH	[12], [20], [23], [27], [30], [32]
25	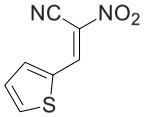	168(EtOH)	8.81 (1H, s, CH) 8.04 (1H, d, J=4.91, CH) 8.00 (1H, d, J=4.02, CH) 7.36 (1H, dd, J=4.02, J=4.91, CH) $CDCl_3$	2225(CN) 1615(C=C)	375(4.25)EtOH	[20], [23], [27], [32]
26	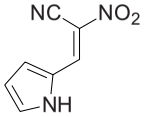	174-175(EtOH)			420(4.67)EtOH	[27]
27	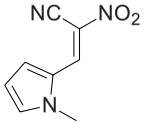	184-186(EtOH)			430(4.54)EtOH	[27]
28	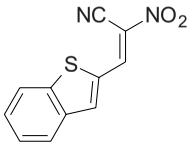	194(CCl_4)				[12]

No.		t_t [°C] (solvent)	1H-NMR δ [ppm]	IR [cm^{-1}]	UV λ (log ε) [nm]	Ref.
29	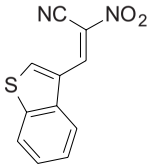	203-204($CHCl_3$ or xylene)				[12]
30	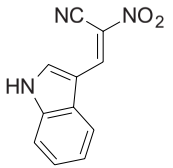	215(CH_3NO_2)				[29]
31	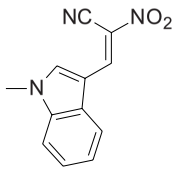	207-208(CH_3NO_2)				[29]
32	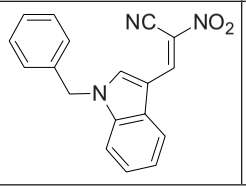	211(CH_3NO_2)				[29]

TECHNICAL TRANSACTIONS 2/2018
CHEMISTRY
DOI: 10.4467/2353737XCT.18.025.7998
SUBMISSION OF THE FINAL VERSION: 10/1/2018

Przemysław Woliński
Agnieszka Kącka-Zych (akacka@chemia.pk.edu.pl)
Faculty of Chemical Engineering and Technology, Cracow University of Technology

Chemistry of 2-aryl-1-cyano-1-nitroethenes. Part II. Chemical transformations

Chemia 2-arylo-1-cyjano-1-nitroetenów. Część II. Chemiczne transformacje

Abstract

This work is a continuation of our study on the chemistry of 2-aryl-1-cyano-1-nitroethenes. In this paper, we describe the reactivity of 2-aryl-1-cyano-1-nitroethenes as a key component in [2+3] and [2+4] cycloaddition reactions, and in other transformations.

Keywords: 2-aryl-1-cyano-1-nitroethene, [2+3] cycloaddition, [2+4] cycloaddition, transformations of 2-aryl-1-cyano-1-nitroethenes, ACN

Streszczenie

Praca stanowi kontynuację studiów dotyczących chemii 2-arylo-1-cyjano-1-nitroetenów. W jej ramach dokonaliśmy przeglądu transformacji 2-arylo-1-cyjano-1-nitroetenów jako komponentów [2+3], [2+4] cykloaddycji oraz w innych reakcjach.

Słowa kluczowe: 2-arylo-1-cyjano-1-nitroeten, [2+3] cykloaddycja, [2+4] cykloaddycja, transformacje 2-arylo-1-cyjano-1-nitroetenów

1. Introduction

The chemistry of substituted 2-aryl-1-cyano-1-nitroethenes (ACNs) is a promising field in modern organic chemistry and accessible compounds for preparation of various important organic components [1]. ACNs have been known since the first half of the twentieth century [2]. Currently, several compounds of this group are known; nonetheless, their chemical properties are not well recognized [3–6]. The chemical transformations of these compounds include [2+3] cycloaddition to nitrogen-containing Three-Atoms-Components (TACs), which occupies an important place among the synthetic tools of organic chemistry [7]. Several examples of the participation of ACNs in Diels-Alder reactions as ethylenes as well as heterodienes are also known [3, 8, 9].

This paper is a continuation of our study on the chemistry of 2-aryl-1-cyano-1-nitroethenes. In the previous paper we characterized the synthetic protocols as well as the physical description of the compounds studied. In turn this part of our study contains the chemical transformations of ACNs as a component in different types of reactions.

2. [2+3] cycloaddition reactions with 2-aryl-1-cyano-1-nitroethenes

Chemical transformations of substituted cyanonitroethenes include [2+3] cycloaddition reactions (1,3-dipolar cycloaddition) to nitrogen containing TACs, which occupies an important place among the synthetic tools of organic chemists. Formed as a result, nitrogen containing heterocycles demonstrates a broad spectrum of significant properties. In particular the 1,2,3-triazole rings constitute a structural fragment of a number of pharmaceuticals [1], photosensitizers [10], and optical bleaching agents [11].

In 2011, *Nosachev, Shchurova* and *Tyrkov* [7] presented a study of the [2+3] cycloaddition reactions of 2-phenyl-1-cyano-1-nitroethene (PCN) (**1**) with arylazides (**2a,b**). Reactions conducted in diethyl ether at room temperature gave a mixture of regioisomeric 1-aryl-4-nitro-5-phenyl-4,5-dihydro-1H-1,2,3-triazole-4-carbonitriles (**3a,b**) and 1-aryl-5-nitro-4-phenyl-4,5-dihydro-1H-1,2,3-triazole-5-carbonitriles (**5a,b**). Finally, 1-aryl-5(4)-phenyl-1H-1,2,3-triazole-4(5)-carbonitriles (**4a,b**, **6a,b**) (Table 1) were formed as a result of spontaneous nitrous acid extrusion from primary [2, 3] cycloaddition products [7].

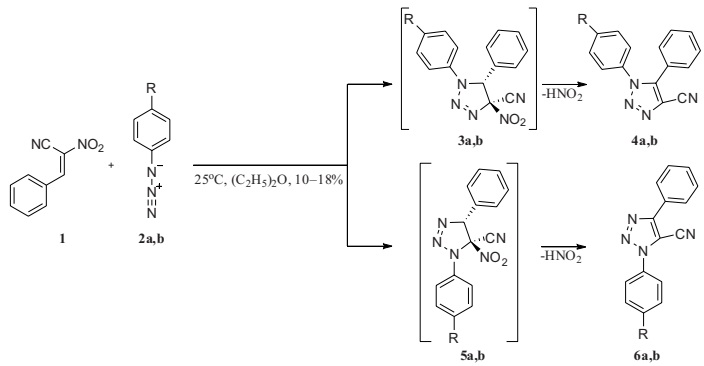

Table 1. Synthesis of 1-aryl-5(4)-phenyl-1H-1,2,3-triazole-4(5)-carbonitriles (**4a,b**, **6a,b**) from PCN (**1**) and arylazides (**2a,b**) [7]

Entry	Azide	R	Product	Yield [%]
1	**2a**	H	**4a**	15
2	**2b**	CH_3	**4b**	18
3	**2a**	H	**6a**	10
4	**2b**	CH_3	**6b**	10

Piet et al [12] also deal with the [2+3] cycloaddition reactions of PCN (**1**) with phenylazide (**2a**) and methylazide (**7**). They obtained 1-methyl-5-phenyl-1H-1,2,3-triazole-4-carbonitrile (**9**) and 1-methyl-4-phenyl-1H-1,2,3-triazole-5-carbonitrile as a result (**11**). In the case of 1,5-diphenyl-1H-1,2,3-triazole-4-carbonitrile (**4a**) and 1,4-diphenyl-1H-1,2,3-triazole-5-carbonitrile (**6a**) the authors do not present the quantities of the compounds obtained (Table 2).

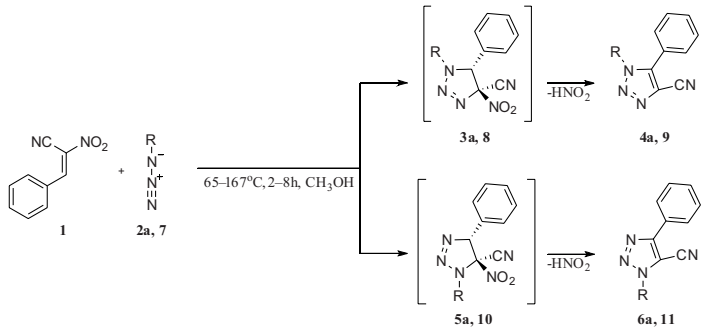

Table 2. Synthesis of 1-methyl-5(4)-phenyl-1H-1,2,3-triazole-4(5)-carbonitrile (**9**)(**11**) and 1,5(4)-diphenyl-1H-1,2,3-triazole-4(5)-carbonitrile (**4a**)(**6a**) [12]

Entry	Azide	R	Product	Ratio
1	**2a**	C_6H_5	**4a:9a**	–
2	**7**	CH_3	**9:11**	0.13

Likewise, *Amantini* et al [13] described the synthesis of 4-aryl-1H-1,2,3-triazole-5-carbonitriles (**15a-g**) through tetrabutylammonium fluoride (TBAF) catalysed [2+3] cycloaddition of (E)-ACNs (**1**, **12a-f**) with azido(trimethyl)silane (**13**). These reagents subsequently experienced aromatization and [1.3]–sigmatropic hydrogen shift, leading to 4-aryl-1H-1,2,3-triazole-5-carbonitriles (**15a-g**) with excellent yield (Table 3).

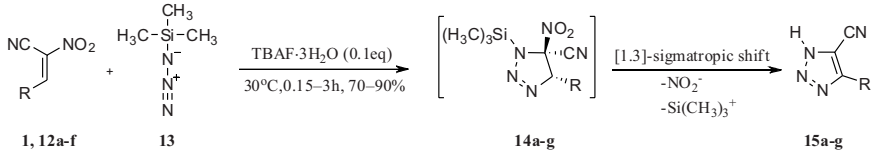

Table 3. Synthesis of 4-aryl-1H-1,2,3-triazole-5-carbonitriles (**15a-g**) through TBAF catalyzed [2+3] cycloaddition [13]

Entry	ACN	R	Time [h]	Product	Yield [%]
1	**1**	C_6H_5	3	**15a**	85
2	**12a**	(4-Cl)-C_6H_4	0.15	**15b**	90
3	**12b**	(4-OCH_3)-C_6H_4	3	**15c**	75
4	**12c**	(4-OH)-C_6H_4	3	**15d**	70
5	**12d**	(3,4-OCH_2O)-C_6H_3	1	**15e**	85
6	**12e**	2-furyl	2	**15f**	75
7	**12f**	2-thienyl	3	**15g**	75

Another example of catalysed [2+3] cycloadditions are the reactions investigated by *Fringuelli's* group [14]. The catalysed process was the reaction between (E)-ACNs (**1**, **16a-e**) and azido(trimethyl)silane (**13**) carried out in the presence of Amberlite IRA900F (Amb-F). These reactions are used for the preparation of 4-aryl-1H-1,2,3-triazole-5-carbonitriles (**15a**, **18a-e**); however, the reaction yield is 60-95% (Table 4).

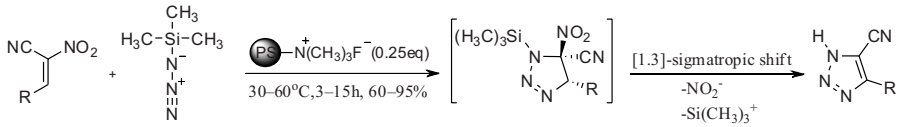

1, 16a-e **13** **14a, 17a-e** **15a, 18a-e**

Table 4. Synthesis of 4-aryl-1H-1,2,3-triazole-5-carbonitriles (**15a, 18a-e**) in the presence of Amb-F [14]

Entry	ACN	R	T [°C]	Time [h]	Product	Yield [%][(a)]
1	**1**	C_6H_5	30	3	**15a**	95
2	**1**	C_6H_5	30	9	**15a**	93[(b)]
3	**1**	C_6H_5	30	3	**15a**	82[(c)]
4	**1**	C_6H_5	30	3	**15a**	83[(d)]
5	**1**	C_6H_5	30	3	**15a**	60[(e)]
6	**1**	C_6H_5	30	3	**15a**	94[(f)]
7	**1**	C_6H_5	30	3	**15a**	95[(f)]
8	**16a**	(2-OCH_3)C_6H_4	60	12	**18a**	92
9	**16b**	(2,4-OCH_3)C_6H_3	60	15	**18b**	90
10	**16c**	(2,4,6-CH_3)C_6H_2	60	14	**18c**	90
11	**16d**	(2,4-Cl)C_6H_3	60	12	**18d**	75
12	**16e**	(2-Cl-6-F)C_6H_3	60	12	**18e**	80

(a) 3.0 eq. of azido(trimethyl)silane (**13**) (b) 0.10 eq. Amb-F. (c) Reaction in 2 ml/mmol of THF. (d) Reaction in 2 ml/mmol of DCE. (e) 0.10 eq. TBAF. (f) Reaction with recovered Amb-F.

Nosachev et al [15] presented the studies of [2+3] cycloaddition of PCN (**1**) to N-phenacyl- (**19a**) or N-acetonyl- (**19b**) isoquinolinium bromides. Those reactions provide an interesting pathway to the hardly accessible isoquinolines (**21a,b**) in high to excellent yield

and full regioselective manner. The authors also obtained 1-nitro-2,3-diphenyl- (**22a**) and 3-methyl-1-nitro-2-phenyl- (**22b**) 2,2a,5,5a,6,10b-hexahydro-1H-benzo[g][1,2,3]triazino-[5,4,3-cd]indolizine-1-carbonitriles resulting from the formation of intermediate hydrazine derivatives of pyrrolidine which undergo a spontaneous heterocyclization into compounds **22a,b** with 30-41% yield (Table 5) [15].

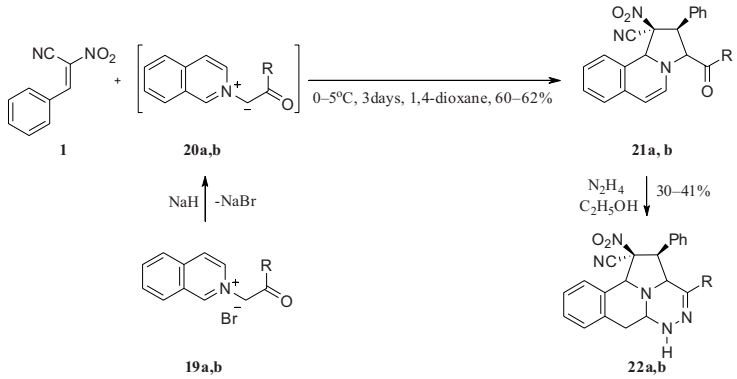

Table 5. Synthesis of isoquinolines (**21a,b**), 1-nitro-2,3-diphenyl- (**22a**) and 3-methyl-1-nitro-2-phenyl- (**22b**) 2,2a,5,5a,6,10b-hexahydro-1H-benzo[g][1,2,3]triazino-[5,4,3-cd]indolizine-1-carbonitriles [15]

Entry	Substrate	R	Product	Yield [%]	Product	Yield [%]
1	**19a**	C_6H_5	**21a**	60	**22a**	41
2	**19b**	CH_3	**21b**	62	**22b**	30

Recently published experimental and quantum-chemical studies confirm that reactions between (E)-ACNs (**1**, **12a,b**, **23**) and diazofluorene (**24**) lead to acyclic 2,3-diazabuta-1,3-diene derivatives (**27a-d**) (Table 6) instead of the expected pyrazoline systems [16]. The quantum-chemical calculations suggest that this could be a consequence of the formation of zwitterionic structures (**26a-d**) in the first reaction stage. The authors explained this as a specific property of the (E)-2-aryl-1-cyano-1-nitroethenes (**1**, **12a,b**, **23**) group.

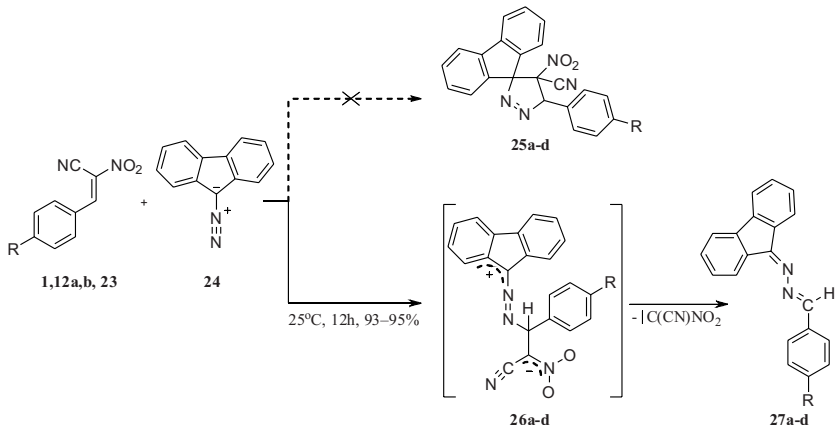

Table 6. Synthesis of 2,3-diazabuta-1,3-diene derivatives (**27a-d**) [16]

Entry	ACN	R	Product	Yield [%]
1	**1**	C_6H_5	**27a**	95
2	**12a**	(4-Cl)-C_6H_4	**27b**	93
3	**12b**	(4-OCH_3)-C_6H_4	**27c**	95
4	**23**	(4-F)-C_6H_4	**27d**	95

3. [2+4] cycloaddition reactions with 2-aryl-1-cyano-1-nitroethenes

Thanks to their specific structure, ACNs can undergo Diels-Alders reactions as a heterodiene component as well as dienophil one. This feature broadens their use significantly. As a result of these reactions biphenyl analogues, norbornenes and benzoxazines derivatives have been produced [7].

Jasiński et al [17, 18], conducted a series of reactions of ACNs (**1**, **12a,b**, **28a,b**) with cyclopentadiene (**29**) in nitromethane which lead to the formation of *endo*- and *exo*-nitronorbornenes (**30a-e**, **31a-e**). After 24 hours, almost full conversion was achieved and the products (**30a-e**, **31a-e**) (Table 7) were isolated by semipreparative HPLC.

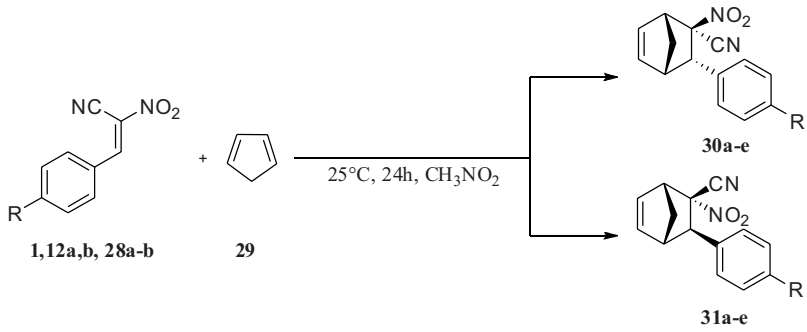

Table 7. Synthesis of nitronorbornenes (**30a-e**, **31a-e**) in nitromethane [17]

Entry	ACN	R	T [°C]	Products	30a-e:31a-e ratio
1	**1**	H	25	**30-31a**	0.14
2	**12a**	Cl	25	**30-31b**	0.15
4	**12b**	CH_3O	25	**30-31c**	0.08
3	**28a**	Br	25	**30-31d**	0.15
5	**28b**	$COOCH_3$	0	**30-31e**	0.17
6	**28b**	$COOCH_3$	25		0.19

Recently Łapczuk-Krygier et al [19] performed cycloaddition of ACNs (**1**, **12a,b**, **23**, **28b**, **32**) to cyclopentadiene (**29**) in ionic liquids. In comparison to the earlier study [17], the authors obtained cycloadducts (**30a-c**, **30e**, **33a,b**, **31a-c**, **31e**, **34a,b**) after only 10

minutes, and varying stereoselectivity which depended on the ionic liquid used (Table 8). They proposed this method as effective and eco-friendly.

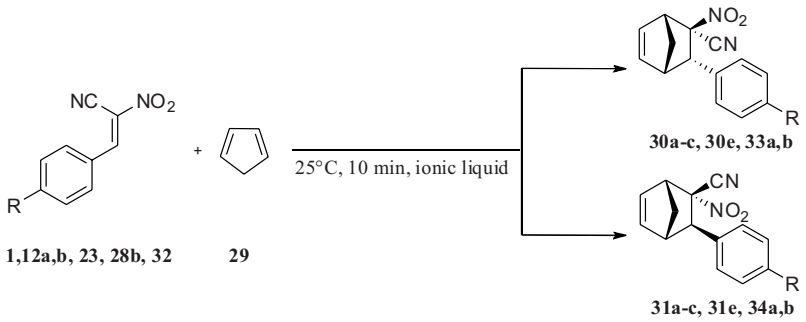

1,12a,b, 23, 28b, 32 **29** **30a-c, 30e, 33a,b** **31a-c, 31e, 34a,b**

Table 8. Synthesis of nitronorbornenes (**30a-c**, **30e**, **33a,b**, **31a-c**, **31e**, **34a,b**) in ionic liquids [19]

Entry	ACN	R	Ionic liquid	Products	Products ratio
1	**1**	H	[BMIM][Cl]	**30a, 31a**	0.16
2		H	[TEAS]		0.16
3		H	[HMIM][HSO_4]		0.19
4		H	[C_6MIM][Cl]		0.14
5		H	[TEAP]		0.13
6		H	[BMIM][BF_4]		0.11
7	**12a**	Cl	[BMIM][Cl]	**30b, 31b**	0.17
8	**12b**	CH_3O	[BMIM][Cl]	**30c, 31c**	0.24
9	**23**	F	[BMIM][Cl]	**33a, 34a**	0.14
10	**28b**	$COOCH_3$	[BMIM][Cl]	**30e, 31e**	0.12
11	**32**	CH_3	[BMIM][Cl]	**33b, 34b**	0.13

Baichurin et al. [20] synthesized *gem*-cyanonitrocyclohexenes (**36a-d**) by cycloaddition of ACNs (**1**, **12b**, **12e-f**) to 2,3-dimetyl-1,3-butadiene (**35**). The reaction was performed in boiling toluene, and after 2-9 hrs the products were isolated with 54-94% yield (Table 9).

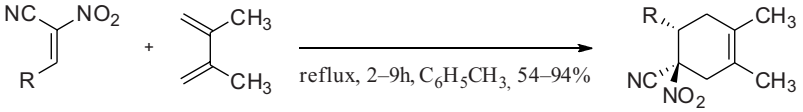

1,12b, 12e-f **35** **36a-d**

Table 9. Synthesis of *gem*-cyanonitrocyclohexenes (**36a-d**) in toluene [20]

Entry	ACN	R	Time [h]	Product	Yield [%]
1	**1**	C_6H_5	3	**36a**	75
2	**12b**	(4-CH_3O)C_6H_4	9	**36b**	94
3	**12e**	2-furyl	2	**36c**	54
4	**12f**	2-thienyl	4	**36d**	83

A series of 2-aryl-1-cyano-1-nitroethenes (**1**, **16b-d**, **32**, **37a-g**) have been used in cycloaddition to four different 1,3-butadienes (**35**, **38a-c**) by *Pizzo* et al [21]. They conducted the reactions in solvent free conditions and generated *in situ* obtaining very good yields (75–88%) of cycloadducts (**39a-n**). Aromatization of (**39a-n**) was achieved by reaction with 1,8-diazabicyclo[5.4.0]undec-7-ene (DBU) in the presence of O_2. Biphenyls (**40a-n**) were isolated in 45-80% yield (Table 10).

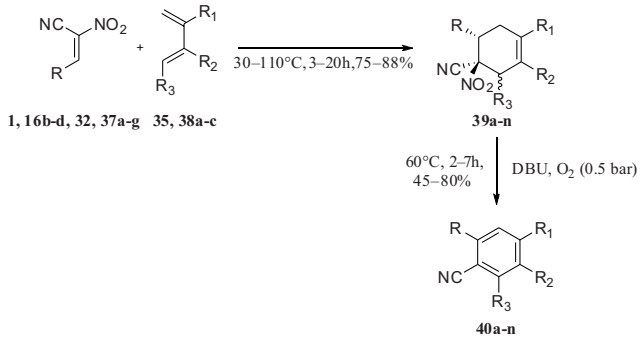

Table 10. Synthesis of cycloadducts (**39a-n**) and biphenyls (**40a-n**) in solvent-free conditions [21]

Entry	ACN	R	Diene	R_1, R_2, R_3	T [°C]	Time [h]	Yield of 39 [%]	Time [h]	Yield of 40 [%]
1	**1**	C_6H_5	**35**	R_1=R_2=CH_3, R_3=H	60	5	86	3	75
2		C_6H_5	**38a**	R_1=R_2=H, R_3=CH_3	60	10	85	5	65
3		C_6H_5	**38b**	R_1=CH_3, R_2=R_3=H	60	12	80	4	70
4	**16b**	(2,4-CH_3O)C_6H_3			30	12	80	5	45
5	**16c**	(2,4,6-CH_3)C_6H_2			30	12	78	3	62
6	**16d**	(2,4-Cl)C_6H_3			60	6	84	5	70
7	**37a**	(2-CH_3)C_6H_4			60	6	85	6	57
8	**37b**	(2-CH_3O)C_6H_4			60	20	88	3	60
9	**37c**	(2-CF_3)C_6H_4			30	12	77	2.5	70
10	**37d**	(2-NO_2)C_6H_4			30	12	78	6	57
11	**37e**	(4-CN)C_6H_4			30	10	85	6	77
12	**37f**	(2-Cl-6-F)C_6H_3			60	12	82	2	70
13	**37g**	(3,5-Br-4-OH) C_6H_2			30	15	75	7	80
14	**32**	(4-CH_3)C_6H_4	**38c**	R_1=R_2=R_3=H	110	12	75	6	65

Vaccaro et al [22] presented an uncatalysed and solvent-free cycloaddition of ACNs (**1**, **12a-e**, **16b**, **32**, **37b**, **37d**, **41a,b**) to 1-(trimethylsilyloxy)-cyclohex-1-ene (**42**). The hexahydro-4*H*-1,2-benzoxazine-2-oxide (**43a-l**) formed was isolated with 80–90% yield (Table 11). The authors showed this reaction to be fully regio- and stereoselective.

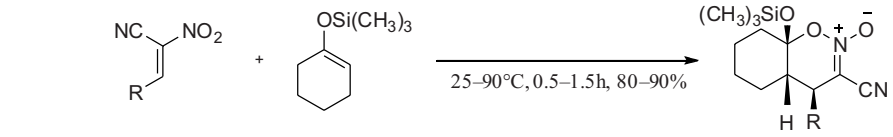

1, 12a-e, 16b, 32, 37b, 37d, 41a,b 42 **43a-l**

Table 11. Synthesis of hexahydro-4*H*-1,2-benzoxazine-2-oxides (**43a-l**) in solvent-free conditions [22]

Entry	ACN	R	T [°C]	Time [h]	Product	Yield [%]
1	**1**	C_6H_5	25	0.75	**43a**	90
2	**12a**	$(4\text{-Cl})C_6H_4$	25	0.75	**43b**	90
3	**12b**	$(4\text{-}CH_3O)C_6H_4$	30	1.25	**43c**	90
4	**12c**	2-furyl	50	0.5	**43d**	86
5	**12d**	$(3,4\text{-}OCH_2O)C_6H_3$	60	0.5	**43e**	80
6	**12e**	2-thienyl	60	0.5	**43f**	84
7	**16b**	$(2,4\text{-}CH_3O)C_6H_3$	90	1.0	**43g**	80
8	**32**	$(4\text{-}CH_3)C_6H_4$	25	1.25	**43h**	85
9	**37b**	$(2\text{-}CH_3O)C_6H_4$	40	1.25	**43i**	87
10	**37d**	$(2\text{-}NO_2)C_6H_4$	30	1.0	**43j**	82
11	**41a**	$(4\text{-}CF_3)C_6H_4$	30	1.0	**43k**	80
12	**41b**	$(4\text{-}CH_3S)C_6H_4$	40	1.5	**43l**	85

In 2001 *Fringuelli* et al. [8] vinyl ethers were used (**44a-d**) in a cycloaddition reaction with ACNs (**1**, **12a,b**) in water. The yields of nitronates (**45a-d**) were very high (75-90%) but a mixture of diastereoisomers was obtained (Table 12). The kinetic aspects of these transformations have also been recently discovered [9]

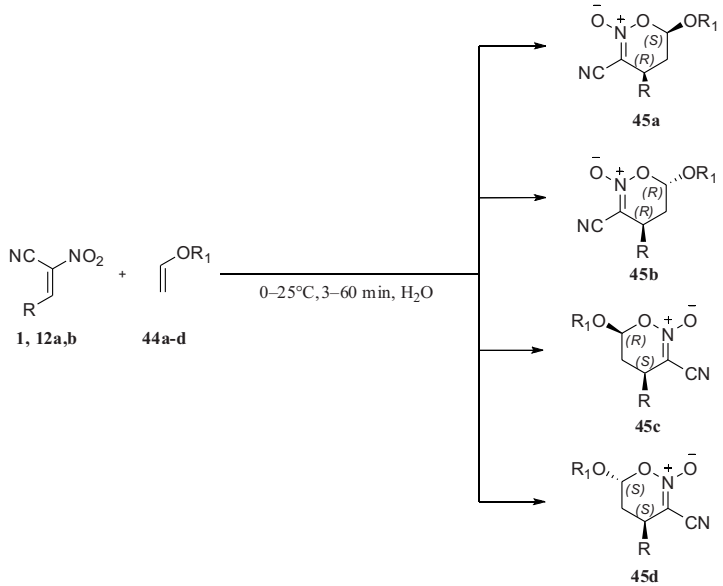

1, 12a,b **44a-d**

Table 12. Synthesis of nitronates (**45a-d**) in water [8]

Entry	ACN	R	R_1	T [°C]	Time [min]	Isomer 45 [%]				Yield [%]
						a	b	c	d	
1	**1**	C_6H_5	C_2H_5	0	3	80	20	–	–	75
2	**12a**	(4–Cl)C_6H_4	C_2H_5	0	20	96	4	–	–	90
3	**12b**	(4–CH_3O)C_6H_4	C_2H_5	25	10	98	2	–	–	85
4	**12a**	(4–Cl)C_6H_4	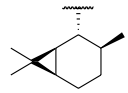	0	30	35	6	54	5	–
5	**12a**	(4–Cl)C_6H_4	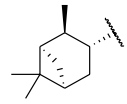	0	30	30	5	60	5	–
6	**1**	C_6H_5	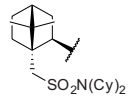	25	60	–	–	85	15	–
7	**12a**	(4–Cl)C_6H_4	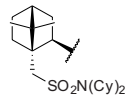	0	60	–	–	85	15	–
8	**12b**	(4–CH_3O)C_6H_4	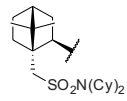	25	60	–	–	83	17	–

In the same year, *Pizzo* et al [3] showed an example of intramolecular cycloaddition in 2-(2'-(3",3"-dimethyl)allyloxyphenyl)-1-cyano-1-nitroetene (**46**) generated *in situ*. This reaction led to the formation of *cis*-4a,10b,-dihydro-1-cyano-4,4,dimethylbenzo[*b*]pyrene- [4,3-*d*][1,2] oxazine-2-oxide (**47**) and its 4a-epimer (**48**) in a 16:1 ratio and with a 60% yield of (**48**).

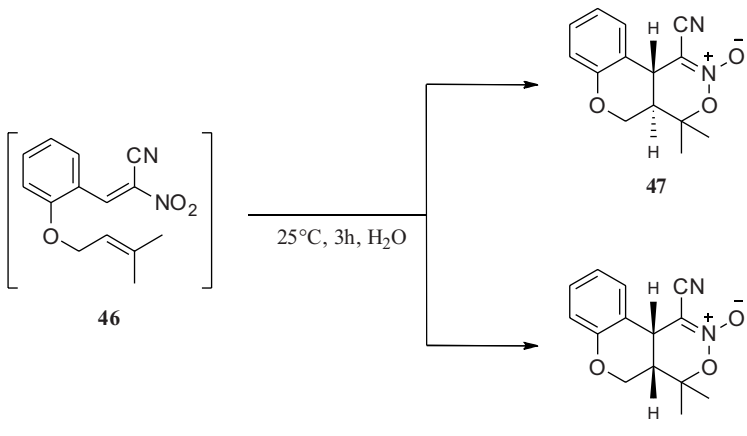

4. Other transformations with 2-aryl-1-cyano-1-nitroethenes

In 1999, *Kislyi* et al [23], found that ACNs (**1**, **12a,b**, **23**) react with cyclohexane-1,3-dione (**49**) or 5,5-dimethylcyclohexane-1,3-dione (**51**) in the presence of catalytic amounts of triethylamine forming 2-amino-3-nitropyrans (**50a-d**, **52a-d**) with good yields (Table 13).

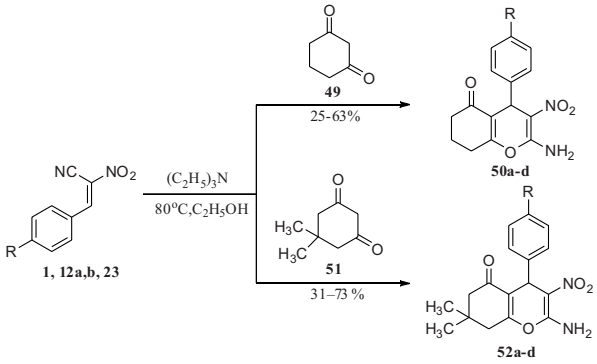

Table 13. Synthesis of 2-amino-3-nitropyrans (**50a-d**, **52a-d**) in the presence of $(C_2H_5)_3N$ [23]

Entry	ACN	R	Product	Yield [%]
1	**1**	H	**50a**	62
2	**12a**	Cl	**50b**	25
3	**12b**	CH_3O	**50c**	63
4	**23**	F	**50d**	30
5	**1**	H	**52a**	73
6	**12a**	Cl	**52b**	31
7	**12b**	CH_3O	**52c**	65
8	**23**	F	**52d**	42

The authors continued work and presented the syntheses of 2-amino-3-nitropyranol-[3,2-c]pyrans (**55a-c**) and 2-amino-3-nitropyranol[3,2,c]chromenes (**57a-c**). These products were obtained with 30-85% yield (Table 14) [24].

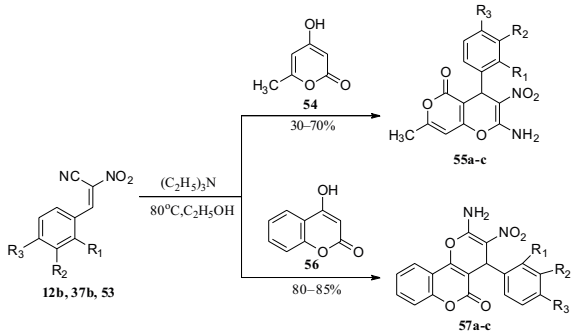

Table 14. Synthesis of 2-amino-3-nitropyranol-[3,2-c]pyrans (**55a-c**) and 2-amino-3-nitropyranol[3,2,c] chromenes (**57a-c**) [24]

Entry	ACN	R_1	R_2	R_3	Product	Yield [%]
1	**12b**	H	H	CH_3O	**55a**	65
2	**37b**	CH_3O	H	H	**55b**	30
3	**53**	H	CH_3O	H	**55c**	70
4	**12b**	H	H	CH_3O	**57a**	85
5	**37b**	CH_3O	H	H	**57b**	80
6	**53**	H	CH_3O	H	**57c**	80

In turn, *Troschutz* and *Luckel* [25] used the PCN (**1**) to synthesize 2,6-diamino-1,4-dihydro-3,5-dinitro-4-phenylpyridine (**58**). They obtained product (**59**) with 40% yield.

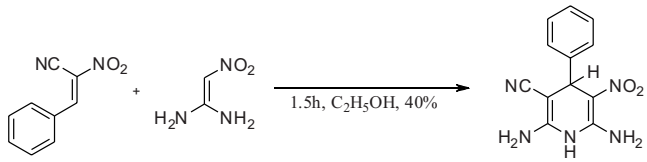

1 **58** **59**

Baichurin et al [26] conducted reactions to prepare 3-(4-dimethylaminophenyl)-2-nitro-4-aryl-propanenitrile (**61a-c**) from 2-aryl-1-cyano-1-nitroethene (**1**, **12b, 12f**) and N,N-dimethlaniline (**60**). The reactions were carried out at room temperature in acetic acid and led to compounds (**61a-c**) with 32–76% yields (Table 15).

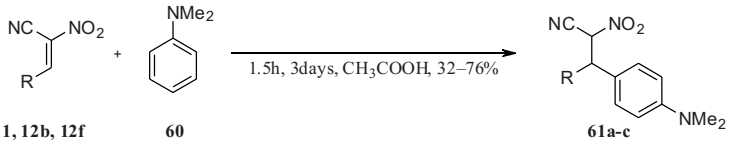

1, 12b, 12f **60** **61a-c**

Table 15. Synthesis of 3-(4-dimethylaminophenyl)-2-nitro-4-aryl-propanenitrile (**61a-c**) [26]

Entry	ACN	R	Product	Yield [%]
1	**1**	C_6H_5	**61a**	75
2	**12b**	$(4\text{-}CH_3O)C_6H_4$	**61b**	76
3	**12f**	2-thienyl	**61c**	32

The reactions of PCN (**1**) with aliphatic and heterocyclic amines with the lowest molecular weights were presented by *Demireva* et al. [27]. They obtained bis-alkylammonium salts of 2,4-dinitro-3-phenylglutarodinitrile (**63a-d**) with 78–84% yields (Table 16).

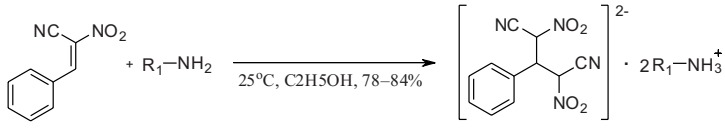

1 **62a-d** **63a-d**

Table 16. Synthesis of bis-alkylammonium salts of 2,4-dinitro-3-phenylglutarodinitrile (**63a-d**) [27]

Entry	Amine	R_1	Product	Yield [%]
1	**62a**	C_7H_{15}	**63a**	80
2	**62b**	C_8H_{17}	**63b**	82
3	**62c**	$C_{17}H_{35}$	**63c**	84
4	**62d**	$C_5H_{11}N$	**63d**	78

In 1984, *Metchkov* and *Demireva* [28] obtained a series of bis(ammonium) salts of 2,4-dinitro-3-(2-furyl)glutarodinitrile (**65a-j**) (Table 17) from 1-nitro-1-cyano-2-(2-furyl) ethane (**12e**) and aliphatic and alicyclic amines (**62b,c, 64a-h**)

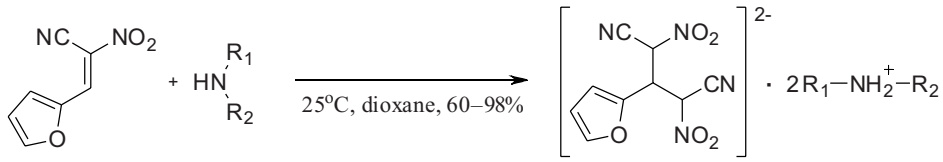

12e **62b,c, 64a-h** **65a-j**

Table 17. Synthesis of bis(ammonium) salts of 2,4-dinitro-3-(2-furyl)glutarodinitrile (65a-j) [28].

Entry	Amine	R_1	R_2	Product	Yield [%]
1	**64a**	H	n-C_3H_7	**65a**	98
2	**64b**	H	n-C_4H_9	**65b**	96
3	**64c**	H	$C(CH_3)_3$	**65c**	60
4	**64d**	H	C_6H_{12}	**65d**	80
5	**62b**	H	C_8H_{17}	**65e**	71
6	**64e**	H	$C_{12}H_{26}$	**65f**	71
7	**64f**	H	$C_{16}H_{33}$	**65g**	73
8	**62c**	H	$C_{17}H_{35}$	**65h**	75
9	**64g**	C_2H_5	C_2H_5	**65i**	83
10	**64h**	-$(CH_2)_5$-		**65j**	83

The same authors [29] presented a synthesis of a series of bis(ammonium) salts of 2,4-dinitro-3-(2-thiophene)glutarodinitrile (**66a-j**). They obtained products (**66a-j**) with good yields, reaching up to 97% (Table 18).

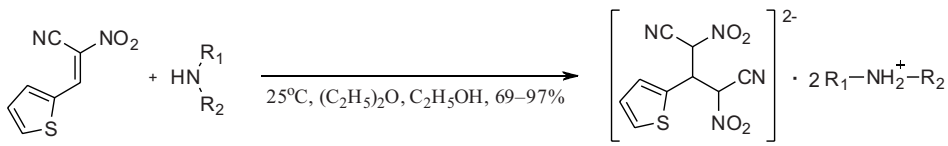

12f **62b,c, 64a-h** **66a-j**

Table 18. Synthesis of bis(ammonium) salts of 2,4-dinitro-3-(2-thiophene)glutarodinitrile (**66a-j**) [29]

Entry	Amine	R_1	R_2	Product	Yield [%]
1	**64a**	H	n-C_3H_7	**66a**	88
2	**64b**	H	n-C_4H_9	**66b**	97
3	**64c**	H	$C(CH_3)_3$	**66c**	97
4	**64d**	H	C_6H_{12}	**66d**	95
5	**62b**	H	C_8H_{17}	**66e**	80
6	**64e**	H	$C_{12}H_{26}$	**66f**	69
7	**64f**	H	$C_{16}H_{33}$	**66g**	82
8	**62c**	H	$C_{17}H_{35}$	**66h**	76
9	**64g**	C_2H_5	C_2H_5	**66i**	96
10	**64h**	-$(CH_2)_5$-		**66j**	52

The authors also showed the synthesis of bis(ammonium) salts of 2,4-dinitro-3-(methoxyphenyl)glutarodinitrile (**68a-j**) with 61–95% yields (Table 19) [30].

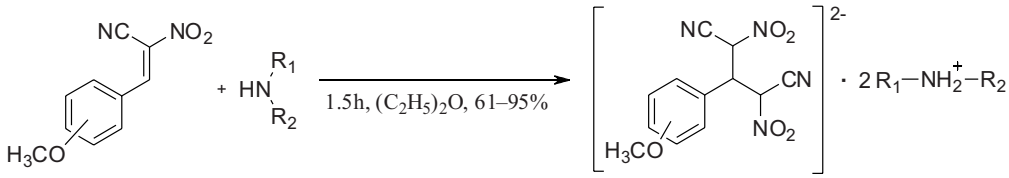

12b, 37b, 53 **64b, 64d, 64i, 67** **68a-f**

Table 19. Synthesis of bis(ammonium) salts of 2,4-dinitro-3-(methoxyphenyl)glutarodinitrile (**68a-f**) [30]

Entry	ACN	Amine	R_1	R_2	Product	Yield [%]
1	2-OCH_3 (**37b**)	**67**	H	H	**68a**	70
2	3- OCH_3 (**53**)	**67**	H	H	**68b**	61
3	4- OCH_3(**12b**)	**67**	H	H	**68c**	77
4	2-OCH_3(**37b**)	**64b**	H	C_4H_9	**68d**	95
5	3- OCH_3(**53**)	**64d**	H	C_6H_{11}	**68e**	92
6	4- OCH_3(**12b**)	**64i**	C_2H_5	C_2H_5	**68f**	76

5. Conclusion

A literature review demonstrated that 2-aryl-1-cyano-1-nitroethenes are mainly applied in the synthesis of carbo- and heterocyclic compounds. These compounds are especially used as ethylene in [2+4] cycloaddition reactions. We also noticed a few examples of [2+3] cycloaddition reactions involving 2-phenyl-1-cyano-1-nitroethenes. As we have shown, there are other examples of uses of ACNs transformations that are mainly involved in bis(ammonium) salts.

References

[1] Grimmett M.R., *Comprehensive Organic Chemistry*, Eds. D. Barton, W.D. Ollis, Pergamon, Oxford 1979, 4, 357–410.

[2] Ried W., Köhler E., Königstein F.J., *Reaktionen mit Nitro-acetonitril*, Liebigs Annalen der Chemie, 1956, 598, 145–148.

[3] Amantini D., Fringuelli F., Piermatti O., Pizzo F., Vaccaro L., *Water, a clean, inexpensive, and re-usable reaction medium. One-pot synthesis of (E)-2-aryl-1-cyano-1-nitroethenes*, Green Chemistry, 2001, 3, 229–232.

[4] Boguszewska-Czubara A., Łapczuk-Krygier A., Rykała K., Biernasiuk A., Wnorowski A., Popiołek Ł., Maziarka A., Hordyjewska A., Jasiński R., *Novel synthesis scheme and in vitro antimicrobial evaluation of a panel of (E)-2-aryl-1-cyano-1-nitroethenes*, Journal of Enzyme Inhibition and Medicinal Chemistry, 2015, 31, 900–907.

[5] Valizadeh H., Mamaghani M., Badrian A., *Effect of Microwave Irradiation on Reaction of Arylaldehyde Derivatives with Some Active Methylene Compounds in Aqueous Media*, Synthetic Communications, 2005, 35, 785–790.

[6] Jasiński R., Mirosław B., Demchuk O.M., Babyuk D., Łapczuk-Krygier A., *In the search for experimental and quantumchemical evidence for zwitterionic nature of (2E)-3-[4-(dimethylamino)phenyl]-2-nitroprop-2-enenitrile – An extreme example of donor–π–acceptor push–pull molecule*, Journal of Molecular Structure, 2016, 1108, 689–697.

[7] Nosachev S.B., Shchurova N.A., Tyrkov A.G., *Reactions of 2-Benzylidenemalononitrile and 2-Nitro-3-phenyl-acrylonitrile with Aryl Azides*, Russian Journal of Organic Chemistry, 2011, 47, 577–580.

[8] Fringuelli F., Matteucci M., Piermatti O., Pizzo F., Burla M.C., *[4 + 2] Cycloadditions of Nitroalkenes in Water. Highly Asymmetric Synthesis of Functionalized Nitronates*, Journal Organic Chemistry, 2001, 66, 4661–4666.

[9] Jasiński R., Kubik M., Łapczuk-Krygier A., Kącka A., Dresler E., Boguszewska-Czubara A., *An experimental and theoretical study of the hetero Diels–Alder reactions between (E)-2-aryl-1-cyano-1-nitroethenes and ethyl vinyl ether: one-step or zwitterionic, two-step mechanism?*, Reaction Kinetics, Mechanisms and Catalysis, 2014, 113, 333–345.

[10] Varma R.S., Kabalka G.W., *Nitroalkenes in the Synthesis of Heterocyclic Compounds*, Heterocycles, 1986, 24, 2645–2677.

[11] Padwa A., Pearson W.M., *Synthetic applications of 1,3-dipolar cycloaddition chemistry toward heterocycles and natural products*, Wiley&Sons, 2002.

[12] Piet J.C., Hetet G.L., Cailleux P., Benhaoua H., Carrier R.,*Reactions des methylazide et phenylazide avec quelquesalcynes et olefins α-nitrees. Syntheseregiospecifique des 1,2,3 triazoles*, Bulletin des Sociètès Chimiques Belges, 1996, 105, 33–44.

[13] AmantiniD., Fringuelli F.,PiermattiO., Pizzo F., Zunino E., Vaccaro L.,*Synthesis of 4-Aryl-1H-1,2,3-triazoles through TBAF-Catalyzed [3+2] Cycloaddition of 2-Aryl-1-nitroethenes with $TMSN_3$ under Solvent-Free Conditions*, The Journal of the Organic Chemistry, 2005, 70, 6526–6529.

[14] Friguelli F., Lanari D., Pizzo F., Vaccaro L., *Amberlite IRA900F as a Solid Fluoride Source for a Variety of Organic Transformations under Solvent-Free Conditions*, European Journal of Organic Chemistry, 2008, 23, 3928–3932.
[15] Nosachev S.B., Del'netskaya K.A., Solov'ev N.A., Tyrkov A.G., *Substituted 1-nitro-2-phenylethenes in reaction with N-phenacyl- and N-acetonylisoquinolinium bromides*, Russian Journal of Organic Chemistry, 2010, 46, 1427–1429.
[16] Jasiński R., Kula K., Kącka A., Mirosław B., *Unexpected course of reaction between (E)-2-aryl-1-cyano-1-nitroethenes and diazafluorene: why is there no 1,3-dipolar cycloaddition?*, Monatschefte für Chemie, 2017, 148, 909–915.
[17] Jasiński R., Rzyman M., Barański A., *Conjugated nitroalkenes in cycloaddition reactions. Part 2. Diels-Alder reactions of E-2-aryl-1-cyano-1-nitroethenes with cyclopentadiene*, Collection of Czech Chemical Communications, 2010, 75, 919–929.
[18] Łapczuk-Krygier A., Ponikiewski Ł., Jasiński R., *The crystal structure of (1RS,4RS,5RS,6SR)-5-cyano-5-nitro-6-phenyl-bicyclo[2.2.1]hept-2-ene*, Crystallography Reports, 2014, 59, 961–963.
[19] Łapczuk-Krygier A., Dresler E., Jasiński R., *Ionic liquids as an effective and eco-friendly medium for synthesis of nitrosubstitutednorborenes analogs*, Przemysł Chemiczny, 2016, 95, 1928–1931.
[20] Baichurin R. I., Aboskalova N. I., Trukhin E. V., Berestovitskaya V. M., *Aryl(hetaryl)-Containing gem-Cyanonitroethenes: Synthesis, Structure, and Reactions with 2,3-Dimethyl-1,3-butadiene*, Russian Journal of General Chemistry, 2015, 85, 1845–1854.
[21] Fringuelli F., Girotti R., Piermatti O., Pizzo F., Vaccaro L., *Uncatalyzed and sol vent-free multicomponent process for the synthesis of biphenyl-2-carbonitrile derivatives*, Organic Letters, 2006, 8, 5741–5744.
[22] Bellachioma G., Castrica L., Fringuelli F., Pizzo F., Vaccaro L., *Catalyst- and solvent-free conditions as an environmentally benign approach to 2-aryl-3-cyano-hexahydro-4H-1,2-benzoxazine-2-oxides*, Green Chemistry, 2008, 10, 327–332.
[23] Kislyi V.P., Nesterov V.N., Shestopalov A.M., Semenov V.V., *Heterocycles with a beta-nitroenamineframent. 1. Synthesis of 2-amino-3-nitro-pyrans from nitroacetonitrile*, Russian Chemical Bulletin, 1999, 48, 1131–1134.
[24] Kislyi V.P., Nesterov V.N., Shestopalov A.M., Semenov V.V., *Heterocycles with a β-nitroenamine fragment. 2. Synthesis of 2-amino-3-nitropyrano[3,2-c]pyrans and 2-amino-3-nitropyrano[3,2,c]chromenes from nitroacetonitrile*, Russian Chemical Bulletin, 1999, 4896, 1135–1138.
[25] Troschütz R., Lückel A., *Nitroketenaminale, 7. Mitt.: Synthese von substituierten 2-Amino-3-nitropyridinen aus 1,3-Biselektrophilen und 2-Nitroethen-1,1-diamin*, Archiv der Pharmazic, 1992, 325, 785–789.
[26] Meichkov T.D., Demireva Z.I., *Synthesis of some bis(ammonium) salts of 2,4-dinitro-3-(2-furyl)glutarodinitrile*, Journal of Chemical and Engineering Data, 1984, 29, 483–484.
[27] Meichkov T.D., Demireva Z.I., Tonicheva E., *Synthese einigerbie-ammonium salze des 2,4-dinitro-3-(2-thienyl)glutaranitrllen*, Zeitschrift für Chemie, 1985, 25, 62–63.

[28] Demireva Z.I., Binev I.G., Juchnovski I.N., *A new, versatile acyl activating reagent for peptide synthesis: asymmetrically selective peptide synthesis by use of optically active 3-hydroxyhydantoin*, Tetrahedron Letters, 1976, 18, 1523–1526.
[29] Baichurin R.I., Aboskalova N.I., Turkhin E.V., Berestovitskaya V.M.,*Arylation of geminally activated nitroethenes*, Russian Journal of Organic Chemistry, 2013, 49, 67–69.
[30] Meichkov T.D., Demireva Z.I., *Die synthese einigerbie-ammonium salze des 2,4-dinitro-3-(methoxyphenyl)glutaranitrllen*, Zeitschrift für Chemie, 1985, 25, 169–170.

TECHNICAL TRANSACTIONS 2/2018
CIVIL ENGINEERING
DOI: 10.4467/2353737XCT.18.026.7999
SUBMISSION OF THE FINAL VERSION: 11/1/2018

Marian Gwóźdź (margwozd@interia.pl)
Faculty of Civil Engineering, Cracow University of Technology

Reliability component differentiation in building structures made of timber

Różnicowanie elementów niezawodności budowlanych konstrukcji drewnianych

Abstract

The design of timber structures according to the current generation of Eurocodes results in new requirements being set for the authors of architectural and building designs with respect to the reliability management of such structures. The reliability problems should be formulated in the building permit design in an unequivocal manner, obliging the authors of the detailed design, as well as the contractors to deliver structures, which have all the operational parameters fully conforming to the expectations of the investor. Substantive and formal basics in this regard are formulated in the Eurocodes: PN-EN 1990, PN-EN 1991, PN-EN 1995 as well as in the related European codes. The reliability management problems of contemporary timber structures are related to the cubature buildings of different life spans, including buildings subjected to the climate loads characterised by several hundred year-long return periods..

Keywords: timber, bearing capacity, reliability, destruction consequence classes, reliability classes, return period, reference period, loads

Streszczenie

Projektowanie konstrukcji drewnianych wg współczesnej generacji norm europejskich stawia przed autorami projektów architektoniczno-budowlanych nowe wymagania w zakresie zarządzania niezawodnością takich obiektów. Problemy niezawodności należy sformułować w projekcie budowlanym w sposób jednoznaczny, zobowiązujący autorów projektów wykonawczych, a także firmy wykonawcze do dostarczenia konstrukcji o parametrach eksploatacyjnych zgodnych z oczekiwaniami inwestora. Podstawy merytoryczne i formalne w tym zakresie są sformułowane w Eurokodach: PN-EN 1990, PN-EN 1991, PN-EN 1995 oraz w europejskich normach pokrewnych. Problemy zarządzania niezawodnością współczesnych konstrukcji drewnianych odniesiono do przypadków budynków kubaturowych o zróżnicowanym okresie użytkowania, w tym poddanym oddziaływaniom klimatycznym o okresie powrotu nawet kilkuset lat.

Słowa kluczowe: drewno, nośność, niezawodność, klasy konsekwencji zniszczenia, klasy niezawodności, okres powrotu, okres odniesienia, obciążenia

1. Introduction

The scope and form of the building permit design according to the Polish regulations [10], treats the reliability of buildings problem in a rather general manner. This makes it possible for the construction companies to erect even large structures according to the so-called replacement designs, even in the cases when the investor delivers his own detailed design with the approved building permit design. In many cases known to the Author, the cubature buildings erected according to the replacement designs have lowered reliability requirements as compared to the investors' original designs. In addition, looking for savings on materials, the authors of replacement designs often select prototypical design solutions, thus posing additional threats to the safe operation. Many buildings erected in the 1990's, such as large area halls covered with roofs of steel or a timber structure may be treated as a negative example of such an approach. The reliability requirements specified for such buildings in the technical description attached to the building permit design most often are limited to a brief reference to the country codes, thus making it possible to underestimate the operating parameters, especially in the area of snow loads. The underestimated cross sections of the roof structures resulted in a permanent need for snow removal, and the costs, which have to be borne by the users, have been incommensurable with the ad hoc benefits gained by the building contractors erecting such structures.

Table 1. Designed life span categories according to PN-EN 1990

Designed life span category	**Designed life span T_d in years**	**Sample structures**
(1)	(2)	(3)
1	10	Temporary structures
2	10–25	Replaceable elements
3	15–30	Agricultural structures and similar
4	50	Ordinary buildings
5	≥ 100	Monumental buildings, bridges

Table 2. Values of conversion coefficients for climate loads according to own research

Return period n [years]	**Conversion coefficients η_d**			
	Actions on structures: snow, wind, temperature			
	s_k	v_b	T_{max}	T_{min}
(1)	(2)	(3)	(4)	(5)
10	0.70	0.90	0.91	0.74
15	0.77	0.93	0.93	0.81
25	0.87	0.96	0.96	0.89
30	0.90	0.97	0.97	0.92
50	1.00	1.00	1.00	1.00
100	1.13	1.04	1.04	1.11
300	1.33	1.10	1.10	1.28
500	1.42	1.12	1.13	1.36

The Ordnance issued by the Minister of Infrastructure on July 3rd, 2003, amending the detailed scope and form of the building permit design, did not introduce any qualitative changes in the area of building reliability management against the previous regulations introduced in 1998 (compare the Polish Law Register no 140, pos. 906). Amendments to the scope of building permit design, taking into account the reliability management rules for the cubature structures according to the Eurocode PN-EN 1990, constitute an efficient remedy against the unfavourable processes described above.

The design of any building structure requires the designed life of the structure T_d to be set, i.e. the time span during which the structure or a component thereof is to serve as intended while subjected to expected maintenance, without the need for major repairs.

The systematic subdivision of the designed life spans into five categories has been introduced in the code PN-EN 1990. This subdivision is listed in Table 1. In most cases building structures are assigned to the fourth category, corresponding to a 50 year-long service time. If the buildings are designed with other assumed service times, the characteristic load values should be corrected, especially the climate loads $\eta_d F_k$, where η_d – a correction factor. Values of the reduction coefficients η_d for various return periods of maximum climate loads, according to the own research [5] are given in Table 2.

2. Analysis of the reliability components for timber structures

In order to differentiate the reliability of the designed building structures the code PN-EN 1990 defines three destruction consequence classes (CC), according to the description specified in Table B1 of the said code. Consequence classes are related to the reliability classes (RC) of structures in such a way, that the consequence class CC3 corresponds to the reliability class RC3, class CC2 – RC2 and class CC1 – RC1. The reliability classes (RC) of structures in the bearing capacity limit state have been defined depending on the recommended minimum value of the reliability factor β_u set for the reference period t = 1 year additionally, in the code PN-EN 1990 one may find the values of the reliability factor determined according to the formula (1) for t = 50 (cf. columns (2) and (7) in Table 3). The reliability factor β (Hasofer, Lind [8]) represents an idea well known in the reliability theory of building structures [1–4], [7–10], [11, 12] and is defined in the probabilistic calculation method of the second level FORM (*First Order Reliability Method*). In particular, the coefficient β is a measure of reliability, which may be specified in the statistical research for random loads and random bearing capacity of the structure. The coefficient β is related to the failure probability P_f of a structure by the following formula:

$$P_f = \Phi(-\beta), \tag{1}$$

where:

Φ – is the Laplace function of the probability distribution of standardised normal distribution, as depicted in Fig. 1.

For the mutually independent random maxima, one may assume that the following relationship holds between the reliability factors specified for the reference periods $T = n$ and $t = 1$ (cf. code PN-EN 1990):

$$\Phi(\beta_n) = \Phi(\beta_1)^n \tag{2}$$

For the selected reference periods n = 10; 15; 25; 30; 50; 100; 300 and 500 – years, the curves according to (2) [6] are compiled in Fig. 2. In addition, the values of reliability factor β_n calculated for these periods in the bearing capacity limit state (LS) for the three reliability classes (RC) are represented in Table 3.

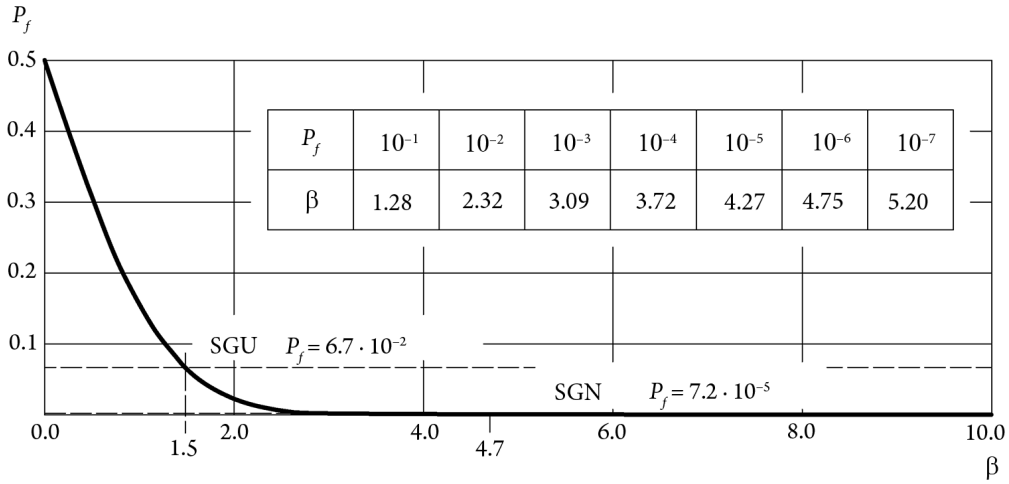

P_f	10^{-1}	10^{-2}	10^{-3}	10^{-4}	10^{-5}	10^{-6}	10^{-7}
β	1.28	2.32	3.09	3.72	4.27	4.75	5.20

Fig. 1. Plot of the P_f – β relationship [6]

In the probabilistic method of the second level, in the case of a linear bearing capacity function:

$$g = R - E, \tag{3}$$

the structural reliability criterion may be expressed by the following inequality

$$\beta = \frac{\overline{R} - \overline{E}}{\sqrt{\mu_R^2 + \mu_E^2}} \geq \beta_u, \tag{4}$$

where:

$\overline{R}, \overline{E}$ – average values,

μ_R, μ_E – standard deviations of random bearing capacities R and load effects E, respectively.

In the basic case the inequality (4) may be replaced by the comparison of computational values: bearing capacity R_d and the corresponding load effect E_d.

$$R_d = \overline{R} - \beta_R \mu_R \geq E_d = \overline{E} + \beta_E \mu_E, \tag{5}$$

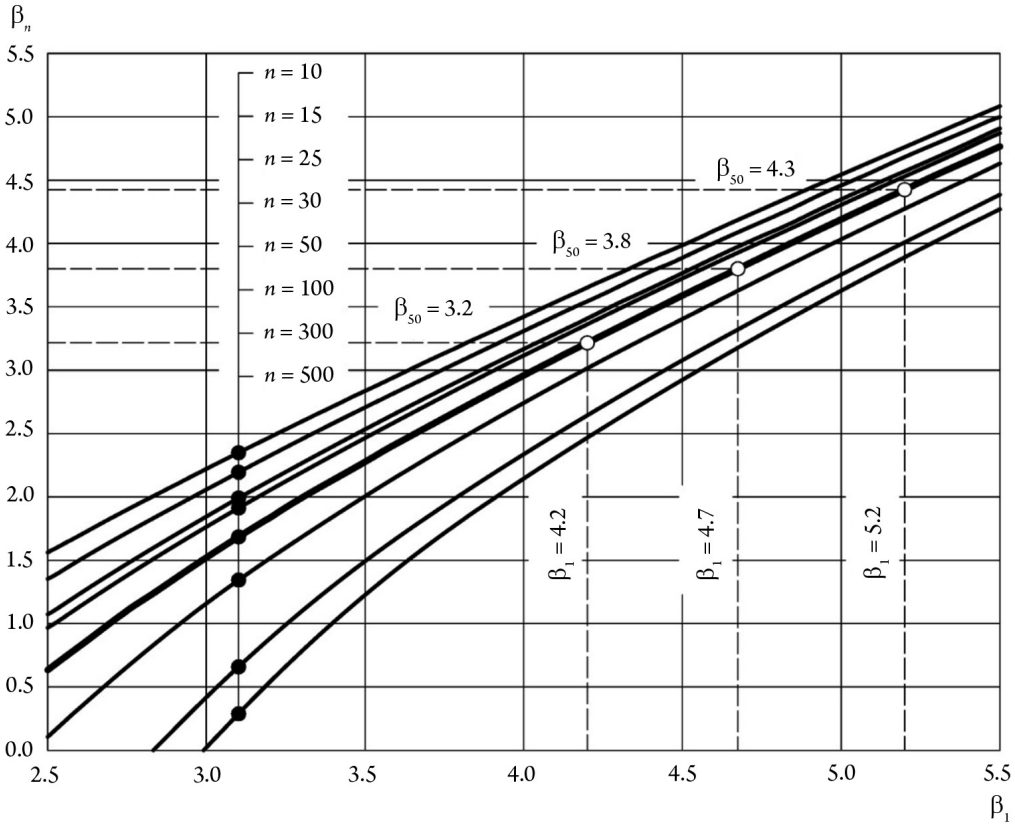

Fig. 2. Plots of the $\beta_1 - \beta_n$ relationships for the selected return periods n (own research)

Table 3. Minimum values of the reliability factor β_u in the bearing capacity limit case for the reliability classes RC1, RC2 and RC3 according to own research.

Reliability factor $\beta_n = \beta_u$									
Reference period n in years									
(RC)	**1**	**10**	**15**	**25**	**30**	**50**	**100**	**300**	**500**
(1)	(2)	(3)	(4)	(5)	(6)	(7)	(8)	(9)	(10)
RC1	**4.20**	3.65	3.54	3.40	3.35	**3.21**	3.00	2.65	2.48
RC2	**4.70**	4.21	4.11	3.99	3.95	**3.83**	3.65	3.36	3.22
RC3	**5.20**	4.75	4.67	4.50	4.53	**4.42**	4.27	4.01	3.89

If the inequality (5) is satisfied, the second level criterion is satisfied as well, subject to the condition that partial coefficients are assumed for β_E and β_R. These coefficients are related to the reliability factor β by the relationships: $\beta_R = \beta|\alpha_R|$, $\beta_E = \beta|\alpha_E|$, where the multipliers $\alpha_R = 0.8$, and $\alpha_E = -0.7$ denote the sensitivity factors having the values listed in the code PN-EN 1990.

The design codes for building structures are usually calibrated for structures of average reliability requirements, i.e. for the RC 2 class. Assuming the specification of partial coefficients assigned to the bearing capacity γ_M for reliability classes other than RC 2 according to the Eurocode 5 one should apply a correction factor K_R of the form listed below to the left side of the formula (5):

$$\bar{R} - 0.8\beta_{RC2}\mu_R = K_R(\bar{R} - 0.8\beta_{RC}\mu_R), \tag{6}$$

thus

$$\frac{1-0.8\beta_{RC2}v_R}{1-0.8\beta_{RC}v_R}, \tag{7}$$

where:

$v_R = \mu_R/\bar{R}$ – timber strength random variation coefficient.

Analogous reasoning may be presented for variable loads Q (having the average value $\bar{Q}$ and standard deviation μ_Q), present on the right-hand side of the formula (5):

$$K_{Fi}(\bar{Q} + 0.7^2{}_{RC2}\mu_Q) = \bar{Q} + 0.7\beta_{RC}\mu_Q, \tag{8}$$

$$\frac{1+0.7\beta_{RC}v_Q}{1+0.7\beta_{RC2}v_Q}, \tag{9}$$

where:

$v_Q = \mu_Q/\bar{Q}$ – random load Q variation coefficient.

For the structure belonging to the RC 3 class, designed for the sample reference period T = 50 years, the reliability coefficients according to Table 3 are equal to: β_{RC2} = 3.83 and β_{RC} = 4.42, respectively; thus, formulas (7) and (9) yield the estimates of the reduction coefficients for bearing capacity and loads:

$$K_R = \frac{1-0.8\cdot 3.83\,v_R}{1-0.8\cdot 4.42\,v_R} = \frac{1-3.06\,v_R}{1-3.54\,v_R} \tag{10}$$

$$K_{Fi} = \frac{1+0.7\cdot 4.42\,v_Q}{1+0.7\cdot 3.83\,v_Q} = \frac{1+3.09\,v_Q}{1+2.68\,v_Q} \tag{11}$$

For the class RC 1, the reliability coefficients according to Table 3 are equal to: β_{RC2} = 3.83 and β_{RC} = 3.21, respectively; and thus, formulas (7) and (9) yield the estimates of reduction coefficients:

$$K_R = \frac{1-0.8\cdot 3.83\,v_R}{1-0.8\cdot 3.21\,v_R} = \frac{1-3.06\,v_R}{1-2.57\,v_R} \tag{12}$$

$$K_{Fi} = \frac{1+0.7\cdot 3.21\,v_Q}{1+0.7\cdot 3.83\,v_Q} = \frac{1+2.25\,v_Q}{1+2.68\,v_Q}. \tag{13}$$

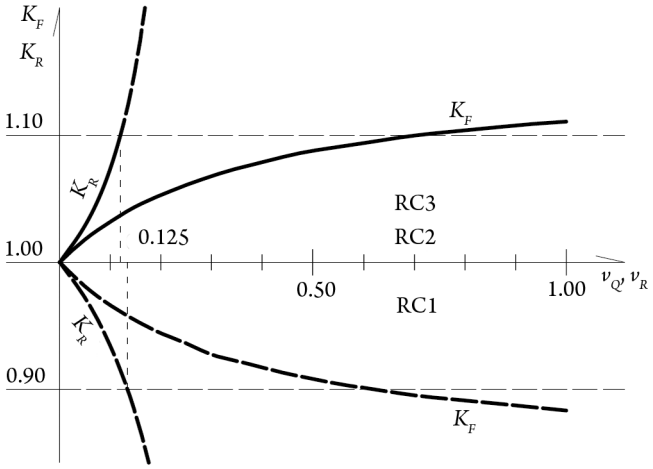

Fig. 3. Plots of the reduction coefficients K_R and K_{Fi} according to the formulas (10)÷(13) (own research)

Graphs of reduction coefficients plotted against the material strength variation coefficient v_R and variable loads variation coefficient v_Q are depicted in Fig. 3. The example values of those coefficients, calculated for the reference periods of T = 50 years and T = 300 years are listed in Table 4. Comparison of numerical data for both periods shows, that quantitative results are convergent, while K_F values recommended in the code PN-EN 1990 and listed in the Table 5 are fully justified for the values presented in Table 4, rounded up to 0.1. One should note, that even large values of the climate loads variation coefficient, for instance describing the uneven snow load on the ground (cf. [13]), for which v_Q = 0.60÷1.00, lead to differences in the reliability measure limited to about 10%.

Table 4. Values of reduction coefficients K_{Fi} and K_R calculated for the reference periods of T = 50 years and T = 300 years according to own research

Reliability class RC3; reference period T = 50 year								
v	0.05	0.100	0.150	0.200	0.400	0.600	0.800	1.000
K_F	1.018	1.032	1.044	1.053	1.079	1.094	1.104	1.111
K_R	1.029	1.074	1.154	1.329				
Reliability class RC1; reference period T = 50 year								
v	0.05	0.100	0.150	0.200	0.400	0.600	0.800	1.000
K_F	0.981	0.966	0.954	0.944	0.917	0.901	0.891	0.883
K_R	0.972	0.934	0.880	0.798				
Reliability class RC3; reference period T = 300 year								
v	0.05	0.100	0.150	0.200	0.400	0.600	0.800	1.000
K_F	1.023	1.037	1.055	1.062	1.094	1.113	1.126	1.136
K_R	1.031	1.077	1.150	1.290				

Reliability class RC1; reference period T = 300 year								
v	0.05	0.100	0.150	0.200	0.400	0.600	0.800	1.000
K_F	0.978	0.960	0.945	0.932	0.898	0.876	0.862	0.852
K_R	0.968	0.928	0.875	0.803				

Table 5. Values of coefficients K_{FI} for actions according to the code PN-EN 1990

Correction factor	Reliability class		
	RC1	RC2	RC3
(1)	(2)	(3)	(4)
K_{Fi}	0.9	1.0	1.1

Correction of the load coefficients γ_F via the correction factors K_{FI} having the values listed in Table 5 constitutes a simple engineering method of differentiating the reliability requirements with respect to the variable loads according to the code PN-EN 1990.

In the recommendations of the code PN-EN 1990 pertaining to the design basics of building structures, a case is considered, where the conditions of the limit state (5) may be expressed by the bearing capacity R and the effect of actions E associated with it in the following form:

$$E_d = E\{F_{di}, a_{di}, \theta_{di}\} \leq R_d = R\{X_{dj}, a_{dj}, \theta_{dj}\}, \tag{14}$$

where index „d" denotes the computational values of:

F_{di} – actions on the structure, $i = 1, 2, \ldots n$,
X_{dj} – mechanical properties of the structural material, $j = 1, 2, \ldots, m$,
a_{di}, a_{dj} – geometrical properties of the structure,
θ_{di}, θ_{dj} – uncertainty parameters of the computational model.

In the code PN-EN 1990, a reliability verification convention has been assumed, according to which the computational values X_d and F_d are usually not entered directly into the limit state equation, but the so-called *representative values* X_{rep} and F_{rep} are used instead. The following may be used as representative values:

- characteristic values, i.e. quintiles for: loads – ηF_k, material strength – ηX_k, and geometrical properties – a_d (where η – conversion coefficients),
- nominal values (central values of geometrical properties a_{nom}).

The computational values F_d and X_d are determined via the multiplication or division of representative values by the applied partial coefficients:

$$F_d = F_{rep}\gamma_F \rightarrow E_d = E(\eta F_k \gamma_P, a_d), \tag{15}$$

$$X_d = \eta X_k / \gamma_M \rightarrow R_d = R(\eta X_k / \gamma_M, a_d). \tag{16}$$

The partial coefficients – γ_F in the formula (15) and γ_M in the formula (16) – account for the random variation of actions (factor γ_f), material strength (factor γ_m) and error in the modelling of these random variables (factors γ_{Sd} and γ_{Rd}, respectively):

$$\gamma_F = \gamma_f \gamma_{Sd}, \gamma_M = \gamma_m \gamma_{Rd}. \quad (17)$$

The structure of partial coefficients according to the formulas (17) explains the basic difference between the limit states method, as applied in the Polish codes PN/B, and the load γ_F and bearing capacity γ_M coefficients method introduced in the Eurocodes. In the European codes perfect modelling of mechanical systems is postulated. Perfect modelling of timber structures results in the need for a numerical model, usually fully 3D, accounting for multi-sourced global and local imperfections. As a consequence of such an approach, the values of bearing capacity coefficients may be lowered with respect to the values known from Polish PN/B codes, since the modelling error of the structure may be justifiably assumed as: $\gamma_{Rd} = 1.0$.

A different interpretation pertains to the modelling of loads, for which $\gamma_{Sd} \geq 1.0$, as all the forecasts of technological, climate and other actions on the structure are inherently burdened with an error.

The values of bearing capacity coefficients for wooden structural components are listed in the part 1–1 of the Eurocode 5 as follows:

- bearing capacity coefficient for components made of solid wood, wooden particle boards and beaverboards $\gamma_M = 1.30$;
- bearing capacity coefficient for components made of glued laminated timber and barbed plate $\gamma_M = 1.25$;
- bearing capacity coefficient for components made of plywood, laminated veneer lumber (LVL) and oriented strand boards (OSB) $\gamma_M = 1.20$.

The dependence of the bearing capacity coefficient γ_M on the variance coefficient of timber strength (cf. PN-EN 1995-1-5) follows from the formula (16):

$$\gamma_M = \frac{R_k}{R_d} = \frac{1 - 1.64 v_R}{1 - 3.04 v_R} \quad (18)$$

where:

R_k, R_d – lower quintiles of the timber bearing capacity at the probability level ω – 5% and ω – 1.35‰, respectively.

For the bearing capacity coefficient $g_M = 1.20$, one obtains from the formula (18) the value of variance coefficient $v_R = 0.100$, and for $g_M = 1.30$ the value of $v_R = 0.130$. According to Table 4, these estimates correspond to the timber strength reduction factor $K_R \approx 1.1$ for the structures of the required reliability class RC3 and $K_R \approx 0.9$ for the reliability class RC1. For highly homogeneous structural materials, such as for instance steel, for which $v_R \leq 0.075$, the reduction coefficients assume the values of $K_R \leq 1.05$ or $K_R \geq 0.95$ for the classes RC3 and RC1, respectively, according to Table 4.

3. An example of the structural components reliability verification

The building structure reliability differentiation method is presented on the example of a timber structure covering the sanctuary in Łagiewniki, erected in Cracow in the years 1999–2002, cf. Fig. 4. Up to 5,000 people may stay in this building at one time; – this justifies the application of destruction consequence class CC3 and the reliability class RC3.

The nominal service time of this structure has been assumed as equal to T_d = 300 years. For this service time one may find in Table 2 the conversion coefficients for climate loads: η_d = 1.33 for snow and η_d = 1.10 for wind speed.

The corrective multiplier for climate loads, according to Table 5, is equal to K_{Fi} = 1.1, and for the roof structure made of glued laminated timber the corrective coefficient has been assumed according to Fig. 3, with a value of K_R = 1.1. The above values result in the following values of load and bearing capacity factors:

- for permanent loads γ_G = 1.35,
- for variable loads $K_{Fi}\,\gamma_Q = 1.1 \cdot 1.50 = 1.65$,
- for strength $K_R\,\gamma_M = 1.1 \cdot 1.25 = 1.375$.

Characteristic actions are subject to correction as well, and especially:

- base value of wind speed pressure according to PN-EN 1991-1-4

$$q_b = 0.5 \cdot 1.25 \cdot 10^{-3}(1.10 \cdot 22)^2 = 0.366\ \text{kN/m}^2,$$

- characteristic value of the snow load on the ground

$$s_k = 1.33 \cdot 1.2 = 1.60\ \text{kN/m}^2.$$

The code values of snow load on the ground, assumed for the building structures assigned to the destruction consequence class CC3, by recommendation should be verified by the statistical forecast.

Fig. 4. The glued laminated timber structure of a roof covering the sanctuary in Łagiewniki. Source: own research

The results of snow load measurements recorded by Polish meteorological stations are documented in [13]. Especially the measurement results for the Cracow Balice station are depicted in Fig. 5, and the 50 years forecast prepared on the basis of those measurements is depicted in Fig. 6.

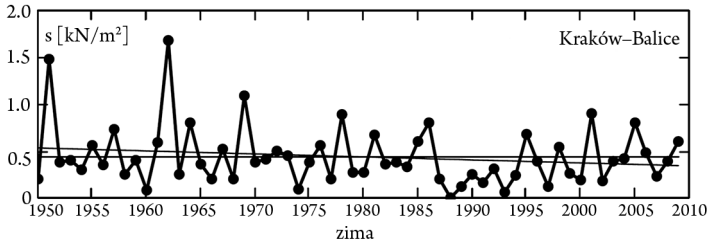

Fig. 5. Results of statistical analyses of snow load on the ground for the 1950–2010 time period at the Cracow Balice meteorological station [13]

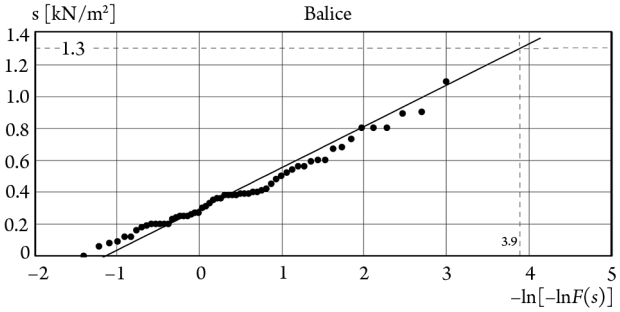

Fig. 6. Statistical forecast of the snow load on the ground for Cracow Balice (own research)

4. Conclusions

Timber structures are especially prone to the differentiation of reliability requirements, as most often these structures are designed as temporary ones, for which the values of reliability measures may and shall be lowered. At the same time, because of high aesthetical values, such structures are willingly applied in many prestigious buildings, to which, as has been presented above, the raised reliability requirements may apply. The verification of the code procedure for the differentiation of reliability requirements performed in this paper has shown, that the reduction coefficient for variable loads K_{Fi} has been correctly specified in the code PN-EN 1990. However, the same verification indicates that for the timber structures belonging to the RC3 class, a value of the bearing capacity reduction coefficient $K_R > 1$ is fully justified (a value of $K_R = 1.10$ is suggested). Additionally, for this reliability class, a statistical verification of the snow loads on the ground assumed according to the code is advised. Long-term observations and measurements performed in 115 meteorological stations, located all over Poland have been

compiled, statistically elaborated and published by the Building Research Institute in Warsaw [13]. In the example considered here, based on Fig. 6, the 50-year forecast indicates the value of $s_k = 1.3\ \mathrm{kN/m^2} > 1.2\ \mathrm{kN/m^2}$ (ordinate on the plot corresponding to the abscissa equal to 3.9).

References

[1] Augusti G., Baratta A., Casciati F., *Probabilistic methods in structural engineering*, Chapman and Hall, London–New York 1984.

[2] Cornell C.A., *Structural safety specification based on second-moment reliability analysis*, Final Report. Symposium on Concepts of Safety of Structures and Methods of Design, London 1969, IABSE, Zurich 1969.

[3] Ferry-Borges J., Castanheta M., *Structural safety*, CEB Bulletin d`Information, No. 78, Copenhague 1971.

[4] Gwóźdź M., Machowski A., *Wybrane badania i obliczenia konstrukcji budowlanych metodami probabilistycznymi*, Wydawnictwo Politechniki Krakowskiej, Kraków 2011.

[5] Gwóźdź M., Machowski A., Żwirek P., *Wybrane zagadnienia niezawodności szkieletów stalowych budynków*, Wydawnictwo Politechniki Krakowskiej, Kraków 2013.

[6] Gwóźdź M., Kuchta K., *Zarządzanie niezawodnością obiektów kubaturowych wg normy PN-EN 1990*, Czasopismo Techniczne, 2-A/2/2011.

[7] Hasofer A.M., Lind N.C., *Exact and invariant second-moment code format*, Journal of Engineering Mechanics Division ASCE, Vol. 100, No. EM1/1974.

[8] Madsen H.O., Krenk S., Lind N.C., *Methods of structural safety*, Prentice Hall 1986.

[9] Nowak A.S., Collins K.R., *Reliability of structures*, McGraw-Hill 2000.

[10] Rozporządzenie Ministra Infrastruktury z dnia 03.07.2003 r. w sprawie szczegółowego zakresu i formy projektu budowlanego. Dz. U. 2003, nr 120, poz. 1133.

[11] Shinozuka M., *Basic analysis of structural safety*, Journal of Structural Engineering, Vol. 109, No. 3/1983.

[12] Thoft-Christensen P., Baker M.J., *Structural reliability theory and its applications*, Springer-Verlag, Berlin 1982.

[13] Żurański J.A., Sobolewski A., *Obciążenie śniegiem w Polsce*, Wydawnictwa Instytutu Techniki Budowlanej, Warszawa 2013.

[14] PN-EN 1990 Eurocode. Basis of structural design. European Committee for Standardization, 2002.

[15] PN-EN 1991-1-3 Eurocode 1. Actions on structures – Part 1–3: General actions – Snow lods. European Committee for Standardization, 2003.

[16] PN-EN 1991-1-4 Eurocode 1. Actions on structures – Part 1–4: General actions – Wind actions. European Committee for Standardization, 2005.

[17] PN-EN 1991-1-5 Eurocode 1. Actions on structures – Part 1–5: General actions – Thermal actions. European Committee for Standardization, 2003.

[18] PN-EN 1995-1-1 Eurocode 5. Design of timber structures – Part 1–1: General – Common rules and Rules for buildings. European Committee for Standardization, 2004.

TECHNICAL TRANSACTIONS 2/2018
CIVIL ENGINEERING
DOI: 10.4467/2353737XCT.18.027.8000
SUBMISSION OF THE FINAL VERSION: 18/1/2018

Dariusz Starkowski (dariusz.starkowski@wsl.com.pl)
Chair of Logistics Bases, Poznan School of Logistics

Load restraint with allsafe products. Part two: choosing a load securing system – a systematic analysis

Wykorzystanie metod zabezpieczenia ładunków przedsiębiorstwa allsafe. Część 2: analiza systemowa doboru systemu zabezpieczenia ładunku w naczepie ciężarowej

Abstract

This is the second part of an article concerning allsafe products (first is available in TT 1/2018, pp. 71–86) – it focuses on the planning role in the supply chain and the mechanisms that need to be taken into account during the process of the road transportation. Furthermore, the paper presents the results of an investigation that relates to the proper functioning of the supply chain in the distribution of 12,000 [kg] of strawberries. A weighted average method was used in reference to an analysis of load securing based on the products of three producers with the aim of indicating the safest and most modern way to secure the load in a semi-trailer. Rules of proper load placement and restraint inside the semi-trailer are also addressed, together with a loading plan associated with the analysis of the technical parameters of a semi-trailer and load securing systems.

Keywords: Road transport, provisions of law, transport centre, transport operation, load-carrying semi-trailer, management, logistic system, cargo security systems

Streszczenie

W drugiej części prezentowanego opracowania (pierwsza dostępna jest w numerze TT 1/2018, s. 71–86) zwrócono uwagę na rolę prawidłowego przebiegu planistycznego łańcucha dostaw analizowanego ładunku w funkcjonowaniu nowoczesnego transportu drogowego. Przedstawiono mechanizmy, jakie muszą być uwzględnione przy organizacji takiego specjalnego przewozu towaru. Zaprezentowano efekty związane z prawidłowym przebiegiem łańcucha dostaw przewozu 12 000 [kg] truskawek. Zastosowano metodę wagową (średniej ważonej), analizując systemy zabezpieczenia ładunków trzech producentów i określając najbezpieczniejszy i najnowocześniejszy sposób zabezpieczenia ładunku w nowoczesnej naczepie ciężarowej dla analizowanego ładunku. Opisano również zasady prawidłowego umieszczenia i zabezpieczenia ładunku na części przewozowej (towarowej) na naczepie drogowej oraz kompleksowy plan załadunku związany z analizą parametrów technicznych dla naczepy ciężarowej oraz systemów zabezpieczenia ładunków.

Słowa kluczowe: Transport drogowy, przepisy prawne, środek transportowy, operacja transportowa, naczepa ciężarowa, system logistyczny, system zabezpieczenia ładunków

1. Introduction

In Poland, the food product market is undergoing constant growth – its worth is currently estimated at PLN 240 billion and it constitutes the largest segment of retail trade. Food transportation has its own rules that apply both to fresh products (including those that require temperature-controlled conditions). It can be said that the organoleptic and physical-chemical qualities of transported products are mainly influenced by the choices of transport packaging made by producers and distributors. Box pallets, plastic containers, thermal trolleys and insulation covers are just some of the packaging options. In order to make the process of road transportation safe, the provision of proper load restraint is significant as properly secured cargo assures not only the stability of the vehicle but also the safety of the driver and other road users. According to statistics, almost 25 [%] of accidents involving trucks in the European Union, result from the improper securing of loads [10]. The responsibility for transport safety rests with the consignor, people preparing the transport, the forwarder and the driver; however, the responsibility of ensuring that the load is secure rests with the driver. The cargo needs to be transported in such a way that does not endanger other road users or the cargo itself. Thus, it is important to use certified, reliable and tested securing systems that guarantee load safety. As road cargo transport constitutes the core of European transport, it is vital to make it no only effective, but also safe. During shipment, objects need to be fundamentally safe and secure – they should not be able to move, tilt, roll in any direction, fall off the vehicle or make the vehicle tip over as a result of jolts or vibrations. Proper load restraint increases the safety of operatives engaged in loading activities, drivers and other road users, such as pedestrians, and also the safety of the vehicle and the cargo. The load needs to be positioned in such a way that prevents human injury or disturbing the stability of the vehicle during transit. The aim of this article is to identify the safest way of transporting 12,000 [kg] of strawberries in the semi-trailers which were selected in the first part of the paper. The results of the analysis of load restraint systems were based on technical data from the three different semi-trailers.

2. Method and materials

This article touches upon the overall problem of the appropriate selection of a vehicle that meets the required technical, constructional and safety standards, complies with the consignor's requirements and is suitable for the given type of load. A comparative method was chosen in order to select the best securing system for the transportation of 12,000 [kg] of strawberries. This method may help the road carrier to select a load securing system that will ensure the safe and successful completion of the task, complying with legal regulations and the needs of the client, at the lowest possible cost. The research tool chosen for this purpose was the weighted average method. The aim of this paper is to select an appropriate method of load restraint, which in this case would be 12,000 [kg] of strawberries with respect to the technical parameters of a semi-trailer, in compliance with the relevant legal regulations.

The first step of proper selection is to determine the intrinsic requirements to be met in transport order, and define the importance of the requirement. The next step is to specify the technical features of the primary and additional parameters for the given vehicle in relation to the previously set requirements. Then, load restraint methods of three restraint manufacturers were compared in the analysed transportation task.

The following parameters were chosen as criteria [9]:

- compliance with legal requirements (homologation) and the possibility of using it in the previously selected semi-trailer,
- meeting requirements concerning the chosen load,
- securing load against damage or theft,
- vehicle's assessment for active and passive safety,
- operational efficiency of vehicle,
- supervision of load securing system.

Levels of relevance (weight) are defined using a scale from 0–10 [8]:

The most important factors were allocated grade (10) and the least important factors, grade (1).

- The first part of the table (Sections I–V) defines the requirements demanded in relation to the vehicle.
- Section IV adopted a degree of relevance according to the scale:
  0 – unimportant
  2 – less important
  4 – advisable
  6 – important
  8 – very important
  10 – necessary
- In the case of a lack of certainty regarding the value of a particular criterion, an intermediate value is adopted (e.g. 3, 5 , etc.).
- The comparative analysis of figures and requirements (with data included in information materials on vehicles) results in the choice of an appropriate type of a vehicle.

The evaluation scale for the standard deviation of each parameter is between 0 and 1 where:

- Parameters of the vehicles initially chosen are written in the second part of the table in Section VI.
- Further, in Section VII standard deviation is determined where:
  0 – significant divergence
  0.3 – divergence
  0.5 – average deviation
  0.7 – minor deviation
  1 – in accordance with the requirements

Weights are multiplied by standard deviation.

The obtained *results are* written in Section VIII and points in each column are added up. The following vehicles are given sections IX, X, XI.

- The highest obtained sum of points is the basis for choosing the most appropriate means of transport with regard to meeting the previously adopted requirements.

A summary table presents examined technical features of vehicles (scale 1 to 10, See Table 1). The more a parameter matches our expectations, the higher rating it gets. The points are then multiplied by weights and the results are divided by the sum of all weights. The next table (see Table 2) contains technical and operating features of the evaluated vehicles (1 to 10 scale) defining how a particular transport feature deals with the comparative factor (e.g. speed and maximum acceleration, driving force depending on engine speed). Again, the more a parameter matches our expectations, the higher rating is given. The points are then multiplied by weights and the results are divided by the sum of all weights. In terms of technical requirements, the following parameters were adopted [8]:

- external parameter characteristics in semi-trailers,
- load securing systems and methods,
- loading-unloading systems in vehicles.

Final selection of a vehicle (semi-trailer) was carried out with the use of weighted average – comparative method, which is average value of technical parameters with weights assigned in such a way, that elements with higher value, have greater impact on the average The type of load and conditions set forth by the consignor are the main criteria that are taken into account. If all weights are the same (all elements are of equal relevance), the weighted average equals the arithmetic average [8]:

$$Zr\ \text{weighted} = \frac{\sum_{i=1}^{n} \text{value}_i \cdot \text{weight}_i}{\sum_{i=1}^{n} \text{weight}_i}$$

Priority – $\sum_{i=1}^{n} \text{value}_i \cdot \text{weight}_i$

Conventional standard deviation – $\sum_{i=1}^{n} \text{weight}_i$

The total of points achieved by a vehicle were divided by total of priority points = weighted average

Choices were facilitated by a substantive analysis that covers, inter alia, research methods and systems of load securing in semi-trailers. Legal requirements and temperature-atmospheric conditions are presented in the first part of the article. A comparative table presents load restraint systems from three producers that modern cooling semi-trailers are equipped with (Table 1) [1–3].

Table 1. Comparison of load restraint systems in cooling semi-trailers

Load restraint system/product	Allsafe	Schmitz cargobull	Loadlok
double-deck system with ATD tracks for flush insertion into the side wall	yes – ATD II system	yes	yes
double-deck system with tracks for gluing and screwing	yes – ATD I system	no	yes
loading beam	yes – several types of beams of different sizes and end pieces (depending on track type) and blocking capacity: 1) classic PL 1000[daN] BC 1100 [daN] 2) heavy duty PL 1350 [daN]/BC 1100 [daN] 3) space 1000 PL [daN]/BC 1100 [daN]	yes	yes
loading beam which may be used as blocking beam	yes – each beam has blocking capacity (BC)	no	no
beams can be stowed under the roof	yes	yes	yes
accessories: release rod	yes	no	yes
accessories: place for hidden release rod	yes	no	no
accessories: beam stop for ATD tracks	yes	no	no
robust loading beam for steel container which may be used for blocking	yes – STD beam with load capacity PL 1000 [daN] and blocking capacity BC 1100 [daN]	no	no
combi tracks	yes	yes	yes
blocking beams to combi tracks	yes – KAT beams of different sizes and load capacity from 800 [daN] to 2800 [daN]	yes	yes
cargo bar with rubber foot	yes – SAM Profi with range 600 [mm]	yes	yes
system for securing roll containers	yes – JF system	no	no
system for roll containers working in temperatures below zero	yes – system with elements inserted at any place of a track	no	no
system for roll containers working in temperatures above zero	yes – system with elements sliding in the track	no	no
clamp fitting to secure roll containers	yes – KERL JF with capacity 500 [daN]	no	no
clamp fitting to secure roll containers with different dimension	yes – KERL JF fittings for containers of three diameters – 25 [mm], 35 [mm] and 45 [mm]	no	no
additional fittings for roll containers securing	Yes – end fitting – KERL JF fix and middle fitting – KERL JF slide	no	no
temperature bulkhead	no	no	yes
temporary temperature wall	no	no	yes

2.1. Characteristics of researched objects

The transportation of food products is demanding and requires specific temperature conditions in vehicles that have been adapted for that purpose. Furthermore, the transport process must not have an impact on the quality of the food. The following points are important considerations in the transportation of food products [7]:

1) Compliance with temperature control requirements for foodstuffs is vital during the distribution process;
2) The chosen means of transport should ensure preservation of the cold chain;
3) Meeting optimum hygiene and cleanliness standards is essential;
4) Vehicles should be equipped with waterproof sealed and non-slip flooring;
5) Workers who deal with loading and unloading should have valid medical checks and use proper protective clothing;
6) The vehicle should meet generally accepted technical standards and be equipped with load restraint systems;
7) The load area should not have acute angles that are hard to reach or clean;
8) Vehicles used for transport of foods should be properly labelled and authorised to carry out food transportation.

The comparative study was based on the following three modern semi-trailers set up for the transportation of strawberries and equipped with load securing systems that meet with the producer's approval:

1) Wielton O4NS34CT refrigerated semi-trailer;
2) Krone Cool Liner refrigerated semi-trailer with Thermo King O4SLX;
3) Krone COOL LINER – 04THERMO refrigerated semi-trailer.

The aim of the analysis is to determine load securing systems used in presented trailers, and ways of securing that can be implemented during loading/unloading.

2.1.1. Characteristics of Wielton 04NS34CT cooling trailer with Loadlok products

The trailer's superstructure is a self-supporting construction made of glued insulated panels, isolated with non-freon polyurethane foam (without thermal bridges), with outer sheets made of glass-fibre laminate (gelcoat). The internal covering layer sheet is made from steel and has a hard PVC film coating. The thickness of the side walls is 60 [mm], secured with aluminium skirting boards up to a height of 300 [mm] and either insert 'an' here or make the noun 'board' plural, depending upon your intended meaning aluminium board with a width of 250 [mm], at a height of 1200 [mm] from the floor. The front wall thickness is 100 [mm], it is reinforced and equipped with cool air ducts. The self-supporting floor is 100 [mm] thick and enables a forklift truck to go inside easily. The non-slipping floor has drainage channels made of stainless steel. The rear wing door creates a 100 [mm]-thick wall, with a frame made of stainless steel (Fig. 1) [6]. The door is secured with four hinges and two revolving rod locks. The O4NS 34 CT – FRC cooling chamber can house thirty-three standard European pallets. Moreover, Thermo King and Carrier Transicold chillers provide cooling. Optionally, trailers can be equipped with an aluminium floor and

a moveable bulkhead. Up to twenty-two decking beams may be installed in the body. Recessed, or surface anchor rails offer optimum load securing through the complete load length [16].

Further analysis of the means of transport that is used for transport of strawberries will focus on two modern means of transport labelled as FRC, in accordance with ATP (the Agreement on the International Carriage of Perishable Foodstuffs and on the special equipment to be used for such carriage.

F – means of transport – chiller trailer.

R – heavy insulation (*K* coefficient $k = 0.4$ [(W/(m²K)].

C – class C – cooler vehicle equipped with devices maintaining temperatures of +12°C to –20°C inclusive.

Fig. 1. Wielton O4NS34CT refrigerated semi-trailer (FRC)

External features and load securing systems are presented in Table 2 [3, 6].

Table 2. External features and load securing systems of Wielton O4NS34CT refrigerated semi-trailer (FRC) with Loadlok products

External features	Securing systems
LOCKS GASKET EXTENSION LADDER	NON-SLIP FLOOR
RUBBER BUFFERS HANDLES SUPPORT LEGS	LOAD FITTING TRACKS STRIP ON THE SIDE WALLS
HINGES ROLL-STOPS BUMPING BLOCK	VERTICAL WALL MOUNTED RAILS
TEMPERATURE SENSOR VENTILATION FLAP	ADDITIONAL SCUFF RAIL ON THE SIDE WALLS
TEMPERATURE SENSOR REFRIGERATOR AND TEMEPRATURE RECORDER	LONGITUDINAL BEAM
DOUBLE-DECKER LOADING SYSTEM	LOADLOCK SYSTEM MOVABLE FLOOR SECTIONS

The most important load securing systems offered by the producer are [3, 6]:

- double-deck system, and movable floor sections (Fig. 2),
- system of load securing tracks on side walls, vertical and horizontal rods (Fig. 3).

Fig. 2. Double-decker loading system, Loadlock system and movable floor sections

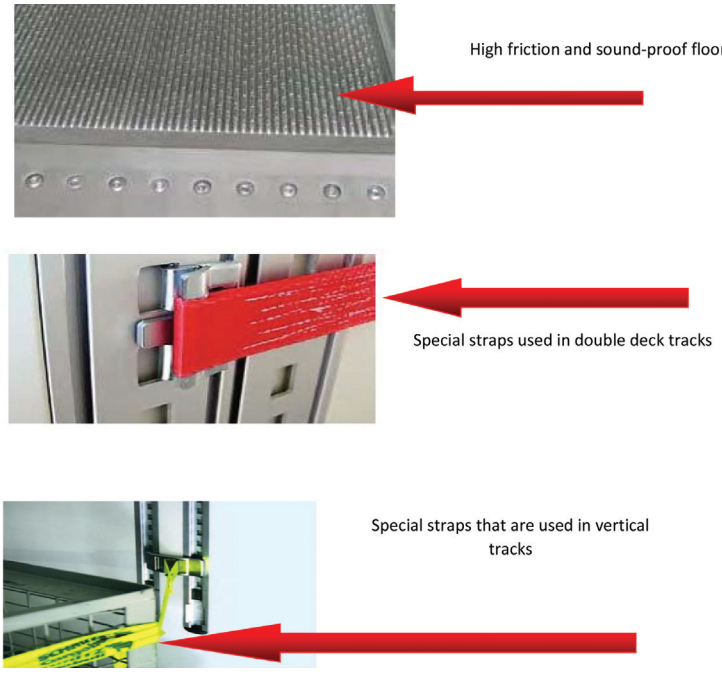

Fig. 3. System of load securing tracks on side walls; vertical and horizontal rods

Non-slip floor with friction coefficient μ – 0.5 (Fig. 4) [3, 6].

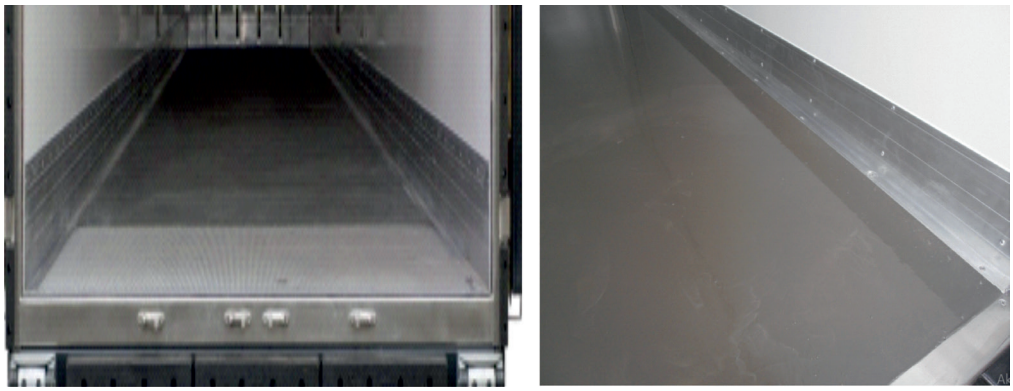

Fig. 4. Non-slip floor

2.1.2. Characteristics of Krone Cool Liner double deck with Thermo King SLX 300 and allsafe loading systems

The Krone Cool Liner has a continuous chassis. Tensile forces are transferred to the chassis – this protects the superstructure during vehicle coupling and uncoupling. The forces involved when docking to the ramp are also absorbed by the chassis. Aluminium profiles ensure good front wall protection and optimal air-flow. The aluminium kick strip is bonded to the side walls and welded to the one-piece, aluminium floor plate in such a way that it is water-tight (Fig. 5) [4]. The side walls are made of GRP panels and the trailer is equipped with ATD tracks for double-deck loading. Furthermore, the trailer has a bolted evaporator guard which is 5 [mm] thick and 68 [mm] high. During the docking manoeuvre, the tail is protected by one horizontal, delta-shape bumper and two impact buffers. The stainless steel rear gantry is suitable for docks and ramps. The door hinges are recessed at the sides to enable optimal door-opening angles.

The German company allsafe GmbH & Co. KG equipped the trailer with two basic systems of load securing, designed for food transport at controlled temperatures [1]:

The double-deck ATD system enables the transport of cargo on two levels, secures delicate loads from damage and enables the transportation of twice the amount of pallets (Fig. 6) [1, 4, 12].

Fig. 5. Krone Cool Liner double deck with Thermo King SLX 300

Fig. 6. ATD double-deck system consists of two elements: loading ATD beam and vertical airline tracks

Table 3. External features and load securing systems of Krone Cool Liner double deck with Thermo King SLX 300 and the allsafe loading systems

External features	Securing systems
Single locks Invisible solid reinforcements Cooling unit	The blocking beam is improved for an increased load capacity
Tracks for telescopic rails and tension straps Two temperature zones Soundproof floor	The blocking beams can be positioned anywhere along the profile
Double-deck system: DOUBLE DECK Adjustable beams HDR Technology increases the resistance of the interior walls to dents	ATD system – ATD loading beams with big loading capacity. Special lashing straps can be used for the double-decker rails
Outer surface – zinc coating Pivoting circulation wall Pallet stoppers	Special lashing straps can also be used in the double-decker rails for additional load securing.
Ferroplast body	Movable floor panels
Insulated ventilation and venting flap	JF system for roll containers

In addition to the elements presented above, there were additional solutions used in the trailer such as special straps and release rods (Figs. 7 & 8) [1, 4].

Fig. 7. ATD system – ATD loading beams with big loading capacity

SAM Profi cargo bars with rubber feet produced by allsafe with additional frames protecting smaller items of cargo.

Fig. 8. Technical solutions (vertical bars) of load protection in refrigerated trailer Krone Cool Liner with ATD double-deck with Thermo King SLX 300

Other features that are worth mentioning are: a pallet stop system, a high friction flooring, connected with a kick strip and rubber-footed cargo bars (SAM Profi by allsafe) that increase the security of transported food products (Fig. 9) [1, 4, 13].

Fig. 9. Vertical and horizontal tracks securing cargo in side walls

Vertical tracks from the double-deck ATD system by allsafe that was previously mentioned. The roof insulating system is another significant securing measure (Fig. 10) [1, 4, 13].

Fig. 10. Insulated roof filled with polyurethane foam, covered with steel sheet (up to 40 mm)

The complex equipment of the presented trailer intended for the carriage of strawberries is shown in (Fig. 11) [1, 4, 11].

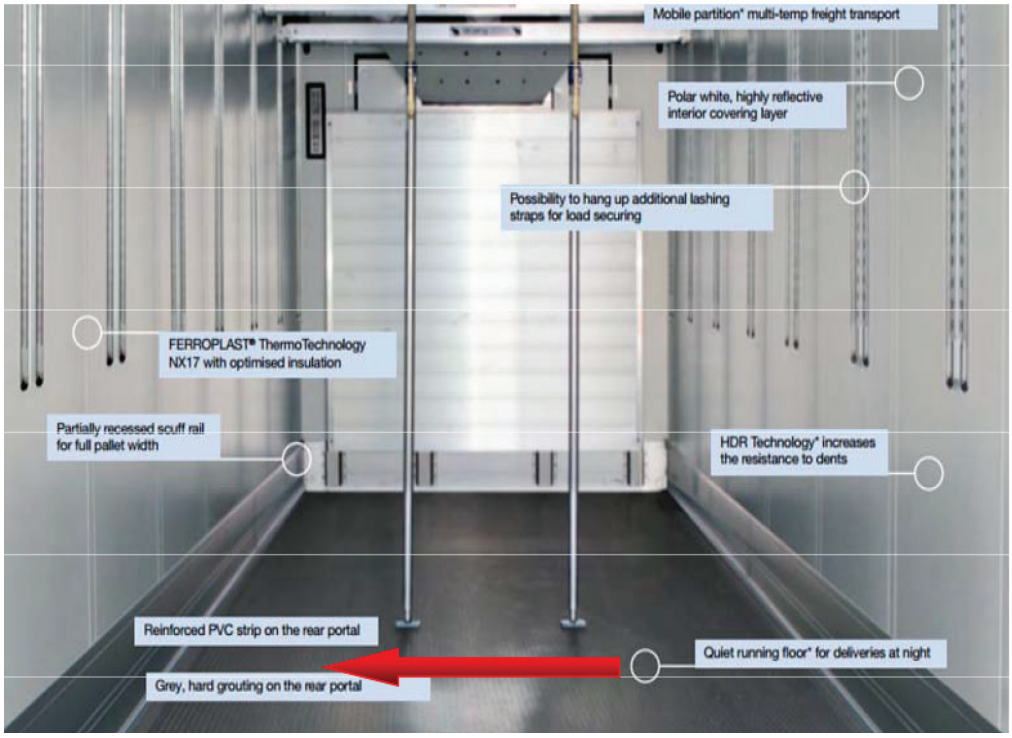

Fig. 11. Complex equipment of a trailer intended for safe food transportation

The JF system consists of the following elements: two airline guide rails installed in the walls and modular fittings KERL JF, KERL slide, KERL fix, which immobilise wheeled containers in a chosen place along the track (Fig. 12) [1, 4].

Fig. 12. JF system

There are two types of modular fittings KERL JF: insert and remove at any position for transport in temperature below zero and non-removable in every position for transport above zero. Another type of fitting is KERL sidle, these are used between cargo units, in cases where there is no need to use the larger KERL JF fitting, and the space between cargo has to be decreased, this type of fitting is advisable (Fig. 13) [1, 4]. The last type of fitting is KERL fix – this is used at the beginning of the track, close to the front wall. It prevents the first pallet unit from moving forward and protects the front wall from damage (Fig. 14) [1, 4].

Fig. 13. KERL JF Modular fitting system

The described trailer is equipped with a tail lift (Fig. 14) [1, 4].

Fig. 14. Tail lift

2.1.3. Characteristics of the Krone 04 COOL LINER – THERMO refrigerated trailer with load securing systems Liner Doppelstock

The circulation wall and the flexible air ducts provide effective air circulation for constant cooling throughout the entire cargo area. The cooling airflow is directed at roof height, it then descends over the freight towards the floor and flows through the pallets, along the side walls and beneath the pallets, back to the bulkhead. Many significant companies that specialise in food transport use Schmitz coolers as the products meet strict HACCP standards. The interior of the trailer has no recesses; moreover, the tracks attached to the walls secure cargo and enable double-deck loading, reducing the possibility of damage and increasing hygiene standards.

The trailer's body is a self-supporting construction made of glued insulated panels isolated with non-freon polyurethane foam (without thermal bridges) with outer sheets made of glass-fibre laminate (gelcoat) (Fig. 15) [5, 9].

Fig. 15. Krone 04 COOL LINER – THERMO semi-trailer Liner Doppelstock

Technical equipment of a trailer and load securing systems are presented in Table 4 [5].

Table 4. Technical equipment of the Krone COOL LINER – THERMO trailer and load securing systems Liner Doppelstock

External features	Securing systems
Additional refrigeration equipment Pallet stoppers	Load securing beams
Air ducts Refrigeration unit	Non-slip floor
Double-deck track Two temperature zones	Additional scuff rails on the side wall.
Guide tracks inserted into side walls compliant with HACCP standards.	Vertical telescopic rods can also be installed as horizontal beams modular fittings compliant with EN 12640
Optional side door	Supporting track
Tail lift Four locks	Longitudinal beam
ROOF	Sandwich type panels covered with steel, temperature sensor pipe, roof lamps, door lighting switch, insulated ventilation and venting flap
FRONT WALL	Strengthened sandwich type panels to improve air circulation, the interior wall is made of a 5 [mm] sheet, the front wall has a cut out for the Carrier and Thermo King units
SIDE WALLS	Steel homogenous sandwich type panels varnished outside, PVC coated inside, aluminium, [300] mm high strip inside, lateral tracks leading to double deck beams 1 600 [mm] high
BACK DOOR	Wing door, set of 3 door hinges V2A, replaceable seal, double locking levers

Figure 16 shows a trailer equipped with fittings that secure the load, compliant with EN 12640, with a loading capacity up to 2 tonnes [5].

Fig. 16. Load securing fitting in the front wall, in accordance with EN 12640

Table 5. Technical parameters and load securing requirements for the examined vehicles

Parameters and basic requirements	**Requirements and technical parameters of refrigerated semi-trailers**										
	Krone COOL LINER – THERMO trailer with load securing systems Liner Doppelstock			**Wielton NS34CT refrigerated semi-trailer with Loadlok products**			**Krone Cool Liner Doppelstock double deck refrigerated semi-trailer and Thermo King SLX 300 with load securing system produced by allsafe**				
Details	Requirements	Value	Requirements and parameters	Standard deviation	Points	Requirements and parameters	Standard deviation	Points	Requirements and parameters	Standard deviation	Points
KERL JF modular fittings	+	10	+	1	0	+	1	0	+	1	10
Tracks and rails on side walls	+	10	+	1	10	+	1	10	+	1	10
Non-slip floor	+	10	+	1	10	+	1	10	+	1	10
ATD II system	+	4	+	1	4	+	1	4	10	0	10
Double deck system	+	6	-	0	0	+	1	6	+	1	6
Load securing beams	+	10	+	1	10	+	1	10	+	1	10
Securing bars possible to install	+	10	+	1	10	-	0	0	+	1	10

Parameters and basic requirements	Requirements and technical parameters of refrigerated semi-trailers										
	Krone COOL LINER – THERMO trailer with load securing systems Liner Doppelstock			Wielton NS34CT refrigerated semi-trailer with Loadlok products			Krone Cool Liner Doppelstock double deck refrigerated semi-trailer and Thermo King SLX 300 with load securing system produced by allsafe				
Vario lock	+	8	-	0	0	-	0	0	+	1	8
Securing bars	+	10	+	1	10	+	1	10	+	1	10
JF System	pneumatic	10	-	0	0	-	0	0	pneumatic	1	10
TOTAL			141			130			**183**		
$\sum_{i=1}^{n} \text{mean}_i$			1.43			1.32			**1.86**		

3. Research results

The results of the research into the technical parameters and load securing requirements for the examined vehicles are presented in Table 5. Adding together all the points assigned to the trailers for each of the assessed criteria produced the following results:

1. Wielton NS34CT refrigerated semi-trailer with Loadlok products – 130 points/1.30.
2. Krone Cool Liner Doppelstock refrigerated semi-trailer and Thermo King SLX 300 with load securing system produced by allsafe – **183/1.86**.
3. Krone COOL LINER – THERMO trailer with load securing systems Liner Doppelstock – 141 points/1.43.

Taking into consideration the technical features and the results achieved through the weighted average method, the Krone Cool Liner double deck refrigerated semi-trailer and Thermo King SLX 300 with load securing systems by allsafe is optimal to perform the transport of strawberries (see Table 5) [4, 5, 6].

For practical reasons, additional empirical research was conducted to shed more light on the proper planning and the carrying out of the presented transport operation. The most advantageous solution for this type of load is the creation of a pallet transport unit. Compliant with the requirements of pallet package, eight layers may be placed on one pallet which makes four packages in each layer. A logistical analysis of load securing during transport operation is presented in (Fig. 17) [11].

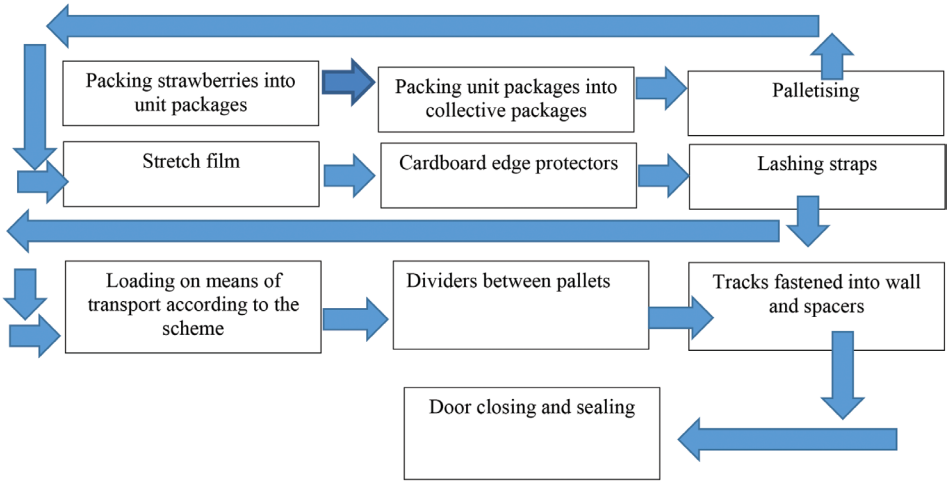

Fig. 17. Technical scheme of load securing during transport operation

Calculation of weight and size of a pallet unit
size:
length: 1200 [mm]
width: 800 [mm]
heigth: 105 [mm] x 8 + 160 [mm] = 1000 [mm]

weigth:
cargo weight: 4 x 5 [kg] x 8 = 160 [kg]
pack weight: 4 x 0.355 [kg] x 8 = 11.36 [kg]
pallet weight: 18 [kg]
pallet unit weight = cargo weight + pack weight + pallet weight = 160 [kg] + 11.36 [kg] + 18 [kg] = 189.36 [kg]

Load unit scheme is presented in (Fig. 18) [11].

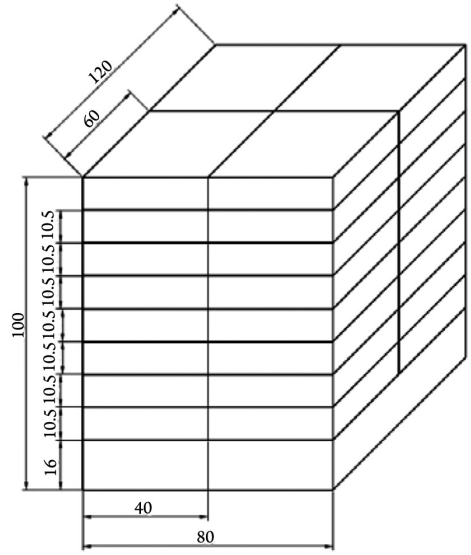

(Fig. 18) [11] Calculated load unit scheme – dimensions in [cm]

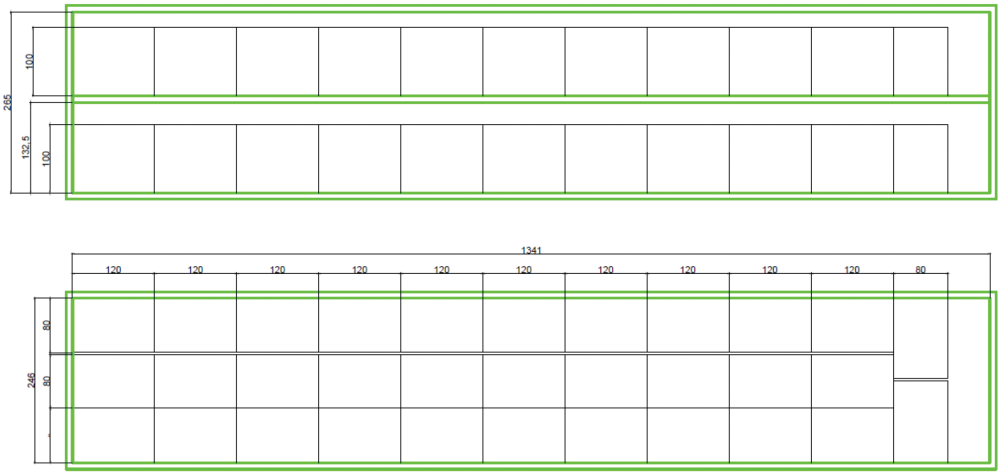

Fig. 19. [11] Example of pallet distribution in a refrigerated semi-trailer with a double-deck loading system

The analysed transport consisted of the carriage of a 12,000 [kg] load – the amount of pallets was calculated on the basis of empirical analysis:

- load weight: 12,000 [kg]
- load unit weight: 189.36 [kg]
- number of load units: 12,000 [kg]/189.36 [kg] = 63.37 [pcs.]

The cargo consists of sixty-four pallet units, and an exemplary way of pallet distribution in a refrigerated semi-trailer is presented in Fig. 19 [11].

$$S_1 = \frac{\left(11 \cdot 189.36\,\text{kg} \cdot 50\,\text{cm}\right) + \left(11 \cdot 189.36\,\text{kg} \cdot 192\,\text{cm}\right)}{11 \cdot 189.36\,\text{kg}} = 121[\text{cm}]$$

$$S_2 = \frac{\left(11 \cdot 189.36\,\text{kg} \cdot 640\,\text{cm}\right) + \left(11 \cdot 189.36\,\text{kg} \cdot 650\,\text{cm}\right)}{22 \cdot 189.36\,\text{kg}} = 640[\text{cm}]$$

$$S_3 = \frac{\left(20 \cdot 189.36\,\text{kg} \cdot 640\,\text{cm}\right) + \left(10 \cdot 189.36\,\text{kg} \cdot 640\,\text{cm}\right) + \left(10 \cdot 189.36\,\text{kg} \cdot 1240\,\text{cm}\right)}{32 \cdot 189,36\,\text{kg}} = 640\,[\text{cm}]$$

$$S_4 = \frac{\left(20 \cdot 189.36\,\text{kg} \cdot 80\,\text{cm}\right) + \left(10 \cdot 189.36\,\text{kg} \cdot 206\,\text{cm}\right) + \left(10 \cdot 189.36\,\text{kg} \cdot 123\,\text{cm}\right)}{32 \cdot 189.36\,\text{kg}} = 122\,[\text{cm}]$$

$S_{(1,2)}(121;640)[\text{cm}]$

$S_{(3,4)}(640;122)[\text{cm}]$

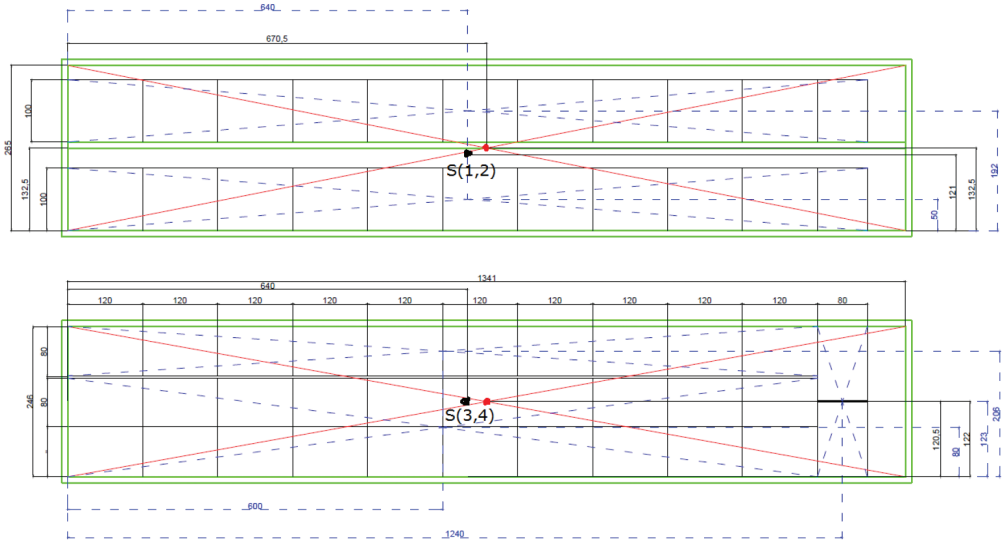

Fig. 20. Determining the centre of gravity in relation to the front wall and floor of the load area

Another significant parameter of a well-planned transport operation is determining the centre of gravity of the vehicle and cargo. The cargo should be placed in such a way that its centre of gravity is as low as possible and as close as possible to the longitudinal axis of the vehicle. This has a significant impact on the stability of the moving vehicle and the safety of the driver, the cargo, and other road users. A procedure for establishing the precise centre of gravity for a load placed in a vehicle is presented in the calculations and picture presented below (Fig. 20) [11].

Determining the centre of gravity enables checking the preliminary permissible maximum axle loads. Determining the axle loads of the trailer was performed with the use of an IT program (Fig. 21) [11]. The total weight of the trailer with the load was 20,000 [kg] (unladen mass 7,960 [kg] + cargo mass 12,000 [kg] = 19,960 [kg]); however, in practice, to use the loading capacity of a vehicle within the maximum permissible laden mass, it is safer to measure axle loads on special scales.

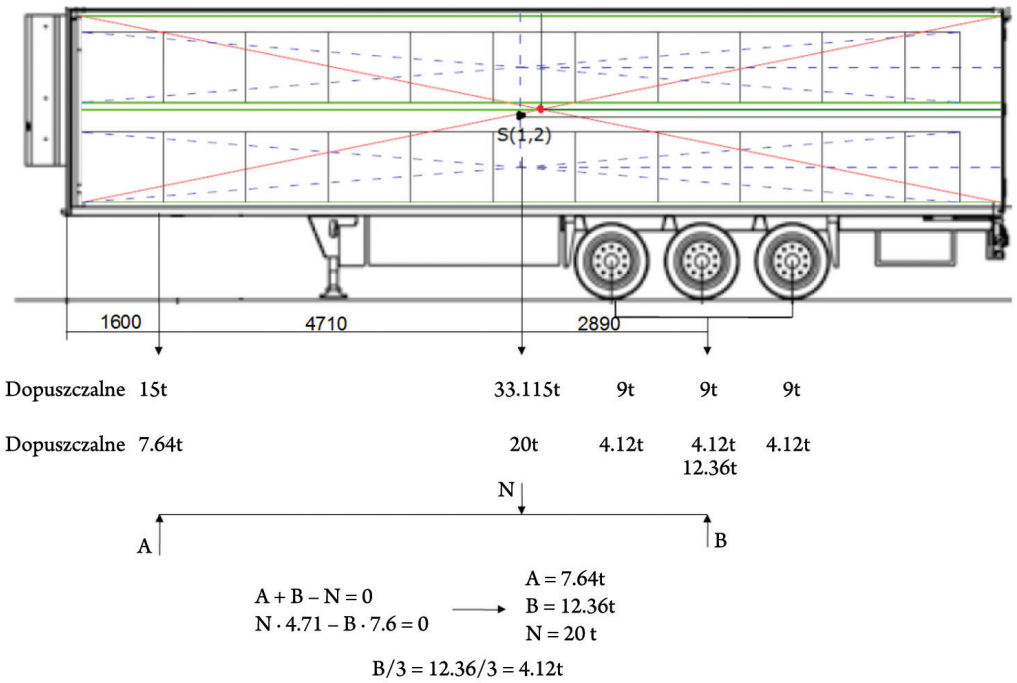

Fig. 21. Axle load calculation with use of determined centre of gravity of the vehicle

In order to select an appropriate method for load securing in a chosen semi-trailer, wall pressure should be calculated as below:
front wall strength:
40% x 12 t = 4.8 t ≤ 5 t
side walls strength:
30% x 12 t = 3.6 t

back wall strength:
25% x 12 t = 3 t ≤ 3.1 t

The producer of the Krone Cool Liner Doppelstock refrigerated semi-trailers with Thermo King SLX 300 allows the following maximum pressure on particular walls (Fig. 23) [4]:

- Front wall: 13.5 t
- Side walls: 10.8 t
- Back wall (door): 8.1 t

Test of the trailer revealed a higher level of strength than the required by the standard EN 12642 (Fig. 22) [4].

To secure the load against careless loading (e.g. leaving empty space that enables the movement of cargo during braking), it is advisable to use a 'pallet stop' system. According to the back wall resistance calculation, the required resistance preventing the load from moving back is three tonnes. It is necessary then to use barrier tracks with a resistance of 2 t (one for each floor): 2 x 2 t ≥ 3 t (requirement fulfilled).

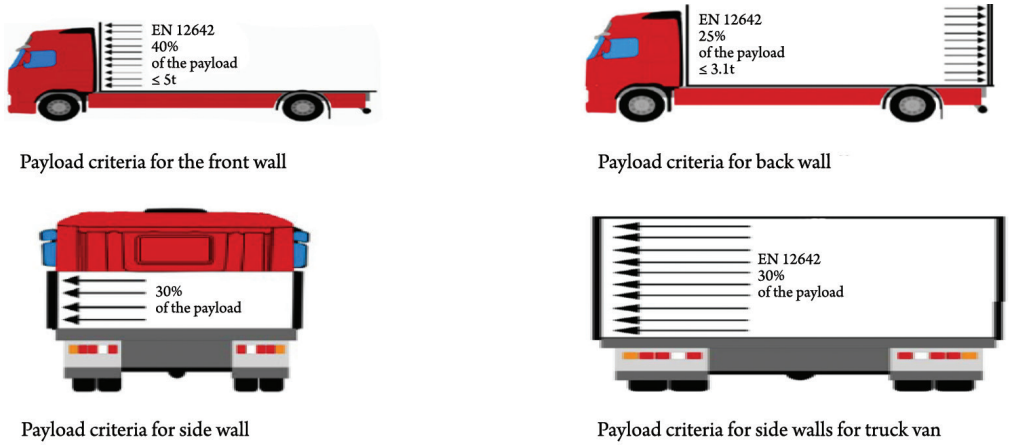

Fig. 22. Payload criteria for walls of box type bodies according to EN12642

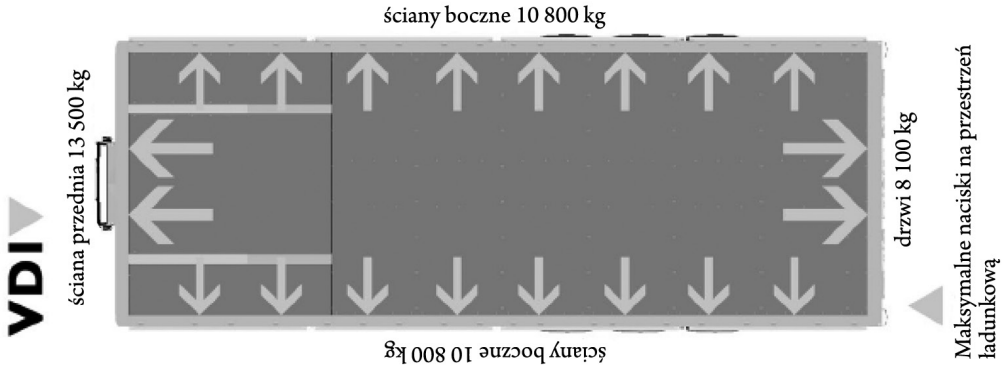

Fig. 23. The strength of side walls in the Krone Cool Liner Doppelstock refrigerated semi-trailer with Thermo King SLX

4. Conclusion

If the load is secured in an improper way, it can not only cause load damage but may also lead to serious economic loss, or tragic road accidents. Achieving technical excellence in the field of load securing has become a goal for many companies who try to outdo each other in new methods, systems and equipment concerned with load securing. The analysis of the technical parameters carried out with the use of the weighted average method and requirements for cargo securing led to the choice of the Krone Cool Liner Doppelstock refrigerated semi-trailer, with Thermo King SLX and allsafe securing systems – this achieved 183 points from the research analysis. The research referred to the technical parameters of a trailer and the requirements that the load securing systems need to meet. The scores achieved by competitive trailers were 141 and 130 points. The key factor that influenced the result most was the usage of modern trailer equipment connected with load securing produced by allsafe. The double deck ATD system by allsafe, allows the loading of sixty-six pallets at a time – the transport task required sixty-four pallets. In the case of the Krone trailer, despite the low rate of loading capacity usage, there would be a need to repeat the transport which would raise the costs. Aside from economic factors, traffic safety parameters also had an impact on the choice of a trailer (EBS with RSP in Schmitz trailer) and an additional 'pallet stop' load securing system that allows either completely avoiding or reducing the required amount of tracks, or reducing the pressure of the load on the front wall that. The analysis of additional parameters influencing safe transport operation revealed that there was a need to use supplementary protection connected with the appearance of free space that may lead to load movement while braking – using a 'pallet stop' system would solve this problem. According to the back wall resistance calculation, the required resistance that would prevent the cargo from moving backwards is three tonnes. It is therefore vital to use two barrier tracks with a resistance of two tonnes (one tonne per floor): $2 \times 2\ t \geq 3\ t$ (requirement fulfilled). It is worth mentioning that the newest directive of the European Parliament and the Council 2014/47/UE of 4 April 2014 on the technical roadside inspection of the roadworthiness of commercial vehicles circulating in the European Union. It was created in order to improve road safety and the environment, the directive establishes minimum requirements for a regime of technical roadside inspections of the roadworthiness of commercial vehicles circulating within the territory of the member states.

References

[1] Materiały techniczno-handlowe przedsiebiorstwa allsafe GmbH & Co.KG [Technical sales materials of allsafe GmbH & Co.KG].

[2] Materiały techniczno-handlowe przedsiębiorstwa Loadlok [Technical sales materials of Loadlok].

[3] Materiały techniczno-handlowe przedsiębiorstwa Schmitz [Technical sales materials of Szmitz].

[4] Materiały techniczno-handlowe dystrybutora naczep chłodniczych Krone Cool Liner [Technical sales materials of Krone Cool Liner].

[5] Materiały techniczno-handlowe naczep Schmitz Cargobull AG [Technical sales materials of Schmitz Cargobull AG trailers].

[6] Materiały techniczno-handlowe naczep Wielton [Technical sales materials of Wielton trailers].

[7] Starkowski D., Bieńczak K., Zwierzycki W., *Samochodowy Transport Krajowy i Międzynarodowy. Kompendium Wiedzy Praktycznej*, Vol. V, Wydawnictwo Systherm D. Gazińska sp. j., Poznań 2012.

[8] Starkowski D., *Zasady i metody doboru środka transportowego podczas planowania operacji transportowej przy pomocy analizy ważonej (wagowej) część 3*, Czasopismo TTS – Technika Transportu Szynowego No. 12/2015, XIX MIĘDZYNARODOWEJ KONFERENCJI NAUKOWEJ „Komputerowe Systemy Wspomagania Nauki, Przemysłu i Transportu", TransComp 2015, Zakopane 2015.

[9] Starkowski D., *Bezpieczeństwo ładunków w transporcie drogowym. Zasady i metody zabezpieczania ładunków w transporcie drogowym, część 3 – Zasady doboru metod oraz systemów zabezpieczenia ładunków w transporcie drogowym*, Monografia – Konferencja w ramach trzeciego kongresu Polskiej Izby Opakowań, Warszawa 2016, Poznań, 27.09.2016, Opakowania w łańcuchu dostaw.

[10] Starkowski D., Bieńczak K., Zwierzycki W., *Samochodowy transport krajowy i międzynarodowy. Kompendium wiedzy praktycznej*, Vol. 1, *Zabezpieczenia ładunków oraz zagadnienia techniczno-eksploatacyjne w transporcie drogowym*, Wydawnictwo Systherm D. Gazińska sp. j. Poznań 2010.

[11] Starkowski D., *Analiza procesu transportowego na przykładzie wybranego przedsiębiorstwa transportowo-spedycyjnego podczas przewozu truskawek, część 4 – Praktyczne wykonanie operacji przewozowej z analizą logistyczną*, Czasopismo Autobusy. Technika. Eksploatacja. Systemy Transportowe 6/2017, XIV konferencja naukowo-techniczna Logistyka Systemy Transportowe Bezpieczeństwo w Transporcie, Szczyrk, 24–27.04.2017.

[12] Starkowski D., *Jak przewozić żywność? Zabezpieczanie żywności w trakcie transportu drogowego (cz. 1). Odpowiedzialność i bezpieczeństwo w transporcie*, Czasopismo Transport i Spedycja 4/2016.

[13] Starkowski D.. *Jak prawidłowo rozmieścić ładunek na różnych typach naczep (cz. 2). Odpowiedzialność i bezpieczeństwo w transporcie*, Czasopismo Transport i Spedycja 1/2017.

[14] Dyrektywa Parlamentu Europejskiego i Rady 2014/47/UE z dnia 3 kwietnia 2014 r. w sprawie drogowej kontroli technicznej dotyczącej zdatności do ruchu drogowego pojazdów użytkowych poruszających się w Unii oraz uchylająca dyrektywę 2000/30/WE (Tekst mający znaczenie dla EOG) wraz z „Międzynarodowymi wytycznymi odnośnie bezpiecznego mocowania ładunków w transporcie drogowym". Międzynarodowa Komisja do spraw Technicznych IRU (CIT) IRU_CIT-2014 version 01. [Directive of the European Parliament and the Council 2014/47/UE of 4 April 2014 on the technical roadside inspection of the roadworthiness of commercial vehicles circulating in the Union Directive 2000/30/EC (Text with EEA relevance) with "International regulations referring to safe cargo securing in road transport".
[15] Zwierzycki W., Bieńczak K., *Pojazdy chłodnicze w transporcie żywności*, Wydawnictwo, Wydawnictwo Systherm D. Gazińska sp. j., Poznań 2006.
[16] Kwaśniowski S., *Pojazdy izotermiczne i chłodnicze*, Oficyna Wydawnicza Politechniki Wrocławskiej, Wrocław 1997.

allsafe
Member of allsafe GROUP

allsafe GmbH & Co. KG – we are German producer of elements and systems for load security in transporters and semi-trailers. Sales around the world are supported with country representatives also in Poland. Our basic values are customer orientation, innovation, fairness and personal responsibility. We are committed to cost-effectiveness, sustainability and safety which all guide our daily business approach. With our standard and promise "Made in Germany" we guarantee high quality brand name products with the highest degree of safety. Visit us on: www.allsafe-group.com or our shop on: www.allsafe24.com

TECHNICAL TRANSACTIONS /2018
ELECTRICAL ENGINEERING
DOI: 10.4467/2353737XCT.18.028.8001
SUBMISSION OF THE FINAL VERSION: 22/1/2018

Krzysztof Schiff (kschiff@pk.edu.pl)
Department of Automatic Control and Technology Information, Faculty of Electrical and Computer Engineering, Cracow University of Technology

An ant colony optimisation algorithm for the triple matching problem

Algorytm mrówkowy dla potrójnego zagadnienia dopasowania

Abstract

In this article, ant colony optimisation algorithms for the triple matching problem are described. This is the first elaborated ant algorithm for this problem. The problem is modeled by means of a 3-dimensional array. The ant algorithm was compared with the Apx3Dmatchnig-F algorithm and tested for different values of ant algorithm parameters. The results of these tests were presented and discussed.

Keywords: triple maximum matching problem, ant colony optimization algorithm, non weighted version

Streszczenie

W artykule został przedstawiony po raz pierwszy algorytm mrówkowy dla problemu potrójnego zagadnienia dopasowania. Problem potrójnego dopasowania zaprezentowano przy pomocy tablicy trój-wymiarowej. Algorytm mrówkowy został porównany z algorytmem Apx3Dmatching-F i przetestowany przy różnych wartościach parametrów algorytmu mrówkowego, a wyniki tych testów zostały zaprezentowane i omówione.

Słowa kluczowe: potrójne maksymalne dopasowanie, algorytm mrówkowy, wersja bez wag

1. Introduction

Triple matching is a generalisation of bipartite matching. Finding the largest triple matching is a well-known NP-hard problem. It is one of Karp's 21 NP-complete problems [1] and until now, there was no polynomial time algorithm for this problem. The DNA algorithm for the triple matching problem was presented in paper [7], but this algorithm is only for molecular not for electronic computer. The approximation algorithm for the triple matching problem have been presented recently in paper [8]. The triple matching is also called the three-dimensional marriage problem [2]. An instance of the three-dimensional marriage problem consists of n boys, n girls and n pets. A matching M consists of k triples (b, g, p) such that each boy, each girl and each pet belong to exactly one triple, but since this problem is very hard to solve, a variant of this problem is studied, which is called the Cyclic Three-Dimensional Matching [3, 4], but this is not the subject of this paper. Until today, there was no ant algorithm for the maximum triple matching problem and since the maximum triple matching belongs to combinatorial problems for which ant algorithms are very suited [5], I decided to elaborate an ant algorithm for this maximal triple matching problem.

2. The triple matching problem

In triple matching, we are given X, Y, Z, T, where:

1) X, Y and Z are 3 disjoint sets, each of size n.
2) $T = \{(x, y, z): x \in X, y \in Y, z \in Z\} \in X \cdot Y \cdot Z$ and we have to find M such that:
   - $M \subseteq T$
   - $|M| = k$
   - for any 2 distinct elements of M, (x, y, z) and (x', y', z'), $x \neq x'$, $y \neq y'$ and $z \neq z'$

The maximum triple matching problem relies on finding max $|M|$.

The triple matching problem and a solution for this problem are presented in Fig. 1. An edge represents a preference. A three-dimensional clique (a triangle) represents a match between boy, girl and pet. A maximum matching at Fig. 1 is presented by three triangles: (B1, G1, P3), (B2, G2, P1) and (B3, G3, P2).

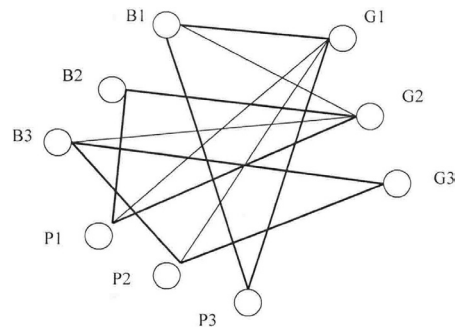

Fig. 1. The triple problem modeled as a 3-dimensional graph and its solution

This instance of the triple matching problem, which is presented in figure 1 as a three-dimensional graph, can be presented by a three-dimensional array M. Any element of this array M equal 1 means that there is a match between boy, girl and pet. If any element of this array M is equal 0, this means that there is no match. All elements of the three-dimensional array M for the instance of the maximum triple matching problem presented in figure 1 are listed below:

$M[b_1, g_1, p_1] = 0$, $M[b_1, g_1, p_2] = 0$, $M[b_1, g_1, p_3] = 1$,
$M[b_1, g_2, p_1] = 0$, $M[b_1, g_2, p_2] = 0$, $M[b_1, g_2, p_3] = 0$,
$M[b_1, g_3, p_1] = 0$, $M[b_1, g_3, p_2] = 0$, $M[b_1, g_3, p_3] = 0$,
$M[b_2, g_1, p_1] = 0$, $M[b_2, g_1, p_2] = 0$, $M[b_2, g_1, p_3] = 0$,
$M[b_2, g_2, p_1] = 1$, $M[b_2, g_2, p_2] = 0$, $M[b_2, g_2, p_3] = 0$,
$M[b_2, g_3, p_1] = 0$, $M[b_2, g_3, p_2] = 0$, $M[b_2, g_3, p_3] = 0$,
$M[b_3, g_1, p_1] = 0$, $M[b_3, g_1, p_2] = 0$, $M[b_3, g_1, p_3] = 0$,
$M[b_3, g_2, p_1] = 0$, $M[b_3, g_2, p_2] = 0$, $M[b_3, g_2, p_3] = 0$,
$M[b_3, g_3, p_1] = 0$, $M[b_3, g_3, p_2] = 1$, $M[b_3, g_3, p_3] = 0$.

The solution for the maximum matching problem consists of three elements of this three-dimensional array M: $M[b_1, g_1, p_3] = 1$, $M[b_2, g_2, p_1] = 1$ and $M[b_3, g_3, p_2] = 1$. Any two of these elements do not concern the same boy, same girl or same pet and thus the constraint 2 c is satisfied.

3. Structure of the ant algorithm

In ant algorithms, each ant is looking for a solution to a problem. If there are m ants, their solutions are compared and the best among them is chosen. This is repeated in each cycle of the ant algorithm, but in each cycle, also the best solution is remembered and an ant mechanism of communication is implemented.

At the beginning of an ant algorithm on all triples, which can be possibly chosen, the maximum quantity of pheromone t_{max} is assigned (line 1). Next, based on a 2-dimensional matrix of preferences between boys and girls bg[][], girls and pets gp[][] and boys and pets bp[][], a 3-dimensional array M[][][] is created. Elements of array M[][][] are equal to 1, when there is a match between boy, girl and pet, and is equal 0 in the other case. Ant algorithms consists of two main loops: one for cycle (line 4) and one for ants (line 6). Vectors allowedb[], allowedg[] and allowedp[] are used in the following way: when any ant finds a triple (b, g, p) then this boy, this girl and this pet can be included into another triple, which is part of the solution for the maximum triple matching problem (line 28), so they are excluded from the allowed boys, girls and pets, which can constitute the next triple. This exclusion is made by assigned a value 0 (line 29–31) to these vectors allowedb[], allowedg[] and allowedp[] for a particular boy, girl and pet. Thus, we can assure that any boys, any girls and any pets can be selected twice into two different triples, and thus, we assure that the received

solution is correct. If elements of these vectors allowedb[], allowedg[] and allowedp[] are equal to 1, this means that these particular boys, girls and pets can be selected into another triple (line 7–9).

The *while(go)* loop is executed when there is another triple (b, g, p), which can be added into the solution (line 13). Inside this loop, each ant calculates a sum of all the pheromones deposited on triples, which can be included into solution (line 16–19), a probability of particular triple selection (line 21–22) and selects one of these triples (line 25–31) based on the rule circle method and adds this triple into the solution (line 28). We can assure that each ant finds a solution, which constitutes of k – triples, so the *while(go)* loop can be executed equal or less than n times.

Each ant checks if a better solution was found, and if so, this solution is remembered (line 32–35). In order to do this, each ant calculates a number of triples *ld*, which were included into the solution. From all solutions received in one cycle, the one, which has the greatest number of triples, is selected *ldb*. This solution *ldb* is compared to the best solution *ldg*, which was found so far by ants (line 36) and the better is remembered. These sizes of the solution are used to calculate the additional quantity of pheromone *dt* which will be deposited on triples.

Next, an ant communication system was implemented (line 37–40): an evaporation mechanism r was used on all existing triples. which can constitute the solution, and an additional quantity of pheromone *dt* is added on all triple,s which constitute the best solution that was found so far (line 40).

The pseudo code of the elaborated ant algorithm for the maximum triple matching problem is presented below as algorithm 1.

Algorithm 1. Ant algorithm for the maximum triple matching problem

```
1.all f[i][j][k] = tmax;
2.based on bg[][], gp[][] and bp[][] a M[][][] is created
3. ldg = 0;
4. for each cycle
5. { ldb = 0;
6. for each ant
        {
7.      for all i allowedb[] = 1;
8.      for all j allowedg[] = 1;
9.      for all k allowedo[] = 1;
10.     for all i,j,k p[][][] = 0;
11.     for all i,j,k solution[][][] = 0;
12.     go = 1;
13.     while(go)
14.  {go = 0;
15.     sumat = 0;
16.     for all i,j,k
17.       if allowedb[] = = 1 && allowedg[] = = 1 && allowedp[] = = 1 && M[][][] = = 1
                  {
18.               go = 1;
19.               sumat = sumat+t[][][];  }
20.     if go = = 1{
                  for all i,j,k
21.                   if allowedb[] = = 1 && allowedg[] = = 1 && allowedp[] = = 1 &&
                      M[][][] = = 1
22.                       p[][][] = t[][][]/sumat;
23.               pr = (rand()/(double)32767);
```

```
24.                 sumap = 0;
        for all i,j,k
25.                 if allowedb[] = = 1 && allowedg[] = = 1 && allowedp[] = = 1 && M[][][] = =
1
26.                                         { sumap = sumap+p[][][];
27.                                         if sumap>pr
28.                         {               solution[][][] = 1;
29.                                                 allowedb[i] = 0; i = n;
30.                                                 allowedg[j] = 0; j = n;
31.                                                 allowedp[k] = 0; k = n; }       }
                    }//if go = = 1
        }//while(go)
32.     ld = 0;
33.     for all i,j,k
34.                 if solution[][][] = = 1 ld = ld+1;
35.     if ld>ldb  ldb = ld;
        }//for each ant
36. if ldb>ldg lg = ldb;
37. dt = (1 / (1 - ( (ldg-ldb)/ldg)));
38. for all i,j,k
39.     if soluution[][][] = = 1
40.                 t[][][] = r*t[][][] +dt
}//for each cycle
```

4. Experiments

Since there are no other ant algorithms even there is no polynomial time exact algorithm for the maximum triple matching problem experiments, which were conducted, concern only the comparison of the elaborated ant algorithm Ant3Dmatching with the approximation Apx3Dmatching-F algorithM [8]. During the first experiment, the size of the problem was changing from $n = 10$ to $n = 50$. The average results from 10 measurements were presented in figure 2 and in table 1. We can see that when the size of the problem is rising, the Ant3Dmatching algorithm allows us to receive a bigger maximum triple matching than the Apx3Dmatching-F algorithm. During the next experiment, the number of cycles was changing from $lc = 50$ to $lc = 250$. The average results from 10 measurements were presented in figure 3 and in table 2. In addition, the Ant3Dmatching algorithm now allows us to obtain a higher maximum triple matching than the Apx3Dmatching-F algorithm.

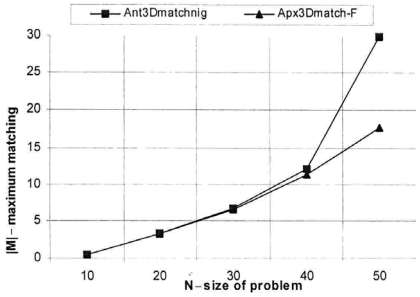

Fig. 2. An average size of maximum matching when $lc = 100$, $lm = 30$, $r = 0.998$ and $q = 0.07$

Table 1. An average size of maximum matching when $lc = 100$, $lm = 30$, $r = 0.998$ and $q = 0.07$

N	10	20	30	40	50
Ant3Dmatching	0.5	3.3	6.7	12.1	29.9
Apx3Dmatch-F	0.5	3.3	6.5	11.4	17.7

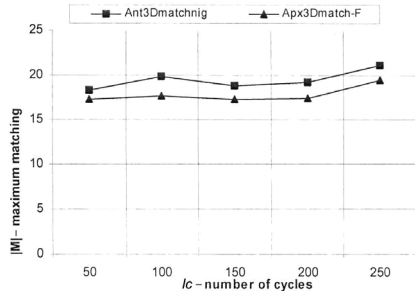

Fig. 3. An average size of maximum matching when $n = 50$, $lm = 30$, $r = 0.998$ and $q = 0.07$

Table 2. An average size of maximum matching when $n = 50$, $lm = 30$, $r = 0.998$ and $q = 0.07$

lc	50	100	150	200	250
Ant3Dmatching	18.3	19.9	18.8	19.2	21.1
Apx3Dmatch-F	17.3	17.7	17.3	17.4	19.5

The third experiment concerns the size of maximum matching when the number of ants was changing from $lm = 10$ to $lm = 50$. The average results from 10 measurements were presented in figure 4 and in table 3. There are no big differences in comparison with the case when the number of cycles was changing and the same occurred when an evaporation rate was changing from $r = 0.990$ to $r = 0.998$: the Ant3Dmatching algorithm has shown its advantage over the Apx3Dmatchnig_F algorithm. The average results from 10 measurements were presented in figure 5 and in table 4 for the case when the evaporation rate was changing.

Table 3. An average size of maximum matching when $n = 50$, $lc = 100$, $r = 0.998$ and $q = 0.07$

lm	10	20	30	40	50
Ant3Dmatching	19.8	20.8	19.9	20.3	20.2
Apx3Dmatch-F	17.6	19.4	17.7	18.4	18.4

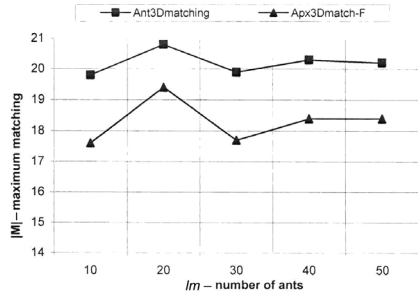

Fig. 4. An average size of maximum matching when $n = 50$, $lc = 100$, $r = 0.998$ and $q = 0.07$

Table 4. An average size of maximum matching when $lc = 100$, $lm = 30$, $n = 50$ and $q = 0.07$

R	0.990	0.992	0.994	0.996	0.998
Ant3Dmatching	19.2	19.0	21.3	19.2	19.9
Apx3Dmatch-F	17.8	17.7	19.6	17.0	17.7

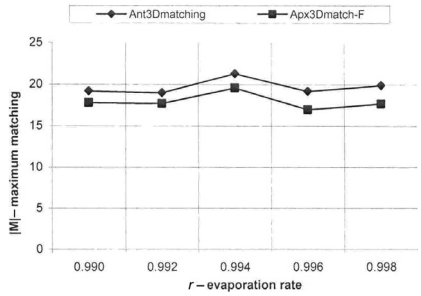

Fig. 5. An average size of maximum matching when $lc = 100$, $lm = 30$, $n = 50$ and $q = 0.07$

The last experiment concerns the size of maximum matching when the density of graph q was changing. The results have been shown in Table 5 and in Fig. 6. We can see that the size of maximum matching is changing when the size of the problem is constant and equal to $n = 50$, and this size of maximum matching received by the Ant3Dmatching algorithm is higher than that received by the Apx3dmatching-F algorithm for different graph density $q = \{ 0.04, 0.07, 0.10, 0.13$ and $0.13\}$. We see that the graph density q is very low. The graph density q is the probability with which the preference between boy and girl or boy and pet or girl and pet exist.

Table 5. An average size of maximum matching when $lc = 100$, $lm = 30$, $n = 50$ and $r = 0.998$

q	0.04	0.07	0.10	0.13	0.16
Ant3Dmatching	6.6	19.9	32.6	39.1	42.8
Apx3Dmatch-F	6.3	17.7	27.9	33.2	38.6

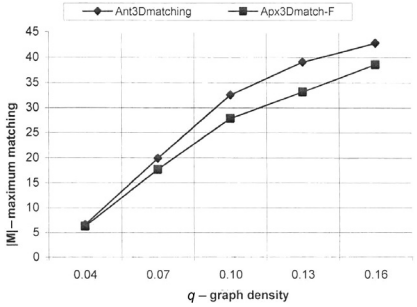

Fig. 6. An average size of maximum matching when $lc = 100$, $lm = 30$, $n = 50$ and $r = 0.998$

5. Conclusions

In this article, for the first time, an elaborated ant algorithm for the maximum triple matching problem is presented. Until now, there was no ant algorithm and no polynomial time exact algorithm for this problem. The elaborated ant algorithm, which is called the Ant3Dmatching algorithm, shows its over-performance over the approximation Apx3Dmatchnig-F algorithm. Thanks to the elaborated ant algorithm, the maximal triple matching problem can be solved very quickly and the size of the received triple matching is bigger than in the case when the Apx3Dmatching-F algorithm is used.

References

[1] Karp R.M., *Reducibility among combinatorial problems*, [in:] R. Miller, J. Thatcher, Complexity of Computer Computations, Plenum, 1972, 85–103.

[2] Knuth, D., *Stable marriage and its relation to other combinatorial problems, An introduction to the mathematical analysis of algorithms*, Amer. Math. Soc., Providence, RI, 1997.

[3] Biro P., McDermid, E., *Three-sided stable matching with cyclic preferences*, Algorithmica 58(1), 2010, 5–18.

[4] Eriksson, K., Sjostrand, J., Strimling, P., *Three-dimensional stable matching with cyclic preferences*, Math. Soc. Sci. 52(1), 2006, 77–87.

[5] Dorigo M., Stützle T., *Ant colony optimization*, Cambridge MIT Press. Proceedings of EvoWorkshops 2002, Berlin, Heidelberg, Springer-Verlag, 2002, 61–71.

[6] Chen J., *Iterative Expansion and Color Coding, an Improved Algorithm for 3D-Matching*, ACM Transactions on Algorithms, 2012, 6.1–6.22.

[7] Cao J., Chang W-L, Guo M., *Using sticker to solve the 3-dimensional matching problem in molecular supercomputers*, Int. J. High Performance Computing and Networking, Vol. 1, 2004, Nos. 1/2/3.

[8] Epifiano F.S., Ogasawara E., Soares J., Amorim M., Souza U., *O Problema de Alocacao deTutores em Aplicacoes de Provas*, XLVI Simposio Brasileiro de Pesquisa Operacional, Salvador, 16–19.09.2014 Brasil, 2014, 3007–3018.

TECHNICAL TRANSACTIONS 2/2018
ENVIRONMENTAL ENGINEERING
DOI: 10.4467/2353737XCT.18.029.8002
SUBMISSION OF THE FINAL VERSION: 22/1/2018

Bernard Twaróg (btwarog@pk.edu.pl)
Institute of Hydraulic Engineering and Water Management, Department of Hydraulic Engineering and Water Management, Faculty of Environmental Engineering, Cracow University of Technology

Interaction between hydraulic conditions and structures – fluid structure interaction problem solving. A case study of a hydraulic structure

Interakcja warunków hydraulicznych oraz konstrukcji – rozwiązywanie problemów FSI na przykładzie obiektu hydrotechnicznego

Abstract

Contemporary analytical and computational techniques enable the researcher to define interaction between varying flow rates, varying volumes of filling water and the deformation and stresses occurring in the structural components of a hydraulic structure. This study aims to describe and create visualisations, under selected operating conditions, of displacements, deformations and stresses of a hydraulic structure resulting from loads generated by hydraulic conditions in standard components of the structure. A sample analysis was carried out for the Niedów earthen dam on the Witka River that failed in 2010 due to a disastrous inflow. The scope of this analysis covers the components of the spillway section: the spillway monolith, the dissipation basin slab and the flip bucket. The results of analytical work and visualisations are shown using the Flow3D software program.

Keywords: hydraulic structure, CFD, stresses, deformations, displacements, spillway section, disaster, FSI solving

Streszczenie

Współczesne techniki analiz i obliczeń pozwalają na określenie wzajemnej interakcji pomiędzy zmienną wielkością przepływu i napełnienia a odkształceniem i naprężeniem, występującymi w elementach konstrukcyjnych obiektu hydrotechnicznego. Tematem proponowanego artykułu, dla wybranych warunków pracy obiektu hydrotechnicznego, jest opis i wizualizacja przemieszczeń, odkształceń oraz naprężeń będących konsekwencją obciążeń generowanych warunkami hydraulicznymi dla typowych elementów obiektu hydrotechnicznego. Przykład analizy został opracowany dla zapory ziemnej Niedów na rzece Witce, która uległa awarii w 2010 roku wskutek katastrofalnego dopływu. Zakres analizy obejmuje elementy sekcji przelewowej: monolit przelewu, płyta niecki wypadowej oraz szykany. Wyniki analiz i wizualizacje są prezentowane z wykorzystaniem oprogramowania Flow3D.

Keywords: obiekt hydrotechniczny, CFD, naprężenia, odkształcenia, przemieszczenia, sekcja przelewowa, katastrofa, rozwiązywanie FSI

1. An introduction to the FSI problems

Interactions between the motions of incompressible fluids and structures immersed in them represent non-linear physics problems that are investigated in a wide scope of scientific and engineering disciplines.

This study discusses the rules for the computation of components of a hydraulic structure affected by the motions of water and presents selected, representative operational examples. A model was developed for extreme operating conditions of the structure; boundary conditions were defined and a sample interaction between the hydraulic structure and the medium (FSI – Fluid Structure Interaction) was analysed using numerical methods.

In interactions between a fluid and a structure, the effects of the surrounding fluid on the structure may be exerted from the inside, from the outside or from both. Contemporary science and engineering studies heavily focus on research into the effects of surrounding fluids on structures and place great emphasis on the description and solving of strongly non-linear and multi-disciplinary problems of FSI (Chakrabarti, 2005; Dowell & Hall, 2001; Morand & Ohayon, 1995).

For most FSI problems, analytical solutions cannot be identified; furthermore, the space for conducting experiments in the laboratory is limited. Therefore, the main emphasis for research is placed on the application and development of numerical methods.

The use of computer techniques in solving FSI problems brings new possibilities on a near daily basis; more effective algorithms have been developed and solved which describe the behaviour of more complex structural designs and interactions between fluids and structures.

Sample applications of FSI are not limited to hydrodynamics and problems of structural dynamics. FSI methods are widely applied in research into bed load transport and sedimentation (Mucha et al., 2004; Tornberg & Shelley, 2004; Wang & Layton, 2009), aerodynamics (Haase, 2001; Zhang Jiang & Ye, 2007), turbulence (Kaligzin & Iaccarino, 2003; Yang & Balaras, 2006), medium flow in irregular geometries (Fadlun et al., 2000; Udaykumar et al., 1996, 2001), electrohydrodynamics (Hoburg & Melcher, 1976), magnetohydrodynamic flows (Grigoriadis et al., 2009), and descriptions of the behaviour of bio-fluids or biomechanics (cell junction and deformation, interaction of blood with the cardiac muscle, the behaviour of the inner ear, the behaviour of jellyfish, the mobility of spermatozoa and many other problems).

The numerical procedures aimed at solving FSI problems may be divided into two approaches – a comprehensive approach and a phased approach. Certainly, both approaches are variously perceived by scientists representing various disciplines.

The comprehensive approach (Hubner et al., 2004; Michler et al., 2004; Ryzhakov et al., 2010) describes fluid dynamics and structures using the same mathematical frameworks, proposing one equation system for the entire problem which is solved using a single algorithm. This approach may potentially achieve greater accuracy in defining interdisciplinary problems but may also require considerable computing power and greater resources and knowledge in order to develop and maintain a highly specialist code.

Unlike the comprehensive approach, the phased approach considers the fluid and the structure in separate computational domains, and in two separated and disjointed numerical meshes and computational algorithms.

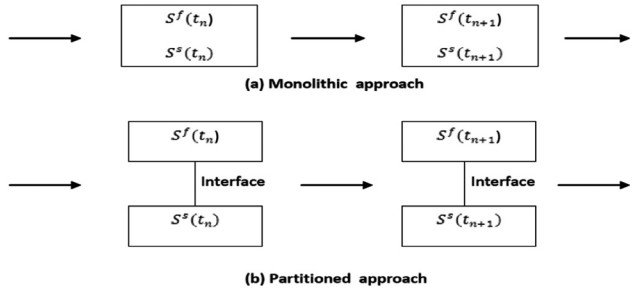

Fig. 1. A schematic diagram of the comprehensive and phased approaches in FSI problem solving [5]

Other generalised approaches are used that are based on the application of matching/conforming and non-matching/nonconforming meshes. The application of matching meshes is dependent upon using meshing methods that take into account the shape of the object (a structure, solid body) and the variation of boundary conditions. Repeated meshing is required to represent motions and deformations of the structure, using a matching or a non-matching mesh.

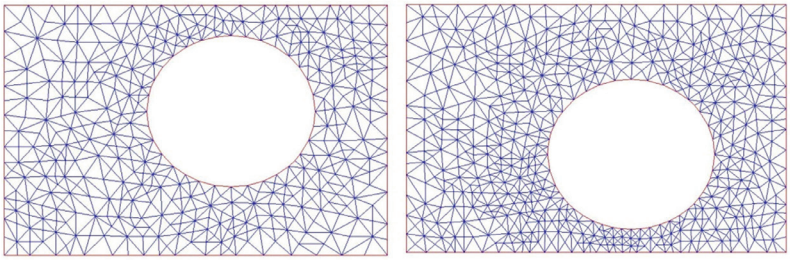

Fig. 2. Sample matching meshes for various times, t_1 and t_2

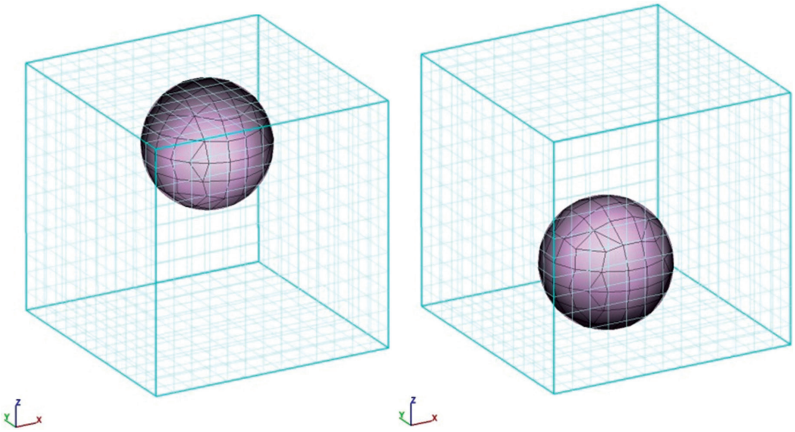

Fig. 3. Sample non-matching meshes for various times, t_1 and t_2

2. FSI problem definition

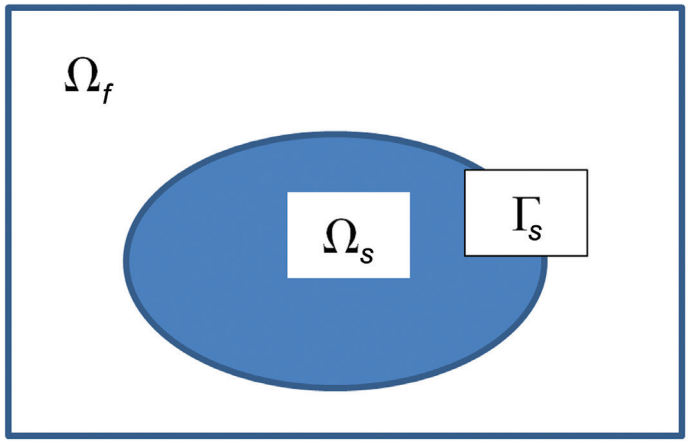

Fig. 4. A schematic diagram of the solid body, fluid domains and the interface domain

Let us assume a computational domain and mark it as Ω with an external boundary Γ. Let the analysed domain contain the area of a rigid body (the structure) Ω_S and the area of fluid Ω_f.

$$\Omega = \Omega_s \cup \Omega_f$$

The area of joint effect of the fluid and the rigid body is defined by the condition

$$\Gamma_s = \Omega_s \cap \Omega_f$$

The equations representing motions of the fluid and the rigid body may be formulated using previously adopted indices and the d'Alembert's principle:

$$p\dot{v}_i - \sigma_{ij,j} + f_i = 0 \qquad \text{Eq. 2.1}$$

where:

f_i – gravity forces

The equation in the solid body domain may be formulated as:

$$\rho^s \dot{v}_i^s - \sigma_{ij,j}^s + f_i^s = 0 \text{ w obszarze } \Omega_S \qquad \text{Eq. 2.2}$$

Consider that the velocity $\dot{v}_i^s$ is a time derivative of the displacement field u_i^s thus:

$$v_i^s = \dot{u}_i^s$$

The first two terms of equation 2.2 describe inertia and the internal stress state, respectively.

For example, when describing the behaviour of a rigid body in the domain of linear deformations using Hooke's law to calculate the stresses, we obtain:

$$\sigma_{ij}^{s} = \lambda \delta_{ij} \varepsilon_{11} + 2G\varepsilon_{ij}$$

where:

σ_{ij}^{s} – the tensor of stresses in the rigid body is expressed as a tensor of deformations and Lamé constants defined by the following equations:

$$\varepsilon_{ij} = \frac{1}{2}(u_{ij} + u_{ji})$$

$$G = \frac{E}{2(1+\nu)}$$

$$\lambda = \frac{E\nu}{(1+\nu)(1-2\nu)}$$

where:

E – Young's modulus,

ν – Poisson's ratio.

In the fluid domain, the equations may be formulated as follows:

$$\rho^{f} \dot{v}_{i}^{f} - \sigma_{ij,j}^{f} + f_{i}^{f} = 0 \text{ in the region of } \Omega_{f} \qquad \text{Eq. 2.3}$$

Internal conditions may be defined as:

$$\dot{v}_{i}^{f} = \frac{dv_{i}^{f}}{dt} = \frac{\partial v_{i}^{f}}{\partial t} + v_{j}^{f} v_{ij}^{f}$$

Assuming incompressible fluids and Newtonian stresses in the fluid, we obtain:

$$\sigma_{ij}^{f} = -p\delta_{ij} + \tau_{ij}$$

where:

$$\tau_{ij} = 2\mu\left(e_{ij} - \delta_{ij}\frac{e_{kk}}{3}\right)$$

$$e_{ij} = \left(v_{ji}^{f} + v_{ij}^{f}\right)$$

Consider that represents the hydrostatic pressure that may be understood *to be in an enforced state* of incompressibility:

$$v_{i,i}^{f} = 0$$

It is often assumed in fluid mechanics that fluid particles do not move at the boundary (the no-slip condition). A viscous fluid has a velocity of zero relative to the boundary

represented by the surface of a solid body during flow. Note that this condition along the interface area of the fluid and solid body surfaces may be defined as follows, using the Dirichlet and von Neumann boundary conditions:

$$v_i^s = v_i^f \text{ na } \Gamma_s \qquad \text{Eq. 2.4}$$

$$\sigma_{ij}^s n_i = \sigma_{ij}^f n_i \text{ na } \Gamma_s \qquad \text{Eq. 2.5}$$

Under real conditions, the differentiation of the displacement conditions in both domains leads to the domain interface equation

$$x_i^s = x_i^f \text{ na } \Gamma_s \qquad \text{Eq. 2.6}$$

3. Matching mesh methods

The matching mesh methods applied to solve FSI problems usually cover three areas: fluid dynamics, solid body motion dynamics and the mesh. The sequence of solving is intuitively comprehensible. Firstly, the equations for the fluid field may be solved for a given moment and specific location of the solid body. The calculated pressure and stress values are related to the solid body and to the external forces. Finally the behaviour of the solid body is calculated and a new mesh is then generated that matches the surface that has changed due to motion or deformation of the solid body. This iterative process may lead, at a purposefully selected time step, to the obtaining of convergent solutions.

4. Flow 3D software

Flow3D is a computer program that uses non-matching mesh methods to solve the FSI problems. It is designed to generate and solve fluid-structure interaction (FSI) problems and provides a platform that includes both fluid flow and solid body mechanics factors.

In the solid-body domain, the FSI module uses the finite element method (FEM) to simulate and analyse stresses and deformations. The stresses in the solid body are caused by external forces exerted on it by the surrounding fluid or by other limitations or constraints imposed on it.

5. Preprocessing – FSI modelling

It is enough to select the FSI option to activate the FSI module in the elements describing the properties of individual components. The choice must be finalised by entering material properties such as the density of the solid body and at least two of the following parameters:

the Young's modulus, the bulk modulus of elasticity, the shear modulus, the yield point, the Poisson's ratio.

Entering the yield point activates a material effort model that predicts local plastic deformations in the locations where the yield point is exceeded by stresses that are calculated according to von Mises theory.

The next step following the definition of material properties consists of the generation of a mesh of finite elements that discretises the solid body domain. By default, the preprocessor uses a Cartesian mesh defined to describe the fluid domain, but local meshes of finite elements may also be generated to describe the solid body.

The FSI model gradually solves the equations of solid body dynamics, so that it is theoretically capable of predicting major deformations with an adequate level of accuracy; however, fluid motions due to displacements at the boundary of the fluid and solid body phases are not updated. Consequently, the mapped dynamics of the solid body have no effect on the fluid behaviour in simulation results when modelling major deformations.

In the current version, the components of the solid body need to be limited by the boundaries of the fluid mesh or by contacts with other components so that motions of those components do not need to be mapped in the behaviour of the surrounding fluid. Therefore, the model must currently be structured so that motions of the components are appropriately limited (i.e. constraints must be imposed on them) in order to obtain a correct simulation.

6. Postprocessing – FSI modelling

The results of modelling of the rigid body behaviour may be viewed separately in the Flow3D interface by selecting the type of rigid body component and the result of calculations using finite elements. The user may select displacements, deformations and stresses along the axis of the adopted coordinate system.

Initially, the interface proposes a visualisation of normal displacements. These are defined as displacements of elements of the solid body surface (positive or negative) in the normal direction of this surface. Negative values of normal displacements present a visualisation of compression; positive values result from expansion. Six components of the deformation and stress tensor may additionally be visually represented.

An averaged value of stresses (ISO – an isotropic state) and stresses calculated according to von Mises theory may also be visually represented.

7. The concept of FSI modelling in Flow3D

Interaction between a fluid and a solid body (FSI – Fluid Structure Interaction) is modelled in Flow3D using fully coupled equations describing the dynamics of the solid body and the behaviour of the fluid. The approach used is not designed only to solve the flow problem. No

finite difference mesh is used in this module; it is replaced with a matching mesh of finite elements that is warped with the solid body.

This solution *is typically adopted* because the equations of solid mechanics are more convenient by far when solving solid body problems.

The current Flow3D software version enables the user to generate a new mesh of finite elements that matches the solid body – it is capable of providing a description of the solid body domain using a tetragonal or hexagonal mesh. The contact area (the interface) between the fluid and the solid body is processed so as to match the nodes of the external mesh with the mesh describing the solid body. The nearest nodes of the external mesh are matched with the nodes located on the solid body surface using the criterion of distance along the normal line to the surface of the solid body.

In certain cases, adjacent nodes are combined or selected nodes are removed.

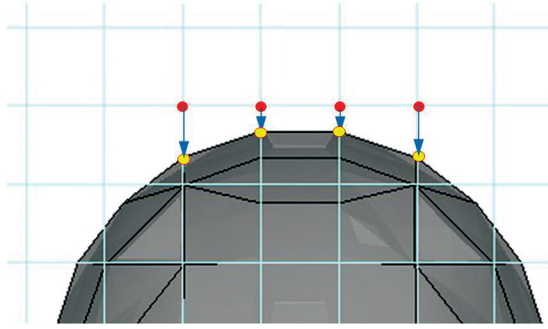

Fig. 5. The diagram represents a simplified 2D version of the problem of 'pulling' the nodes of the external mesh towards the nodes of the solid body mesh

The diagram shows a simplified version of the node pulling process. The developers of the program adopted the philosophy of a fully automated node matching process without external adjustment by the user.

8. The equations used in the Flow3D software

The basic equation used to describe motion of a rigid body is the d'Alembert principle:

$$\rho\frac{d^2x}{dt^2}=\nabla\boldsymbol{\sigma}+\rho\boldsymbol{b} \qquad \text{Eq. 8.1}$$

where:

- ρ – density of the rigid body,
- t – time,
- x – point coordinates,
- $\boldsymbol{\sigma}$ – Cauchy stress tensor,
- $\boldsymbol{b}$ – body forces.

The stress tensor is a measure of the stress state in a rigid body; it is related to material deformations and to other internal stresses in a rigid body – the program also enables the user to solve the problem of stresses caused by thermal phenomena. Deformation is a measure of the physical distortion affecting the body and is also represented by a tensor.

The approach adopted in this study is based on minor, gradual deformations. Consequently, the increment of deformation in one time step is calculated using the following formula:

$$E' = \frac{1}{2}\left\{[\nabla(\delta x)]^T + \nabla(\delta x)\right\} = \frac{1}{2}\left[\frac{\partial(\delta x)_i}{\partial x_j^n} + \frac{\partial(\delta x)_j}{\partial x_j^n}\right] e_i e_j \qquad \text{Eq. 8.2}$$

where:

E' – increment of deformation,
i, j – indices describing Cartesian coordinated in the directions,
e_i – unit vector in the system,
δx – describes the displacement vector.

$$\delta x = x^{n+1} - x^n \qquad \text{Eq. 8.3}$$

where:

x^n – represents the location of the point in the preceding rigid body at the moment,
x^{n+1} – represents the location of the point in the rigid body at the moment.

The Couchy stress tensor for the moment $n + 1$, σ^{n+1}, is calculated based on Hooke's linear model:

$$\sigma^{n+1} = \sigma^n + \left(K - \frac{2}{3}G\right) tr(E') + 2GE' \qquad \text{Eq. 8.4}$$

where:

$n, n + 1$ – represent time indices,
K – bulk modulus of elasticity,
G – shear modulus,
$tr(E')$ – the trace of the deformation tensor, i.e. the sum of its components on the main diagonal.

The bulk modulus of elasticity describes the resistance of an isotropic body to volume changes when the body is subject to isometric compression or expansion. The shear modulus describes the resistance of the body to shear. Both modulus forms are obtained from a functional dependence of the elasticity module and Poisson's ratio.

The FSI module in Flow3D is executed when a combination of at least two elements is given in material parameters.

The algorithm uses dependencies between material constants:

$$K = \frac{E}{3(1-2\nu)}, \quad G = \frac{E}{2(1+\nu)} \qquad \text{Eq. 8.5}$$

The acceleration conditions (8.1) are solved based on the locations of points on the body at various times:

$$\rho\frac{d^2x}{dt^2}=\rho\left(\frac{x^{n+1}-2x^n+x^{n-1}}{\Delta t^{n+1}\Delta t^n}\right) \qquad \text{Eq. 8.6}$$

9. The finite element method used in Flow3D

The equation (8.1) contains three-dimensional differential equations, solved at each time step, where x^{n+1} are unknown (σ^{n+1} are calculated directly from x^{n+1} and previous values σ in the equation 8.2). In the finite element method (FEM), the weighted remainder method is used to solve the equation (8.1). The method may be formulated as:

$$0=\int_\Omega \boldsymbol{\Psi}\left[\nabla\sigma^{n+1}+\rho\boldsymbol{b}-\rho\left(\frac{x^{n+1}-2x^n+x^{n-1}}{\Delta t^{n+1}\Delta t^n}\right)\right]d\Omega \qquad \text{Eq. 8.7}$$

where:

$\boldsymbol{\Psi}$ – the function of weights in the domain Ω.

By differentiating and minimising the formula:

$$\nabla(\boldsymbol{\Psi}\sigma^{n+1})=\boldsymbol{\Psi}\nabla\sigma^{n+1}+\nabla\boldsymbol{\Psi}\sigma^{n+1} \qquad \text{Eq. 8.8}$$

we obtain from the equations (8.7, 8.8):

$$0=\int_\Omega\left[\boldsymbol{\Psi}\nabla\sigma^{n+1}-\boldsymbol{\Psi}\rho\boldsymbol{b}+\boldsymbol{\Psi}\rho\left(\frac{x^{n+1}-2x^n+x^{n-1}}{\Delta t^{n+1}\Delta t^n}\right)\right]d\Omega-\int_\Omega\nabla(\boldsymbol{\Psi}\sigma^{n+1})d\Omega \qquad \text{Eq. 8.9}$$

The conditions on the right side of (8.9) may be recorded using Green's theorem:

$$0=\int_\Omega\left[\boldsymbol{\Psi}\nabla\sigma^{n+1}-\boldsymbol{\Psi}\rho\boldsymbol{b}+\boldsymbol{\Psi}\rho\left(\frac{x^{n+1}-2x^n+x^{n-1}}{\Delta t^{n+1}\Delta t^n}\right)\right]d\Omega-\oint\mathbf{n}(\boldsymbol{\Psi}\sigma^{n+1})d\Gamma \qquad \text{Eq. 8.10}$$

In the equation (8.10), $\boldsymbol{n}$ represents a normal vector pointing to the outside of the surface of domain , represents an infinitesimal portion of the solid body domain that constitutes the boundary domain. The indices n–1, n, and n+1 describe the time for each variable analysed. The last condition on the right side is non-zero at the boundary of the analysed domain. The weight function $\boldsymbol{\Psi}$ consists of a series of basic functions that differ from zero only around the point on the solid body they refer to and equal zero in all other points. Consequently:

$$\boldsymbol{\Psi}(x)=\sum_{i=1}^{nnodes}\psi_i \qquad \text{Eq. 8.11}$$

where:

nnodes – total number of nodes in the mesh used to discretise the domain,

x – coordinate of the point in the adopted frame of reference,

Ψ_i – represents the local values of the weight function close to the node.

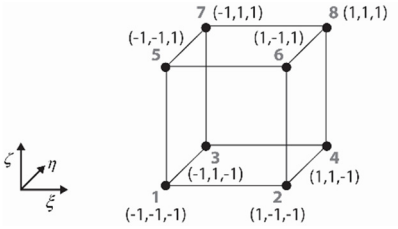

Fig. 6. Sample element of a tetragonal mesh

Let us assume a domain whose vertices correspond to 8 nodes, as in Fig. 6. The values of function Ψ_i corresponding to those nodes are non-zero while all the remaining nodes that do not relate to this element equal zero. Thus, considering the equation (8.11), we may formulate the equation (8.10) as follows:

$$0=\sum_{k=1}^{nnodes}\int_{\Omega}\left[\nabla\psi_k\sigma^{n+1}-\psi_k\rho\boldsymbol{b}+\psi_k\rho\left(\frac{x^{n+1}-2x^n+x^{n-1}}{\Delta t^{n+1}\Delta t^n}\right)\right]d\Omega-\sum_{k=1}^{nnodes}\oint\psi_k(\mathbf{n}\sigma^{n+1})d\Gamma \quad \text{Eq. 8.12}$$

The above equation is applied to each element. Since ψ_k in the equation (8.12) are non-zero only for elements that share the node k, the equation 8.12 actually leads to the system *nnodes*, and as there are three Cartesian directions, we obtain 3 x *nnodes* equations.

The function Ψ_k is recorded for each element. The basic functions are calculated within each element using computational coordinates, regardless of element orientation.

Sample forms of the weight function:

$$\Psi_1=\frac{1}{8}(1-\xi)(1-\eta)(1-\zeta)$$

$$\Psi_2=\frac{1}{8}\xi(1-\eta)(1-\zeta)$$

$$\Psi_3=\frac{1}{8}(1-\xi)\eta(1-\zeta)$$

$$\Psi_4=\frac{1}{8}\xi\eta(1-\zeta)$$

$$\Psi_5=\frac{1}{8}(1-\xi)(1-\eta)\zeta$$

$$\Psi_7 = \frac{1}{8}(1-\xi)\eta\zeta$$

$$\Psi_8 = \frac{1}{8}\xi\eta\zeta$$

The indices describe local nodes. The basic functions are both used as weight functions and represent the position and displacement:

$$\boldsymbol{x} = \sum_{k=1}^{nnodes} \boldsymbol{x}_k \psi_k \qquad \text{Eq. 8.13}$$

$\boldsymbol{x}$ – describes the position of point in the domain solved,
$\boldsymbol{x}_k$ – refers to the value in node k,
ψ_k – represents the value of basis function in node k.

10. Boundary conditions in the solid body domain

The interaction between the fluid and the solid body domain and the evolution of the stress tensor determine boundary conditions on the solid surface. If the surface area of the solid remains in contact with the fluid, the local pressure determines the force of interaction in the equation (8.12). Consequently:

$$\boldsymbol{n}\sigma^{n+1} = -\boldsymbol{n}p_{fluid} \qquad \text{Eq. 8.14}$$

The minus sign on the right side results from the adopted convention of stress signs – a compressive stress is negative.

If the boundary surfaces of the solid body are adjacent to the fluid domain boundary, the type of boundary condition defines the conditions imposed on the solid body. The domains adjacent to the boundary walls are steady; consequently, the nodes are attached to the boundary and may not move. If the symmetry condition is met, the nodes may freely move along the boundary, but may not move to the inside or to the outside of the solid body domain. For other boundary conditions, the pressure value is used to calculate motion based on the equation (8.14).

When an FSI component comes into contact with another component (either a standard or FSI component), the interface is always fixed, i.e. the nodes on the interface do not move during simulations. Full conjugation between two FSI components does not exist for that reason.

11. Sample FSI analysis

A sample FSI analysis was carried out using a model of the Niedów dam which was destroyed in the disaster of 7 August 2010. This dam break on the Witka River resulted from a limited flow capacity due to erroneous settings of limit switches, preventing the full opening of the dam Tainter gates [6–8].

11.1. Characteristics of the analysed structure (the Niedów dam)

The Niedów impounding structure was built in 1962 on the Witka River in order to create a reservoir feeding the Turów Power Plant, the Bogatynia region and a weir power station with water. The earthen dam is located on kilometre 2.8 of the Witka River course which is a right-bank tributary of the Nysa Łużycka River, with the confluence on kilometre 167.3

The structure consisted of:

- an earthen dam
- a spillway block
- a hydroelectric plant
- a pumping station

Fig. 7. The Niedów dam and the reservoir of the town of Zgorzelec, before and after the failure

A Creager-type, three-bay spillway was used to discharge significant amounts of flood water through the impounding structure. The bays with a width of 6.70 m were closed by Tainter gates lifted with the use of roller chains. The total length of the spillways amounted to 20.10 m.

The crest of the spillway was at an elevation of 204.00 m above sea level. With an elevation of the water table in the reservoir corresponding to the normal impoundment level (NIL) of 210.0 m above sea level, the unit capacity of the spillway was defined as $q = 25.0\ m^2s^{-1}$. The elevation of the dam crest was 211.60 m above sea level, and the depth of water flowing over the crest reached around 0.4 m on the day of disaster.

A peak of 211.96 m above sea level was recorded at the Witka water-level gauge at 5:10 pm. A peak of 212.05 m above sea level occurred in the dam cross-section at 5:42 pm.

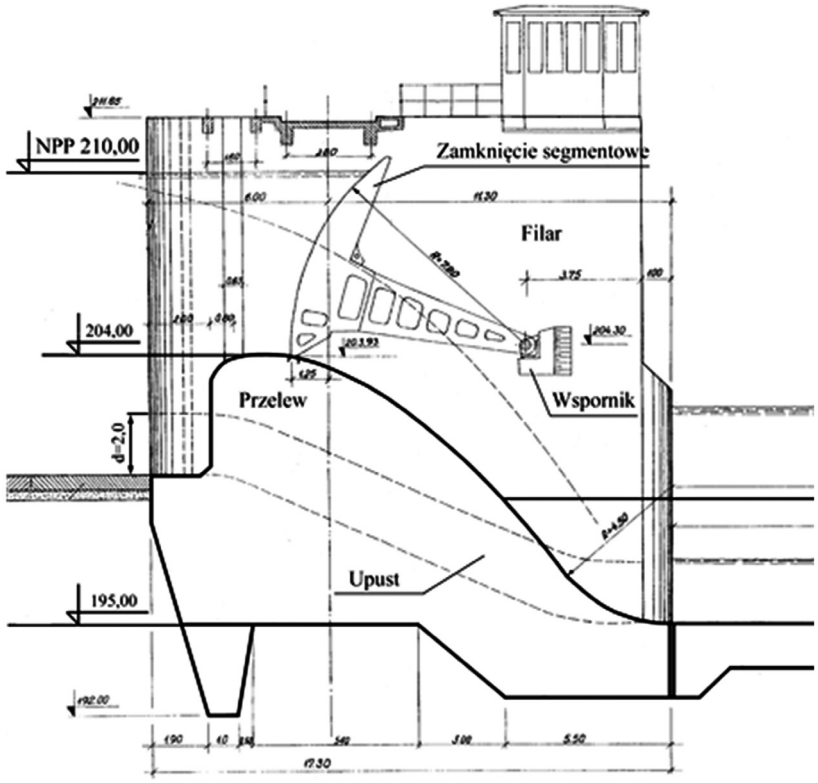

Fig. 8. Cross section of the spillways [6]

The water overflow resulted in the erosion of the downstream embankment in both dam sections; consequently, the bitumen pavement in the left dam section eroded first, then concrete facing slabs were breached and the left wing of the upstream abutment was broken off and collapsed. This caused an increase in the water outflow in the left section of the dam. Erosion of the downstream embankment occurred first in the right section of the earthen dam, then the dam increasingly eroded towards the spillway block. Water outflow caused erosion at two-thirds of the dam length to the right of the spillway block, and practically the entire dam on the left bank side. The erosion process ended at around 7:00 pm, when the reservoir was empty.

11.2. Assumptions for the FSI analysis

The following material parameters were assumed for all elements of the spillway section covered by the FSI analysis:

- material – concrete,
- density – 2300 kg/m^3,
- Young's modulus – 3.0 e+10 Pa,
- Poisson's ratio – 0.2.

The operating conditions of the structure were defined as those in place during the extreme circumstances that occurred on 7 August 2010 which led to the erosion of the dam earthen body [8]; an elevation of water table at 212.05 m above sea level was assumed. The positions of Tainter gates were set as they were at the time immediately preceding the disaster. The analysis aimed to replicate the maximum stress values that occurred in selected components of the spillway section [7, 8].

The FSI analysis was carried out for one spillway section with two boundary pillars and for the dissipation basin with the flip bucket located in the analysed section.

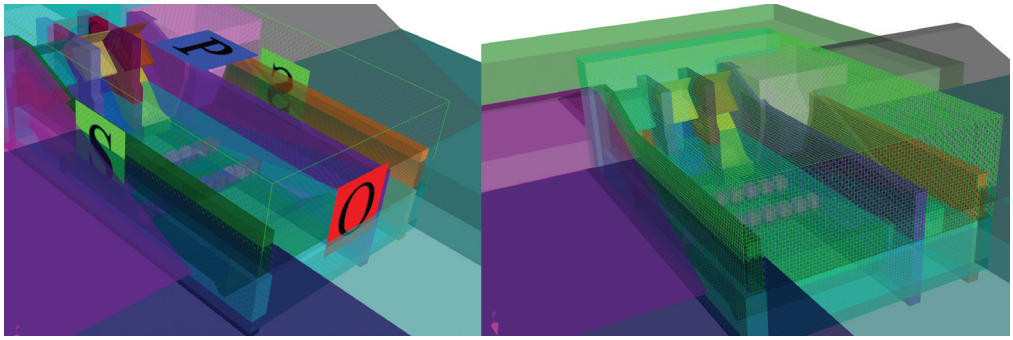

Fig. 9. Allocation of meshes used to discretise the analysed components of the spillway section [7, 8]

The modelling process was limited to the first minutes of the simulation under extreme operating conditions of the structure, preceding the moment of the erosion of the earthen body (changes in the hydraulic conditions affecting the load exerted on the structure). The meshes used to discretise the domain were allocated so as to provide nodes for the analysed components. The filtration under the structure and through the earthen body of the dam was ignored in the modelling process.

11.3. Results of the analysis

The following components of the spillway section were covered by the FSI analysis:

- the dissipation basin slab,
- the flip bucket,
- the spillway monolith.

The simulation was carried out using Flow3D software with the FSI option activated. The analysis covered deformations, stresses and displacements. The simulation model was defined for a linear range of operation of the components, in the domain described by Hooke's law.

Selected results of the analysis representing the evolution of the stress field due to the flow of breaching water in individual components of the section are given below. The selected stress states show changes in their values from a hydrostatic load until the moment of the formation of a hydraulic jump.

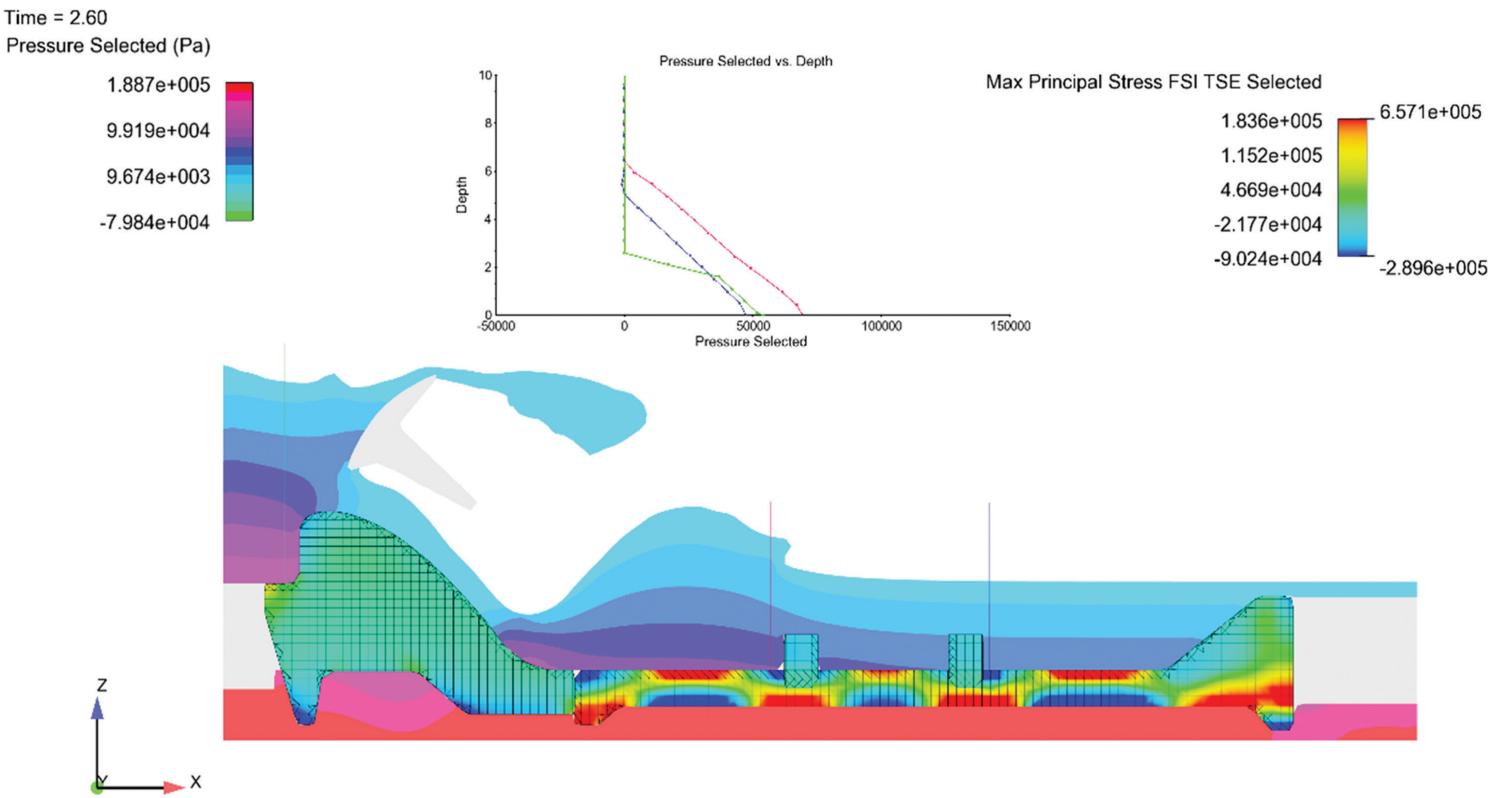

Fig. 10. Values of pressure [Pa] and maximum main stresses [Pa] in the structural components of the spillway section, $t = 2.6$ s

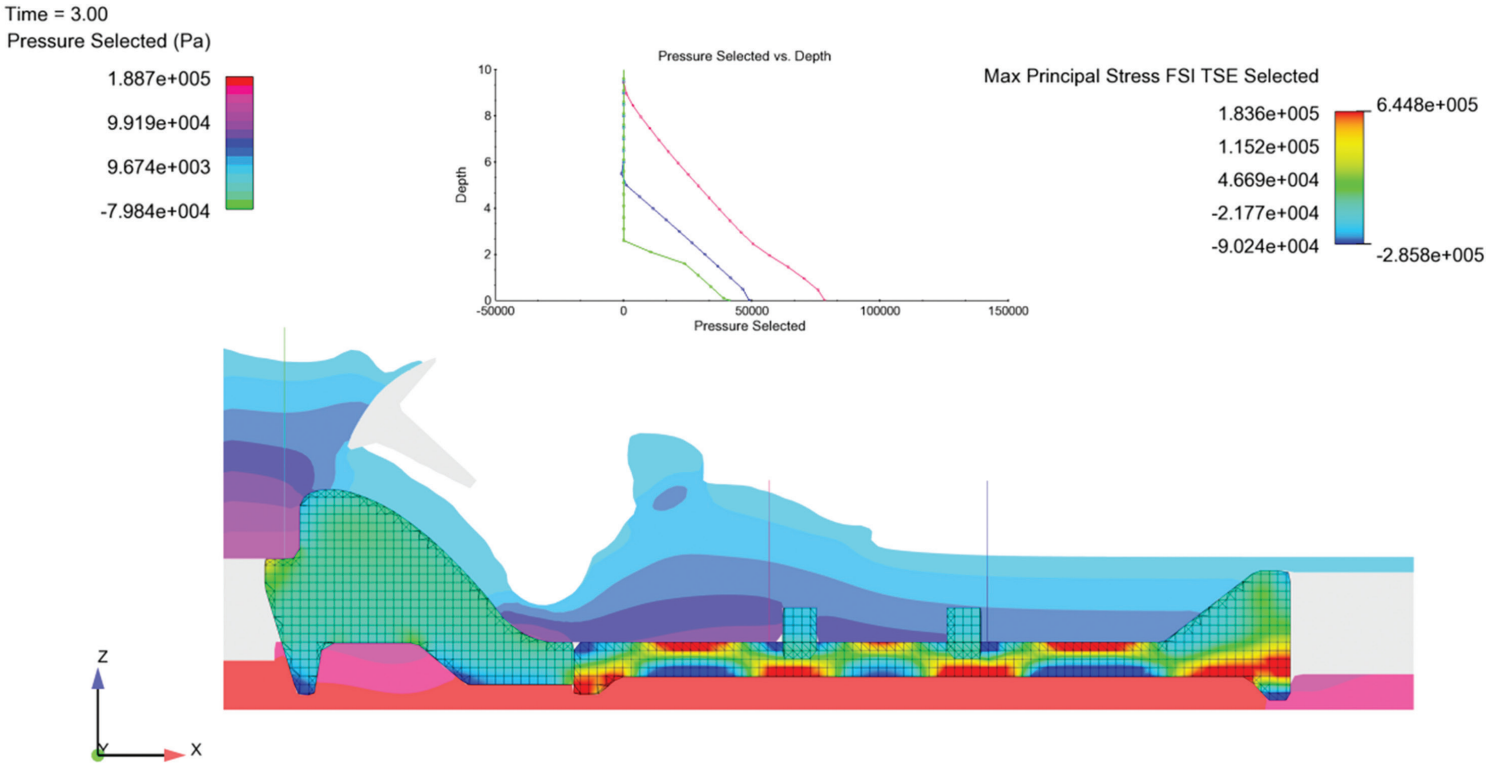

Fig. 11. Values of pressure [Pa] and maximum main stresses [Pa] in the structural components of the spillway section, t = 3.0 s

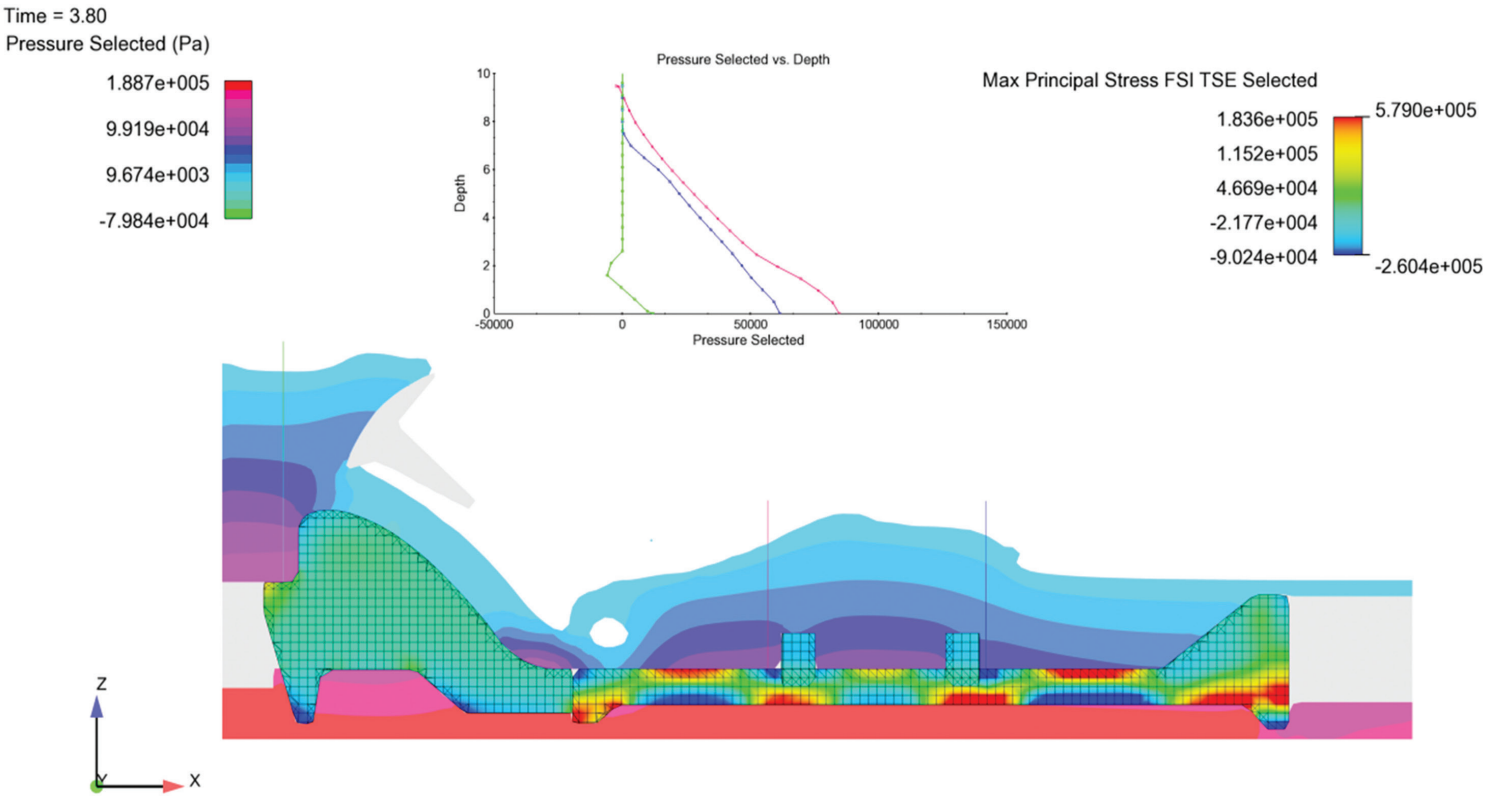

Fig. 12. Values of pressure [Pa] and maximum main stresses [Pa] in the structural components of the spillway section, $t = 3.8$ s

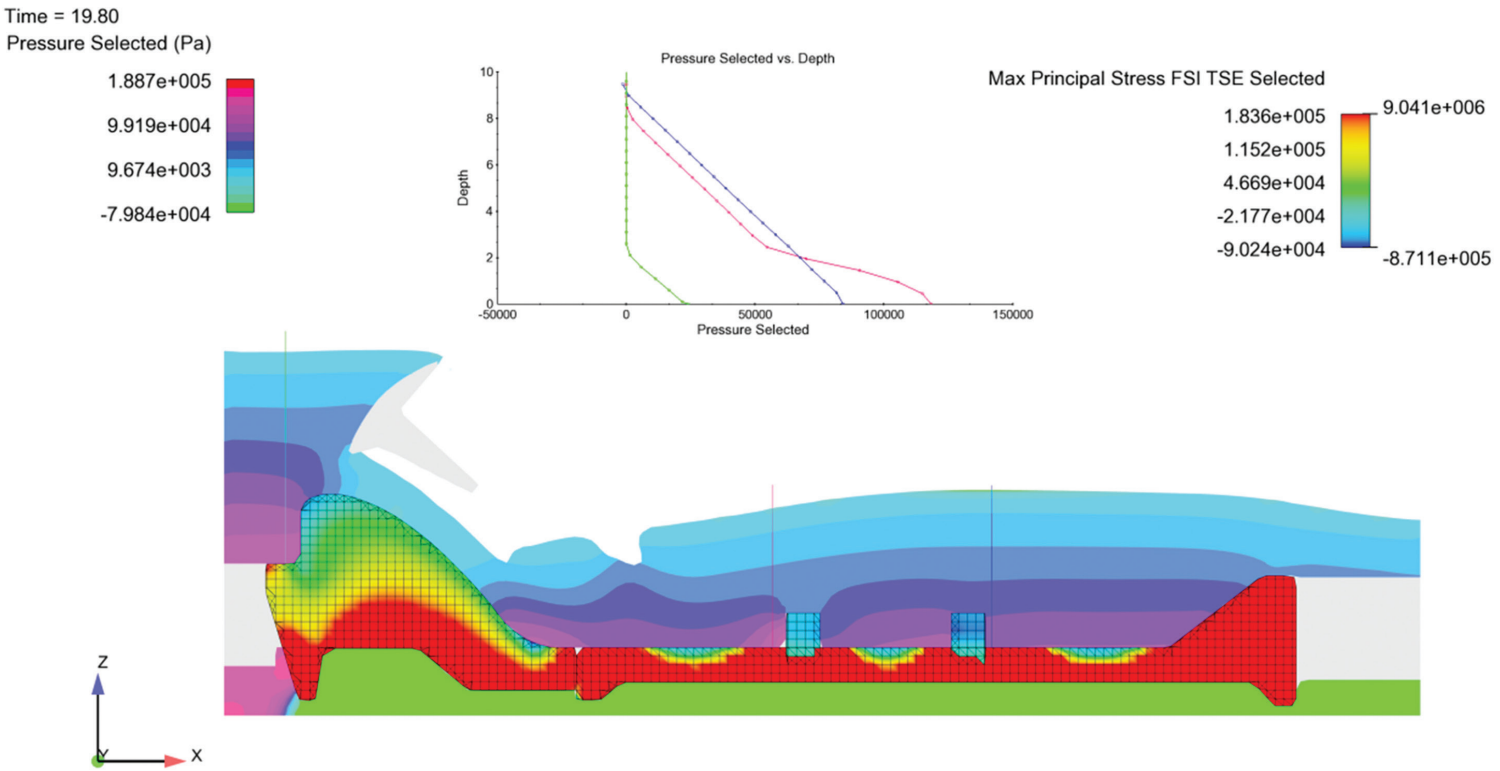

Fig. 13. Values of pressure [Pa] and maximum main stresses [Pa] in the structural components of the spillway section, $t = 20$ s

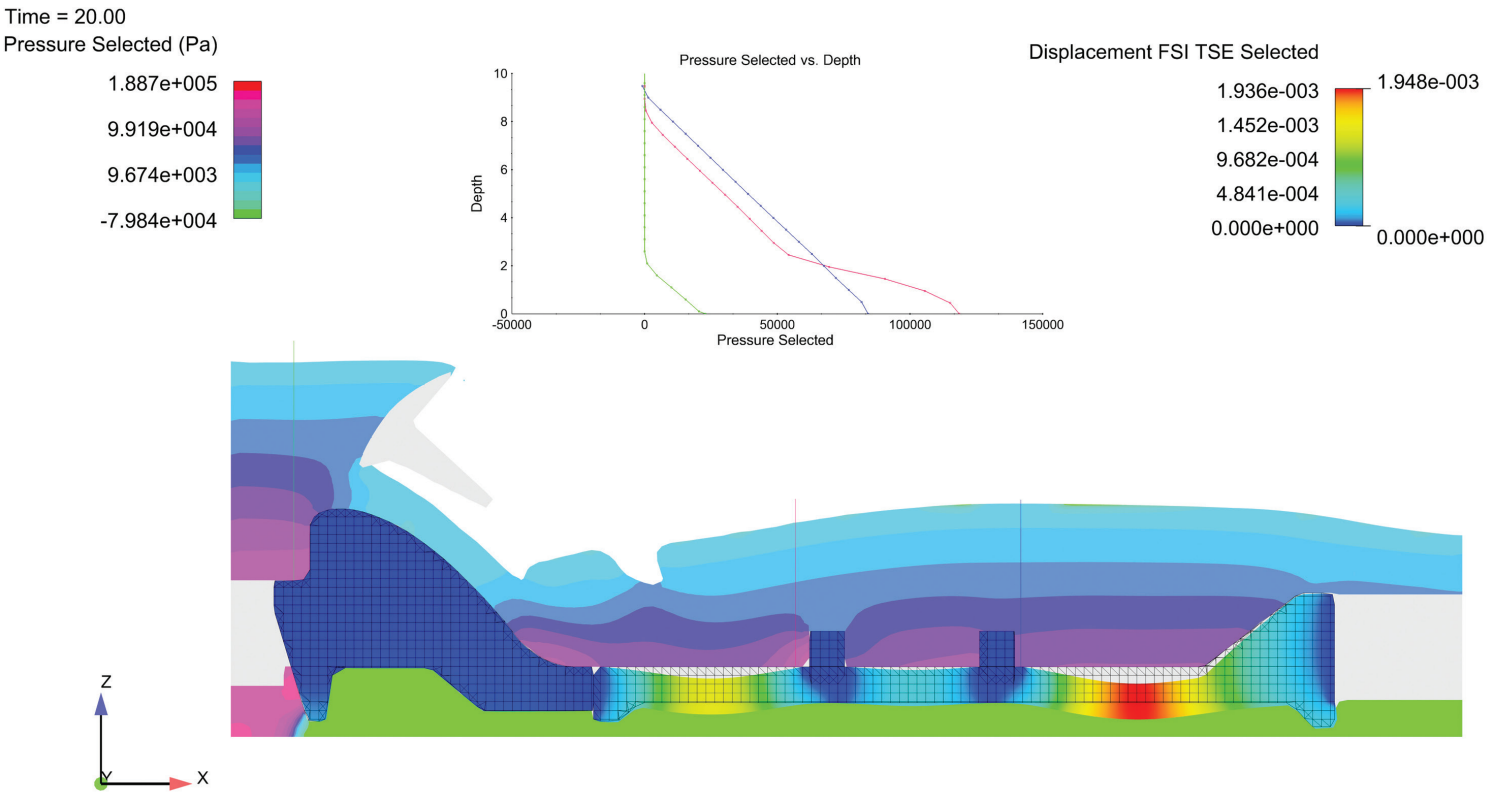

Fig. 14. Values of pressure [Pa] and values of displacements in a distorted scale [Pa] in the structural components of the spillway section, $t = 20$ s

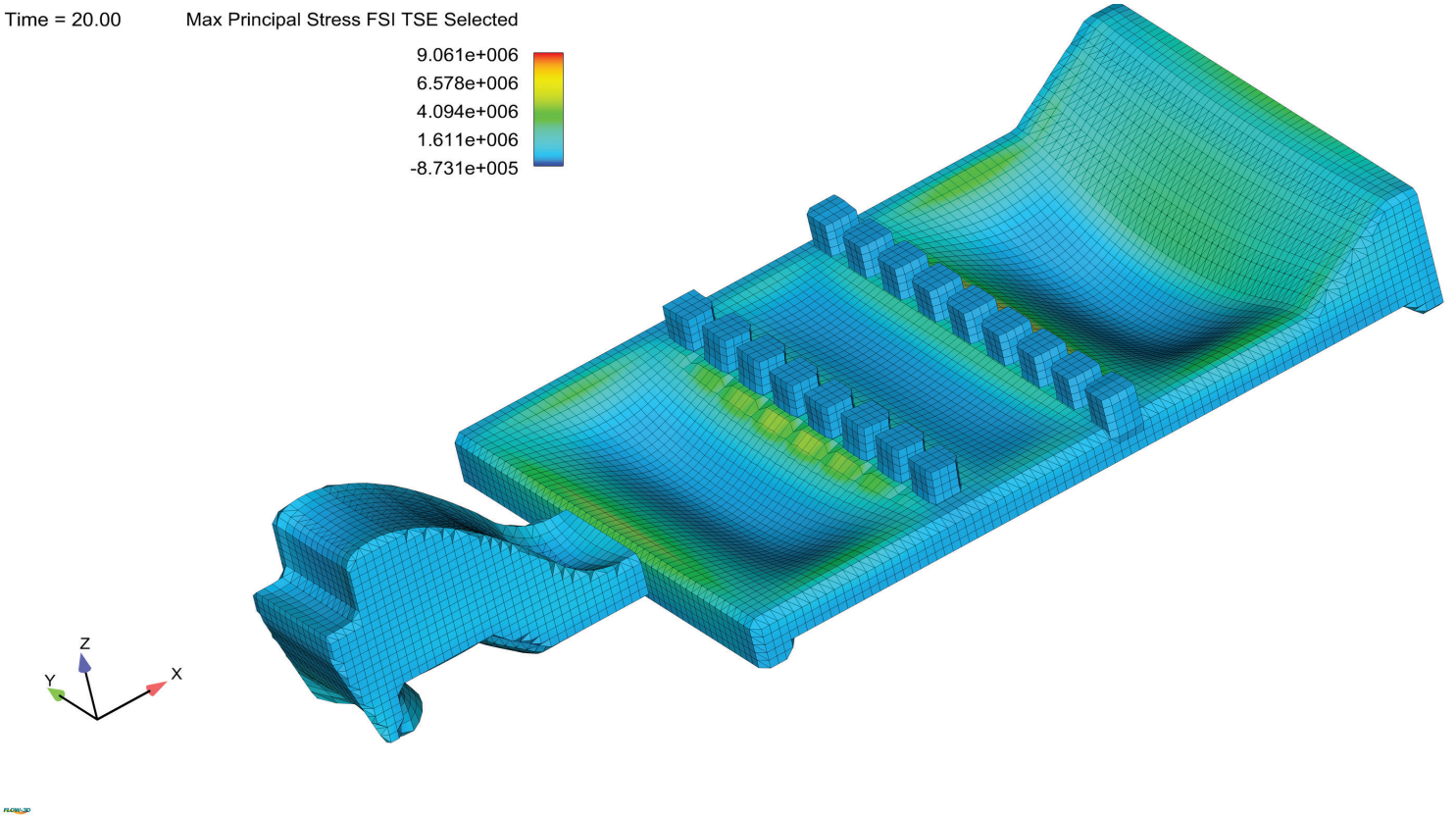

Fig. 15. Values of normal compressive and tensile stresses occurring in the spillway monolith and in the basin slab at the selected moment, $t = 20$ s

12. Conclusion

The methods and algorithms used to solve FSI problems have been dynamically developed over recent years. This development has mainly been driven by the demand observed in numerous scientific and engineering disciplines where FSI problems are identified and play an increasingly important role. A rapid increase in computation efficiency is favourable for the application of demanding calculation techniques. FSI numerical research has become a separate discipline. Due to the interdisciplinary nature of FSI problems, the development of this discipline is conditional upon contributions made by engineers and research representing various disciplines.

The completed FSI analysis of selected concrete (and reinforced concrete) components of the spillway section of the destroyed structure shows the potential of contemporary computational methods as used to identify domains subject to varying stress values.

The analysis covering the first several dozens of seconds of *see above note* the operation of the structure during a disaster resulted in the identification of two distinct phases of structural component operation in terms of stress variation. The first phase displays a considerable variation of inflow and velocity, mainly in the dissipation basin (formation of the hydraulic jump) in the spillway section, and consequently, by a considerable variation in the pressures that generate a stress state with the values of normal stresses reaching ±1e+6 Pa (Fig. 10–12). In the second phase of operation of the structure, the outflow from the basin initially stabilizes with a submerged hydraulic jump. Larger pressure, but at lower velocities, and the generated stress state is characterised by normal stress values reaching ±1e+7 Pa (Fig. 14). The conditions change over the following seconds, because the structure erodes and is finally destroyed.

Considerable variation of normal stress values and their arithmetical signs occurs in the dissipation basin slab during the first phase of operation. The variation indicated by the arithmetical sign of normal stress occurs alternately with along the basin slab. The spillway monolith is subject to lower stress values – these are mainly compressive. Layers of compressive and tensile stresses are formed mainly in the second phase – the tensile stresses occur in the spillway monolith in the foundation section and the compressive stresses occur in the area near the surface; tensile stresses prevail in the dissipation basin slab. The flip bucket is subject to compressive stresses in both phases of variation of the conditions.

References

[1] Brebbia C.A., *Fluid Structure Interaction V. Wessex Institute of Technology*, UK, WITpress, Southhampton, Boston 2009.

[2] Hammack E. Allen, Fong Moira T., Stockstill Richard L., *Calculating Forces on Components of Hydraulic Structure*, US Army Corps of Engineers, ERDC/CHL CHETN-IX-21, August 2009.

[3] Bandringa H., *Immersed boundary methods, Institute of Mathematics and Computing Science*, University of Groningen, August 2010.
[4] Peskin Charles S., *The immersed boundary method,* Acta Numerica, 2002, 479–517c, Cambridge University Press, DOI: 10.1017/S0962492902000077.
[5] Hou G., Wang Jin, Layton A., *Numerical Methods for Fluid-Structure Interaction – A Review*, Commun. Comput. Phys., Vol. 12, No. 2, pp. 337-377, August 2012, DOI: 10.4208/cicp.291210.290411s.
[6] Kostecki S., Rędowicz W., *The Washout Mechanism of the Niedów Dam and its Impact on the Parameters of the Flood Wave*, Procedia Engineering, 91, Wrocław 2014, 292–297, DOI: 10.1016/j.proeng.2014.12.062.
[7] Twaróg B., Failure *of Dam Niedów in Poland Preliminary Analysis and Conclusions*, Flow 3D Americas Users Conference, Canada, Toronto 2014.
[8] Twaróg B., *Katastrofa zapory Niedów – modelowanie z wykorzystaniem FLOW-3D, Wybrane problemy planowania i zarządzania w warunkach kryzysowych*, Chapter: II. *Wybrane narzędzia wspierające proces podejmowania decyzji (Selected tools supporting the decision-making process)*, M. Maciejewski, T. Walczykiewicz (eds.), IMGW PIB Poland, 95–106.

TECHNICAL TRANSACTIONS 2/2018
MECHANICS
DOI: 10.4467/2353737XCT.18.030.8003
SUBMISSION OF THE FINAL VERSION: 22/12/2017

Dominik Kwiatkowski (dkwiatkowski@pk.edu.pl)
Edward Lisowski
Dominik Kwiatkowski, Edward Lisowski, Institute of Applied Informatics,
Faculty of Mechanical Engineering, Cracow University of Technology

Nonlinear static analysis of air cushion in SolidWorks Simulation 2016

Badania nieliniowe poduszki pneumatycznej w programie SolidWorks Simulation 2016

Abstract

The paper presents the results of research for load lifting process for a single pneumatic cushion. The load lifting process has been simulated in SolidWorks Simulation using the model of Mooney-Rivlin for hyper-elastic material. Research was conducted based on a simplified 3D model and drawn up a mathematical model of pneumatic cushions determining of non-linear static characteristics for the lifting height depending on the weight of the load and supply pressure. The results compare with the results of laboratory tests conducted for the platform equipped with four air cushions.

Keywords: CAD 3D, FEM, Mooney-Rivlin, air cushion

Streszczenie

W artykule przedstawiono wyniki badań dla procesu podnoszenia ładunku dla pojedynczej poduszki pneumatycznej. Proces podnoszenia ładunku zasymulowano w programie SolidWorks Simulation, wykorzystując model Mooney-Rivlin'a dla materiału hiper-sprężystego. Bazując na uproszczonym modelu 3D i opracowanym modelu matematycznym poduszki pneumatycznej, przeprowadzono badania statyczne nieliniowe, wyznaczając charakterystyki dla wysokości podnoszenia w zależności od masy ładunku i ciśnienia zasilającego. Otrzymane wyniki porównano z wynikami badań laboratoryjnych, przeprowadzonymi dla platformy wyposażonej w cztery poduszki pneumatyczne.

Słowa kluczowe: CAD 3D, MES, Mooney-Rivlin, poduszka pneumatyczna

1. Introduction

Transportation systems on air cushions designed to transport heavy load are used in industrial halls and production plants where the low value of system's displacement in the direction of the height of lifting (Y-axis) is the significant parameter.

In order to estimate such a value, it can be simulated as a simplified system reducing its to one air cushion. In this research software specialised in solving problems connected with nonlinear static analysis and possibility of defining hyper-elastic material was used. A program used in this purpose was SolidWorks Symulation 2016.

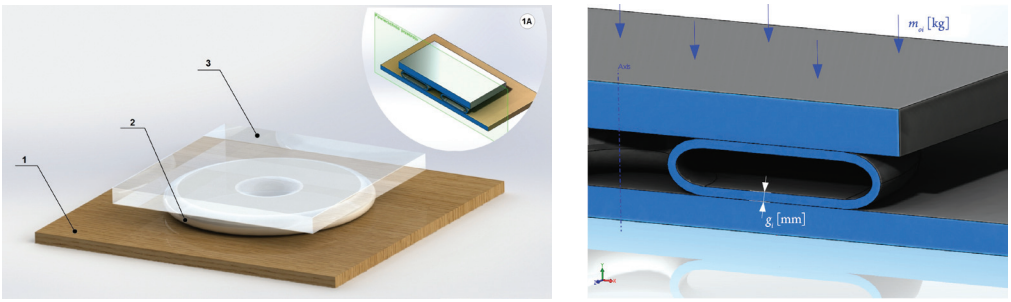

Fig. 1. Simplified geometrical model of air cushion, where: 1 – work surface; 2 – rubber toroid; 3 – rigid carrier plate; 1A – Cross-section view of air cushion; g_i – rubber toroid thickness, m_{oi} – load

A simplified geometric model is shown in the Fig. 1 where – for the needs of research – the parameter for thickness of a toroid made of a hyper-elastic material with value $g = 2$ [mm] and three configurations of load: $m_{o1} = 500$ [kg], $m_{o2} = 750$ [kg], $m_{o3} = 1000$ [kg] are introduced.

To calculate pressures which are present in- and under air cushion during system's work, mathematical model of air cushion and results of laboratory research for value of lifting basing on study [1] was used.

2. Hyper-elastic material model

To define the material of the toroid element, the Mooney-Rivlin hiper-elastic model [2] was used. This model describes material made from sythetic rubber from the group EPDM (ethylene propylene diene monome) [3].

The Mooney-Rivlin strain energy density function is expressed as [4]:

$$W_1 = A(\mathrm{I}-3)+B(\mathrm{II}-3)+X\left(\frac{1}{\mathrm{III}^2}-1\right)-1+Y(\mathrm{III}-1)^2 \tag{1}$$

$$W_2 = C(\mathrm{I}-3)(\mathrm{II}-3)+D(\mathrm{I}-3)^2+E(\mathrm{II}-3)^2+F(\mathrm{I}-3)^3 \tag{2}$$

$$W = W_1 + W_2 \tag{3}$$

where:

A, *B*, *C*, *D*, *E* and *F* – are Mooney material constants,

I, II, III – invariants of the right Cauchy-Green deformation tensor,

and

$$X = 0.5A + B \tag{4}$$

$$Y = \frac{\left[A(5\nu - 2) + B(11\nu - 5)\right]}{\left[2(1 - 2\nu)\right]} \tag{5}$$

where:

ν – Poisson's ratio.

To define the hyper-elastic material in SolidWorks, data shown in the Fig. 2 were used.

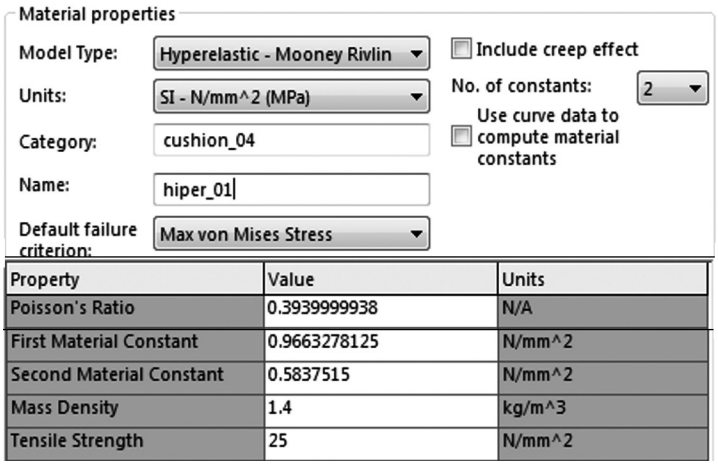

Property	Value	Units
Poisson's Ratio	0.3939999938	N/A
First Material Constant	0.9663278125	N/mm^2
Second Material Constant	0.5837515	N/mm^2
Mass Density	1.4	kg/m^3
Tensile Strength	25	N/mm^2

Fig. 2. The definition of properties for hyper-elastic material in SolidWorks

3. Definition of properties for FEM

In order to realize a simulation for air cushion with proper loading and supply pressure where height research was taken into consideration, contacts between elements, boundary conditions and type of the mesh and its density were defined.

The model used for strain and displacement calculations was reduced to cross-section, so it means to 2D model.

For this simplified model, a program generated 2D linear triangular elements which have got three degrees of freedom in every node: two transations and one rotation. Translation degrees of freedom are motions in global directions *X*, *Y*. Rotation degrees of freedom are rotation around global axis *Z*.

Parameters of the mesh was prepared according to thickness of toroid. For example, for $g_1 = 4$ [mm] (Fig. 3), max element size was equal 4 [mm]; min element size was equal 0.5 [mm]. In the areas where the biggest strains and deformations were forecasted, the mesh refined.

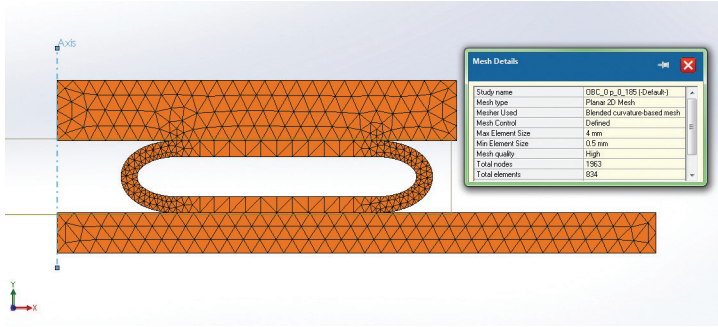

Fig. 3. The definition of properties for mesh where $g = 4$ [mm], the other variants depend on the thickness of rubber toroid

Then, a contact of elements occuring in the model was defined. A bonded contact for edges between rigid carrier plate and toroid was created (Fig. 4 – red color). The mesh must not have been compatible. If the is compatible, the program merges common nodes along cooperation sufrace. In other case, it applies constrain equations internally to symulate a link.

To make a link between work surface and toroid there was created constrain without penetration (Fig. 4 – blue color). This constrain does not allow to penetration of elements but it allows to creating gaps [5].

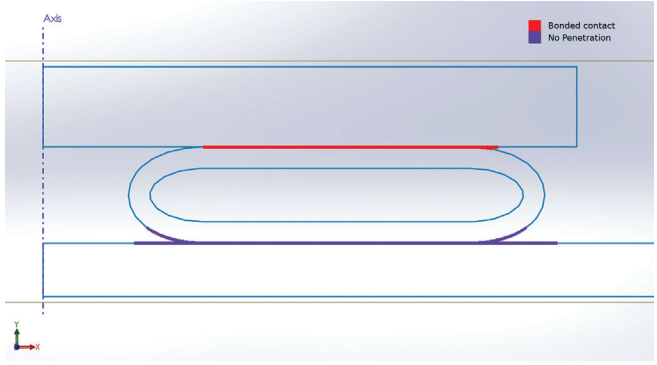

Fig. 4. The definition of component contact, where color red color – bonded contact, blue color – no penetration

In the next stage, restraints were defined. For work surface (Fig. 5), fixed possibility of motion in direction *Y*-axis and in direction *X*-axis. When defining strengthening for the rigid carrier plate (Fig. 5), it was decided to divest one degree of freedom for *X*-axis on side of the plate because of the possibility of decline state of balance with simulation calculations.

For bottom edges of toroid, a displacement on *Y*-axis which is variable in time was defined to simulate a moment of transition of air cushion from state of work to state of lifting with possibility of moving a load. The second state is connected with occuring an air film between work surface and working layer of toroid. A value R_y assessed from 0 to 1 [mm] in time of simulation 10 [s].

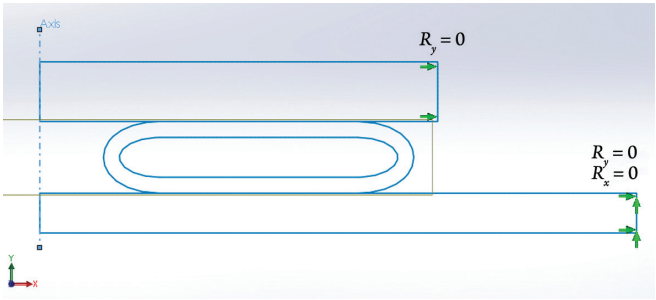

Fig. 5. The definition of restraints for work surface and rigit carrier plate

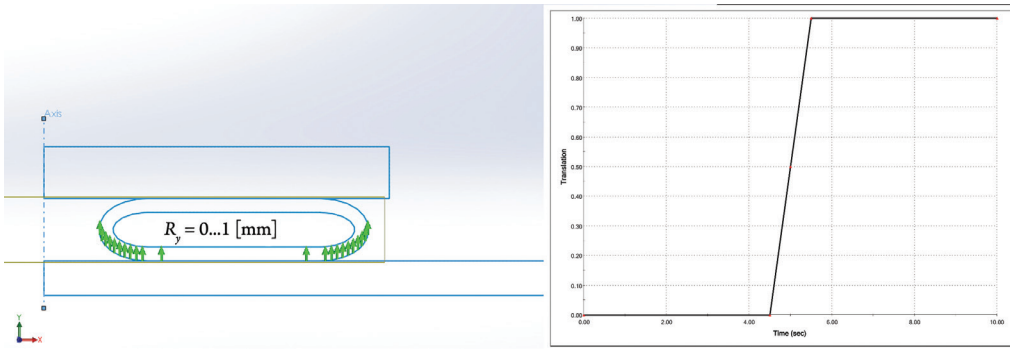

Fig. 6. The definition of restraints for rubber toroid in left and curve of *Y* translation in time (R_Y[t]) for rubber toroid in right

After defining restraints, defining of external loadings for the model has begun. Rigid carrier plate was loaded with a force equaling a mass of the loas in three variants (Fig. 7). The load was picked according to laboratory results for the system of four air cushions and respectively calibrate in proportion to simulation of single air cushion.

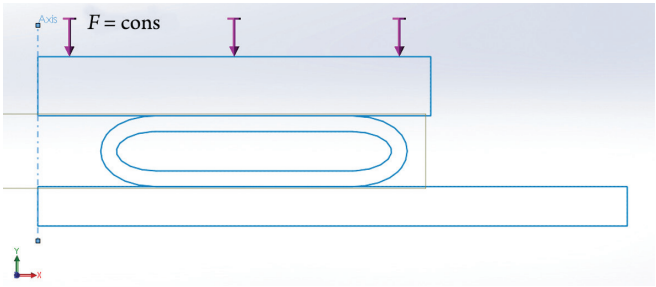

Fig. 7. The definition of external load for rigid carrier plate for the three variants:
1) $F = 1250$ [N]; 2) $F = 1875$ [N]; 3) $F = 2500$ [N]

Then, pressure variable in time $p_2(t)$ found in the toroid. A change of the value in time stems from increasing quantity of air during work inside the air cushion, so that inside the toroid. Both direction of pressure and characteristics are shown in the Fig. 8.

For the rigid carrier plate pressure variable in time $p_{31}(t)$ simulating pressere found in chamber under the air cushion which modifies slightly its value in the moment of occuring an air film was also defined (Fig. 8).

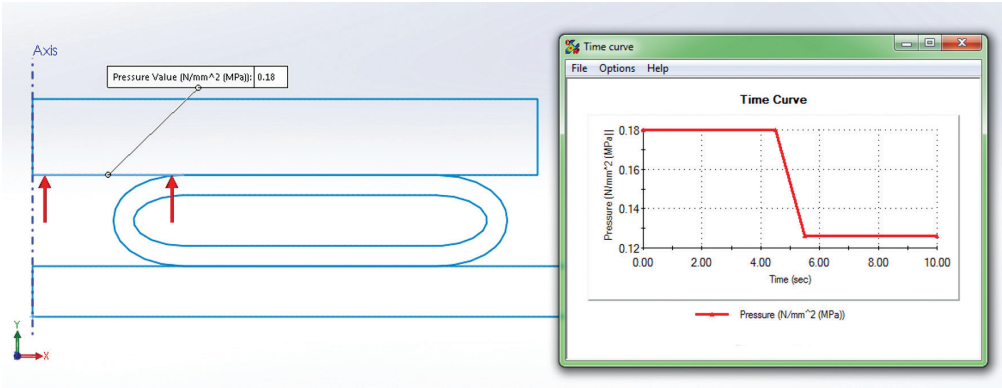

Fig. 8. Left image present the definition of pressure $p_2(t)$ inside of rubber toroid, one example. Right image present definition of pressure $p_{31}(t)$ for rigid carrier plate, one example

Additionally, two components pressure found in the chamber under air cushion was defined (Fig. 9). Second component, $p_{32}(t)$, occurs on external layer of the toroid inside the object. Its value decreses with moment of occuring an air film.

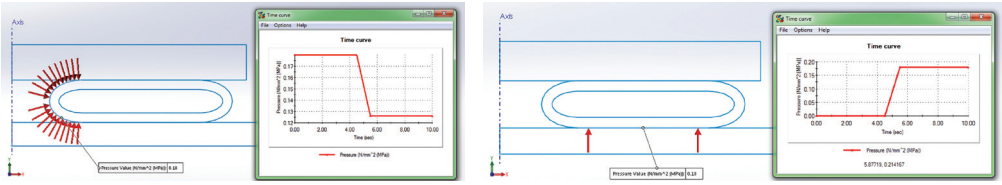

Fig. 9. Left image present the definition of pressure $p_{32}(t)$ for outside of rubber toroid, one example. Right image present the definition of pressure $p_{33}(t)$ for outside of rubber toroid, one example

Third component, $p_{33}(t)$, occurs under toroid and appears in the moment of appearing of an air film.

The model prepared this way was submitted for simulation for various values of supply pressure p_1.

4. Results of the simulation

As a result of the simulation for every configuration, a picture of a map of equvalent strains von Mises, maps of deformations and maps of displacements were obtained (Fig. 10). In that, there was a possibility of estimating height of air cushion lifting according to every case of value of supply pressure.

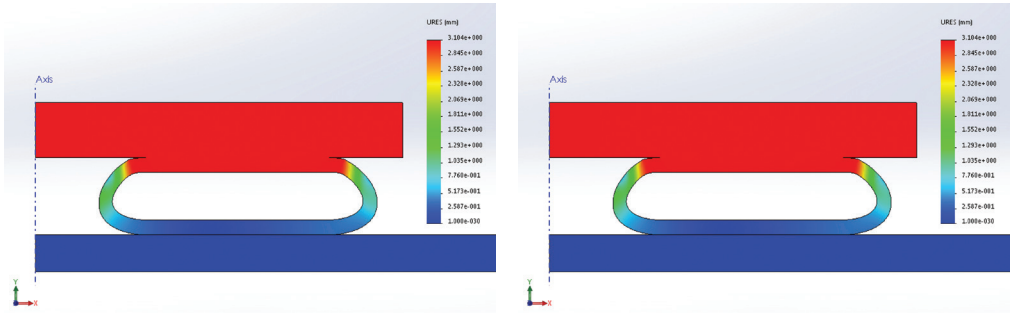

Fig. 10. Example of von Mises stress (left image) and *Y*-displacement (right image)

Gathered data let create characteristics (Fig. 11) for three cases of loading with possibility to compare them with results had done in laboratory (blue color).

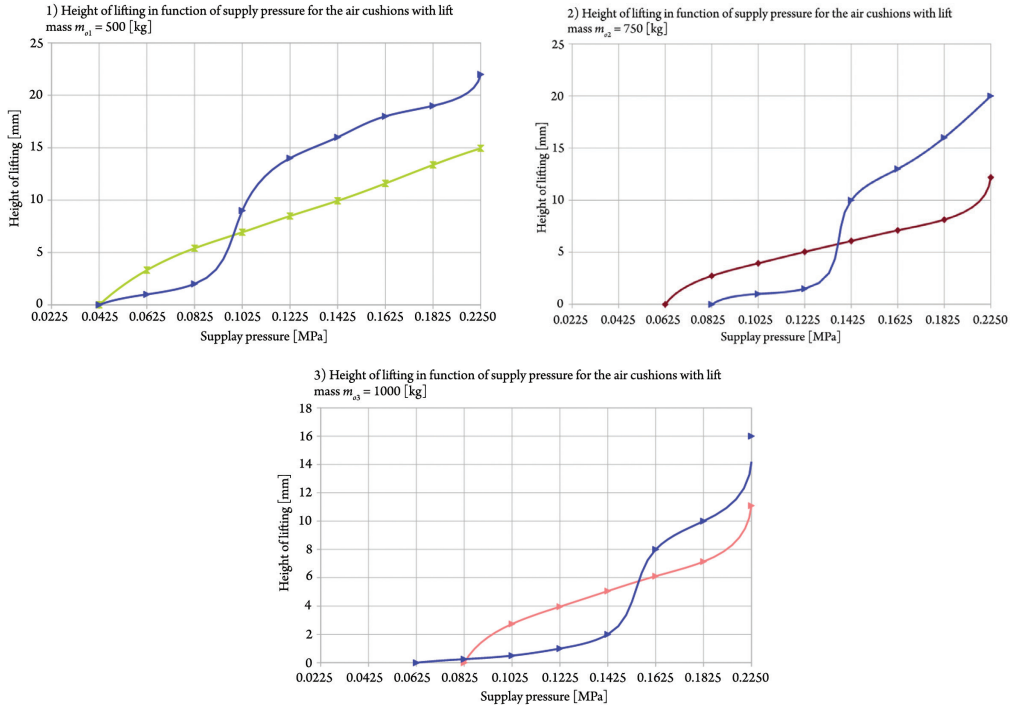

Fig. 11. Height of lifting in function of supply pressure for the air cushions with lift mass: 1) m_{o1} = 500 [kg] 2) m_{o2} = 750 [kg], 3) m_{o3} = 1000 [kg]

5. Summary

Too large difference in results for the geometry akin to a real object shows that picked model used in the symulation must be verified. With this end of view, further studies with consulting change of hyper-elastic material model, omitting simplifying model to flat model and symulation whole system on four air cushions as well as additional laboratory rasearch will be done.

References

[1] Lisowski E., Filo G., *Automated heavy load lifting and moving system using pneumatic cushions*, Automation in Construction, Vol. 50, 2015, 91–101.

[2] I-Shih L., *A note on the Mooney-Rivlin material model*, Continuum Mechanics and Thermodynamics, Vol. 24, 2012, 583–590.

[3] Jaszak P., *Modelowanie gumy za pomocą metody elementów skończonych*, Elastomery, Vol. 20, No. 3 , 2016, 31–39.

[4] http://help.solidworks.com, Mooney-Rivlin hiper-elastic model.

[5] http://help.solidworks.com, Contact between elements.

TECHNICAL TRANSACTIONS 2/2018
MECHANICS
DOI: 10.4467/2353737XCT.18.032.8005
SUBMISSION OF THE FINAL VERSION: 16/1/2018

Krzysztof Wach (krzysztof.wach@mech.pk.edu.pl)
Krzysztof Wach, Institute of Automobiles and Internal Combustion Engines, Faculty of Mechanical Engineering, Cracow University of Technology

Measurements of the angular and linear displacements of steered wheel

Pomiary kątowych oraz liniowych przemieszczeń koła kierowanego

Abstract

This paper concerns the use of a prototype measuring instrument for conducting measurements of the linear and angular displacements of a steered wheel in relation to the car body. The theoretical principles of the measurement are presented, as are the notation method and a solution to the system of equations of the geometric constraints of the instrument's mechanism. In the research section, the manner in which the measurements were conducted is discussed and sample results are described. A preliminary analysis of the results is performed in the summary section.

Keywords: car, suspension, steered wheel, prototype measuring instrument, angular and linear displacements, perturbation method

Streszczenie

Praca dotyczy pomiarów przemieszczenia i orientacji koła kierowanego względem nadwozia pojazdu wykonanych za pomocą prototypowego przyrządu pomiarowego. Przedstawione zostały teoretyczne podstawy pomiaru, jak również sposób zapisu i rozwiązywania układu równań więzów geometrycznych mechanizmu przedmiotowego przyrządu. W części badawczej omówiono sposób przeprowadzania pomiarów oraz przedstawiono przykładowe wyniki. W podsumowaniu została dokonana ich wstępna ocena i analiza.

Słowa kluczowe: samochód, zawieszenie, koło kierowane, prototypowy przyrząd pomiarowy, przemieszczenia kątowe oraz liniowe, metoda perturbacji

1. Introduction

Suspension and steering systems are two of the most important vehicle's systems affecting the safety of the vehicle. In order to achieve the desired dynamic behaviour of cars in different driving situations, numerous computer simulations and actual road tests have been carried out using specialised measuring apparatus [1–10]. Modern car suspensions are complicated spatial mechanisms with flexible constraints [11–13] – this is one of the reasons why the real kinematic steering ratio changes in relation to the speed of the vehicle [14]. This change results in a significant difference between the actual and the theoretical steering angle. Measurements of linear and angular displacements of steered wheel taken during experimental car rides, such as the real steering angle, are very important. The results of these measurements are essential with regard to vehicle handling and stability improvements in the process of designing new suspension systems [15–17]. The measurement of the position and orientation of the steered wheel relative to the car body is very difficult and complicated – only a few studies on this topic can be found in the literature. Measured values are not obtained directly but as a result of complex calculations [15, 18–24].

2. The prototype measuring instrument

The proposed instrument for measuring the translation and rotation of a steered wheel is composed of two plates – external and internal – connected with nine links with linear displacement sensors s_i, i = 1–9 built in. The external plate is fixed to the vehicle body, while the inner plate is connected to the axis of rotation of the steered wheel. The connection is made using a bearing hub. The links of the instrument are attached to both plates via ball joints, there are 9 joints named H_i, i = 1–9 in the case of the external plate, and three joints named D_j, j = 1–3 in the case of the inner plate. A characteristic feature of the joints D_j is that each of them realises the function of three ball joints with a common centre [21–24]. A schematic diagram of the prototype instrument is shown in Fig. 1.

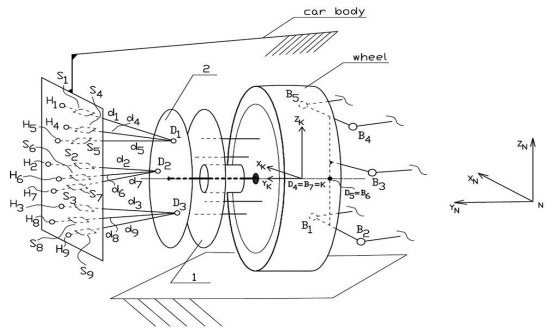

Fig. 1. Schematic diagram of a measuring instrument for the determination of the translation and rotation of a steered wheel: 1 – disc attached to a rim, 2 – disc immobilised against a stub axle. Points B_k, k = 1–5 are the centres of ball joints of a sample suspension. Detailed notation described in text [22]

Elongations of the instrument's links s_i, i = 1–9 are recorded during the measurement process. They are then substituted to a system of nine equations (1)–(3), which is solved using a so-called perturbation method [25, 26]. Coordinates of the centres of the ball joints D_j, j = 1–3 are obtained as a result.

$$\vec{r}_{D_1H_i}^{\,T} \cdot \vec{r}_{D_1H_i} = (l_{D_1H_i} + s_i)^2, \text{ for} \begin{cases} i=1, \\ i=4, \\ i=5, \end{cases} \tag{1}$$

$$\vec{r}_{D_1H_i}^{\,T} \cdot \vec{r}_{D_2H_i} = (l_{D_2H_i} + s_i)^2, \text{ for} \begin{cases} i=2, \\ i=6, \\ i=7, \end{cases} \tag{2}$$

$$\vec{r}_{D_3H_i}^{\,T} \cdot \vec{r}_{D_3H_i} = (l_{D_3H_i} + s_i)^2, \text{ for} \begin{cases} i=3, \\ i=8, \\ i=9, \end{cases} \tag{3}$$

Next, coordinates of two additional points lying on a wheel rotation axis D_n, n = 4,5 are calculated using formula (4):

$$\vec{r}_{D_jD_n}^{\,T} \cdot \vec{r}_{D_jD_n} = (l_{D_jD_n})^2, \text{ for } j=1-3, n=4,5 \tag{4}$$

Knowing coordinates of points D_j, j = 1–3 and D_n, n = 4,5 it is possible to determine a unit vector lying on the wheel rotation axis. Steering δ and camber γ angles, (see formulas (5) and (6)), as well as lateral displacements of steered wheel ΔK_y are then calculated.

$$\delta_k = -\text{arctg}\left(\frac{e_{kx}}{e_{ky}}\right), \tag{5}$$

$$\gamma_k = -\arcsin\left(e_{kz}\right), \tag{6}$$

It is necessary to know the initial configuration of the instrument mechanism at the start of the measurement process. The coordinates of ball joints centres H_i, i = 1–9 were determined using the coordinate measurement method, while the coordinates of the centres of the ball joints D_j, j = 1–3 were calculated using mathematical dependences. The theoretical analysis of the measurement of angular and linear displacements of a steered wheel using the prototype instrument and the determination of the initial configuration of the instrument mechanism have been widely described in earlier works [20–22, 24].

The initial configuration of the prototype instrument mechanism is shown below in millimetres:

H_1(113.6, –11.2, 61.0);	H_4(0.0, 1.3, 36.5);	H_7(–113.9, –12.9, 59,3);
H_2(177.9, –11.8, –50.0);	H_5(–64.9, –11.1, 146.8);	H_8(–177.6, –12.4, –50.6);
H_3(50.1, 1.1, –50.2);	H_6(63.7, –10.3, 147.3);	H_9(–49.8, 1.1, –50.0);
D_1(69.3, –232.2, –40.0);	D_2(–69.3, –232.2, –40.0);	D_3(0.0, –232.2, 80.0);

3. Measurements of the linear and angular displacements of a steered wheel

The test bench measurements of linear and angular displacements of a steered wheel were conducted on a car with independent (MacPherson) front wheel suspension. During the execution of the measurements the front wheels of the car were placed on turntables, while the rear wheels were placed on plates of the same height. An internal plate of the instrument was kinematically attached to the wheel using a bearing hub. The possibility of the plate rotating against its lateral axis y_w, was taken away. The external plate, parallel to the previous plate, was attached to the body of the car. Figure 2 shows an overview of a vehicle with a prototype measuring instrument mounted on the front left wheel.

Fig. 2. An overview of a tested vehicle with the prototype measuring instrument mounted on the front left wheel

It was important to appropriately configure the instrument before starting the measurement process. The configuration consisted of:

- setting up the internal and external plates in a position parallel to each other;
- unambiguous determination of a origin of the coordinate system;
- setting up proper angular position of internal plate in relation to the external plate.

In addition to the procedure described above, measurements of the steering rack displacements were carried out. The position of the steering rack was measured using optical linear displacement sensor with an accuracy of 0.02 mm. The method of mounting the sensor in the test car is shown in Fig. 3.

Fig. 3. Optical sensor of the linear displacements of the steering rack mounted in a test car: 1 – analogue-to-digital converter, 2 – sensor's housing, 3 – movable strip of a sensor, 4 – rack and pinion housing

Data from all sensors went to an analogue-to-digital converter and then to a notebook. The scheme of the measuring configuration is shown in Fig. 4; an overview is presented in Fig. 5.

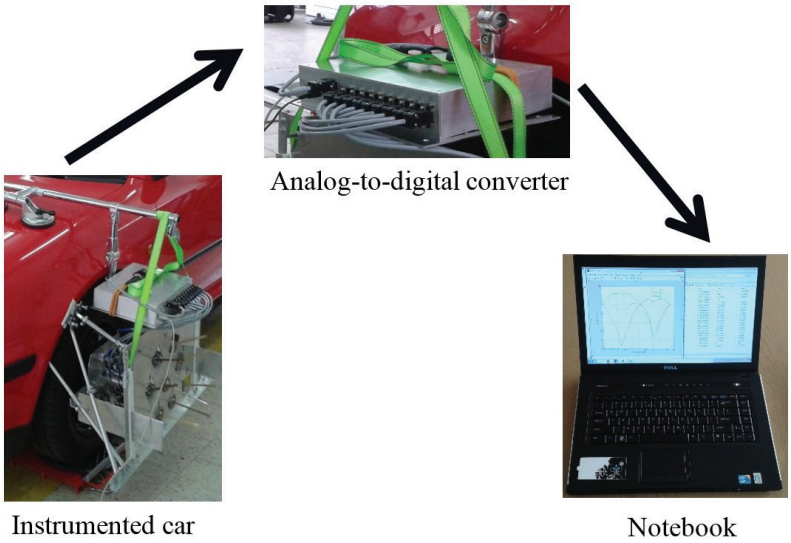

Fig. 4. Scheme of the measuring configuration

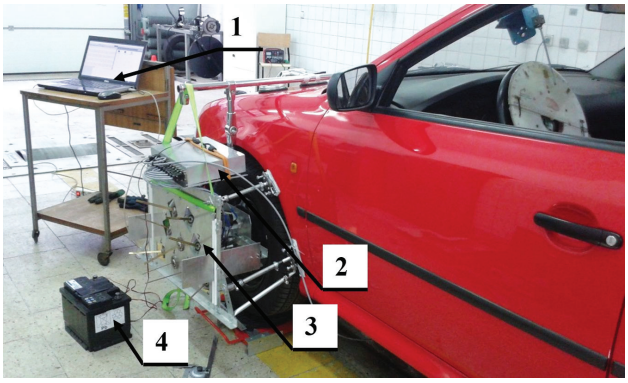

Fig. 5. An overview of the measuring configuration 1 – notebook, 2 – analogue-to-digital converter, 3 – prototype measuring instrument, 4 – battery

During the execution of the measurements the wheels were being turned left, then right, then left again, while the instrument links elongations and steering rack displacements were being simultaneously registered. Changes of linear dimensions of instrument links were used to calculate the steering and camber angles and the lateral displacements of the car wheel. At the same time, the steering angle was measured using a universal protractor with a vernier scale of 0°05'. Data registration was made at approximately every 2° of steering angle. The measurements were conducted for three different suspension deflections: neutral position, 43 mm compression and 57 mm rebound.

4. Results of measurements

4.1. Instrument links elongations

Example characteristics of instrument links elongations against steering rack displacement u_p and suspension deflection q are shown in Fig. 6.

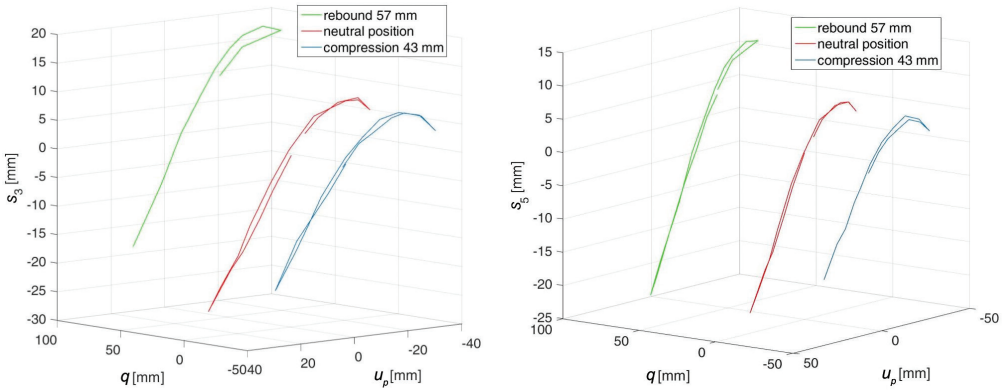

Fig. 6. Elongations of links s_3 and s_5 of prototype instrument against steering rack displacement u_p and suspension deflection q

4.2. Characteristics of suspension

Instrument links elongations s_i, i = 1–9 were used to calculate the characteristics of the suspension: camber γ and steering δ angle and lateral displacements of steered wheel ΔK_y against steering rack displacement u_p and suspension deflection q. Figures 7 to 9 show objective suspension characteristics.

Comparative values of steering angle δ obtained using the prototype measuring instrument and an universal protractor for three different suspension deflections are shown in Figs. 10 to 12.

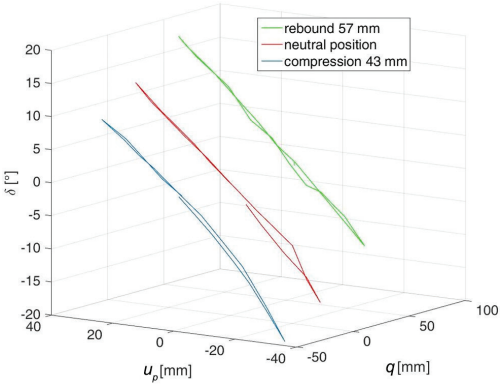

Fig. 7. Steering angle δ against steering rack displacement u_p and suspension deflection q

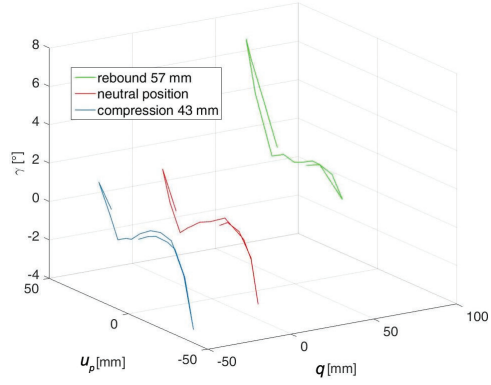

Fig. 8. Camber angle γ against steering rack displacement u_p and suspension deflection q

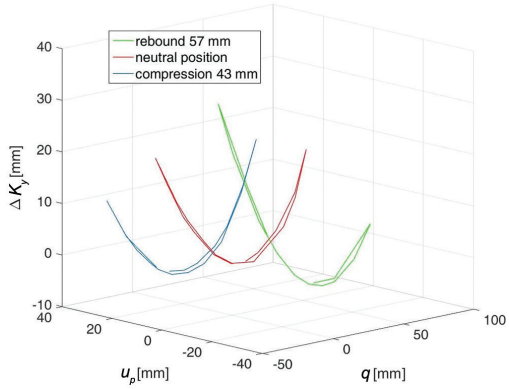

Fig. 9. Lateral displacements of steered wheel ΔK_y against steering rack displacement u_p and suspension deflection q

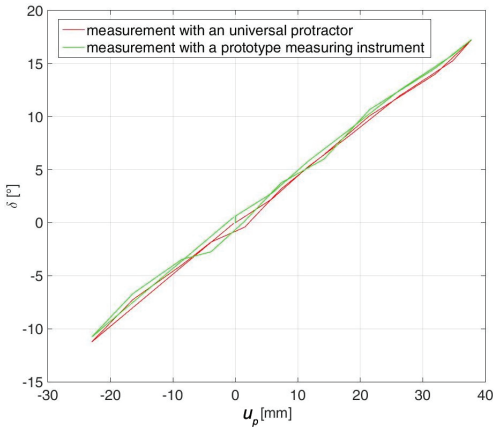

Fig. 10. Steering angle δ against steering rack displacement u_p for 57 mm rebound

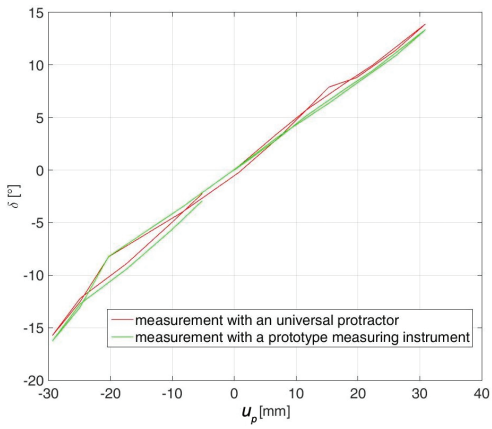

Fig. 11. Steering angle δ against steering rack displacement u_p for neutral position of suspension

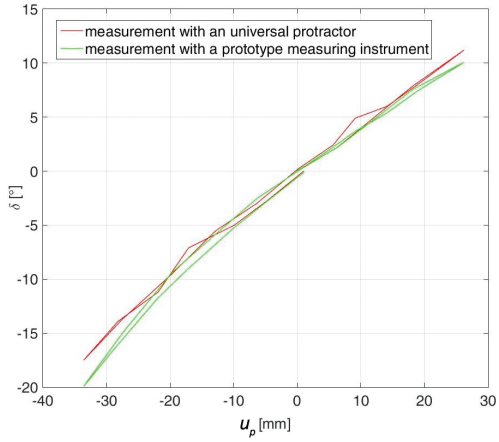

Fig. 12. Steering angle δ against steering rack displacement u_p for 43 mm compression

5. Summary

Results of preliminary measurements of translation and rotation of a steered wheel have been presented in this paper. The measurements were conducted using a prototype measuring instrument. As a result, camber γ and steering δ angle, and lateral displacements of a steered wheel ΔK_y against steering rack displacement u_p and suspension deflection q, were obtained. Steering angle δ values, obtained through the use of the prototype instrument, were compared with an analogous values achieved with an universal protractor. An analysis of the comparison for three different suspension deflections shows that, qualitatively, the results are very similar to each other. There is also a quantitative similarity, although some differences are visible especially with regard to marginal measured values of the steering rack displacement in the case of 43 mm compression of suspension.

The presented results show that the proposed method of measurement of linear and angular displacements of the steered wheel is accurate, despite the presence of some differences between values achieved using the prototype instrument and those achieved with a universal protractor.

The discussed measurements were preliminary, their results will be helpful for optimisation of the proposed method of measurement.

References

[1] Jonsson J., *Simulation of Dynamical Behaviour of a Front Wheel Suspension*, Vehicle System Dynamics, Vol. 20(5)/1991, 269–281.

[2] Lozia Z., *An analysis of vehicle behaviour during lane-change manoeuvre on an uneven ROAD surface*, Vehicle System Dynamics, Vol. 20(sup1)/1992, 417–431.

[3] Ammon D., Gipser M., Rauh J., Wimmer J., *High Performance System Dynamics Simulation of the Entire System Tire-Suspension-Steering-Vehicle*, Vehicle System Dynamics, Vol. 27(5–6)/1997, 435–455.

[4] Baumal A.E., McPhee J.J., Calamai P.H., *Application of genetic algorithms to the design optimization of an active vehicle suspension system*, Computer Methods in Applied Mechanics and Engineering, Vol. 163(1–4)/1998, 87–94.

[5] Gobbi M., Mastinu G., Doniselli C., *Optimising a Car Chassis*, Vehicle System Dynamics, Vol. 32(2–3)/1999, 149–170.

[6] Sancibrian R., Garcia P., Viadero F., *Fernandez A., De-Juan A., Kinematic design of double-wishbone suspension systems using a multiobjective optimisation approach*, Vehicle System Dynamics, Vol. 48(7)/2010, 793–813.

[7] Vilela D. Barbosa R.S., *Analytical models correlation for vehicle dynamic handling properties*, J. Braz. Soc. Mech. Sci. & Eng., Vol. 33(4)/2011, 437–444.

[8] Balike K. P., Rakheja S., Stiharu I., *Development of kineto-dynamic quarter-car model for synthesis of a double wishbone suspension*, Vehicle System Dynamics, Vol. 49(1–2)/2011, 107–128.

[9] Shim T., Velusamy P.C., *Improvement of vehicle roll stability by varying suspension properties*, Vehicle System Dynamics, Vol. 49(1–2)/2011, 129–152.
[10] Mántaras D. A. Luque P., *Virtual test rig to improve the design and optimisation process of the vehicle steering and suspension systems*, Vehicle System Dynamics, Vol. 50(50)/2012, 1563–1584.
[11] Reimpell J.,Betzler W., *Podwozia samochodów. Podstawy konstrukcji*, WKŁ, Warszawa 2002.
[12] Kanpczyk J., Dzierżek S., *Elastokinematic Analysis of Five-rod Suspension with Flexible Joints, Including Effects of Shock Absorber*, Vehicle System Dynamics, Vol. 29(sup1)/1998, 270–79.
[13] Cao D., Song X., Ahmadian M., *Editors' perspectives: road vehicle suspension design, dynamics, and control*, Vehicle System Dynamics, Vol. 49(1–2)/2011, 3–28.
[14] Abe M., *Vehicle Handling Dynamics, Second Edition: Theory and Application*, Butterworth-Heinemann, 2015.
[15] Janczur R., *Analityczno- eksperymentalna metoda badań sterowności samochodu*, Politechnika Krakowska, Ph.D. Thesis, Kraków 2002
[16] Struski J., *Quasi- statyczne modelowanie sterowności samochodu*, Wydawnictwo Politechniki Krakowskiej, Monografia 144, Kraków 1993.
[17] Struski J., *Przyrząd do pomiaru dynamicznego kąta skrętu koła kierowanego*, Patent No. P–267693.
[18] Blumenfeld W., Schneider W., *Opto- elektronisches Verfahrenzur Spur- und Sturz-winkelmessung am fahrenden Farzeug*, ATZ 87(1)/1985, 17–21.
[19] Struski J,. Kowalski M., *Podstawy teoretyczne uogólnionych zagadnień z zakresu parametryzacji układów prowadzenia kół względem nadwozia*, Technical Transactions, 6-M/2008, 119–129.
[20] Struski J., Wach K., *Analiza mechanizmu przyrządu pomiarowego do wyznaczania translacji i rotacji zwrotnicy z kołem kierowanym*, Technical Transactions, 3-M/2012, 87–100.
[21] Struski J., Wach K., *Teoretyczne podstawy wyznaczania przemieszczeń liniowych oraz kątowych koła kierowanego*, Czasopismo Logistyka – Nauka [Electronic document], Optical Disc CD, Vol. 4/2015, 5840–5849.
[22] Wach K., *The theoretical analysis of an instrument for linear and angular displacements of the steered wheel measuring*, IOP Conference Series: Materials Science and Engineering IOP, Vol. 148(1)/2016.
[23] CORSYS- DATRON RV-4 *Wheel Vector Sensor for Simultaneous Measurement of all Wheel Positions and Orientations in* 5 *Axes*, User manual, Vol. I, Wetzlar, Germany 2008.
[24] Wach K., Kupiec R., *Determination of initial configuration of mechanism of an instrument for measuring the translation and rotation of a steered wheel*, Technical Transactions, 6-M/2017, 197–2017.
[25] Grzyb A., *On a perturbation method for the analysis of the kinetostatics of mechanisms*. Akademie Verlag, ZAMM, Z. Angew. Math. Mech. 72/1992, T615–T618.
[26] Grzyb A., Struski J., *Metody wyznaczania kinematyki wielowahaczowych zawieszeń* kół ogumionych, Teka Komisji Naukowo-Problemowej Motoryzacji, Vol. 16/1998, 9–17.